WINTER/SPRING 1982 ● VOLUME 3, NUMBER 1 ● MOLECULAR LASER ISOTOPE SEPARATION

Los Alamos Science

LOS ALAMOS NATIONAL LABORATORY

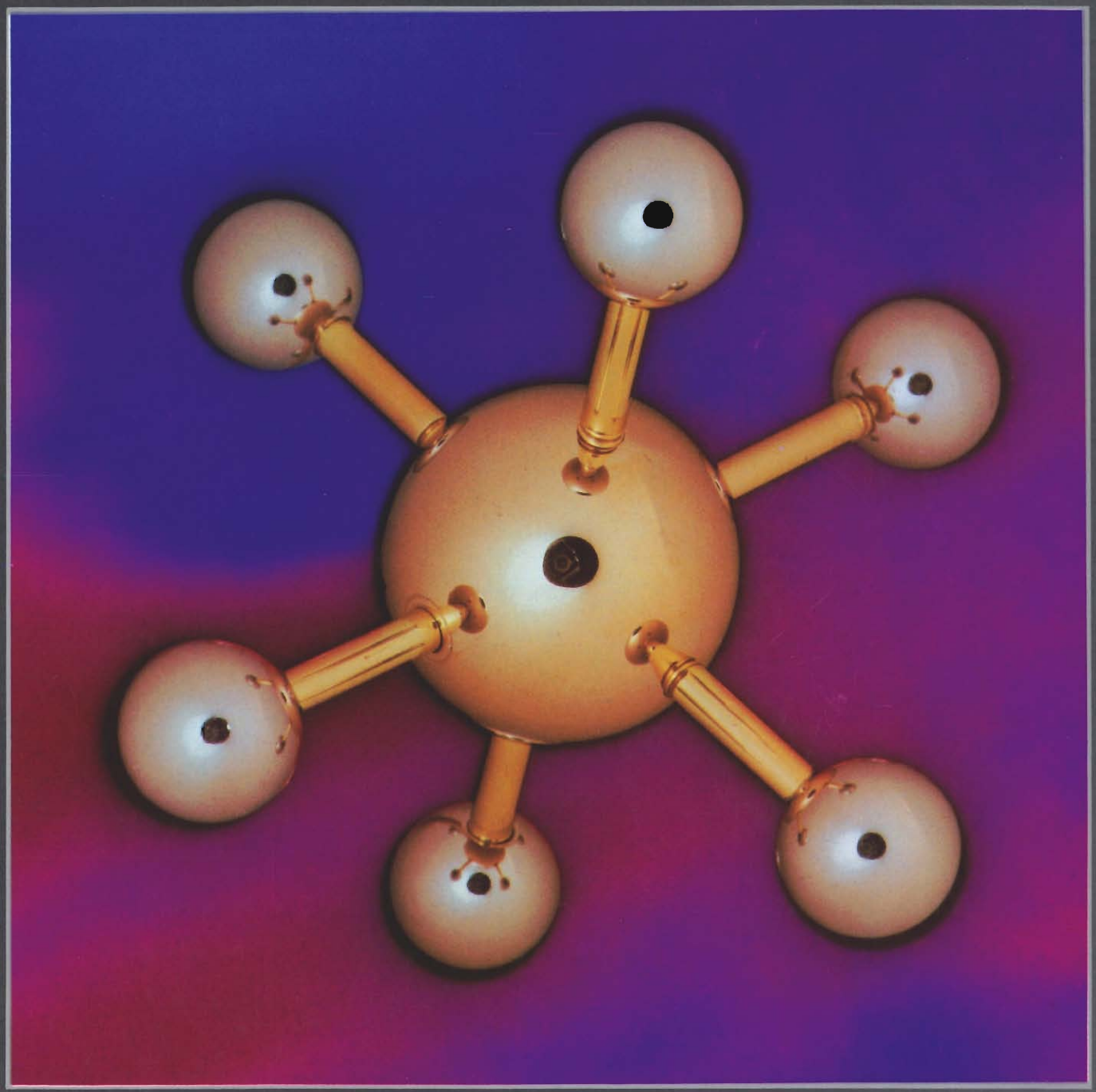

Inside This Issue

EDITOR'S NOTE

About ten years ago Los Alamos scientists ventured into a new frontier of scientific research, the interaction of lasers with molecules. It was the beginning of laser-induced chemistry—a field that holds much promise for the future.

The initial project that captured the imagination of both the scientists and the funding agencies was a clever scheme to produce enriched uranium. Bypassing the need for huge diffusion plants and their enormous consumption of electrical power, the idea was to use the intense, single-frequency light of lasers to break the chemical bonds of only those molecules containing the fissionable isotope uranium-235. This valuable nuclear fuel, which is only a minor constituent of uranium ore, would thus be prepared easily and cheaply in the more concentrated form required for nuclear reactor applications.

To take this idea, which originally was based almost entirely on intuition rather than experimental fact, and to make it not only work, but also work economically and efficiently, has been a prodigious task and one that is not yet complete. It has required the development of new high-power lasers that now enable chemists to "see" into chemical reactions in somewhat the same way that the microscope enables the biologist to see into the structure of microorganisms. It has required a new and deep understanding of molecular dynamics that has revolutionized the field of infrared spectroscopy. It has required an understanding of the remarkable nonlinear process of multiple-photon excitation whereby molecules absorb light energy much as a sponge absorbs water. And it has required tremendous dedication and perserverance.

Not only have the scientists had to face numerous disconcerting surprises offered up by nature, but they have had to work under the burden of perhaps overzealous classification (in a number of instances, concepts and results that originated at Los Alamos and were classified were later published by others in the open literature) and under the formidable pressure of management milestones—milestones based, perhaps of necessity, more on a priori assumptions rather than on proven facts about how nature works.

At present the program is facing a point of decision. Of three competing processes, the Los Alamos process may or may not be chosen to go forward with an advanced engineering program designed to lead to a demonstration plant. Even as we prepare this issue, Los Alamos scientists are in the laboratory working almost around the clock to show that molecular laser isotope separation will be able to produce the enrichments and the product throughput required to make the process economical. The latest results have come very close to the design parameters specified for a full-scale plant. These results were obtained in part by modifying the laser systems and will therefore affect the proposed plant design. But it is hoped that the decisionmakers will look favorably upon these changes. Despite the promising results to date, evaluation of the program is clouded by uncertainties in the laser and optical equipment costs. Then too, the future of the program, and in fact of all advanced isotope separation programs, is clouded by the decreasing demand projections for enriched uranium in the United States.

Whatever the outcome of the present competition, Los Alamos is proud of the program's technical achievements. According to the program leaders, the investment in this technology has produced dollar for dollar as much new knowledge, as measured by the number of research papers, as direct funding in basic research. And undoubtedly the related research on laser development and laser-induced chemical reactions has made an enormous contribution to the general field of applied photochemistry.

Perhaps it is fitting that in this issue devoted to a field of high scientific interest, high risk, high promise, and at the moment high drama, we honor Bernd Matthias through a personal memoir by one of his dearest friends. He was a man who loved risk, loved life, and more than anything loved the adventure of science.

Necia Grant Cooper

Cover photograph by H. W. Johnson and R. E. Duran

Editor:	Necia Grant Cooper
Art, Design, and Production:	M. A. Garcia
Science Writer:	Roger Eckhardt
Associate Editor:	Nancy Shera
Assistant Editor:	Judith M. Lathrop
Editorial and Production Assistant:	Elizabeth P. White
Production Assistant:	Judy Gibes
Computergraphic Illustrations:	Rongriego, Robert S. Hotchkiss
Illustrators:	Anita Flores, Monica Fink (type), Jim Mahan, Don DeGasperi (airbrush), Gerald S. Martinez, Gayle Fulwyler Smith
Photography:	Henry F. Ortega, LeRoy N. Sanchez, H. W. Johnson, R. E. Duran
Black and White Photo Laboratory Work:	Dan Morse, Ivan Worthington, Ken Lujan, Chris Lindberg, Ron Levy, Ernie Burciaga
Phototypesetting:	Chris West, Kris Mathieson
Pasteup:	Judy Gibes, Kathy Valdez
Printing:	M. A. Garcia, Robert C. Crook, William H. Regan, Jim E. Lovato

Errata: On page 131 of the article "Keeping Reactors Safe from Sabotage" (Volume 2, Number 1), we erroneously cited Ronald L. Cubitt rather than Richard L. Cubitt.

Los Alamos Science

FALL 1982 • VOLUME 3, NUMBER 3

CONTENTS

On the cover.
A unique "mirror" for lasers fluoresces as it reflects the phase-conjugate version of an incident laser beam. Ultraviolet light from a xenon fluoride laser enters a cell of liquid hexane from the left. There stimulated Brillouin scattering generates the reflected beam, which exactly retraces, in reverse, the path of the incident beam. (Photo by Henry Ortega)

Address mail to
LOS ALAMOS SCIENCE
LOS ALAMOS NATIONAL LABORATORY
MAIL STOP M708
LOS ALAMOS, NEW MEXICO, 87545

Los Alamos Science is published by Los Alamos National Laboratory, an Equal Opportunity Employer operated by the University of California for the United States Department of Energy under contract W-7405-ENG-36.

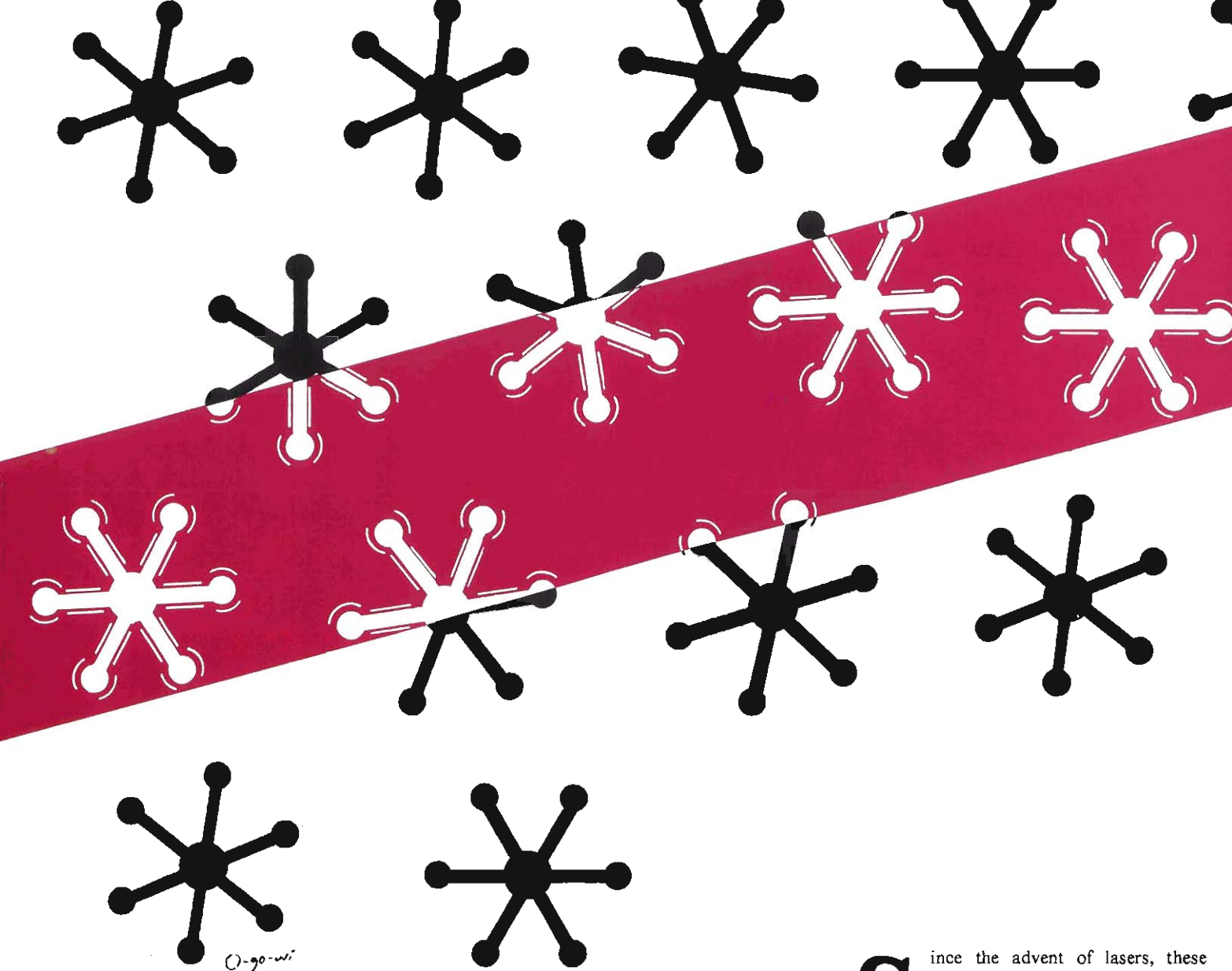

Based on recent discoveries in science and advances in engineering, the Los Alamos molecular laser isotope separation process appears to be an economical method for uranium enrichment.

by Reed J. Jensen, O'Dean P. Judd, and J. Allan Sullivan

Since the advent of lasers, these unique sources of highly intense and nearly monochromatic radiation have been proposed as tools to induce or catalyze chemical reactions. Of all the reactions investigated, laser isotope separation has received the most attention worldwide and may be the first major commercial application of lasers to chemistry.

Laser isotope separation was first demonstrated nearly a decade ago for boron and to date has been applied on a laboratory scale to many elements throughout the periodic table. But the goal is to find laser processes that are more economical than conventional separation techniques. Los Alamos researchers have developed a practical process for separating sulfur isotopes based on laser irradiation of sulfur hexafluoride molecules, and the Soviets have developed commercially applicable laser processes for separating both sulfur and carbon isotopes.

However, the primary motivation behind the generous funding of this field is the

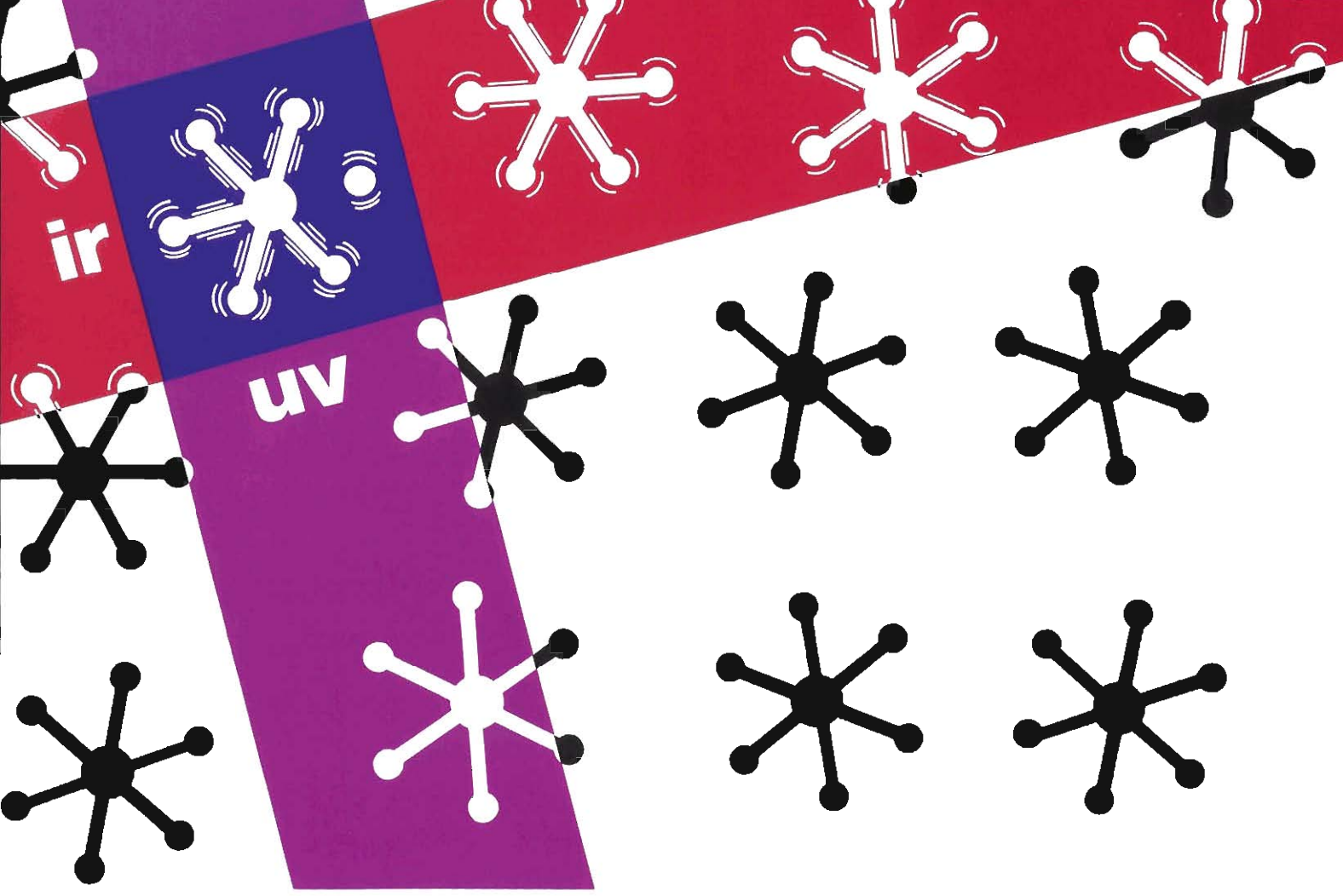

Separating Isotopes With Lasers

promise of an economical method for producing bulk quantities of enriched uranium, the fuel of nuclear reactors. Here, success has been much harder to achieve. But the difficulties encountered have been beneficial in the larger perspective, having stimulated fundamental scientific advances that are strongly influencing the broad field of laser chemistry. Among them are the discovery of multiple-photon processes, a revolution in infrared spectroscopy of heavy molecules, an increased understanding of molecular electronic structure and of condensation processes in cooled gases, the development of new, high-intensity, tunable laser systems, and practical methods for producing gas flows at low temperatures. These advances have also contributed to major progress in the Laboratory's molecular laser isotope separation process for uranium.

Natural uranium is a mixture of isotopes and contains 99.3 per cent uranium-238 and only 0.7 per cent of the fissile isotope uranium-235. To increase the concentration of uranium-235 to that required of reactor fuel, the two isotopes must be sorted according to some difference in their chemical or physical properties. But the electronic and therefore the chemical properties of the two isotopes are so nearly identical that chemical processing is difficult and inefficient. Conventional methods for separating isotopes of uranium, as well as those of other elements, rely instead on physical processes that are affected by the small differences in the masses of the different isotopes.

The gaseous diffusion method, which currently produces most of the enriched uranium for nuclear reactors, consists of passing gaseous uranium hexafluoride molecules (UF_6) through a series of chambers separated by porous barriers. The lighter molecules, those containing uranium-235, diffuse through the barriers slightly faster. So in each successive chamber the concentration of uranium-235 relative to that of uranium-238 increases slightly. More than a thousand chambers are needed to increase the concentration of uranium-235 to the fuel assay of 3.2 per cent required for light-water reactors. Gaseous diffusion thus requires a very large and expensive facility and, moreover, consumes large amounts of electrical energy.

Other separation techniques based on mass differences include the gas centrifuge, multiple distillation, and electromagnetic separation. Of these, the gas centrifuge is being explored as an alternative to gaseous diffusion (see sidebar "Economic Perspective for Uranium Enrichment").

What may prove to be more economical is a separation process driven by lasers. The idea is quite simple. Since atoms or molecules containing different isotopes have slightly different energy levels, they have slightly different absorption spectra—that is, they absorb radiation with different frequencies (Fig. 1). Consequently, radiation of a particular frequency can selectively excite an

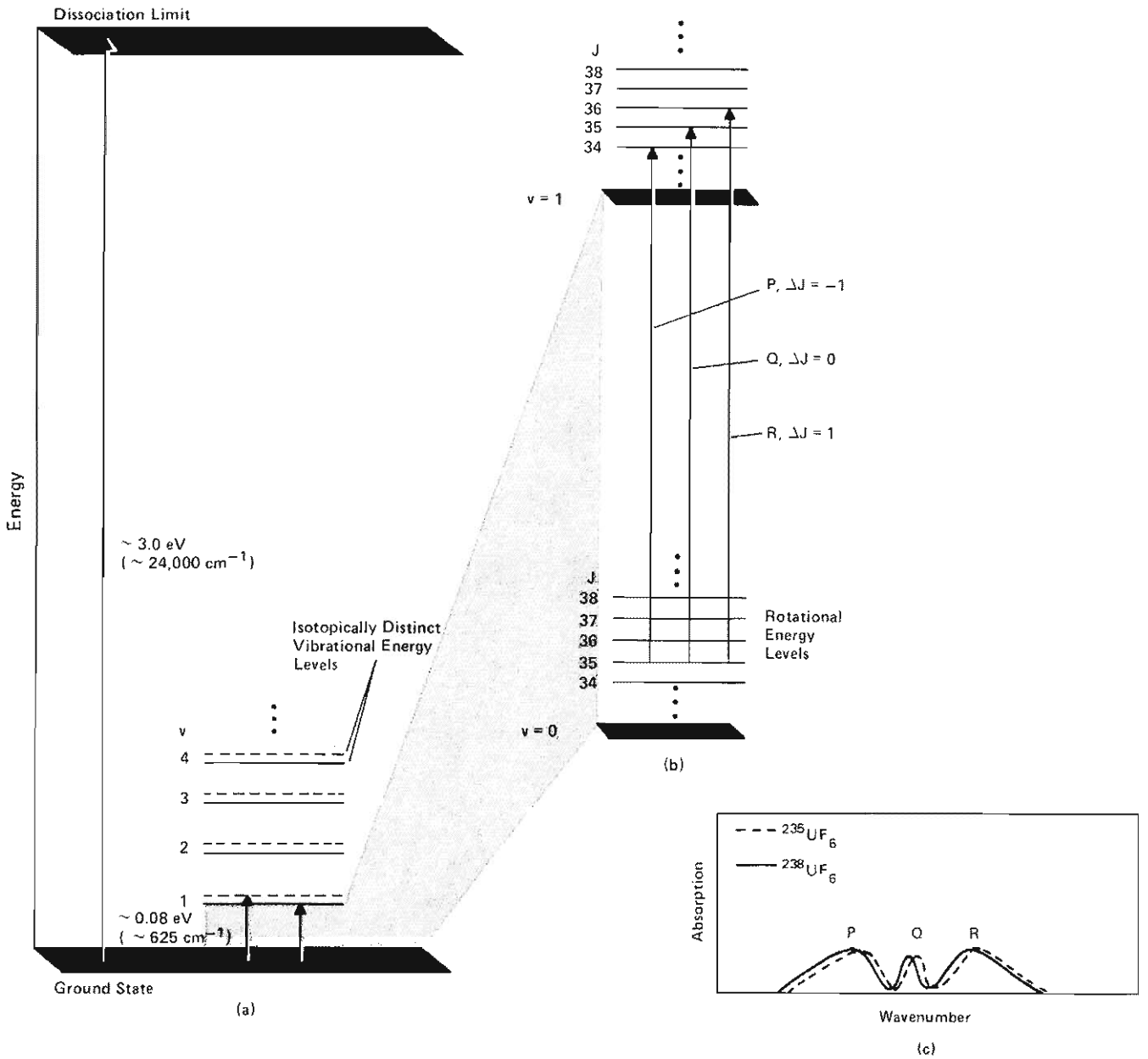

Fig. 1. The shift in vibrational energy levels of one molecular isotopic species relative to another shown in (a) is reflected in (c) as a shift in the infrared absorption spectra. (a) Within the ground electronic state of a molecule are many vibrational states resulting from oscillatory motion of the nuclei about their equilibrium positions. Shown here schematically are the energy levels for a vibrational mode of UF_6 known as the ν_3 mode. The energy levels are labeled by v, *the number of vibrational energy quanta of the state. The arrows represent absorptions of infrared photons that raise a molecule from the ground state to the first vibrational state. The different lengths of the arrows for the two isotopic species represent the different photon energies, or frequencies, needed to excite the two isotopic species. The difference, although small (less than 1.25 $\times$ 10^{-4} electron volt, or 1 reciprocal centimeter, for UF_6), allows selective excitation by nearly monochromatic laser light. (b) One of the vibrational transitions indicated in (a) is shown in more detail. Each vibrational state is split into many rotational states labeled by* J, *the number of rotational angular momentum quanta of the state. At room temperature molecules typically populate rotational states with high* J *values. During a transition between vibrational states, the change in* J, ΔJ, *is restricted to −1, 0, or +1. Such allowed transitions are denoted as* P-,Q-, *and* R-*branch transitions, respectively. (c) The infrared absorption bands of $^{235}UF_6$ and $^{238}UF_6$ from 620 to 630 reciprocal centimeters include transitions from the ground state to the first excited state of the ν_3 vibrational mode. Absorptions that excite the ν_3 mode occur over a broad band of frequencies because molecules in the ground state occupy many rotational states and the molecules in each rotational state can undergo* P-, Q-, *or* R-*branch transitions to the first excited vibrational state. The absorption band of $^{235}UF_6$ is shifted slightly to higher frequencies relative to that of $^{238}UF_6$.*

atom or molecule containing one isotope to a higher energy level and leave other isotopic species undisturbed. Then, depending on the type of excitation, the selectively excited species can be separated from the others by conventional physical or chemical methods.

For selective excitation to be practical as a separation technique, it must produce a large change in some chemical or physical property of the excited species. One possibility is to excite a molecule to such a high energy level that its chemical reactivity increases substantially. The molecule can then react with another chemical species, and the product containing the desired isotope can be separated from the mixture by conventional techniques. This type of bimolecular process has many applications in selective photochemistry.

However, the more widely studied laser isotope separation techniques involve only photons and a single atomic or molecular species. For example, the atomic vapor process under development at Lawrence Livermore National Laboratory uses selective photoionization to separate uranium isotopes. Through a multistep excitation process laser photons selectively ionize atoms of uranium-235. The ions are then separated from the neutral uranium-238 atoms by an electric field.

The separation technique being studied at Los Alamos uses selective photodissociation of molecules into stable fragments. As discussed below in more detail, a molecule can be excited to the point of dissociation in several ways. A two-step process is the basis of our technique. An infrared laser selectively excites vibrations of gaseous UF_6 molecules containing uranium-235 ($^{235}UF_6$). These vibrationally excited molecules are then dissociated by an ultraviolet laser into uranium pentafluoride ($^{235}UF_5$) plus a fluorine atom. The $^{235}UF_5$ molecules coalesce to form particulates that are easily separated from the remaining gas.

The various techniques for isotope separation have been investigated vigorously at Los Alamos and at many other research centers around the world since the early 1970s when high-intensity tunable lasers became available. However, isotope separation based on selective photoexcitation of atoms and molecules is not a new idea. In fact, photochemical separation was attempted with conventional radiation sources long before the invention of lasers. In 1922 efforts were made to separate the two naturally occurring chlorine isotopes by irradiating them with white light that had been filtered through a cell containing only the more abundant chlorine isotope. These experiments were unsuccessful. About ten years later Stanislaw Mrozowski suggested that mercury isotopes might be separated by selective excitation with the 253.7-nanometer resonance line of a mercury arc lamp and subsequent reaction with oxygen. This separation was achieved experimentally by Kurt Zuber in 1935. In the early '40s Harold Urey proposed a photochemical method for separating uranium isotopes, but his proposal lost in competition with the gaseous diffusion technique. After the war, an enlarged effort to separate mercury isotopes by photochemical techniques succeeded in producing small amounts of product. Carbon and oxygen isotopes were also separated by using a strong spectral line of an iodine lamp to excite carbon monoxide molecules.

These pre-laser experiments involved a one-step process in which absorbed photons with frequencies in the visible or ultraviolet spectral region selectively excite electronic states of one isotopic species. Although this technique works in a few isolated cases, it is not generally applicable in molecules. Most molecules have very broad, structureless electronic absorption bands, and selective excitation is not possible.

These early efforts were also limited by the radiation sources then available. Photochemical isotope separation requires highly monochromatic, highly intense radiation. The few reasonably monochromatic discharge lamps were not very intense and covered only a small number of wavelengths. Monochromatic sources at other wavelengths were created from conventional white light sources (for example, with filters or gratings), but their intensity was even lower.

High-intensity tunable lasers have removed many of the limitations of the early experiments. Lasers can be tuned to match any absorption feature that shows a distinct isotope shift. In particular, high-intensity infrared lasers can selectively excite the isotopically distinct vibrational levels of molecules. Because of its high monochromaticity, laser light can excite a desired species with reasonable selectivity even when absorption features of other isotopic species partially overlap those of the desired isotopic species. Thus, both the tunability and high monochromaticity of the laser are crucial for selective excitation.

Other properties of laser light contribute to the efficiency of selective excitation. First, since laser light has a high degree of spatial and temporal coherence, a laser beam can propagate over long distances and interact efficiently with large volumes of process material. Second, a high-intensity laser beam can saturate the absorbing material. In other words, the beam contains so many photons that almost all the molecules that can be excited will be excited. Finally, the laser pulses are short compared with the average time for the selectively excited molecules to lose their energy either through collisions with unexcited molecules or through other loss channels. Short pulses are essential if the excitation process is to be isotopically selective and efficient in its use of laser photons.

Laser photons are quite expensive and represent the major cost in any laser chemistry process, including laser isotope separation. To illustrate, a mole (6×10^{23}) of photons costs about 1 to 3 dollars, whereas chemical reagents typically cost about 10 to 20 cents per mole. Efficient use of laser photons is therefore a primary factor determining the economy of a laser isotope

continued on page 8

SIDEBAR 1:

Economic Perspective for Uranium Enrichment

The future demand for enriched uranium to fuel nuclear power plants is uncertain. Estimates of this demand depend on assumptions concerning projections of total electric power demand, financial considerations, and government policies. The U.S. Department of Energy recently estimated that between now and the end of this century the generation of nuclear power, and hence the need for enriched uranium, will increase by a factor of 2 to 3 both here and abroad. Sale of enriched uranium to satisfy this increased demand can represent an important source of revenue for the United States. Through fiscal year 1980 our cumulative revenues from such sales amounted to over 7 billion dollars, and until recently foreign sales accounted for a major portion of this revenue. The sole source of enriched uranium until 1974, the United States now supplies only about 30 per cent of foreign demand. New enrichment capacity planned in this country should include means of reducing enrichment costs to permit capturing a larger share of the foreign trade in this commodity. Laser isotope separation shows promise of accomplishing this goal.

Currently, gaseous diffusion is the process by which uranium is enriched at the large-scale production facilities in the United States. Three such facilities exist (at Oak Ridge, Tennessee; Paducah, Kentucky; and Portsmouth, Ohio) whose total enrichment capacity will soon reach 27.3 million separative work units per year.

Separative work units (abbreviated SWU) are the customary measure of the effort required to produce, from a feed material with a fixed concentration of the desired isotope, a specified amount of product enriched to a specified concentration and tails, or wastes, depleted to a specified concentration. For example, from feed material with a uranium-235 concentration of 0.7 per cent (the naturally occurring concentration), production of a kilogram of uranium enriched to about 3 per cent (the concentration suitable for light-water reactor fuel) with tails depleted to 0.2 per cent requires about 4.3 SWU.

Gaseous diffusion is based on the greater rate of diffusion through a porous barrier of the lighter component of a compressed gaseous mixture. For uranium enrichment the gaseous mixture consists of uranium hexafluoride molecules containing uranium-235 ($^{235}UF_6$) or uranium-238 ($^{238}UF_6$). The enrichment attainable per diffusion unit is quite low, being limited theoretically to less than the square root of the $^{238}UF_6$ to $^{235}UF_6$ mass ratio, or about 1.004. Therefore, the slightly enriched product from one diffusion unit, consisting of a compressor and a diffusion chamber, is passed through a second unit whose product in turn is passed through a third unit, and so on. (The theory of separative work and optimal arrangement of separation units was pioneered by R. E. Peierls and P. A. M. Dirac.) To enrich uranium from 0.7 per cent uranium-235 to about 3 per cent requires approximately 1250 units. Gaseous diffusion plants are therefore very large and expensive.

They have, however, proved very reliable. The main disadvantage of the process is the great amount of electric power required to operate the many compressors. A standard gaseous diffusion plant operating at full capacity demands about 3000 megawatts electric. For comparison, a typical large electric power plant produces 1000 megawatts electric. As the cost of electric power increases, its consumption becomes an increasingly important factor in the cost of enriched uranium. (In fiscal year 1980 about 75 per cent of the production costs at gaseous diffusion plants was for electricity.)

With the expectation of reducing power consumption, attention is now focused on the gas centrifuge, another method for enriching uranium. The Gas Centrifuge Enrichment Plant now being constructed at Portsmouth, Ohio will contribute 8.75 million SWU per year to the national enrichment capacity by 1994. In a gas centrifuge $^{235}UF_6$ and $^{238}UF_6$ are separated by the centrifugal force imposed on UF_6 by a rapidly rotating container. For this process a considerably smaller number of centrifuge units (less than 10) are required to reach the desired enrichment. However, the throughput per centrifuge unit is very small compared to that of a diffusion unit—so small, in fact, that it is not compensated by the higher enrichment per unit. To produce the same amount of reactor-grade fuel requires a considerably larger number (approximately 50,000 to 500,000) of centrifuge units than diffusion units. This disadvantage, however, is outweighed by the considerably lower (by a factor of 20) energy consumption per SWU for the gas centrifuge.

Compared to diffusion and the centrifuge, laser isotope separation offers the potential for much greater enrichment and throughput per separation unit. Therefore, a laser isotope separation facility would be much smaller, including only about ten separation units. In addition, the process would consume an equal or lesser amount of energy per SWU than the gas centrifuge. These advantages lead directly to reduced capital and operating costs.

For a laser isotope separation process involving selective excitation of $^{235}UF_6$ molecules with infrared lasers and their dissociation with an ultraviolet laser, a facility with the standard capacity of 8.75 millions SWU per year is estimated to cost about 1 billion dollars. (Laser costs account for approximately half of the direct capital costs.) This is considerably lower than the estimated cost of a new gaseous diffusion plant (about 5 billion dollars) or that of a gas centrifuge plant (about 6 billion dollars). The annual operating cost for a laser isotope separation facility is estimated to be about 100 million dollars, in contrast to about 500 million for a gaseous diffusion plant and 100 to 200 million for a gas centrifuge plant. Our estimates of capital and operating costs for a laser isotope separation facility indicate a cost per SWU of about $30; the current commercial cost for enriched uranium is $110 per SWU.

The considerably lower cost per SWU for laser isotope separation opens the possibility of turning the large stockpile of wastes from gaseous diffusion plants into a valuable uranium resource. These wastes contain about a third of the $^{235}UF_6$ originally present in the feed material and are estimated to amount to more than 500,000 metric tons by the end of 1990—an amount containing enough uranium-235 for 1800 reactor-years of operation.

These advantages imply that laser isotope separation should be thoroughly investigated as a potentially economical process for large-scale production of enriched uranium. ■

continued from page 5

separation process.

We said earlier that a fairly large amount of energy must be deposited in a molecule to make a substantial change in its physical or chemical properties. In the pre-laser experiments this energy was deposited through a one-step, or single-photon, process. When high-intensity infrared lasers became available, new multistep excitation processes became possible. Unlike the single-photon process, these multistep methods can achieve isotopic selectivity on virtually all atoms or molecules.

In the sections that follow, we will describe these excitation methods and their application to isotopes of medium and heavy elements. Great success has been achieved in separating medium-weight isotopes with infrared photons through what is known as multiple-photon excitation and dissociation. Progress has also been made on the more difficult problem of separating isotopes of heavy elements such as uranium. Laboratory-scale experiments based on the infrared-plus-ultraviolet dissociation of UF_6 have been very successful. The lasers and gas flow systems necessary to scale up the process have been built, and designs for a full-scale plant have been studied. But challenges still remain in both the science and engineering needed to optimize the process and its economics on a large scale. The physics of the molecular excitation is not sufficiently defined to choose process parameters that optimize selectivity, and some problems associated with irradiating large volumes of material have yet to be solved. But we are rapidly drawing nearer to our goal.

Molecular Laser Isotope Separation Methods

Three methods of molecular photodissociation have been used successfully to separate isotopes: a single-photon process, in which a

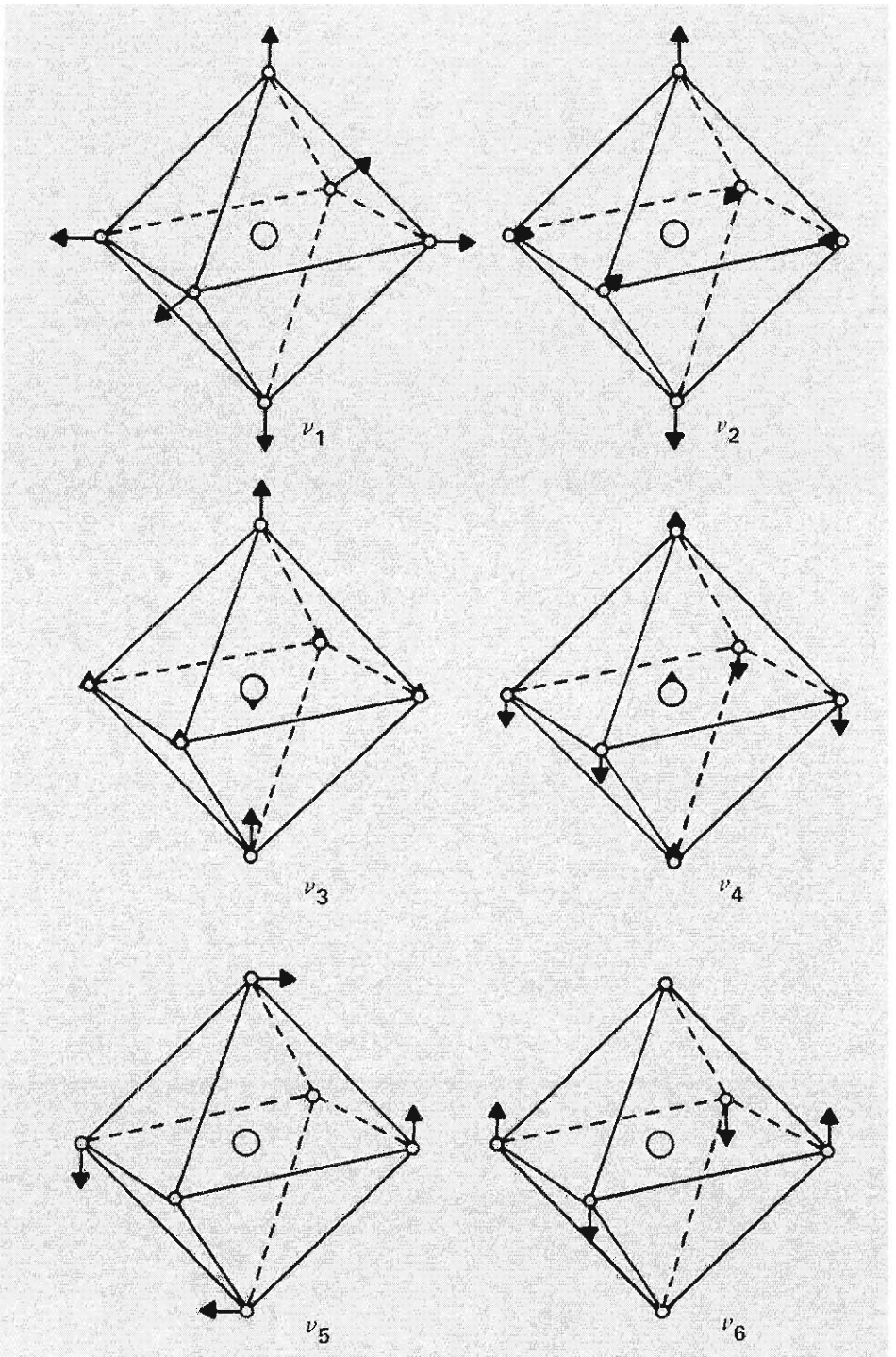

Fig. 2. In the ground-state configuration the fluorine nuclei in a sulfur hexafluoride (SF_6) molecule occupy the vertices of a regular octahedron about the central sulfur nucleus. Shown here are the six fundamental vibrational modes that, singly or in combination, describe the complex motion of SF_6 and other octahedral molecules, such as UF_6. Only the ν_3 and ν_4 modes can be excited by absorption of infrared photons, and, since only these modes involve motion of the sulfur nucleus, any shifts due to sulfur isotopes are confined to these particular modes. The ν_3 mode stretches one S-F bond and compresses a second S-F bond that is colinear with the first. The ν_4 mode bends the four coplanar S-F bonds.

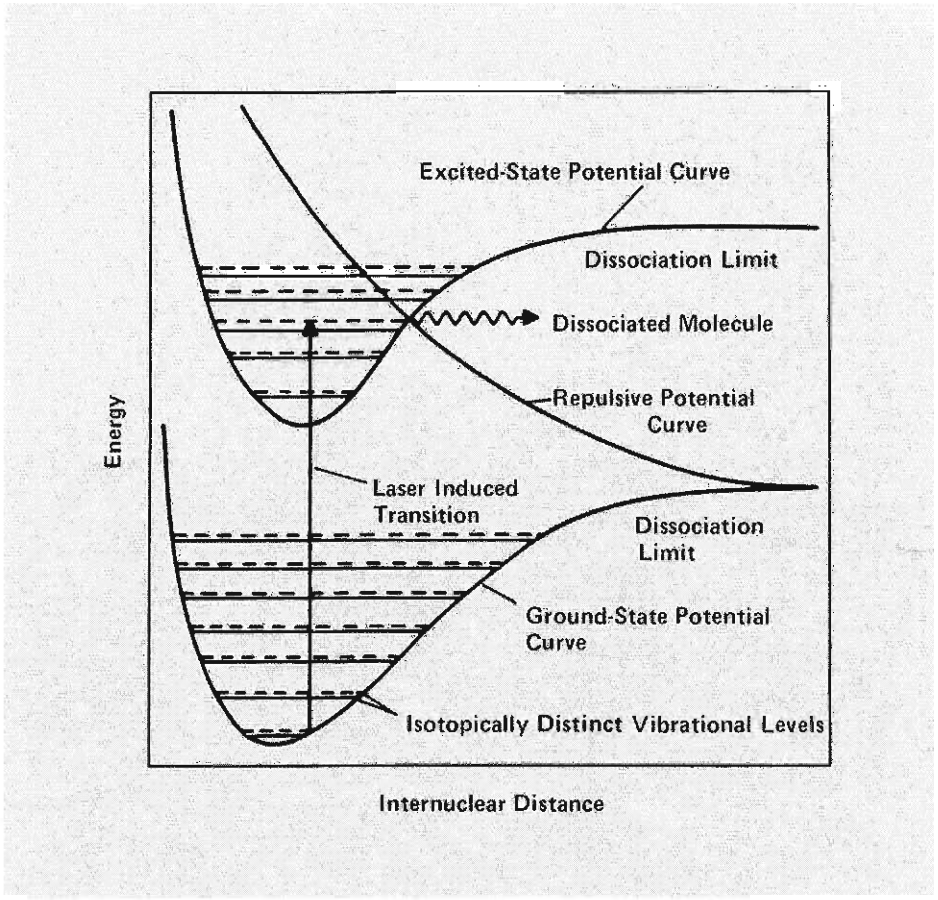

Fig. 3. Predissociation. The three potential energy curves depict the molecular binding energy as a function of internuclear distance. The curves for the ground electronic state and the bound excited electronic state exhibit energy minima and thus represent stable molecular configurations. The curve for the repulsive electronic state represents an unstable configuration in which the molecule dissociates because the forces are always repulsive. The usual photodissociation process involves a transition directly to a repulsive electronic state. The arrow represents a photon-induced transition of one isotopic species to a vibrational state within the bound excited electronic state. This transition can result in predissociation in which the molecule tunnels from the bound excited electronic state to the repulsive electronic state and then dissociates.

visible or an ultraviolet photon excites a molecule to a "predissociative" state; a two-step process, in which an infrared photon excites a vibrational state of a molecule and an ultraviolet photon dissociates the excited molecule; and a multistep infrared process, in which infrared photons excite successively higher and higher vibrational states of a molecule until its dissociation limit is reached.

In all these processes, including predissociation, selectivity is based on the isotopically distinct energies of the molecule's vibrational states. In a vibrational state the nuclei of a molecule undergo oscillatory motion about the ground-state configuration (Fig. 2) at some frequency. This frequency depends on the masses of the nuclei. In particular, molecules containing lighter isotopes vibrate at higher frequencies. Consequently, vibrational excitation of a molecule containing a lighter isotope requires absorption of a photon at a higher frequency. This mass-dependent shift in the absorption spectrum has been exploited to dissociate molecules of one isotopic species selectively and thus achieve isotope separation.

PREDISSOCIATION. The usual photodissociation process involves a photon-induced transition from a bound ground electronic state to an electronic state for which the internuclear forces are always repulsive. The lifetime of such a repulsive electronic state is so short that dissociation follows the transition with nearly unity probability. Predissociation (Fig. 3) involves a photon-induced transition not directly to a repulsive electronic state but to a predissociative state—a vibrational state within a bound excited electronic state that is energetically coupled to the repulsive electronic state. That is, the bound excited and repulsive electronic states have the same energy (the curve-crossing energy) at some internuclear distance greater than the equilibrium internuclear distance for the ground electronic state. Then, if the bound excited and repulsive electronic states have certain symmetry relations and if the energy of the vibrational state is near the curve-crossing energy, dissociation occurs by tunneling from the bound excited electronic state to the repulsive electronic state. This dissociation by tunneling is called predissociation because it requires a photon energy less than that required for dissociation directly from the repulsive electronic state. By tuning a laser to the frequency matching the transition energy of the isotopic species of interest, that species can be selectively excited and dissociated.

A requirement for isotopic selectivity of predissociation is that the shift of the vibrational energy levels for the different isotopic species be greater than their energy widths. The energy width of a state is determined in

part by its lifetime, and longer-lived states have narrower energy widths. Predissociative states in some molecules are relatively long-lived, and selective predissociation not only works but also has a high quantum yield. That is, if the molecule absorbs a photon of the right frequency to raise it to a predissociative state, it will almost always dissociate rather than decay to lower-energy states through emission of photons.

One successful application of this process is the predissociation of formaldehyde (H_2CO) to produce carbon monoxide enriched in carbon-13. Laser photons with a wavelength of 334 nanometers excite $H_2{}^{13}CO$ molecules to a vibrational level of an excited electronic state that predissociates into hydrogen and carbon monoxide molecules. Some of the $H_2{}^{12}CO$ molecules also dissociate, but early experiments produced carbon monoxide with a concentration of carbon-13 greater by a factor of 3 or 4 than its initial natural isotopic abundance.

Predissociation of formaldehyde with a laser of different wavelength has also been studied as a practical way to separate hydrogen and deuterium. From an equal mixture of H_2CO and D_2CO, products have been obtained with deuterium-to-hydrogen ratios of 9, in contrast to the original ratio of 1. Although these results seem impressive, the natural abundance of deuterium is so small (about 0.015 per cent) that the enrichment must be increased significantly for any practical application.

This process is being actively investigated by the Canadians at Ontario Hydro for production of the heavy water needed in their CANDU (Canadian deuterium uranium) power reactors. A CANDU reactor requires about 800 kilograms of heavy water per megawatt of capacity, and at the present cost of $250 per kilogram, the heavy-water inventory represents about 15 to 20 per cent of the total capital cost of the reactor. Recent predissociation experiments at Ontario Hydro show enrichments on the order of 1000, and experiments based on multiple-photon dissociation have also demonstrated high enrichments. These results indicate that laser isotope separation may be a potentially promising technology for low-cost production of heavy water.

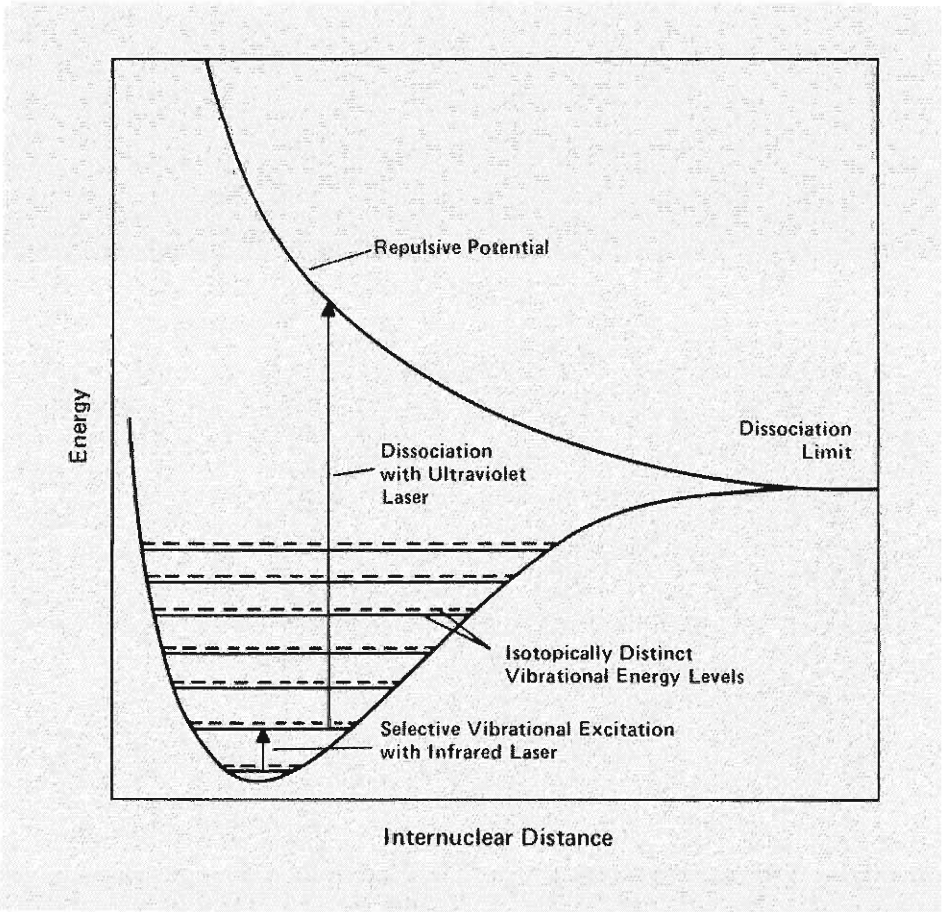

Fig. 4. In two-step photodissociation, an infrared laser selectively excites a vibrational level of one isotopic species and thereby raises molecules of that species closer to the dissociation limit. An ultraviolet laser then raises the excited molecules to an unstable electronic configuration represented by the repulsive potential. The molecule then dissociates into stable chemical fragments. (Predissociation can also occur in the ultraviolet step.)

TWO-STEP PHOTODISSOCIATION. In predissociation a single laser provides both the isotopic selectivity and the dissociation. The quantum yield for this process is quite high, but selectivity is limited to a few molecules with distinct features in their electronic absorption spectra. However, we can make photodissociation selective in a very wide range of molecules by breaking the process into two steps, the first providing high selectivity and the second efficient dissociation (Fig. 4).

In the first step infrared lasers selectively

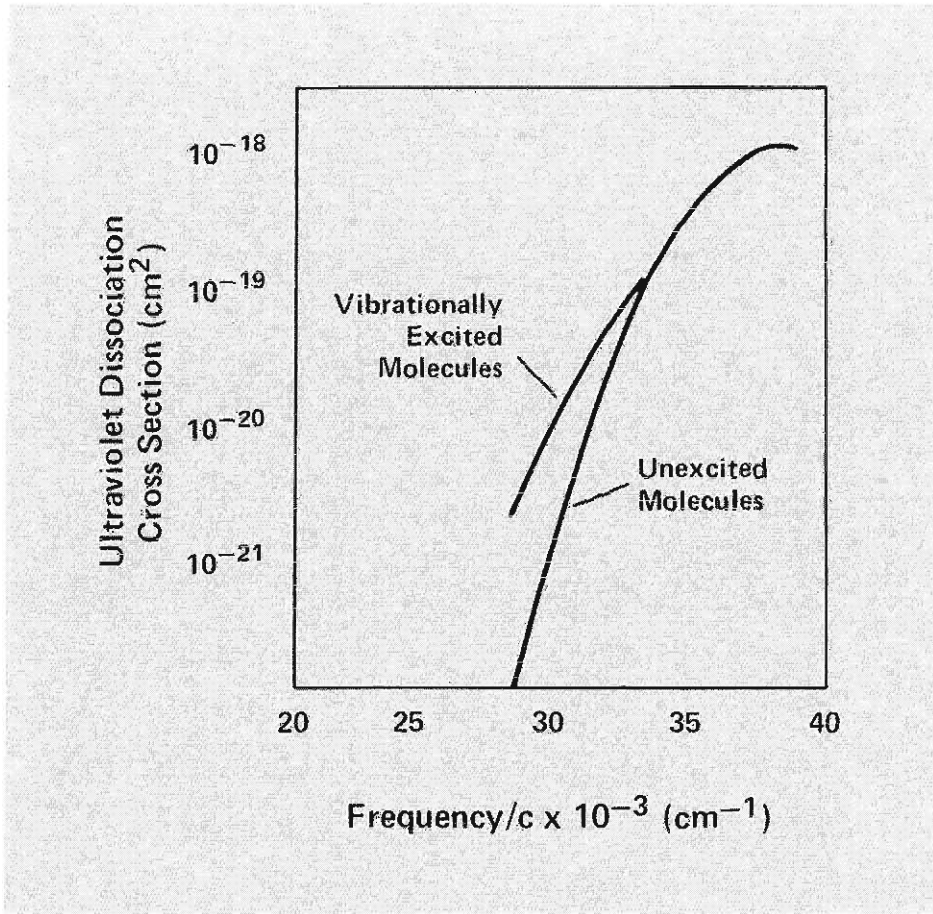

Fig. 5. The effect of vibrational excitation induced by an infrared laser on the ultraviolet dissociation cross-section spectrum of CF_3I. Vibrational excitation increases the dissociation cross section at a given ultraviolet frequency and shifts the spectrum to lower frequencies. At about 29,000 cm^{-1} the dissociation cross section for the selectively excited molecules is about 10 times larger than that for the unexcited molecules. Data from "Laser Isotope Separation of Carbon by Multiple IR Photon and Subsequent UV Excitation of CF_3I Molecules," I. N. Knyazev, Yu. A. Kudriavtzev, N. P. Kuzmina, V. S. Letokhov, and A. A. Sarkisian, Applied Physics 17, 427-429 (1978).

excite the vibrational states of one isotopic species and not the others. To date most experiments involving selective vibrational excitation have dealt with molecules whose vibrational transition frequencies overlap the output frequencies of the carbon dioxide (CO_2) laser. This laser operates at several wavelengths centered around 10 micrometers with a pulsed optical output that can be varied over a wide power range.

The second step is dissociation of the selectively excited moleucles with an ultraviolet laser. Figure 4 shows that dissociation from a vibrationally excited state requires an ultraviolet photon with an energy, and hence frequency, lower than that required for dissociation from the ground state. In an ideal situation the lower-frequency ultraviolet photons will not dissociate the unexcited molecules, and the selectivity of the first step will be preserved.

In this two-step process the excitation and the dissociation must occur on a time scale that is short compared to the lifetime of the intermediate vibrational state. Otherwise, the excited molecules can lose their vibrational energy through collisions to other isotopic species or to lower-energy vibrational states not accessible to dissociation. Since the CO_2 laser is normally operated with a pulse length of 50 to 100 nanoseconds, which is shorter than the lifetime of the vibrational state, most vibrationally excited molecules will not lose their energy before being dissociated by the ultraviolet laser pulse if the pressure of the absorbing molecular gas is sufficiently low. For 100-nanosecond pulses the gas pressure must be a few torr or less to avoid the effects of collisions.

Two-step photodissociation has been applied successfully to the separation of carbon isotopes in trifluoroiodomethane (CF_3I). This molecule has a strong vibrational absorption at a frequency covered by the CO_2 laser. Among the parameters influencing the dissociation are the frequency of the ultraviolet laser and the fluence of the infrared laser. (The fluence, or time-integrated intensity, of a laser beam is a measure of its energy per unit beam area.)

Figure 5 shows the ultraviolet dissociation cross section, or dissociation probability, as a function of ultraviolet photon frequency. Before infrared excitation the dissociation cross-section spectra for different isotopic species are nearly the same. The cross section is zero at low frequencies and then rises steeply to a nearly constant value. Infrared excitation increases the photodissociation cross section at a given frequency and shifts the threshold for dissociation to lower frequencies (to the red). This shift allows one to

choose an ultraviolet laser frequency at which the dissociation cross section is large for excited molecules (the selected isotopic species) and small for unexcited molecules. If the infrared excitation were perfectly selective, the ratio of the dissociation cross section for the excited molecules to that for the unexcited molecules at a given ultraviolet frequency would be a direct measure of the highest enrichment attainable.

Figure 6 shows that the dissociation cross section increases with the fluence of the infrared laser. Therefore, one might expect better selectivity at higher fluences. But because the selectivity of the infrared excitation is finite, some molecules of the unwanted isotopic species are vibrationally excited. Higher infrared fluence increases the dissociation cross section of these molecules also. Consequently, higher fluence increases the concentration of the unwanted isotopic species in the product and thus degrades the overall selectivity. A similar situation holds in the case of heavy elements.

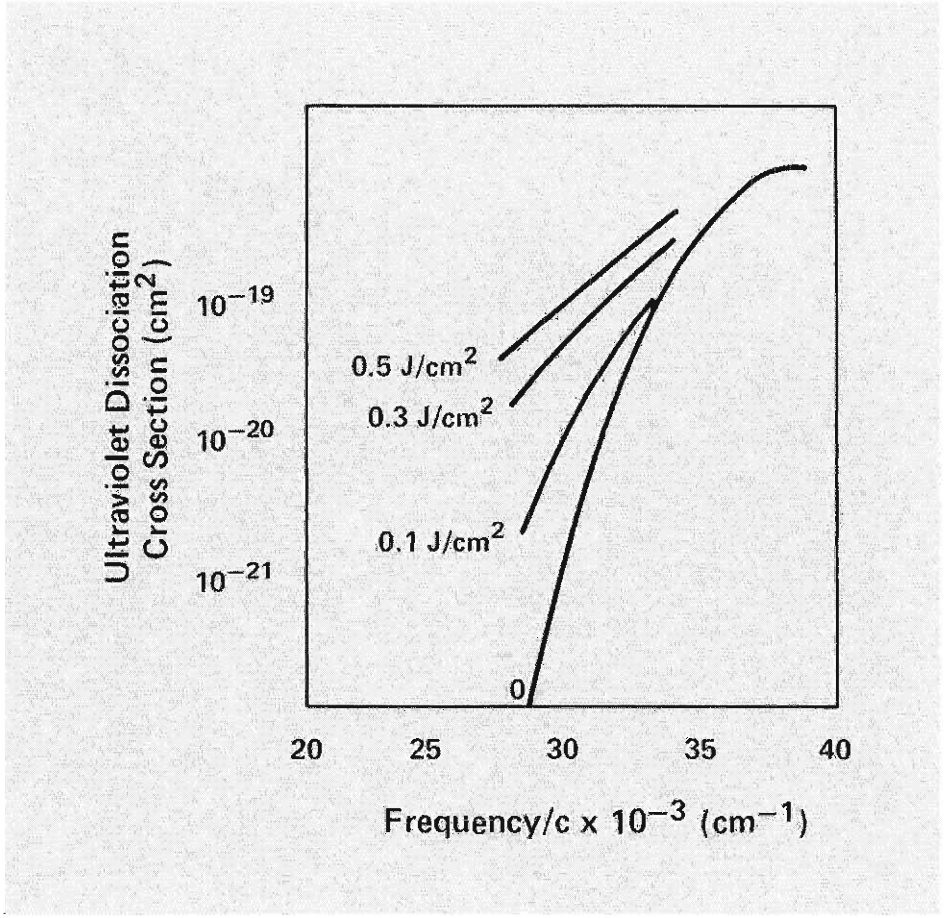

Fig. 6. The low-frequency edge of the ultraviolet dissociation cross section spectrum for CF_3I. Each curve is labeled by the fluence of the infrared laser pulses that provided vibrational excitation of the molecules. As the infrared fluence increases, the cross section at a particular ultraviolet frequency increases and the threshold frequency for dissociation shifts more and more to the red, that is, to lower frequencies. This red shift indicates that higher infrared fluences raise the molecules to higher vibrational states. Data from source cited in Fig. 5.

MULTIPLE-PHOTON DISSOCIATION. Figure 6 also shows that the threshold frequency for ultraviolet dissociation shifts more and more to the red as the infrared laser fluence increases. These relatively large shifts clearly indicate that the CO_2 laser is exciting the molecules to very high vibrational states. Thus, many photons of equal energy are being absorbed by a single molecule, a very surprising result! If molecular vibrations were governed by forces that increased linearly with displacement, as they are in a harmonic oscillator, the energy difference between vibrational states would be constant and photons with this constant energy could "resonantly" induce transitions to higher and higher vibrational states (Fig. 7a). But most molecular vibrations are anharmonic, that is, they involve nonlinear forces. The anharmonicity results in progressively smaller energy differences between vibrational states. Thus, as a molecule's vibrational energy increases, it should absorb infrared photons of lower energy and its interaction with constant-energy photons should quickly become nonresonant and ineffective.

The discussion above suggests that a molecule should absorb only one photon at the frequency corresponding to the energy of the transition from the ground state to the first vibrational state. In fact, this type of resonant absorption is observed in diatomic and many triatomic molecules. Experiments have shown, however, that polyatomic molecules can absorb many single-frequency infrared photons, and these photons can excite the molecule to high vibrational states and even to the dissociation limit (Fig. 7b). Even more intriguing is the fact that this multiple-photon process can be isotopically selective and can therefore be used for isotope separation.

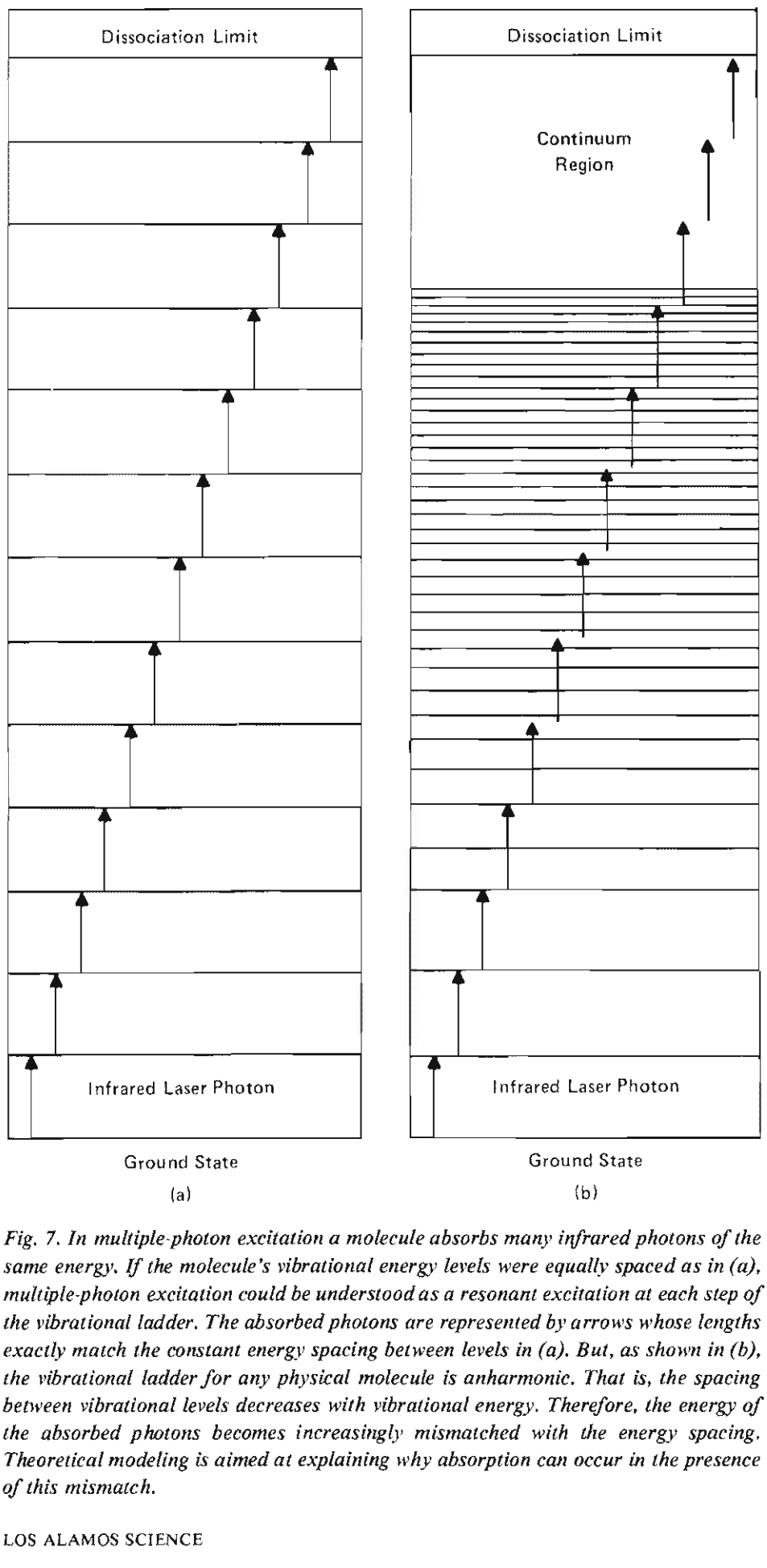

Fig. 7. In multiple-photon excitation a molecule absorbs many infrared photons of the same energy. If the molecule's vibrational energy levels were equally spaced as in (a), multiple-photon excitation could be understood as a resonant excitation at each step of the vibrational ladder. The absorbed photons are represented by arrows whose lengths exactly match the constant energy spacing between levels in (a). But, as shown in (b), the vibrational ladder for any physical molecule is anharmonic. That is, the spacing between vibrational levels decreases with vibrational energy. Therefore, the energy of the absorbed photons becomes increasingly mismatched with the energy spacing. Theoretical modeling is aimed at explaining why absorption can occur in the presence of this mismatch.

Between 1971 and 1973 a number of Los Alamos researchers, with the encouragement of Keith Boyer, pioneered experiments leading to the discovery of multiple-photon excitation phenomena. In the course of work with tetrafluorohydrazine (N_2F_4), John Lyman and Reed Jensen published experimental results showing that dissociation occurs in response to infrared-laser-induced vibrational excitation and that the distribution of vibrational energy in the molecules is far from thermal equilibrium. To our knowledge the first correct explanation of multiple-photon excitation and dissociation and the first suggestion of their application to isotope separation were summarized in a Laboratory memorandum by C. Paul Robinson in 1973. Then in 1975 experiments at the Institute of Spectroscopy in the Soviet Union and at Los Alamos were reported that demonstrated these amazing phenomena for sulfur hexafluoride (SF_6). The results were clear: under collisionless conditions, a polyatomic molecule could absorb 45 photons, a 0.1-electron volt photon source could break a 4-electron volt chemical bond, and multiple-photon dissociation could exhibit isotopic selectivity.

Since 1975 there has been an explosion of theoretical and experimental studies of this phenomenon throughout the scientific centers of the world. It now appears that multiple-photon excitation occurs in all polyatomic molecules. The process occurs most readily at high radiation intensities but is also clearly manifest at low intensities. Also, it occurs over a broad range of the frequencies within a given absorption feature of a molecule. Theory and experiment have provided a qualitative description of the excitation mechanism, which is primarily a multistep process rather than a multiphoton process involving virtual states. (The latter may, however, be important at some excitation frequencies.)

For some molecules the experimental results can be understood in terms of quantitative theoretical models. But these models

are not unique; conceptually different models can be made to fit the experimental data. Moreover, collisional effects have not been modeled nor is their inclusion straightforward. Additional work will be required to provide a satisfactory and detailed understanding of the complex interaction between the molecules and the radiation field (see "Multiple-Photon Excitation" in this issue). There still exist two basic questions. How is the absorbed energy distributed among the various vibrational modes of a molecule at different degrees of vibrational excitation? And how does absorption of one photon affect the absorption probability for the next?

Despite these uncertainties we know that multiple-photon excitation plays a key role in all molecular isotope separation processes that include vibrational excitation. And the process provides an efficient means of separating isotopes in medium-weight molecules using infrared lasers alone.

The three photodissociation techniques described above can be used to separate isotopes of most elements. Table I lists some of the elements whose isotopes have been separated at Los Alamos. This list could be extended substantially by including published results from other research institutions.

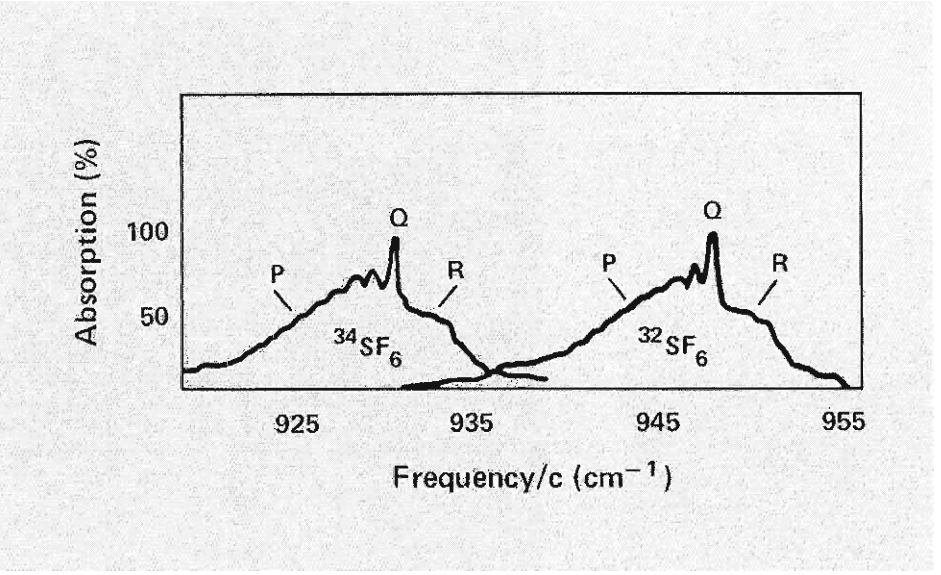

Fig. 8. The low-intensity ν_3 absorption bands of $^{34}SF_6$ and $^{32}SF_6$. The absorption band for the heavier isotopic species is shifted to the red by 17 cm^{-1}. The Q-branch peaks correspond to transitions in which J *does not change. The* P *and* R *branches correspond to transitions in which* $\Delta J = -1$ *and* $+1$*, respectively (see Fig. 1).*

Laser Isotope Separation in SF_6

A more detailed look at the work done on separating sulfur isotopes will illustrate specific features of selective multiple-photon excitation, as well as generic considerations involved in the development of a practical molecular isotope separation process.

The four naturally occurring isotopes of sulfur and their abundances are sulfur-32 (95.0 per cent), sulfur-33 (0.76 per cent), sulfur-34 (4.22 per cent), and sulfur-36 (0.02 per cent). The odd-nucleon isotope sulfur-33 is of value as a tracer because its presence can be detected by nuclear magnetic resonance techniques. Its applications include agricultural studies and structural studies of proteins.

The Los Alamos process for separating sulfur isotopes is based on SF_6, an octahedrally symmetric molecule like UF_6. Some researchers refer to SF_6 as the hydrogen atom of multiple-photon excitation because it is the molecule most studied in the attempts to understand the phenomenon. Here we will discuss only those results relevant to isotope separation.

Portions of the low-intensity infrared absorption spectra of $^{32}SF_6$ and $^{34}SF_6$ at room temperature are shown in Fig. 8. Absorption at these frequencies induces excitation of the ν_3 vibrational mode of the molecule's ground electronic state (see Fig. 2). There are many absorbing transitions corresponding to different initial and final rotational states of the ν_3 vibrational mode. The highest peak for each isotope, labeled *Q* in Fig. 8, results primarily from transitions in which *J*, the quantum number for the molecule's rotational angular momentum, does not change. The other portions of the ν_3 absorption band, called *P* and *R* branches, correspond to ν_3 transitions in which *J* decreases and increases, respectively, by unity. Note the 17-reciprocal centimeter (cm^{-1}) isotope shift of the *Q*-branch peak from 931 cm^{-1} for $^{34}SF_6$ to 948 cm^{-1} for $^{32}SF_6$.

In early investigations of SF_6, we could not even resolve the smaller peaks near the *Q*-branch peaks nor could we identify the specific transitions that give rise to the *Q*-branch peaks. Thanks to the revolution that has occurred over the past seven years in high-resolution molecular spectroscopy, we now know what transitions are being excited in the *Q* branch as well as the origin of the subsidiary peaks. Called hot bands, the subsidiary peaks are due to ν_3 vibrational transitions from low-energy vibrational states rather than the molecule's ground state (see "The Modern Revolution in In-

TABLE I
MOLECULAR LASER ISOTOPE SEPARATION SUCCESSES AT LOS ALAMOS

Molecule	Isotopes	Laser System	Dissociation Mechanism
H_2CO (in liquid Xe)	$^{1,2}H$	Frequency-doubled dye laser (319 nm) and HeCd laser (325 nm)	Predissociation
BCl_3	$^{10,11}B$	CO_2 laser (10 μm) plus ultraviolet flashlamp	Two-step photodissociation
BCl_3	$^{10,11}B$, $^{35,37}Cl$	CO_2 laser (10 μm)	Multiple-photon dissociation
CF_2Cl_2	$^{12,13}C$	CO_2 laser (10 nm)	Multiple-photon dissociation
CS_2	$^{12,13}C$, $^{32,34}S$	ArF laser (193 nm)	Predissociation
CS_2 (in liquid N_2, Ar, or Kr)	$^{12,13}C$	Iodine resonance lamp (206 nm)	Predissociation
O_2	$^{16,18}O$	ArF laser (193 nm)	Predissociation
UO_2F_2 (in liquid CH_3OH)	$^{16,18}O$	Dye laser (448 and 455 nm)	Predissociation
SiF_4	$^{28-30}Si$	CO_2 laser (9 μm)	Multiple-photon dissociation
SF_6, SF_5Cl, S_2F_{10}, SF_5NF_2	$^{32,34}S$	CO_2 laser (10 μm)	Multiple-photon dissociation
MoF_6	$^{92,94-98,100}Mo$	CO_2 laser (9 μm)	Multiple-photon dissociation
UF_6	$^{235,238}U$	Raman-shifted CO_2 laser (16 μm) plus ultraviolet laser	Two-step photodissociation

frared Spectroscopy" in this issue). This detailed spectroscopic data has provided the basis for quantitative theoretical models of the excitation process.

Pulses from a CO_2 laser tuned near either of the isotopically distinct Q-branch peaks of the ν_3 vibrational mode of SF_6 will selectively dissociate that isotopic species if the laser intensity is sufficiently great. The dissociated molecules, namely SF_5, then undergo further dissociation to SF_4, which is then converted to SOF_2 for separation from the other chemical species by fractional distillation.

The selectivity of this process depends on both the laser frequency and its fluence. Figure 9 shows the probability for dissociation of SF_6 as a function of laser fluence at a laser frequency of 944 cm^{-1}. We see that at low fluences only the $^{32}SF_6$ molecules are dissociated, but at higher fluences the other isotopic species may also dissociate. This decrease in selectivity is predominantly due to a broadening of the vibrational states' energy widths in the presence of intense radiation fields.

At high laser intensity we can achieve the best selectivity for $^{32}SF_6$ by tuning the laser to the red of its 948-cm^{-1} peak in the low-intensity spectrum, or closer to the excitation frequency of the unwanted isotopic species. We can see this quantitatively in Fig. 10, where the dissociation spectrum at high laser intensity is superimposed on the low-intensity absorption spectrum. Why this laser tuning is optimum for $^{32}SF_6$ seems puzzling until we realize that the laser is pumping molecules up the entire ladder of vibrational states, all the way to dissociation. Since the energy difference between vibrational states decreases as the molecules reach higher states, those molecules some distance up the ladder will more readily absorb radiation at frequencies lower than the frequency required to reach the first vibrational state. Thus, the frequency for selective vibrational excitation at high intensity is red-shifted from that at low intensity.

One measure of the efficiency of an

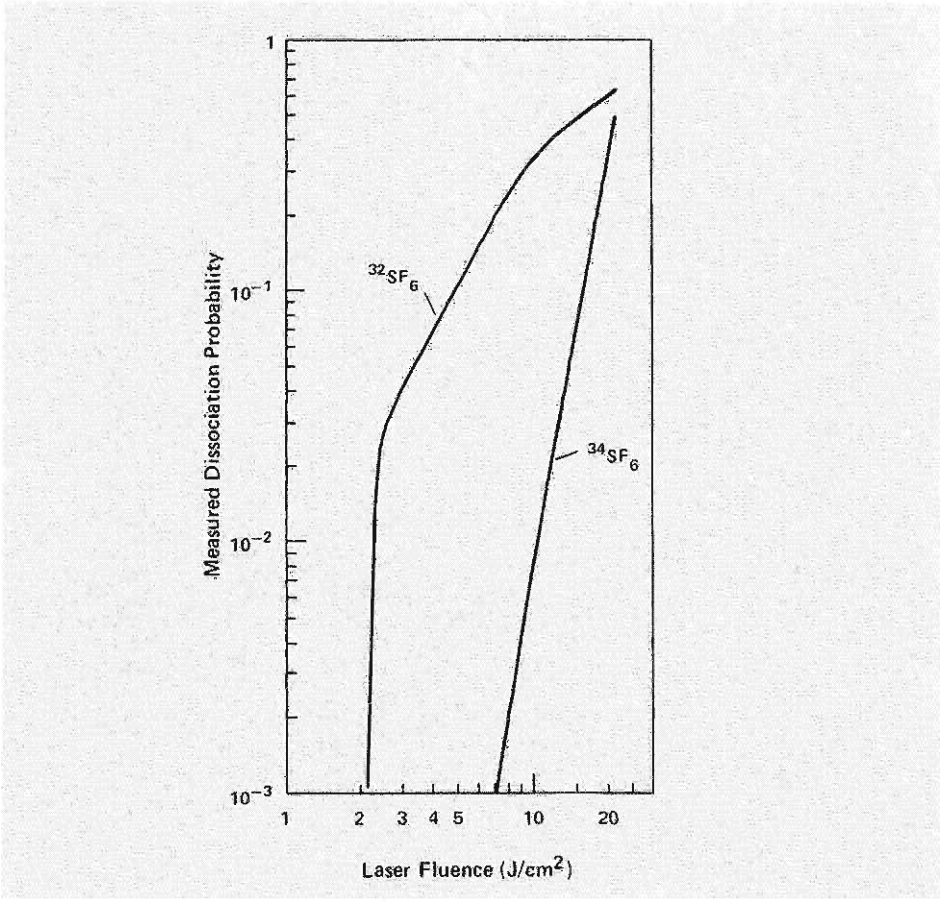

Fig. 9. Probability of dissociation for $^{32}SF_6$ and $^{34}SF_6$ as a function of CO_2 laser fluence. The laser is tuned to 944 cm^{-1}, slightly to the red of the Q-branch peak of $^{32}SF_6$ and far to the blue of the Q-branch peak of $^{34}SF_6$ (see Fig. 8). The dissociation probability increases sharply with laser fluence. At low fluences only $^{32}SF_6$ dissociates, but at high fluences $^{34}SF_6$ also dissociates. With the laser tuned to 944 cm^{-1}, the best compromise between selectivity and the amount of $^{32}SF_4$ produced is achieved with fluences in the range of 2 to 8 J/cm^2. Data from "Energy and Pressure Dependence of the CO_2 Laser Induced Dissociation of Sulfur Hexafluoride," W. Fuss and T. P. Cotter, Applied Physics 12, 265-276 (1977).

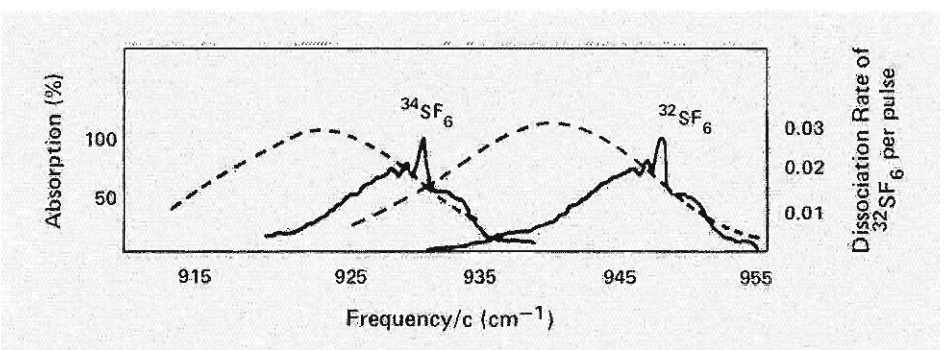

Fig. 10. Comparison of the high-intensity multiple-photon dissociation probability spectra (dashed) and the low-intensity absorption spectra for $^{34}SF_6$ and $^{32}SF_6$ shows that the best selectivity for multiple-photon dissociation of $^{32}SF_6$ occurs with the high-intensity laser tuned to the red of its low-intensity absorption peak. This red shift is caused by the anharmonicity of the molecule's vibrational energy ladder. Dissociation probability data from "Explanation of the selective dissociation of the SF_6 molecule in a strong IR laser field," R. V. Ambartsumyan, Yu. A. Gorokhov, V. S. Letokhov, G. N. Makarov, and A. A. Puretskii, JETP Letters 23, 22 (1976).

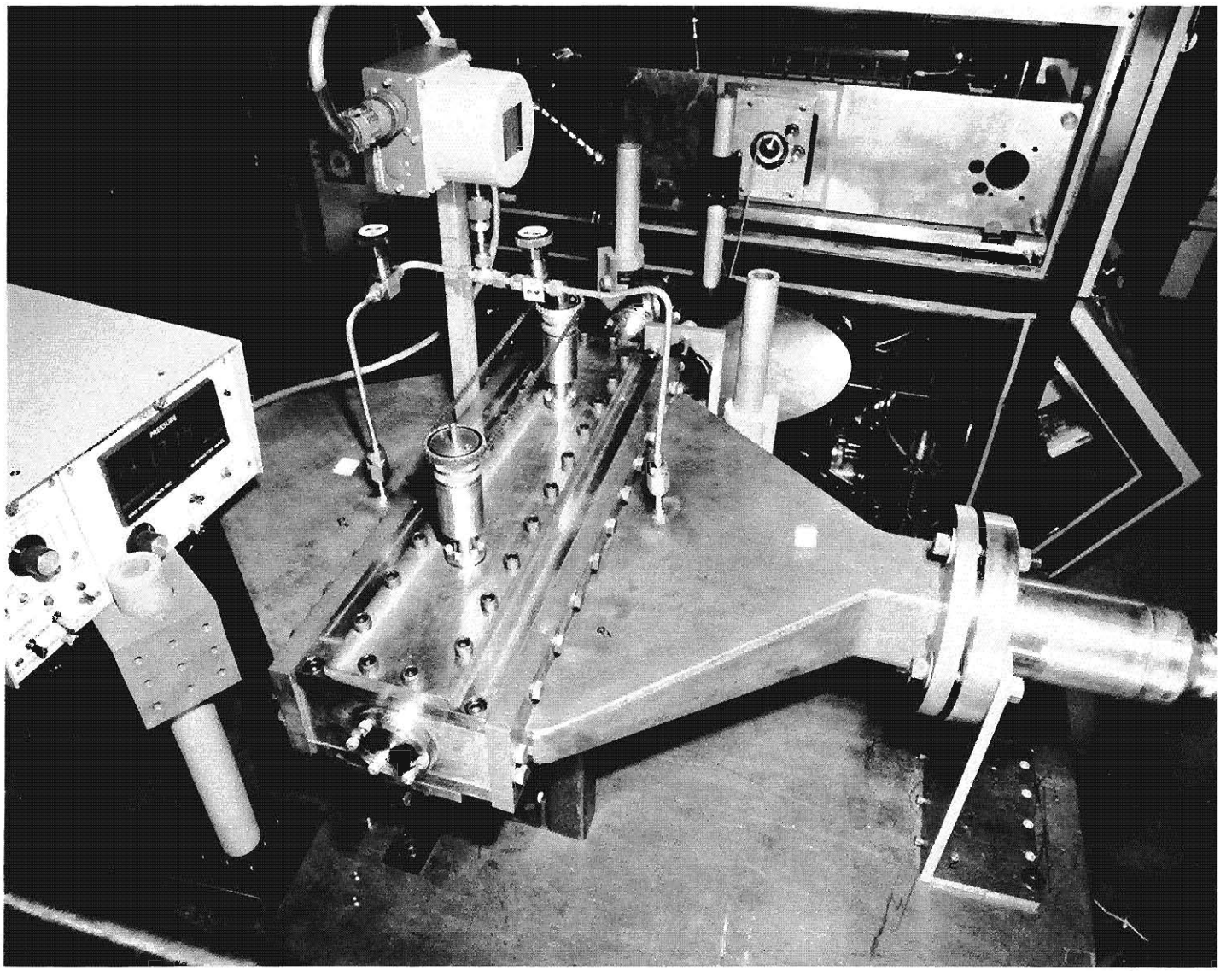

Fig. 11. Photograph of plant prototype constructed at Los Alamos for production of sulfur-33 and sulfur-34 by multiple-photon dissociation of SF_6. Shown are the gas expansion area leading into the photolysis chamber (center front) and the high-repetition-rate pulsed CO_2 laser (center rear).

isotope separation process is the enrichment parameter β. In the case of the sulfur isotopes, β for, say, sulfur-34 is defined as

$$\beta_{34} = \frac{(^{34}N/^{32}N)_{\text{product}}}{(^{34}N/^{32}N)_{\text{feed}}} ,$$

where ^{34}N and ^{32}N are the number densities of sulfur-34 and sulfur-32, respectively. The laboratory experiments based on multiple-photon dissociation of SF_6 with single-frequency infrared radiation have produced values of β_{34} as high as 1000.

To see how well the process would work on a larger scale, Los Alamos scientists have constructed and operated a small plant prototype for production of sulfur-33 and sulfur-34 by multiple-photon dissociation. The prototype (Fig. 11) consists of a gas recirculation system that provides a continuous flow of SF_6 gas through an irradiation zone and a CO_2 laser with an output energy of 0.5 joule per pulse that irradiates the gas at a repetition rate of 200 hertz. Dimensions of the irradiation zone in centimeters are 50 by 0.3 by 0.3. The laser, tuned to the $^{32}SF_6$ high-intensity absorption peak, selectively dissociates the molecules by multiple-photon excitation and produces $^{32}SF_4$ plus fluorine atoms. Back reaction of the fluorine atoms with $^{32}SF_4$ is prevented by adding hydrogen and a small amount of water vapor to the system. A fast chemical reaction occurs that converts SF_4 to SOF_2, which is chemically inert and can be separated from the other chemical species.

After a fixed period of operation, the gas is pumped from the system, and the various chemical species are separated in a distillation column. In 6 hours this system produces about 1 gram of SF_6 with a β_{34} of about 2.2

and a β_{33} of about 2.0. More than 99 per cent of the sulfur atoms in the SOF_2 distillate are the sulfur-32 species.

Multiple-Photon Excitation of Heavy Elements

In SF_6 multiple-photon dissociation was achieved by tuning high-intensity CO_2 lasers to the red of the absorption peak of the lighter isotopic species. Both the frequency shift and the high intensity were necessary for efficient dissociation of the lighter molecules. But these conditions can also compromise the selectivity. Since the laser is tuned closer to the unwanted isotopic species' absorption peak and since this absorption feature is broadened by the strong electromagnetic field, the probability of exciting and dissociating both isotopic species is increased and the selectivity is reduced.

For SF_6 the isotope shift is large enough that the red shift and the power broadening of the absorption peak at high intensities do not destroy the selectivity. But for heavy elements, whose isotope shifts may be smaller by a factor of 10 or more, these effects can reduce the selectivity drastically. In fact, the red shift in the absorption peak of the excited species can be much larger than the isotope shift between species.

These problems can be circumvented to a large degree by using two infrared lasers with different frequencies and intensities (Fig. 12). A low-intensity laser is tuned near the resonant frequency of the ground-to-first-vibrational-state transition of the lighter molecule. This laser selectively excites the lower vibrational states of the molecule. A second high-intensity laser is tuned to the red-shifted absorption peak of the excited molecules. This laser interacts predominantly with those molecules tagged by the first laser and excites them to higher vibrational states and, at sufficiently great intensities, to dissociation.

In principle, one could replace the second high-intensity laser with additional infrared lasers of lower intensity to provide a more nearly resonant excitation up the entire vibrational ladder to dissociation. Another alternative is to use two-frequency infrared excitation followed by dissociation with an ultraviolet laser. As discussed below, this latter scheme has been chosen for separation of uranium isotopes. Optimization of any laser isotope separation process with respect to the excitation method and the exact laser tunings depends on the individual molecule. In evaluating the tradeoffs, the economics of the process plays an important role.

The advantages of two-frequency infrared excitation for the heavier elements has been

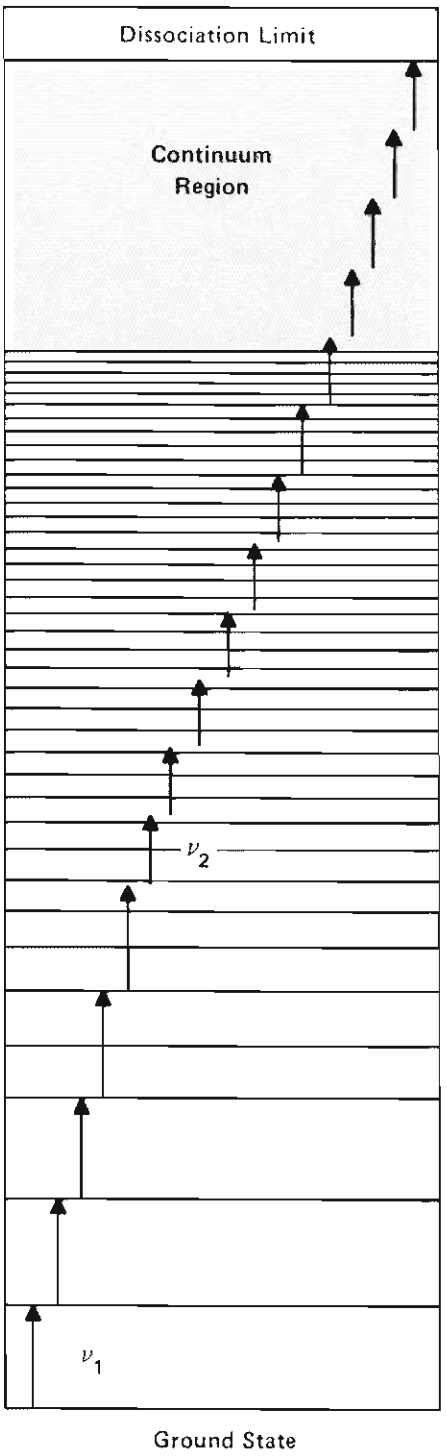

Fig. 12. Isotopic selectivity of multiple-photon excitation in heavy elements can be enhanced by using two infrared lasers. A first low-intensity infrared laser selectively excites molecules of one isotopic species to the first few low vibrational levels. A second infrared laser, lower in frquency and higher in intensity than the first, interacts predominantly with those molecules excited by the first laser and excites them to high vibrational levels. These molecules can then be dissociated with either an ultraviolet laser or with the second infrared laser at sufficient intensities. Note that the distribution of vibrational levels becomes a quasi-continuum at high energies. Rotational and Coriolis splitting of the high-energy levels makes the distribution even more continuous. The near continuum of levels leads to an almost resonant excitation by the second laser.

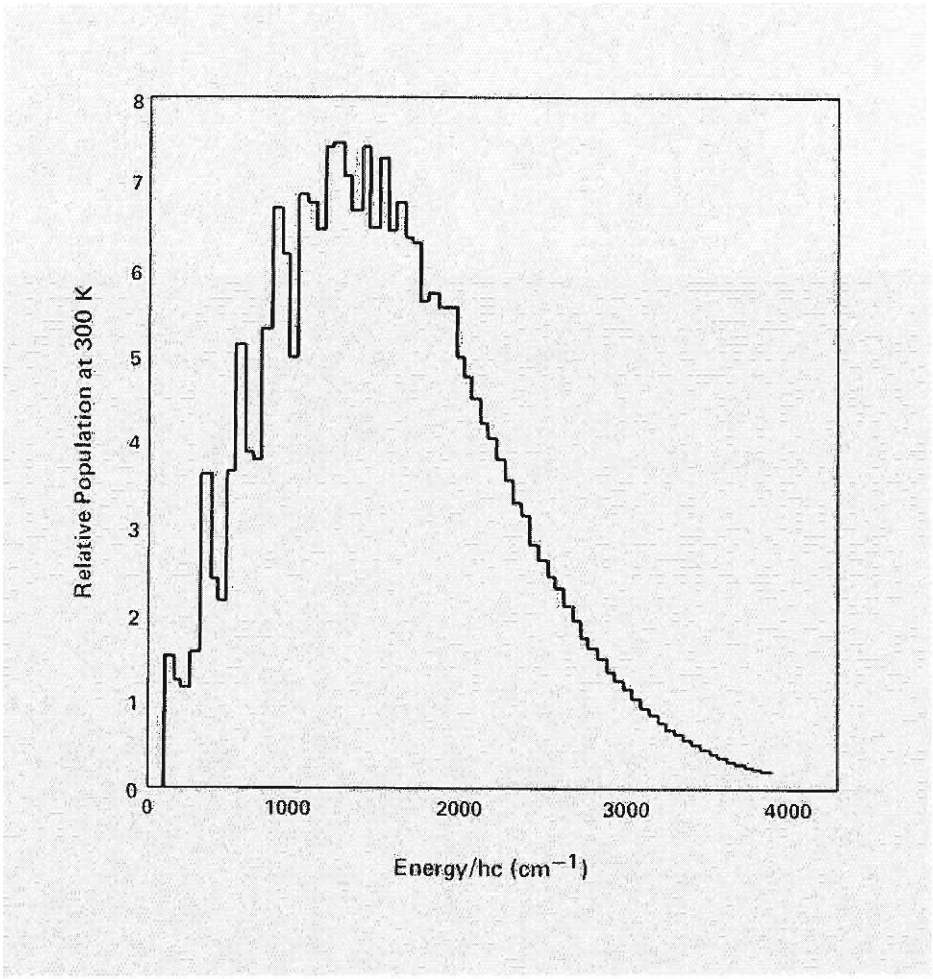

Fig. 13. At room temperature only a very small fraction (about four-thousandths) of the molecules in a sample of UF_6 at room temperature occupies the ground state. Most of the molecules are distributed as shown here among many vibrational states. (The lowest vibrational state is at 143 cm^{-1} and the lowest state of the ν_3 vibrational mode is at 628 cm^{-1}. At 300 kelvin the thermal energy is 210 cm^{-1}.) Therefore, at room temperature only a small fraction of the molecular population can be excited with a narrow bandwidth laser.

demonstrated for osmium by Soviet researchers. They separated osmium-187 (1.6 per cent) and osmium-192 (41 per cent) by selective dissociation of osmium tetroxide (OsO_4) with a pulsed CO_2 laser. The isotope shift in the absorption spectrum of this molecule is 1.3 cm^{-1}. Single-frequency excitation produced a β_{187} of only 1.15. With two-frequency excitation β_{187} was increased to 1.5. Since the fractional increase of the enriched product varies as $\beta - 1$, the two-frequency excitation increased this quantity by a factor of 3.

The Uranium Enrichment Process

The primary motivation behind laser isotope separation studies at Los Alamos has been the development of an efficient, economical process for enriching uranium. Our early decision to focus on a molecular rather than an atomic process was based in part on the fact that a molecular process offered more possibilities. For several reasons the molecule selected was UF_6. One reason was that the techniques for handling this gas were well known from its use in gaseous diffusion plants. We chose a two-step (infrared-plus-ultraviolet) photodissociation process, several years before the discovery of multiple-photon dissociation.

The idea was to selectively excite the ν_3 vibrational mode of $^{235}UF_6$ (analogous to the ν_3 mode of SF_6 shown in Fig. 2) and then dissociate the excited molecules with an ultraviolet laser into fluorine atoms and $^{235}UF_5$. The UF_5 molecules condense into particulates that are easily separated from the process material.

The first step in this process, selective excitation by infrared lasers, is the most critical and has been much more difficult to achieve in UF_6 than in SF_6. The reasons are twofold. First, although the CO_2 laser conveniently covered the 10-micrometer region corresponding to the frequencies of the SF_6 ν_3 vibrational mode, no lasers were available at the frequencies of the UF_6 vibrational transitions. The strongest absorption in UF_6 corresponds to ν_3 transitions around 16 micrometers; consequently, we had to design new high-intensity pulsed lasers at these frequencies. Our success represented a first—usually a laser is developed before its applications are known. However, development of the appropriate laser systems at the required frequency and intensity specifications took some time and was a pacing item during the early years of the program (see sidebar "Lasers for Uranium Enrichment").

The second set of problems arises from the fact that uranium is a heavy element, much heavier than sulfur. The isotope shift of the ν_3 vibrational mode of UF_6 is less than 1 cm^{-1} compared to 17 cm^{-1} for SF_6. The power broadening mentioned in the previous section therefore becomes much more serious. Moreover, because the fundamental vibration modes of UF_6 are much lower in energy than those of SF_6, at room temperature most of the UF_6 molecules are not in the ground vibrational state but are distributed among thousands of vibrational states (Fig. 13). Even high-energy vibrational states of UF_6 (those with energies much greater than thermal energy) are populated at room temperature because of their large degeneracies. Hence only a small fraction of the molecular population can be accessed with a narrow bandwidth laser. In addition, the ν_3 absorption band of UF_6 is significantly broadened and red-shifted at room temperature, and any spectral features with an isotope shift are obscured within the room-temperature bandwidth of about 30

continued on page 22

SIDEBAR 2:

Lasers for Uranium Enrichment

Like radar and sonar, the acronym laser (light amplification by stimulated emission of radiation) has achieved the status of a familiar word. But the principles upon which lasers operate may not be so familiar. Atoms or molecules can exist only in certain definite energy levels. In the presence of a photon with an energy equal to the difference between the energies of two such levels, atoms or molecules can undergo either of two processes, absorption or stimulated emission. In absorption, the more familiar process, an atom or molecule in the lower energy level absorbs the photon and makes a transition to the upper energy level. In stimulated emission an atom or molecule in the upper level makes a transition to the lower level and emits a photon. The emitted photon and the stimulating photon are spatially and temporally coherent (that is, they have the same phase and energy) and travel in the same direction. If the upper energy level has a greater population of atoms or molecules than the lower level (a condition known as population inversion), an intense field of coherent radiation can be produced as the emitted photon in turn stimulates another atom or molecule in the upper level to emit a photon, and so on. The atoms or molecules are then said to be lasing.

Developing a working laser is not as simple as explaining its operating principle. The first requirement is a collection of atoms or molecules among whose energy levels are suitable upper and lower levels between which lasing can occur. (Suitable here refers to the ease of producing and maintaining a population inversion. That is, the upper level must be easily populated, and the lower level, as it is populated by lasing, must be easily depopulated.) Then, this active medium must be "pumped" to achieve a population inversion. Electron bombardment or exposure to an intense light source are common methods of pumping. And usually the active medium must be contained within a suitable optical cavity, such as a pair of highly reflecting mirrors. The cavity provides the feedback for lasing. To extract energy from the cavity, one of the mirrors is partially transmitting. The output of the cavity is an intense, highly monochromatic beam of light.

Compared to light from other sources, laser light can be much more intense, monochromatic, and directional. Lasers producing such light with wavelengths ranging from the ultraviolet to the far infrared are now available. In fact, some lasers can be tuned to cover a wide range of wavelengths. The many applications of laser light take advantage of one or more of its unusual properties.

Normally, a laser is developed *before* its applications are conceived. But our program for enriching uranium presented the reverse situation—the application was at hand, but lasers with the required properties did not exist.

The properties demanded of an infrared laser for the first step in our enrichment scheme, selective vibrational excitation of $^{235}UF_6$ molecules, were a wavelength near 16 micrometers, narrow frequency bandwidth, high energy per pulse (greater than 0.1 joule), and short pulse length (on the order of 0.1 microsecond). Another highly desirable, if not mandatory, property was tunability, either continuous or in discrete steps. Our search for such a laser began about eight years ago with suggestions from

within and without the Laboratory. Among the suggestions were the following: a 16-micrometer CO_2 laser based on different vibrational levels of the molecule than is the 10.6-micrometer CO_2 laser; an optical parametric oscillator based on the nonlinear crystal cadmium selenide (CdSe); nonlinear frequency mixing of carbon monoxide (CO) and CO_2 lasers in the semiconductor cadmium germanium arsenide ($CdGeAs_2$), a material referred to at the time as unobtainium; optically pumped carbon tetrafluoride (CF_4) or ammonia (NH_3) lasers; and frequency shifting of the output of the 10.6-micrometer CO_2 laser by Raman scattering.

Because of early success with the optical parametric oscillator and the frequency-mixed CO-CO_2 laser, these two lasers were the main tools for our early experiments. Later, the optically pumped CF_4 and NH_3 lasers were demonstrated experimentally and were developed as high-energy lasers. These are still used in some of our experiments. The 16-micrometer CO_2 laser was successfully demonstrated but proved to have the wrong frequency for the process.

The most powerful laser system at 16 micrometers results from Raman scattering of the 10.6-micrometer CO_2 laser's output by the second rotational energy level in parahydrogen. (Raman scattering refers to an interaction of photons with a molecule in which the scattered photons undergo a frequency change determined by the molecule's rotational or vibrational energy levels.) Suggested early in the program, this concept is covered by a patent issued to its Los Alamos originators. We did not pursue its development until it was experimentally demonstrated about three years ago at Stanford University and at Exxon Nuclear Co., Inc. A system based on this concept is now the major 16-micrometer laser under development for the program. Its energy per pulse is greater than 1 joule, its pulse length is typically 50 nanoseconds, and its frequency is variable over a sufficient range. In addition, the system is efficient, converting as much as 40 per cent of the 10.6-micrometer input energy into 16-micrometer laser light.

The second step of our enrichment scheme, dissociation of the vibrationally excited $^{235}UF_6$ molecules into $^{235}UF_5$, required a laser with a wavelength in the ultraviolet and, like the infrared laser, with high energy per pulse, short pulse length, and tunability. The rare-gas halide lasers, which were developed in 1975, satisfied these requirements. The rare-gas halides belong to a class of diatomic molecules, referred to as excimers, that have a stable excited electronic state and an unstable ground state. This situation is ideal for a laser because a population inversion is easily produced and maintained.

The first rare-gas halide lasers yielded only millijoules of energy and were cumbersome to operate. The technology grew rapidly, however, and today these devices are relatively compact, easy to operate, and produce energies in excess of several joules at repetition rates of one to several hundred hertz.

The rare-gas halide lasers that we have used for isotope separation experiments (and their wavelengths in nanometers) are ArF (190), KrF (254), XeBr (282), XeCl (308), and XeF (354). The wavelengths of these lasers can be increased or decreased by Raman scattering involving vibrational levels of hydrogen, deuterium, or methane. These additional wavelengths provide the opportunity to study the enrichment process as a function of ultraviolet laser frequency over a very broad range.

Much of the technology of rare-gas halide lasers and their Raman shifting was pioneered at Los Alamos. In terms of intensities and repetition rates, the rare-gas halide lasers available today are suitable for use in a production plant prototype. The goals of current development include the increased reliability and longer operational life required for a full-scale plant. ■

continued from page 19

cm^{-1}. The only way to increase the ground-state population and narrow the absorption features is to cool the gas.

Figure 14 shows the collapse of the UF_6 population into the ground state and a few low-energy vibrational states as the temperature is decreased. This collapse simplifies the ν_3 absorption band, as shown in Fig. 15. At room temperature and relatively high density the band has very broad features that obscure the *Q*-branch peaks of both isotopes. But at low temperature a medium-resolution spectrum shows sharp, well-separated *Q*-branch peaks for the two isotopic species.

More detailed low-temperature spectra have been obtained by scanning across the ν_3 absorption band with a tunable semiconductor diode laser. A significant effort has gone into determining the exact value of the isotope shift and identifying the specific rotational-vibrational transitions that can be excited in this frequency interval. Figure 16 shows a high-resolution scan near the $^{235}UF_6$ *Q*-branch peak. In the Los Alamos uranium enrichment process the infrared laser is tuned to a frequency in this region. A spectrum at even higher resolution would show many additional rotational subcomponents within the structure of Fig. 16. As discussed in "The Modern Revolution in Infrared Spectroscopy," these subcomponents are due to Coriolis forces and octahedrally invariant tensor forces. The choice of a particular frequency for the selective infrared excitation is based on this detailed knowledge of the low-intensity absorption spectrum.

EXPANSION SUPERCOOLING OF UF_6. Knowing that any uranium enrichment process would require cooling the UF_6 gas to low temperature before infrared excitation, we sought an efficient and practical means of

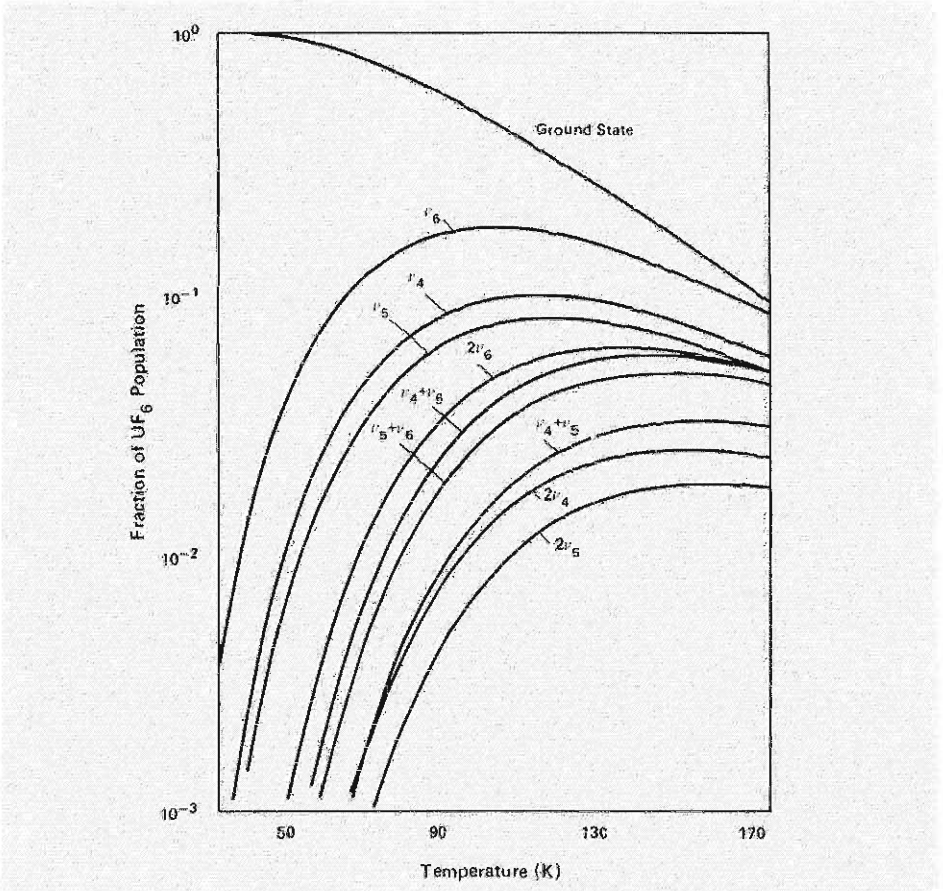

Fig. 14. Calculated thermal populations in the ten lowest vibrational levels of UF_6 as a function of temperature. As the temperature decreases, a greater fraction of the molecules occupies the ground state and the lower vibrational levels. This situation leads to greater selectivity of vibrational excitation and access to a larger UF_6 population.

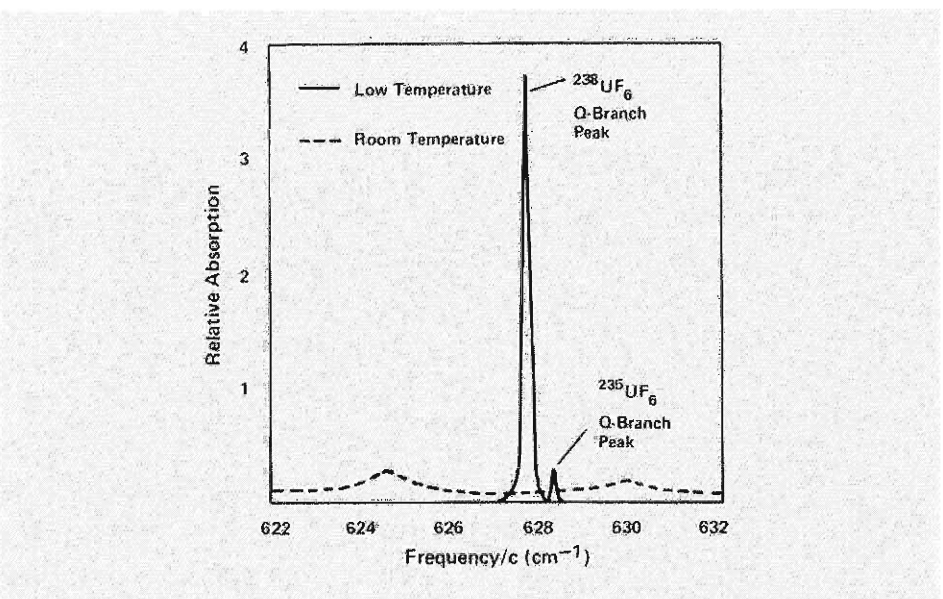

Fig. 15. The ν_3 absorption band of expansion-cooled natural-assay UF_6 exhibits narrow, distinct Q-branch peaks for $^{238}UF_6$ and $^{235}UF_6$. In contrast, the room-temperature band is broad and the isotopic features are merged. (For clarity the $^{235}UF_6$ peak is increased in height. The Q-branch peak heights for a sample containing the natural mixture of uranium isotopes are in the ratio of about 140 to 1.)

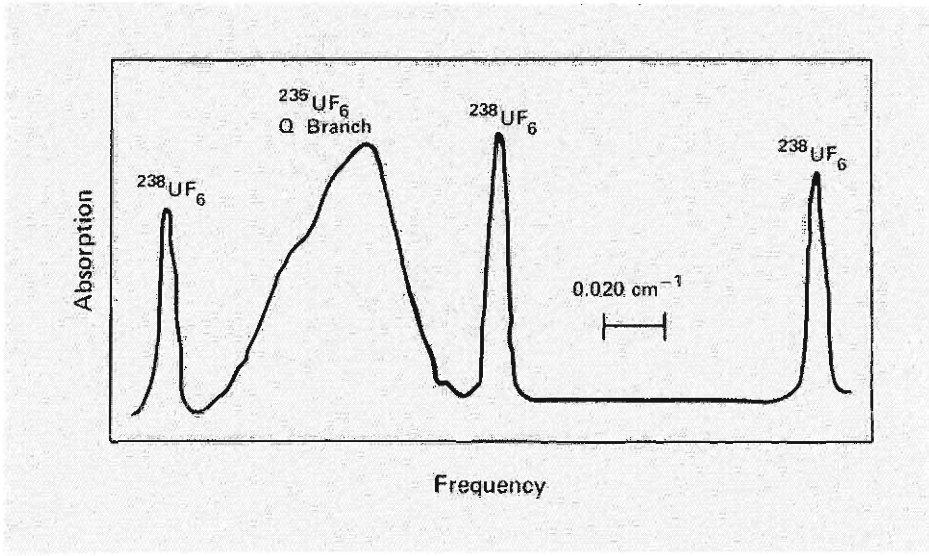

Fig. 16. A small portion of the ν_3 absorption band of UF_6 at high resolution. This scan of a sample enriched to 3 per cent in uranium-235 was obtained with a tunable semiconductor diode laser. The sharp peaks labeled $^{238}UF_6$ result from R*-branch transitions in $^{238}UF_6$.*

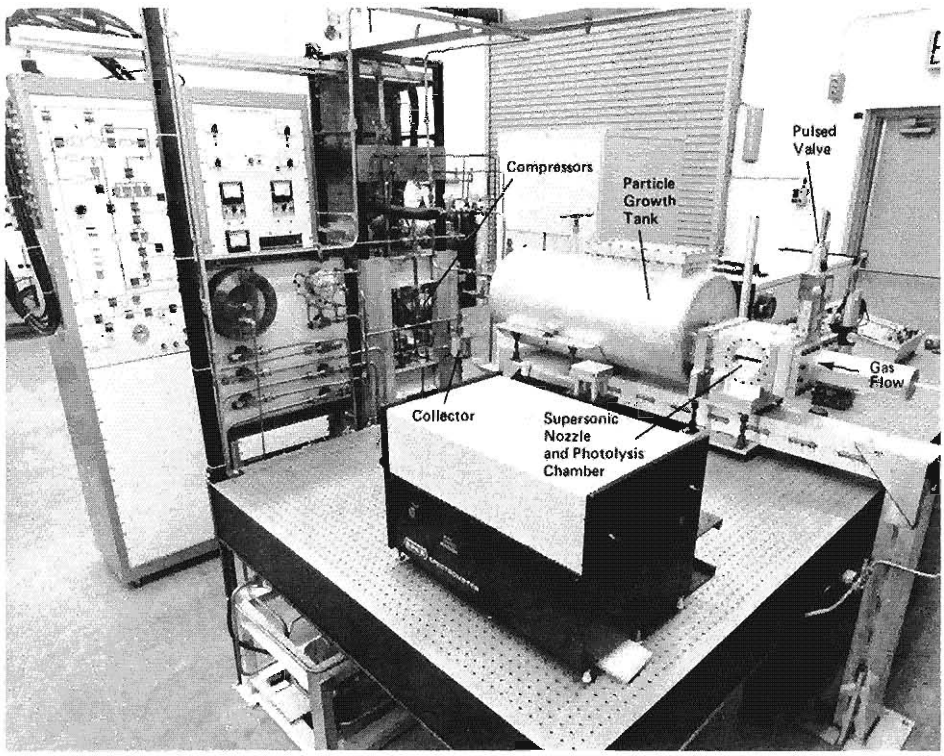

Fig. 17. Photograph of pulsed recirculating loop. This compact system provides a high density of supercooled UF_6 monomers for spectroscopic measurements and enrichments experiments. The system is simple and operates routinely for several hours.

cooling. Static cooling was impossible because the very low vapor pressure of solid UF_6 would provide too few molecules in the gas phase, and it is these molecules on which the laser process is designed to work. Early in the program Theodore Cotter suggested the use of a supersonic nozzle for expansion supercooling, a cooling method that was subsequently used not only in the isotope separation experiments but also in the high-resolution spectroscopy experiments. (Expansion supercooling has since become standard practice in high-resolution spectroscopy.)

The major question concerning this cooling method was whether the gas emerging from the nozzle would remain in the gas phase long enough for the lasers to act on single molecules. After expansion the gas is in a nonequilibrium state of supersaturation and has a strong tendency to condense within the flow. At a given temperature the major factor controlling condensation is the UF_6 number density in the flow-cooled region. The theory of homogeneous condensation was not well developed at the start of the project. We have since developed detailed theories and performed extensive experiments on condensation showing that expansion supercooling is a suitable technique. Measurements indicate that the nozzle produces uniform supersonic flow in the central core with only small turbulent-flow boundaries near each wall of the flow channel.

The ratio of final to initial temperature during supersonic expansion is equal to $(P/P_0)^{\gamma-1/\gamma}$, where P and P_0 are the final and initial pressures and γ is C_p/C_v, the ratio of specific heats at constant pressure and constant volume. When γ is very nearly unity, as it is for a gas of large polyatomic molecules such as UF_6, the initial pressure and/or the nozzle area expansion ratios must be very large to achieve substantial cooling. To circumvent this constraint, small amounts of UF_6 are mixed with a carrier gas consisting of atoms or small molecules (for example, argon or nitrogen) with a larger γ. Under these conditions substantial gas cooling can be achieved with only modest initial pressure and nozzle area expansion ratios. The carrier gas also provides a collisional environment that ensures continuum fluid flow and thermal equilibrium among the vibrational, rotational, and translational degrees of freedom of the UF_6 before irradiation.

The first infrared absorption measurements on UF_6 at low temperature were

accomplished in a blowdown mode in which the supersonic gas flow from the nozzle was dumped into a large (150 cubic meter) evacuated tank. The duration of continuous supersonic flow, which was set by the volume of the dump tank, was about 20 seconds. The time between runs was 2 hours. Despite the slow turnaround time, this setup provided many of the early data on shifts and simplifications in the UF_6 spectrum at low temperature.

Experiments are now done in a closed-cycle system known as a pulsed recirculating loop (Fig. 17). Since the lasers used in the experiments are pulsed at low repetition rates, a continuous gas flow and a large compressor train to move the gas through the system were unnecessary. To produce a pulsed gas flow coincident with the laser pulse, the recirculating loop includes a fast-acting hydraulic valve at the entrance to the nozzle. The valve is actuated at a typical rate of 1 hertz and provides a fully supersonic flow of cooled gas lasting about 2 milliseconds at the nozzle exit. With this system experiments can be performed at UF_6 densities and temperatures that are nearly the same as those for a full-scale plant. The only scaling required is increasing the area of the gas flow and the cross-sectional area of the irradiation zone.

SELECTIVE PHOTODISSOCIATION OF UF_6. After expansion through the nozzle, the cooled gas is irradiated by a sequence of infrared and ultraviolet laser pulses (Fig. 18). Either one or two infrared lasers tuned in the 16-micrometer range provide selective vibrational excitation of $^{235}UF_6$. The two-frequency infrared excitation described above provides higher selectivity than single-frequency excitation. The first

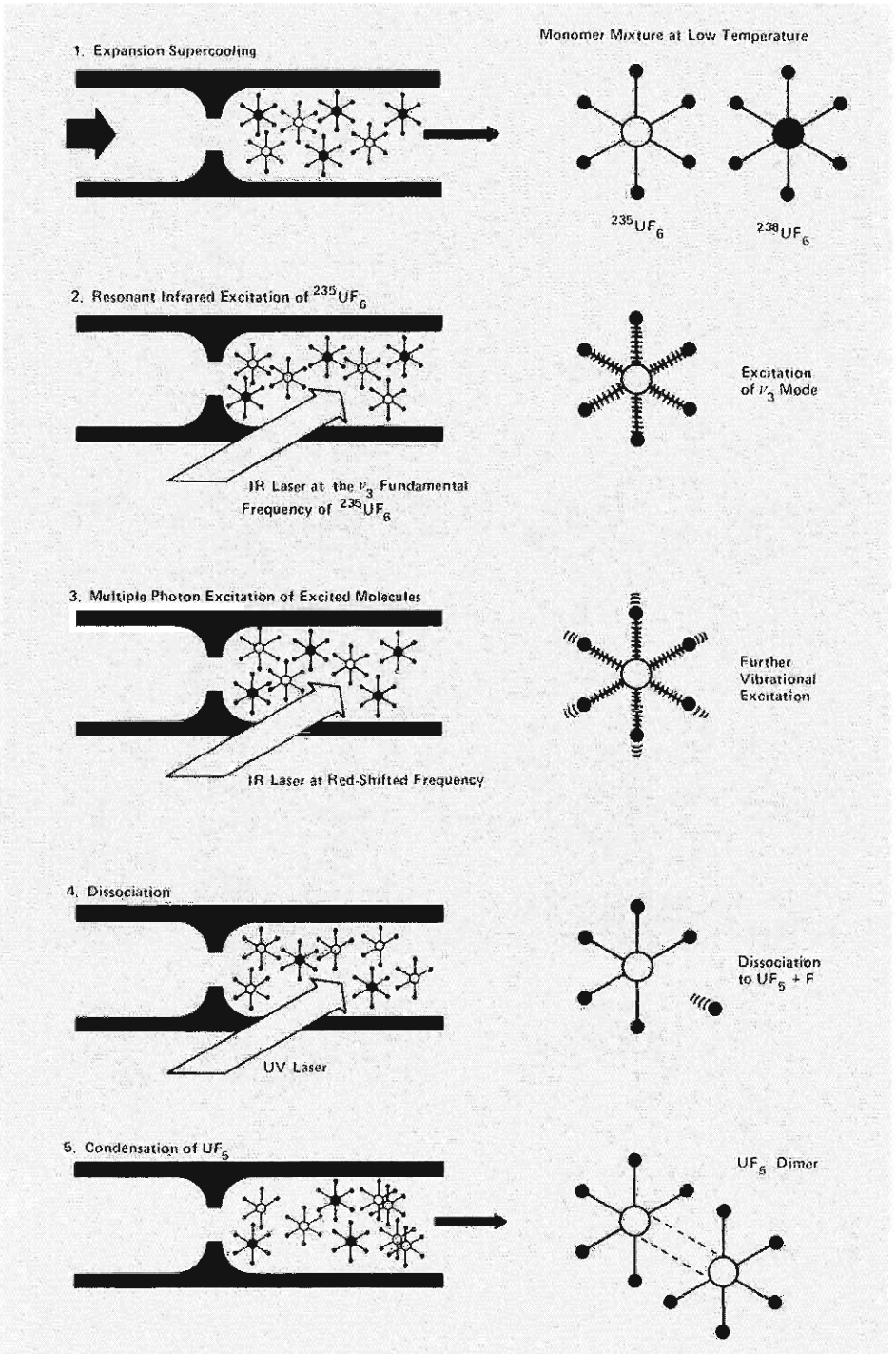

Fig. 18. The Los Alamos uranium enrichment scheme involves irradiating expansion-cooled UF_6 gas with infrared and ultraviolet lasers. The expansion supercooling produces a substantial density of UF_6 monomers at low temperature. Two infrared lasers selectively excite the ν_3 vibrational mode of $^{235}UF_6$ molecules, and the excited molecules are dissociated by an ultraviolet laser. The UF_5 product forms particulates that are easily separated from the gas flow.

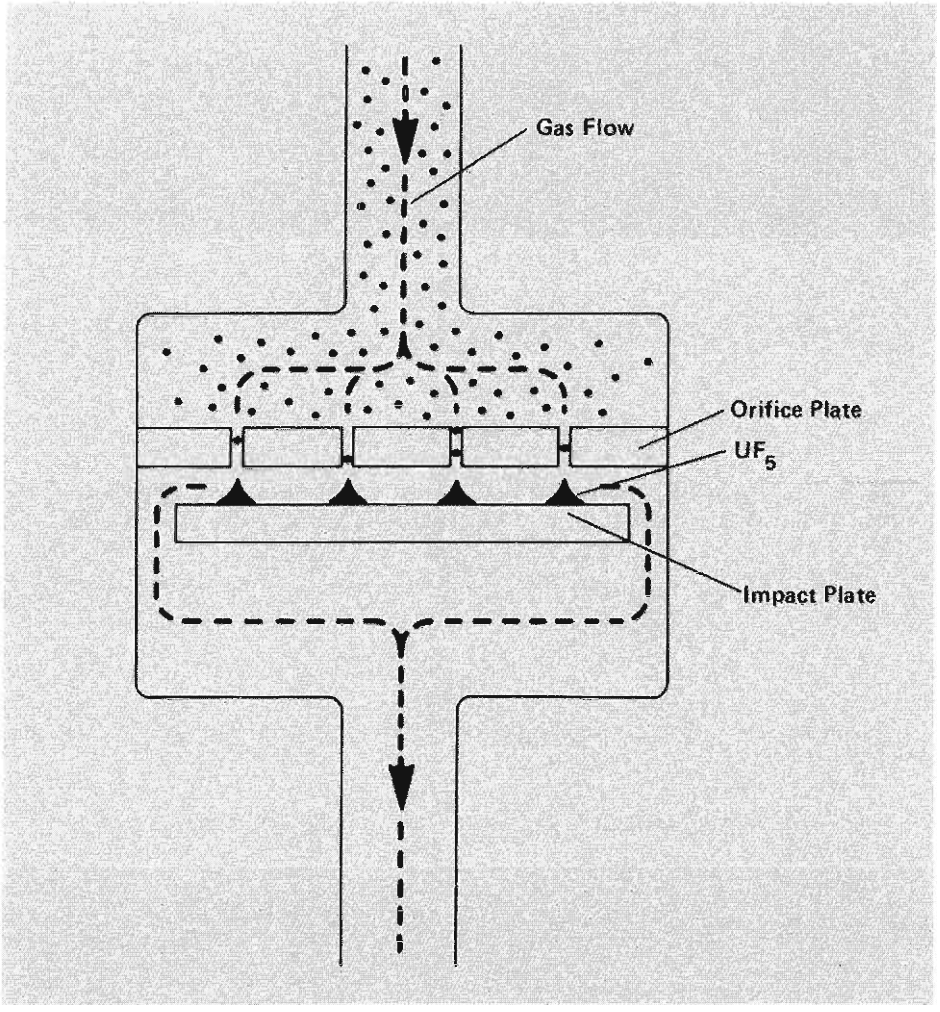

Fig. 19. Cross-sectional view of sonic impactor for collection of enriched product. The UF_5 molecules formed by dissociation of UF_6 aggregate to more massive particulates that are separated from the gas flow in the sonic impactor. The gas reaches sonic velocities as it passes through small holes in the orifice plate and then bends around to the exit port. The massive UF_5 particulates cannot negotiate the bend and instead collect on the impact plate.

low-intensity laser is tuned near the resonant frequency of the $^{235}UF_6$ Q branch, and the second high-intensity laser is tuned far to the red of this peak to achieve maximum excitation of the $^{235}UF_6$ molecules. Since multiple-photon excitation can occur over a fairly wide range of frequencies, especially at high intensity, the second laser will also excite some $^{238}UF_6$ molecules. But the probability for ultraviolet dissociation is substantially higher for the highly infrared-excited $^{235}UF_6$ molecules than for the $^{238}UF_6$ molecules. The physics of the infrared excitation is complex and depends on a number of parameters. These parameters are now being systematically varied to minimize excitation of $^{238}UF_6$ and thereby increase the infrared selectivity even further.

The infrared excitation produces a change in the ultraviolet dissociation spectrum similar to that shown previously for CF_3I. Thus, an ultraviolet laser tuned near the low-frequency edge of the dissociation spectrum of unexcited molecules will provide large dissociation yields for $^{235}UF_6$ and small dissociation yields for $^{238}UF_6$. In addition, ultraviolet dissociation of UF_6 to UF_5 is very efficient, occurring with a near unity quantum yield in the 200- to 300-nanometer wavelength region.

Although ultraviolet dissociation has been chosen for the Los Alamos uranium enrichment process, the intensity of the second infrared laser can be increased to provide dissociation without an ultraviolet laser. At present both methods are being considered.

POSTPHOTOLYSIS CHEMISTRY AND COLLECTION OF ENRICHED PRODUCT. A primary concern regarding this stage of the process was whether the UF_5 and UF_6 molecules might exchange fluorine atoms before being separated. But the UF_5 molecules rapidly form dimers in the supersonic flow; these dimers are relatively immune to exchange of fluorine with UF_6.

After being irradiated, the process gas containing the enriched UF_5 first passes through a supersonic diffuser, which returns the gas to higher pressure and room temperature. The enriched material in the form of particulates is then separated from the gas stream and collected on a simple sonic impactor (Fig. 19). The gas reaches sonic velocities as it passes through a series of small orifices in a flat plate. At the exit of the orifice plate the gas flow bends around to an exit port. The massive particulates traveling

at sonic velocities cannot negotiate the turn and impact on a backing plate. A typical run time for a collection experiment is 1 to 2 hours. Figure 20 shows a sample of enriched material collected on the impact plate.

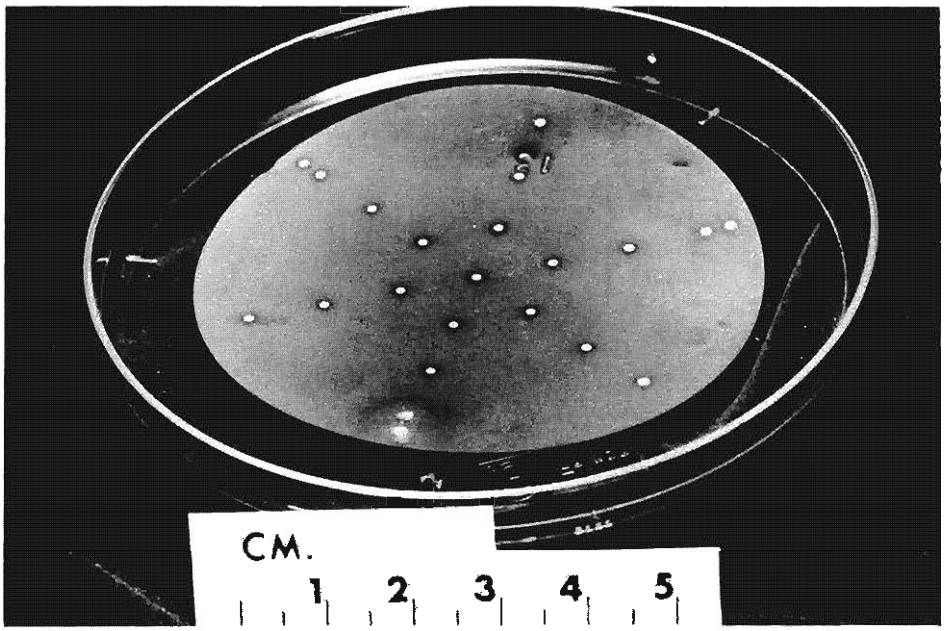

Fig. 20. Sample of enriched material produced by laser irradiation of UF_6 gas and collected in a sonic impactor.

DIAGNOSTICS. The samples collected from this system constitute the major source of data and confidence for projected performance of a full-scale plant. Each collection experiment yields an enrichment parameter for one set of operating conditions, but such experiments give little information about the intermediate steps of infrared excitation, ultraviolet dissociation, and postphotolysis chemistry. Morever, collection experiments are time-consuming and expensive. We have therefore developed a real-time diagnostic technique that does not involve an assay of the solid material.

Based on detection of the fluorescence induced in UF_6 by a low-intensity ultraviolet laser, the technique (Fig. 21) directly measures the number density of UF_6 before and after photolysis and thus the number density of UF_5 produced during photolysis. Experiments are performed separately on each isotopic species as a function of the intensities and frequencies of the infrared and ultraviolet lasers and other important parameters. With this technique we have obtained many of the fundamental data about vibrationally enhanced photodissociation of UF_6. From the ratio of the enhanced dissociation for the two isotopes we can also project the intrinsic enrichment attainable for uranium with the molecular laser isotope separation process.

RESULTS OF THE URANIUM ENRICHMENT EXPERIMENTS. The collection and laser-induced fluorescence experiments clearly show that vibrational excitation of UF_6 produces enhanced ultraviolet photodissociation of the molecule, that uranium can be enriched with this technique, that high values of β can be achieved, and that the enriched materical can be collected with little or no degradation by postphotolysis processes.

But the process must not only work—it must work efficiently and economically. The two parameters used most often to characterize the figure of merit for an isotope separation process are θ, the cut, and α, another measure of enrichment. The cut is the fraction of UF_6 dissociated at each stage of enrichment. Obviously the larger the cut and enrichment, the fewer the number of stages needed in a full-scale plant. The enrichment parameter α, unlike β, depends on the cut. For enrichment in uranium-235 it is defined by

$$\alpha = \frac{(^{235}N/^{238}N)_{\text{product}}}{(^{235}N/^{238}N)_{\text{tails}}} = \frac{\beta(1-\theta)}{1-\beta\theta} .$$

The economics of the process improves as α and θ increase.

In 1976 milligram amounts of slightly enriched uranium were produced at Los Alamos by the molecular laser isotope separation process. Since then the major experimental efforts have focused on increasing α and θ for this process. But these two parameters are not independent. For example one can increase θ by increasing the intensity of either the infrared or the ultraviolet laser, but this increased intensity will saturate and broaden the absorption features and thereby reduce the selectivity and decrease α.

The process parameters that determine α and θ include the frequencies and intensities of the lasers and the temperature of the UF_6 gas. Currently, enrichment experiments are aimed at determining a set of parameters that optimize α and θ. Values for α and θ achieved in the experiments to date show that the molecular laser isotope separation process is economically competitive with other separation methods. But since the entire parameter space has not been studied

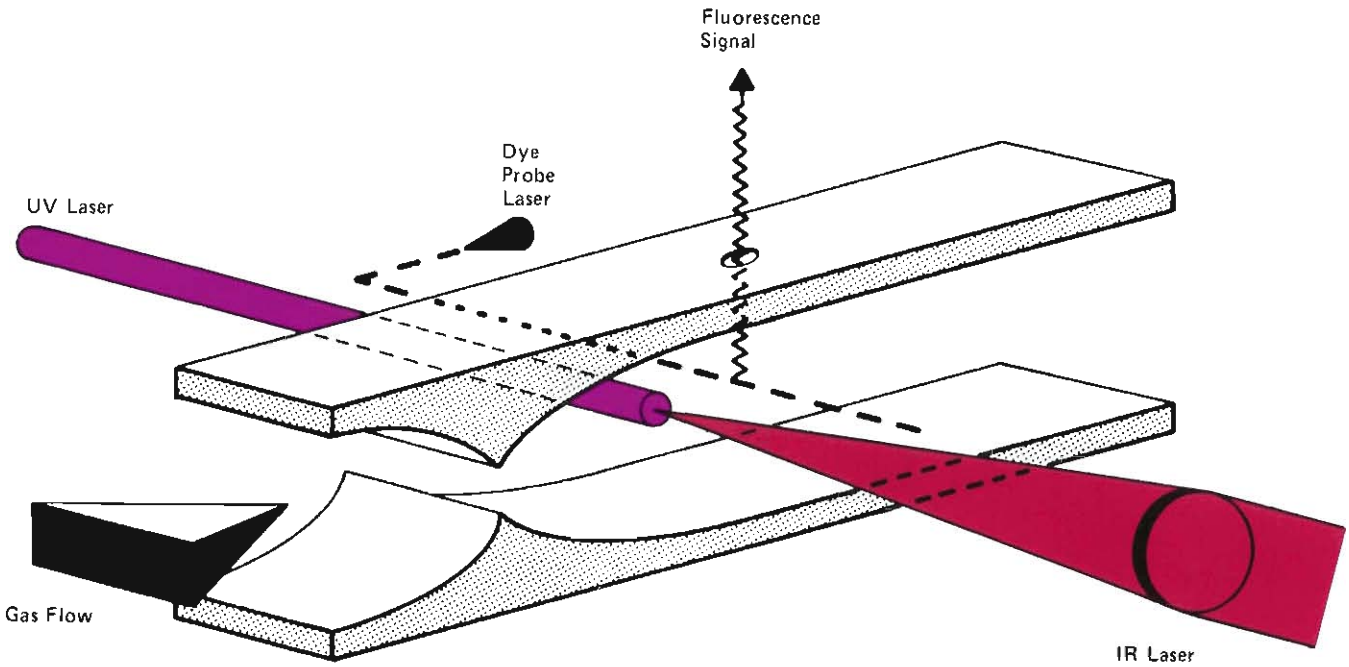

Fig. 21. Real-time diagnostic technique for determining the number density of UF_5 produced during photolysis. A low-intensity dye laser induces fluorescence in the UF_6 molecules within a small volume about 1 centimeter downstream of the photolysis zone. The fluorescence is detected by a high-gain photomultiplier before and after the volume has been irradiated by the infrared and ultraviolet laser pulses. The difference is a direct measure of the UF_5 produced during photolysis. In experiments using this diagnostic technique, the infrared laser beam can be focused to provide high fluences.

(in particular, the selectivity of the multiple-photon process as a function of laser frequency and intensity and UF_6 temperature is uncertain), additional work will be required before we know with certainty that we have achieved the optimal set of operating parameters.

Engineering Considerations

Concurrent with the experimental research efforts to optimize α and θ, we have undertaken the engineering design studies needed to convert a small-scale laboratory experiment into a full-scale production plant. In these studies we have specified the production plant in as much detail as possible, identified the scaling required, and designed two intermediate-scale facilities in which plant equipment can be developed and the process can be evaluated. One of these facilities, the preprototype, is now assembled; the other, the demonstration module, is still in the design stage. We will first discuss some aspects of the scaling involved in our concept of a production plant and then briefly describe the intermediate-scale facilities.

SCALING UP. The performance goals for a production plant include the following.

- Product assay: $\geq 3.2\%$
- Tails assay: $\leq 0.1\%$
- Capacity: 8.75 MSWU/year
- Availability: $\geq 90\%$
- Product cost: $\leq \$40$/SWU

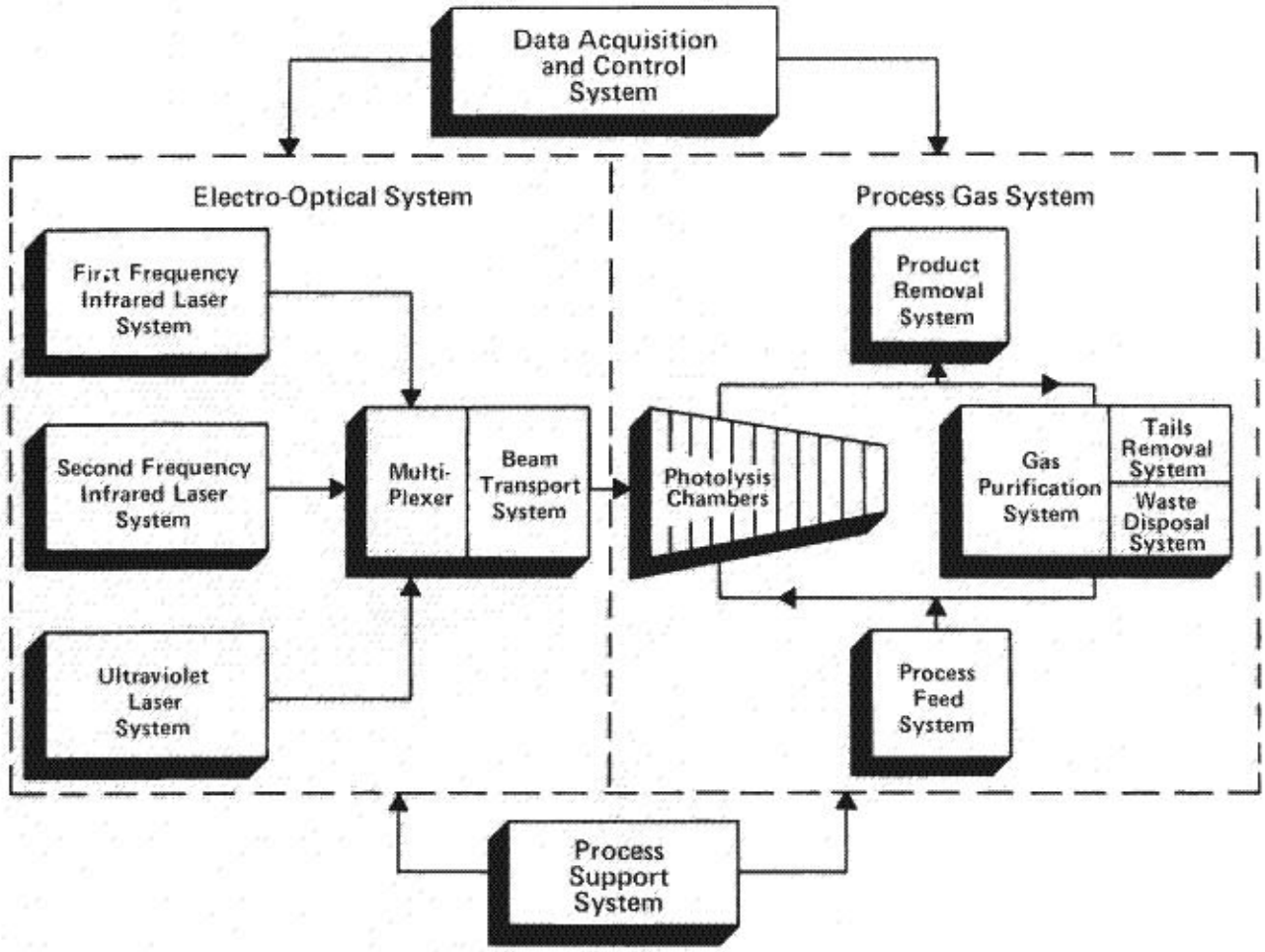

Fig. 22. Four major systems compose a production plant for uranium enrichment by laser irradiation of UF_6 gas. Shown here schematically is the organization of the more important equipment items and subsystems.

In more concrete terms a plant must produce an annual throughput of 1,500,000 kilograms of reactor-grade uranium, with tails depleted to 0.1 per cent, at a cost of about $600 per kilogram. Obviously, developing reliable plant equipment to meet these goals is not a trivial task.

The equipment for a production plant can be grouped into four major systems: the process gas system, which includes the photolysis chambers and the components providing the flow of process gas; the electro-optical system, which includes the lasers and the beam-transport optics; the data acquisition and control system; and the process support system. Figure 22 shows these systems schematically.

The design of a production plant begins with the choice, guided by the product cost goal, of an α and θ combination. To arrive at a product cost less than $40/SWU, current calculations show that α must be greater than 3 and θ must be between 0.05 and 0.30, depending on α. The choice of α and θ strongly influences the design of the photolysis chamber, as does the need to minimize diffraction and other optical losses. Other parameters influencing its design are the UF_6 number density and the temperature and pressure of the process gas.

For the values of α and θ believed to be attainable, a plant must have not one but several photolysis chambers to achieve the desired product assay. The chambers are arranged in what is commonly referred to as an enrichment cascade (Fig. 23); the term

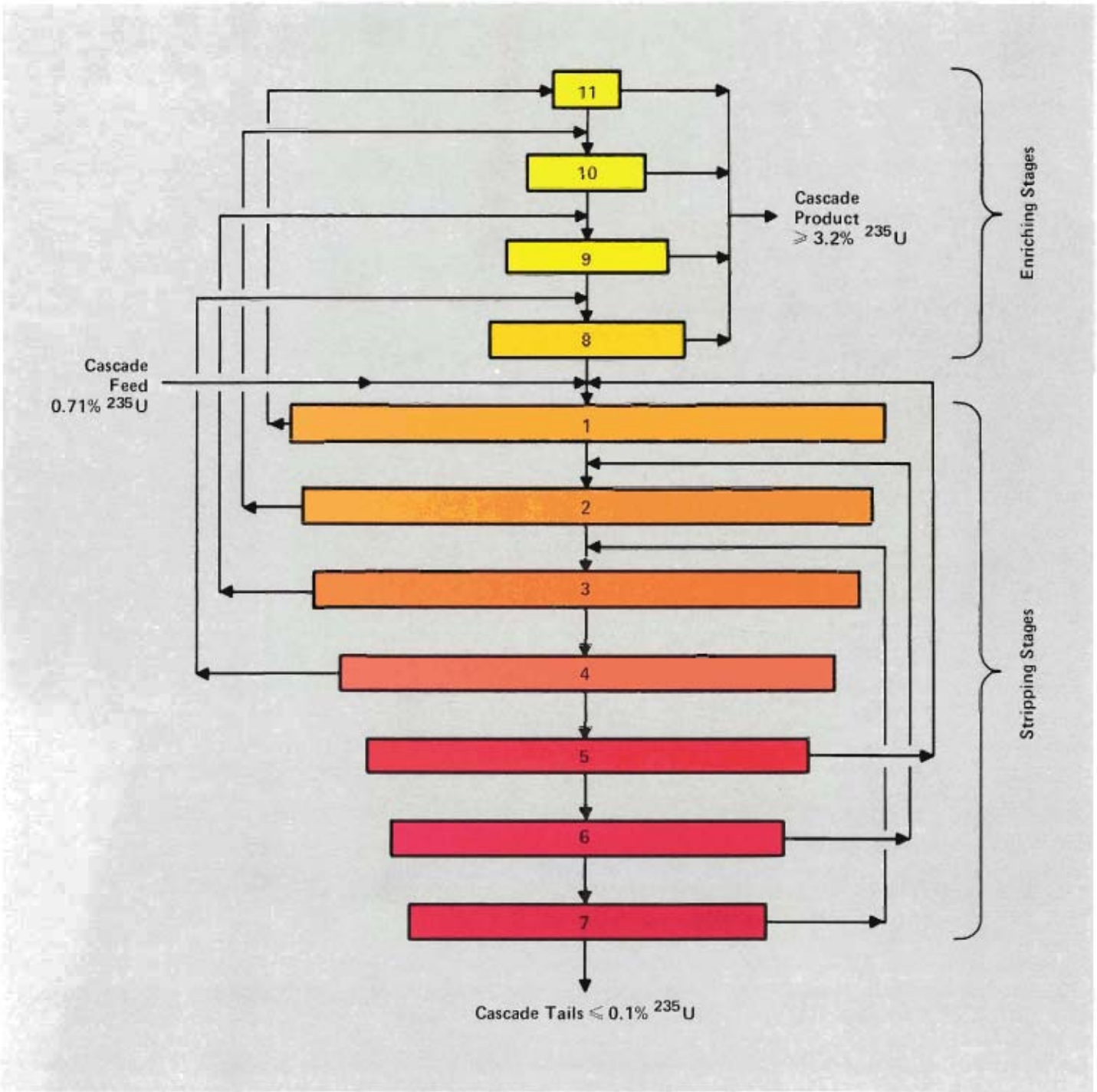

Fig. 23. Schematic gas flow pattern in an 11-stage cascade for uranium enrichment by laser irradiation of UF_6 gas. Each stage consists of a photolysis chamber and associated equipment. The relative volumetric flow through a stage is indicated by the area of the rectangle representing the stage. The incrementally enriched stream from each stage (shown here exiting to the right or left) flows to another stage for further enrichment, and the incrementally depleted stream from each stage flows to another stage for further depletion. This recirculating flow pattern avoids losses of separative work that would occur if streams of unlike assay were mixed.

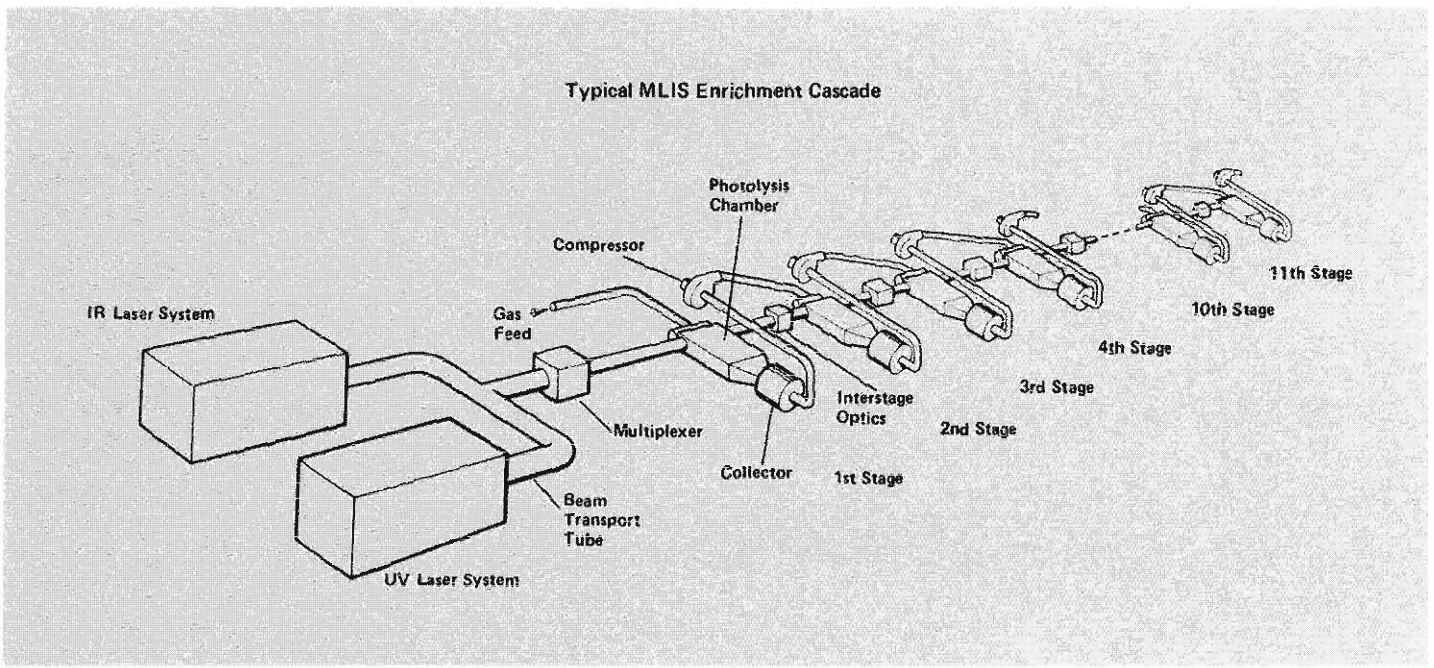

Fig. 24. Possible arrangement for integrating the laser systems and the cascade stages in a production plant for uranium enrichment by laser irradiation of UF_6 gas. Single banks of infrared and ultraviolet lasers service the entire cascade. Interstage optics adjust the fluences of the beams at each stage of the cascade.

stage refers to a single chamber and its associated equipment. The number of stages in an enrichment cascade depends directly on the α and θ combination chosen. In general, low α and θ values lead to a large number of stages, which in turn leads to increased complexity, large size, high energy consumption, and high capital costs for the plant.

Each photolysis chamber in the cascade includes a nozzle that might be as much as 8 meters wide, in contrast to the single 20-centimeter nozzle used in the laboratory experiments. Further, the gas flow though the chambers must be continuous rather than pulsed. Each stage must include a compressor system for moving the gas and equipment for collecting the enriched UF_5, converting it back to UF_6, and returning it either to the cascade or to the final product stream. A feed system, a gas purification system, a tails removal system, and a waste disposal system service the entire cascade.

All of the equipment necessary for the process gas system is within the current state of the art. In particular, the flow equipment developed for gaseous diffusion plants can be translated in a relatively straightforward manner to a molecular laser isotope separation plant.

The electro-optical system for a production plant must be capable of uniformly irradiating the gas flow through each photolysis chamber with the required infrared and ultraviolet laser fluences. The laboratory experiments were performed with a small beam size and a low repetition rate (about 1 hertz). Both these parameters must be increased considerably in a production plant.

The required increase in beam area implies a similar increase in beam energy to maintain the same fluence. The CO_2 and XeCl lasers used in the experiments can be scaled to higher energies by ganging several laser heads together in what is termed a master oscillator power amplifier chain. Several chains are necessary for each laser type. Individual high-energy beams must then be combined spatially to achieve the required beam area. To irradiate all of the gas flowing through a plant-scale nozzle, the repetition rate of the laser pulses must be about 10,000 hertz. Direct extrapolation of current technology to achieve such high rates from a single laser is not likely. However, the required rate can be achieved by temporally combining reliable, long-lived lasers with repetition rates of about 1250 hertz. A system known as a multiplexer combines the laser beams temporally and a reflective mirror arrangement called a dihedral combiner performs the spatial combination.

The electro-optical system must also compensate for the reduction in beam fluence that occurs as the beam progresses through

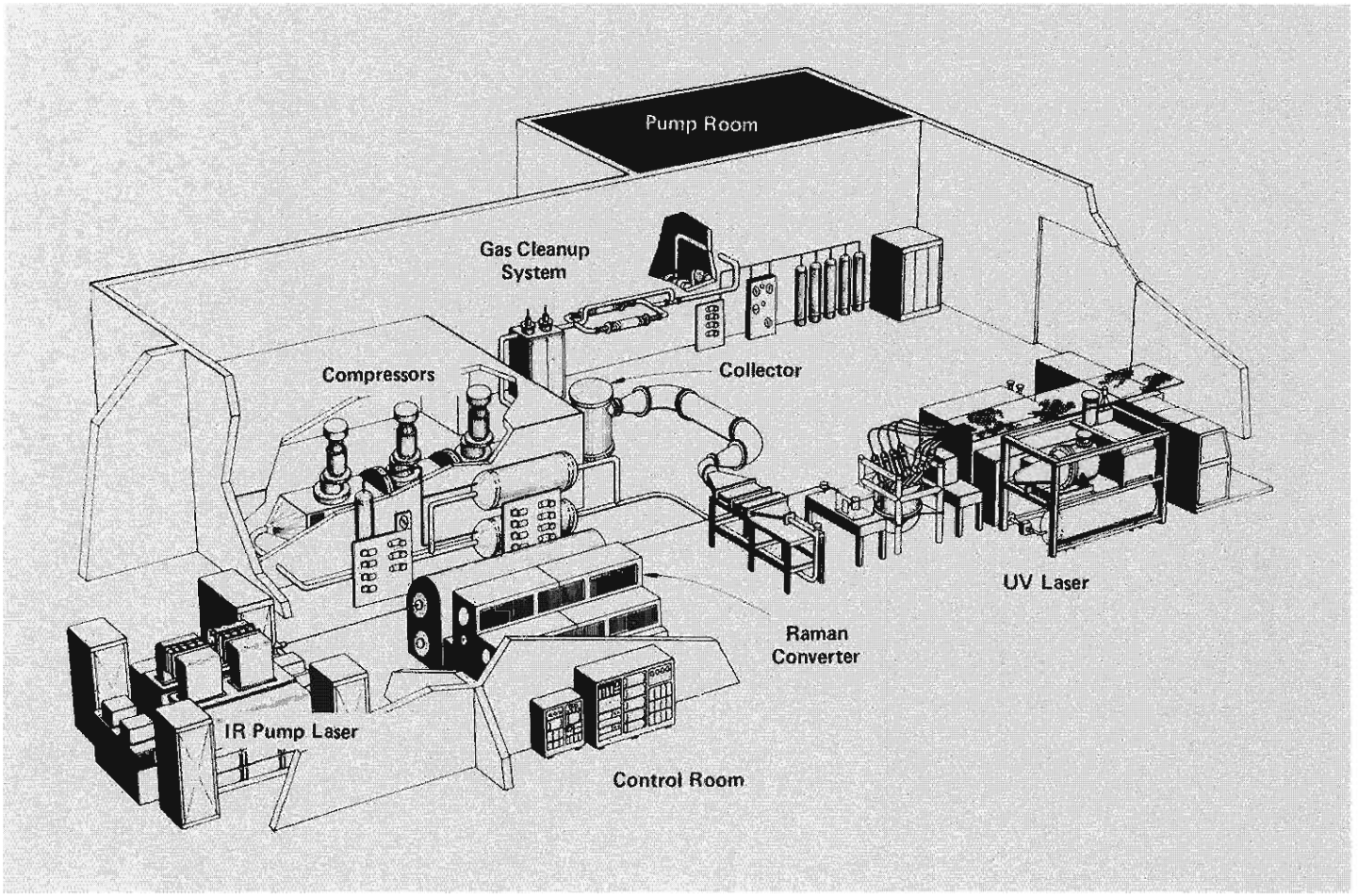

Fig. 25. The Laboratory's preprototype for testing the molecular laser isotope separation process at a scale intermediate between that of the laboratory experiments and a production plant.

each photolysis chamber. This fluence reduction, which is due to absorption, degrades the enrichment. It is not large, however, and can be limited by restricting the width of the photolysis chambers. In addition, the beam transport system includes interstage optics that adjust the beam area to the required fluence as it is transmitted from one chamber to the next. With this approach the laser beams can be adjusted to provide optimum fluence at each stage of the cascade.

Data acquisition and process control for a plant demand no new technology. Existing computers and instrumentation can meet all of the requirements for continuously monitoring and controlling the electro-optical and process gas systems. Equipment for the process support system, such as cooling towers, gas liquefaction plants, and electrical power system, is standard and can be obtained in the sizes required.

Integration of the cascade stages with the electro-optical system is a major design and engineering problem. Figure 24 shows schematically how this might be accomplished. A typical production plant might consist of two integrated cascades that share common subsidiary systems.

We have carried out an extensive production plant design at a conceptual level. That is, detailed design of equipment is bypassed in favor of an approach that clearly identifies the function, size, and performance requirements for each piece of equipment and each system. This level of detail is sufficient for reasonable costing, for studying design tradeoffs, and for establishing the goals that can be achieved by scaling the process and the equipment.

THE PREPROTOTYPE. Our first step toward a production plant was design and assembly of a preprototype by the Laboratory's Applied Photochemistry Division. This facility will test the process and equipment at a scale significantly larger than that of the pulsed-flow experiments. The preprototype (Fig. 25) includes a gas flow system capable of continuous operation, lasers designed to operate at 1000 hertz, and a subscale plant-type collector. The short lifetimes of

the switching elements in the laser systems will limit the tests primarily to short-duration (10-minute) runs. The gas flow area in the preprototype is approximately five times greater than that in the pulsed recirculating loop. The repetition rate of the lasers is sufficient to irradiate only about 1 per cent of the available UF_6. The preprototype demonstrates that scaling the process gas system is straightforward and relatively inexpensive, but scaling the photon supply is expensive and will require further engineering.

The preprototype will not address the requirements for spatial and temporal multiplexing, process staging, or interstage optics. Other issues not readily addressed by the preprototype are gas cleanup requirements for recycling and propagation of the laser beams on a plant scale.

THE DEMONSTRATION MODULE. The questions of scale not addressed by the preprototype can be answered with our next step toward a production plant, the demonstration module. The present plan is to complete the module in the late 1980s. It will be capable of demonstrating all critical aspects of a production plant. Most optical equipment and a beam transport system will be demonstrated at plant design conditions. These components will be incorporated into a multinozzle configuration with sufficient design flexibility to permit their optimization and refinement. A fully integrated stage will incorporate full-scale or directly scalable hardware. Data on the performance, reliability, maintenance, and lifetime of the lasers will establish production plant design criteria and realistic economic parameters.

Conclusions

We have concentrated in this article on the use of lasers to separate uranium isotopes. The primary reason for pursuing the development of a laser process for separating isotopes of any element is an economic one. In the case of uranium the cost of the product from more conventional methods is high enough to warrant introduction of the more selective and technology-intensive laser methods. We believe the high cost of the photons involved can be offset by the reduction in capital and operating costs and electric power consumption relative to conventional processes.

The intense research effort in this area has led to significant advances in our fundamental knowledge of photon-molecule interactions and in the technology of lasers. The application of this new knowledge and technology to more general areas in chemical processing—selective chemical synthesis, purification, reaction-rate control, and catalysis—has only just begun. ■

Further Reading

V. S. Letokhov and C. B. Moore, "Laser Isotope Separation," Soviet Journal of Quantum Electronics 6, 129-150 and 259-276 (1976).

C. D. Cantrell, S. M. Freund, and J. L. Lyman, "Laser-Induced Chemical Reactions and Isotope Separation," in *Laser Handbook, Vol. III*, M. L. Stitch, Ed. (North Holland Publishing Co., Amsterdam, 1979).

V. S. Letokhov, "Laser-Induced Chemical Processes," Physics Today 33, 34-41 (November 1980).

AUTHORS

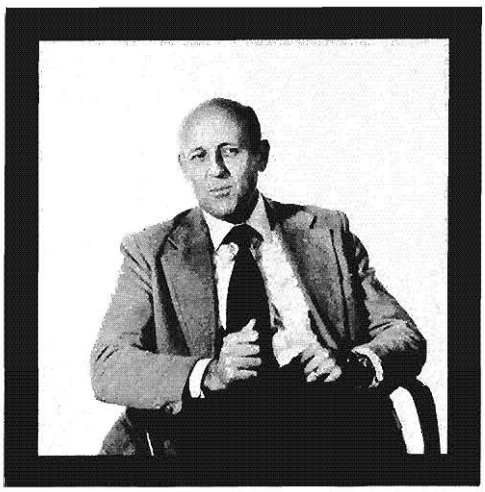

Reed J. Jensen received his Ph.D. in physical chemistry from Brigham Young University in 1965. After a postdoctoral appointment at the University of California, Berkeley, he joined the Laboratory's GMX Division. Following a two-year teaching experience with Brigham Young University, he returned to Los Alamos to initiate a program in chemical laser research. He played a key role in advancing the technology of high-energy pulsed chemical lasers. His experience with the interaction of laser radiation and chemical kinetics led him directly into the field of laser isotope separation. During this period he, along with several coworkers, advanced the concept for the molecular laser isotope separation process described in this article. His promotion to the post of Assistant Division Leader of the Laser Division was followed in 1976 by an appointment as Alternate Division Leader of the newly formed Applied Photochemistry Division. In 1980 he was named Division Leader of the Applied Photochemistry Division and Program Manager for molecular laser isotope separation. Under his direction approximately 225 scientists and technicians pursued research and development in laser isotope separation, laser-induced chemistry, applied photochemistry, spectroscopy, and related fields. In 1981 he was named Deputy Associate Director for molecular laser isotope separation. (Photo by LeRoy N. Sanchez)

O'Dean P. Judd received his Ph.D. in physics with a specialty in plasma physics from the University of California at Los Angeles in 1968. For several years he worked at the Hughes Research Laboratory on microwave electronics, plasma physics, and high-energy lasers. He joined the Laboratory's Theoretical Division in 1972 as an Associate Group Leader of its Laser Theory Group. There he did theoretical work on atomic and molecular physics, lasers, and nonlinear optical interactions for the laser fusion and laser isotope separation programs. In 1974 he became Group Leader of the Laser Division's Advanced Laser Group, whose task was the development of high-energy visible and ultraviolet lasers. In 1977 he joined the Applied Photochemistry Division Office and worked on problems related to uranium isotope separation and multiple-photon excitation processes in polyatomic molecules. Currently he is a Project Manager for high-energy laser concepts in the Defense Science and Technology Office. He is a consultant on lasers to the National Oceanic and Atmospheric Administration and is an Adjunct Professor of Physics in the Institute of Modern Optics and the Department of Physics and Astronomy at the University of New Mexico. His theoretical and experimental interests include lasers and quantum electronics, nonlinear optics, atomic and molecular physics, plasma physics, and laser chemistry. (Photo by LeRoy N. Sanchez)

J. Allan Sullivan earned a Bachelor of Science and a Master of Science in aeronautical engineering from the University of Colorado. After receiving a Ph.D. in mechanical engineering from the University of Michigan, he served for a short time as an Assistant Professor at Colorado State University and then joined the Laboratory in 1966. In his first few years with the Laboratory, he worked on advanced nuclear reactor concepts and computer codes for transient reactor behavior. In association with C. P. Robinson, he helped pioneer some of the early research in laser development and isotope separation at the Laboratory. In 1974 he was appointed Group Leader of what is now the LIS Engineering Group in the Applied Photochemistry Division. This group worked on advanced engineering for the then fledgling molecular laser isotope separation program. In 1977 he served a short time as the Alternate Director for the Reactor Behavior Division of EG&G, Idaho Falls and then returned to the Laboratory's Applied Photochemistry Division. There he served as a project leader for novel instrumentation applications of lasers and as an industrial liaison officer. In 1980 he was assigned to the Department of Energy's Office of Advanced Isotope Separation where he represented the Laboratory's interests in formulating the criteria for deciding which advanced isotope separation technology will be scaled to production facilities. At present he is the Program Manager for engineering implementation of the molecular laser isotope separation program. (Photo by LeRoy N. Sanchez)

by Judith M. Lathrop

*footnotes to a program

The molecular laser isotope separation program at Los Alamos was the first major program in applied photochemistry. Like every technology involving fundamentally new phenomena, this effort had disconcerting surprises as well as satisfying discoveries. Participants in the early years of the program gave us this glimpse of basic research at work.

The molecular laser isotope separation program was formally established at Los Alamos in 1972, but early discussions and preliminary work began the year before. Throughout the summer of 1971 Reed Jensen of J Division and his graduate student John Lyman were doing CO_2 laser induced chemical reactions with SF_6 and N_2F_4. In October that year Roy Greiner, a spectroscopist in GMX-2, sent a memo about the possibilities for uranium laser isotope separation to Keith Boyer, who was to be leader of a new laser division. During the fall an informal uranium task force collected information and read the literature. On the first of February 1972, L Division became operational, and Keith Boyer asked Paul Robinson to assemble the task force on a more formal basis. From various areas of the Laboratory came a core group: Ted Cotter, Roy Feeber, Roy Greiner, Burt Lewis, Reed Jensen, and Paul Robinson. Along with other interested chemists and physicists, they met each week for hours of discussion.

It appeared that monochromatic high-intensity radiation from lasers would make isotope enrichment possible, since in previous attempts the inadequacies of conventional discharge lamps had been the major handicap. The group's first major decision was to work with uranium-bearing molecules rather than with uranium atoms. For one thing, Avco Corporation was already working with atomic uranium. For another, producing uranium atoms requires very high temperatures. Those in the group who had worked on the rocket reactor for the Rover project were well aware of all the difficulties in dealing with uranium at very high temperatures. Also, some of the chemists had experience with uranium hexafluoride (UF_6) gas and thought the molecular approach offered more latent technical possibilities.

The goal of the project was to induce photodissociation of UF_6 molecules containing uranium-235. There seemed to be a variety of possible approaches, but the one that caught everybody's imagination, because it was conceptually so straightforward and so credible, was the idea of using infrared laser radiation to excite the vibrations of the UF_6 molecules containing uranium-235 without affecting any of the molecules containing uranium-238. It seemed quite likely this first step would increase the susceptibility of the ^{235}U-bearing molecules to dissociation by means of ultraviolet radiation. Two steps had already appeared in a French patent for selective ionization, but the French method had not been attempted and did not even mention photodissociation.

Every new concept is contingent upon what is not known. Just how possible was dissociation with lasers? In a book titled *The Chemistry of Uranium* by Katz and Rabinowitch was a tantalizing hint. The text reported that an attempt to measure the UF_6 Raman spectrum with ultraviolet light had failed because a fluffy white solid kept forming. It was possible that the solid was the product of dissociation. In the experiment the UF_6 had been dissolved in Fombic's fluid. Would dissociation also occur in a gas? A sort of bible for the group was an Oak Ridge report, written by R. L. Farrar, Jr. and D. F. Smith, that summed up all that was then known about uranium isotope separation; among other things it clearly indicated that at room temperature UF_6 infrared bands were about 30 times wider than the frequency difference between the peaks of the absorption bands for the two isotopic species. The Los Alamos spectroscopists had to agree

that the amount of enrichment possible at room temperature would be very small.

Cooling the gas seemed a possible solution but had its own problems. During April Roy Greiner did calculations that showed how at very low temperature the infrared absorption bands of UF_6 would become much narrower and the absorption features sharper. However, simple static cooling was out of the question because it would only freeze the gas to an unusable solid. Ted Cotter, who had experience in gas dynamic cooling, suggested that the low temperature could be obtained, for a brief moment, by mixing UF_6 with a light carrier gas and making a supersonic expansion through a nozzle. Because lasers are capable of pulses as short as 100 nanoseconds, the rapidly flowing gas would, relatively speaking, just be sitting there letting things happen to it. It seemed likely that the vapor pressure of the cold UF_6 would be very low, but Reed Jensen pointed out that a slit nozzle could extend the optical path length of the irradiation zone to as much as a meter.

By the first of May the group had at least a conceptual solution to the problems of cooling. There remained the question of how much energy would be required to break apart the strongly bonded UF_6 molecule. Working from a number of chemical papers, Burt Lewis did an "absolutely monumental" calculation that suggested UF_6 would dissociate with 76 kilocalories per mole, which corresponded to light just short of 4000 angstroms. It was energy that lasers could provide.

The pieces of the puzzle had come together, and early in July 1972 patent application was filed for the mainline process. Experiments began. In the attic of the CMR building, a dank place filled with pipes, Paul Robinson, Burt Lewis, and Al Zeltmann of CNC-2 constructed a commercial nitrogen laser and a 1-meter-long cell to hold UF_6. In September they were successful: when the laser was turned on, gas pressure gradually dropped, gas molecules disappeared, a white solid formed. Photodissociation had occurred. Furthermore, the experiment was reversible with the introduction of fluorine gas.

Meanwhile an attempt at spectroscopy was started. Jack Aldridge arrived "just" for the summer, but stayed on as a permanent member of the group. At a firing site on Two-Mile Mesa, a slit nozzle from earlier laser experiments was fitted into a 55 gallon drum patched with teflon putty and pumped out to create a vacuum. Some gas dynamics data were collected, but spectroscopy was impossible without a bigger blowdown system. The group's fluid dynamics engineer was Al Sullivan, who now built at TA-46 a structure declared worthy of pharaohs. An old Rover reactor aluminum pressure vessel, as a feed vessel, was coupled through a nozzle with an irradiation region to a huge space simulation chamber previously used to test arc-jet thrusters. With this enormous contraption the team had 20 seconds of gas flow before the chamber was filled. Al Sullivan, Jack Aldridge, and David Fradkin, who had come along with the space chamber, did experiments of SF_6 in N_2 gas and by late summer of '72 had proved that spectral simplification could be done in a supersonic gas stream. The Department of Military Applications was impressed by the summer's work and granted half a million dollars toward equipment for cooling UF_6.

The basic ideas and physical principles for the mainline process were quite correct from the beginning; however, experimental progress altered many of the quantitative details and required advances in many disciplines. To start in a lighter vein, the classified project was having trouble getting supplies. Early in 1973, to expedite matters, the project received the title JUMP, a term chosen as a suggestion rather than an acronym. (This was later modified to JUMPer to comply with code book

regulations.) The project was again expedited in the fall of '73 by what was informally called the "Harold Resonance." Harold Agnew, Director of the Laboratory, made available to the project both personnel from other divisions and moneys from his discretionary fund.

When the group began to cool UF_6, they discovered they could not nearly reach the estimated concentrations of supercooled gas. Since then Bud Lockett has made substantial improvements in the theory that describes the kinetics of condensation. However, at that time they simply had to accept an unexpected homogeneous condensation, had to live with lower concentrations, and had somehow to provide proportionally more optical path length in the gas.

There was to be a similar experience with the estimations for possible selectivity. The group had a model that gave a surprisingly good interpretation of the observed onset of ultraviolet absorption by UF_6 in the 400 nanometer region at room temperature. In the model the ultraviolet absorption spectrum of each vibrationally excited molecule was exactly a step function of frequency, and the position of the step shifted in frequency in exact proportion to changes in vibrational energy. According to the model very high selectivity would be possible at a sufficiently low temperature. After a while the group was to discover that nature uses a gentle ramp rather than a step function.

But before the group could make significant discoveries about spectra and isotopic selectivity, they had to have the right lasers. In the beginning there were no lasers at suitable wavelengths. They went to Ken Nills, a researcher in diode lasers at Lincoln Laboratory, and asked him to develop what they needed. Ken Nills designed a semiconductor diode laser, flew with it to Los Alamos, and ran spectroscopy with the group. By early summer of '74 the group had observed and confirmed to five figures the frequency required for isotopic selectivity.

The 16-micron absorption band was easily the strongest absorption feature of UF_6. Los Alamos had no laser at 16 microns. There were also possibly usable bands near 12 microns and 8 microns, but there were no lasers available at those wavelengths, either. The Los Alamos scientists found themselves in the position of having to design lasers to a priori specifications—something that had never been done. Steve Rockwood was placed in charge of a laser development group. The first usable laser at 16 microns, and the workhorse of the early experiments, was the hydrogen fluoride, optical parametric oscillator (HF OPO) laser, a unique, tunable laser developed by George Arnold and Bob Wenzel. Later the group obtained 16 micron laser light by shifting the output of the CO_2 lasers with the hydrogen Raman cell.

Other problems were solved and other advances made as the project matured. DeForrest Smith, one author of the Oak Ridge report, agreed to come part time to Los Alamos. His advanced calculations remarkably predicted the fine structure that would result from rotational energy changes in a vibrational peak, and he became a decision-making member of the team.

One persistent problem was the large amount of gas that flowed through the irradiation region during the 20-second run. Early in 1974 Keith Boyer suggested a pulsed valve that could provide a millisecond flow of gas coordinated with the laser pulses. The pulse valve was integrated into a recirculating loop, a system which has been steadily improved.

Problems were sometimes solved with outside help. The program sponsored research at other national laboratories, universities, and industries. For example, the AEC eased classification restrictions to allow a team from the Gaseous Diffusion Plant at Oak Ridge to instruct the Los Alamos group in systems for handling UF_6, using gaseous diffusion technology. Later, Sandia Laboratories developed a rare-gas halide laser to be used in the ultraviolet region. The Sandia team then joined the Los Alamos project.

A sad comedy of errors that developed in the U.S. Patent Office provided diversion from purely scientific problems. The first series of patent applications were filed early in July 1972 and became the concern of the Special Laws Administration. The AEC Division of Classification held the original research application of July 3, 1971, as Restricted Data until the material could be examined. In September the application was placed under Secrecy Order and was upgraded to Secret Restricted Data in February 1973. In August 1973, when an application for an improved mainline process was filed, the Laboratory received indications that the U.S. government was becoming less interested in classification and more interested in the possibilities of patents. From then until 1978 the applications went through a bewildering series of indecisions connected with weapons proliferation. Meanwhile an unclassified German application for much the same material was filed with another section of the Patent Office in 1975, was accepted without a complete interference search, and issued into the literature in 1977. In fact, a comprehensive patent for the Los Alamos mainline process is yet to be issued to the Laboratory.

The difficult problems in the research into laser isotope separation have led to important advances in basic science. The development of narrow linewidth tunable lasers has brought about a revolution in molecular theory. Advances in infrared molecular spectroscopy have yielded precise and detailed knowledge of complex polyatomic molecules, not just as static objects but also as dynamic ones. Scientists can now label most of the myriad spectral features as transitions between identified states and can evaluate the information to determine the structure of the molecule, its shape, and its resistance to deformation.

The interaction of experimental and theoretical work on the project has resulted in new understanding of electronic spectra. Electronic structure, which involves the motion of electrons in the molecule, is qualitatively different from molecular structure, which deals with the arrangements, the rotations, and the vibrations of atoms within the molecule. Excitation of electronic states in the two-step method of laser isotope separation involves frequencies in the ultraviolet region. It was the scant knowledge of electronic structure that caused poor predictions of the absorption edges in the ultraviolet region of UF_6 when the project began. Now scientists know where the electronic energy states are and how the overlapping of a number of transitions contributes to the observed spectrum of the cold gas.

As for the old problem of supercooling the gas, that has become a matter of engineering mastery. One now needs only a simple piece of apparatus that occupies no more floor space than a desk. Flick a switch and, lo and behold, there is one's chosen very cold gas to look at.

Perhaps the most extraordinary discovery of the whole project has been multiple-photon excitation. That polyatomic molecules can absorb many single-frequency infrared photons was not even suspected at the beginning. Between 1971 and 1973 the first hints of the phenomenon appeared in the work being done. Between 1973 and 1974 both Los Alamos and the Institute of Spectroscopy in the Soviet Union demonstrated multiple-photon excitation leading to isotopically selective dissociation in sulfur hexafluoride (SF_6). Multiple-photon excitation is now known to occur in all polyatomic molecules at both high and low laser intensities and is an essential part of the infrared step of the Laboratory's uranium enrichment process. The details of this complicated phenomenon are still being studied, but clearly multiple-photon excitation will play a major role in laser isotope separation and other areas of applied photochemistry.

Molecular laser isotope separation is still a program in progress, a technology not yet technically complete, but already its research has provided entirely new fields of knowledge. ■

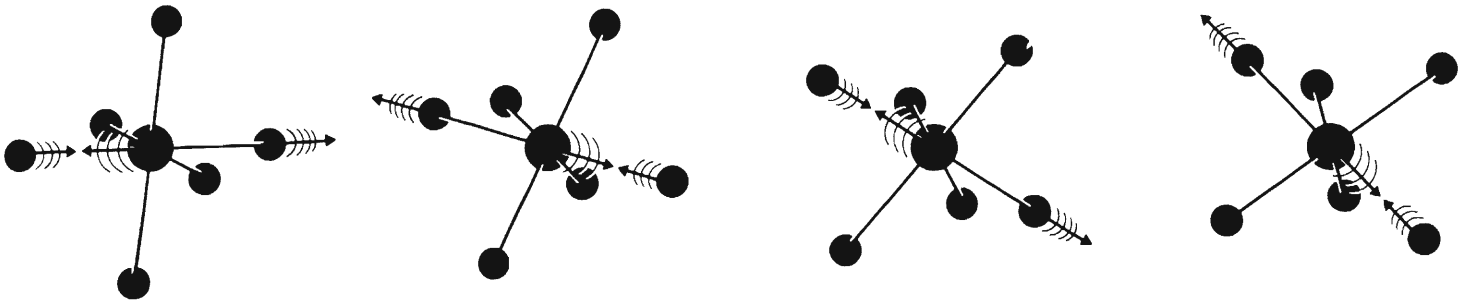

the modern revolution in

by Robin S. McDowell, Chris W. Patterson, and William G. Harter

Lasers have revealed a surprising order to the complex motions of vibrating, rotating molecules.

One of the most exciting challenges in modern science has been to unravel the detailed code of molecular spectra because this code speaks directly of a molecule's energy levels. In other words, the allowed energies and motions of a molecule can be delicately probed by seeing which photons of known frequency tickle the molecule into excited states. In particular, to understand the vibrational motions important for chemical reactions, it is necessary to decipher the portion of the electromagnetic spectrum called the infrared (see sidebar "The Absorption Spectrum—The Signature of Molecular Motions").

However, the infrared spectra of highly symmetric molecules, even of those with only a half dozen or so atoms, appear at first to be a hopeless jumble of finely spaced energy transitions. In fact, only ten years ago the sight of the thousands upon thousands of fine absorption peaks massed together in each absorption band of octahedrally or tetrahedrally symmetric molecules, such as UF_6 or SiF_4, was enough to make an experienced spectroscopist blanch. But spectroscopists persevered and, using lasers as a source of precisely tuned infrared photons, discovered patterns with surprising order. This newly found order not only makes possible the detailed assignment of each absorption peak to a specific energy transition, but also increases our understanding of the allowed motions of these molecules. As it turns out, it is the high degree of molecular symmetry that accounts for both the array of closely spaced transitions and the ordered pattern of absorptions.

The spur to this breakthrough has been laser photochemistry. In particular, knowledge gained about the vibrations of the octahedral molecule uranium hexafluoride (UF_6) has been useful in designing the Los Alamos molecular isotope separation process for uranium. Since the initial, isotopically selective step in this process is vibrational excitation of UF_6, an understanding of its infrared spectrum is imperative. This is especially true for the heavy, symmetric UF_6 molecules since the vibrational frequencies of the various isotopic species differ by only small amounts and since there is considerable overlap in the complex array of possible absorptions.

Moreover, one version of the separation processes involves driving the molecule into a high state of excitation, to the point of dissociation. An understanding of this process requires knowledge of the full ladder of energy levels, not just of the lower rungs.

To achieve such excitation, each molecule must absorb many photons. This multiple-photon process involves intense radiation fields that drive populations of molecules up and down the vibrational energy ladder. Thus the rates at which molecules change their vibrational motion become important.

Although infrared spectroscopy was an already mature and well-established field of research, its capabilities, both theoretical and experimental, were challenged by the need to understand these phenomena. Fortunately, the recent advances in designing lasers as tunable sources of very-narrow-linewidth infrared radiation revolutionized this field, and theoretical developments accelerated to keep pace. This article discusses the comprehensive unraveling of the infrared spectrum for the first step up the vibrational energy ladder and the determination of the next few rungs; the article "Multiple-Photon

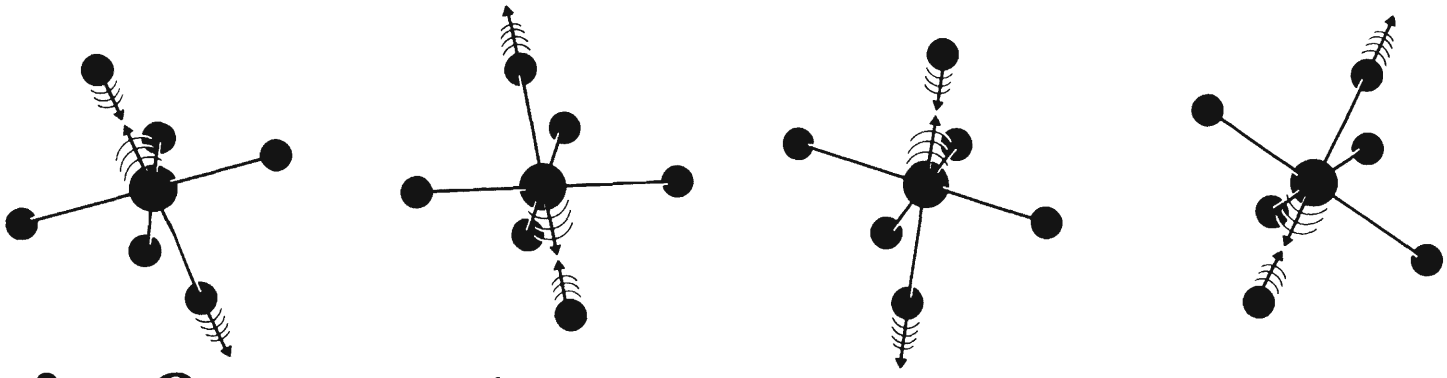

infrared spectroscopy

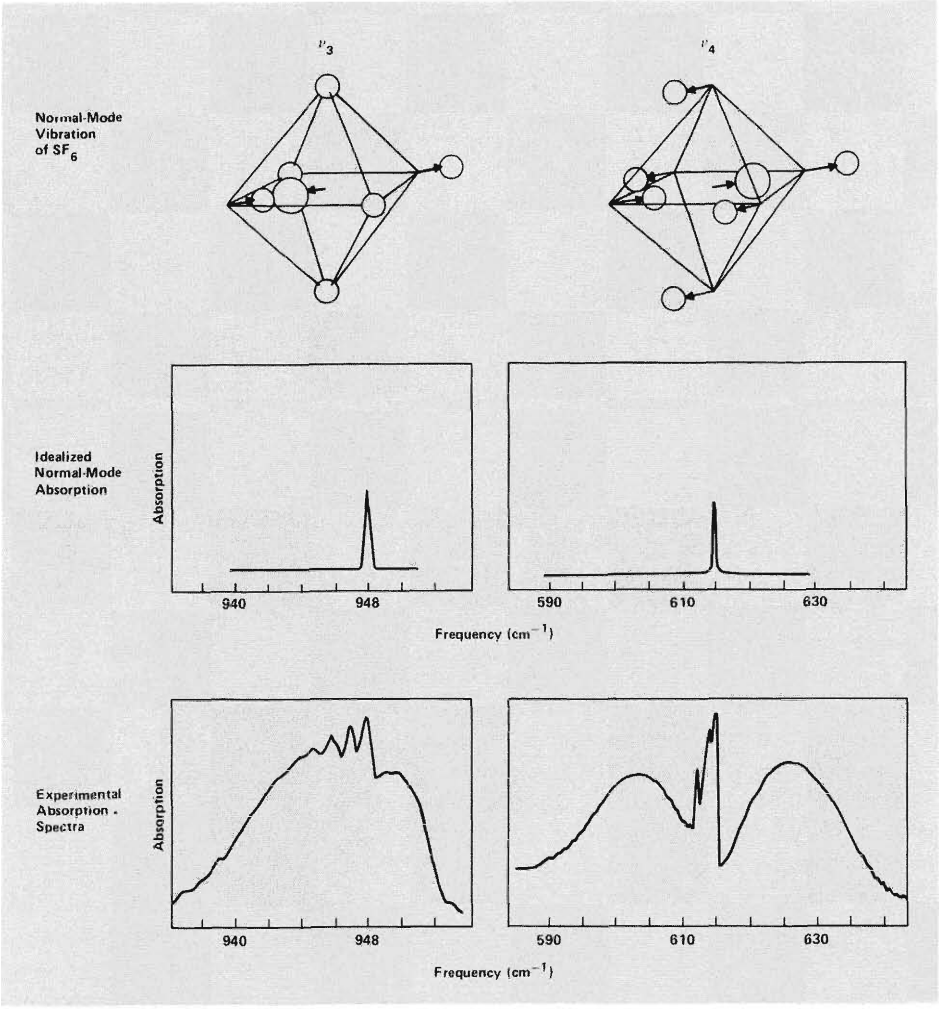

Fig. 1. The two infrared-active vibrations of SF_6 and associated spectra. The ν_3 normal mode is principally an S-F bond stretching motion, whereas the ν_4 mode is an F-S-F bending motion. If these vibrations were harmonic and no molecular rotation occurred, then the spectra would look like the graphs labeled Idealized Normal-Mode Absorption. Much of the width and structure seen in the Experimental Absorption Spectra are due to small rotational energy changes that accompany the large change in vibrational energy. (All spectra in this article have absorption increasing in the up direction.)

Excitation" in this issue deals with excitation to dissociation in the presence of intense radiation fields.

The Complexity of Molecular Motion

People not familiar with modern infrared spectroscopy are apt to picture a vibrating molecule as a collection of atomic point masses held together by rather rigid springs. In fact, much infrared spectroscopy has been based on just such a model. The rigid springs allow only small oscillations about equilibrium, resulting in near-harmonic vibrations. Moreover, the molecule vibrates with only a certain number of characteristic motions, or normal modes, that are independent of each other. The particular frequency of a mode depends on the strengths or force constants of the bonds that are stretching or bending and on the masses of the atoms that are moving. This model is justified by the fact that the normal modes that interact with radiation are easily identified at low resolution as absorption peaks in either infrared spectra or Raman radiation-scattering spectra.

Figure 1 shows the ν_3 and ν_4 vibrational modes for sulfur hexafluoride (SF_6) along with their infrared absorption spectra. As can be seen, the experimental absorption peaks have considerable width and structure compared to the idealized absorption of normal-mode vibrations. This structure is typical and is due primarily to small changes in rotational energy that occur simultaneously with the larger changes in vibrational energy. The basic pattern of rotational energy levels can be explained using as a model the same rigid molecule, but now rotating. In this approach the rotational

continued on page 42

the absorption spectrum-

SIDEBAR 1:

the signature of molecular motions

Photons absorbed by a molecule induce transitions, separately or in combination, between its quantized rotational, vibrational, and electronic energy states. Rotational energy states involve motions of a molecule that produce a net angular momentum about its center of gravity. Vibrational energy states involve oscillations of the nuclei about the center of gravity. And electronic energy states involve motions of the bonding electrons. Therefore, encoded in a molecule's absorption spectrum is much information about its dynamics and structure. The basis for decoding this information is the fact that the energy of an absorbed photon equals the difference between two of the molecule's energy states.

One can approximate the energy difference ΔE between two adjacent rotational energy states of a gaseous molecule by assuming that the molecule is a rigid rotor, that is, by assuming that no molecular deformation accompanies the rotation. Then,

$$\Delta E = \left(\frac{h}{2\pi}\right)^2 \frac{J+1}{I} ,$$

where the rotational quantum number J can assume any nonnegative integral value and I is the molecule's moment of inertia about the axis of rotation. Note that ΔE is inversely proportional to I and increases with increasing J. Numerical values of ΔE based on reasonable estimates of I correspond to the energies of photons in the microwave and far infrared. Thus, the absorption spectrum of a molecule in this region provides information about its moment of inertia, that is, about bond lengths and bond angles.

Vibrational energy states are regarded as being the result of bending or stretching of individual bonds, skeletal motions of the molecule as a whole, or combinations and overtones of these motions. For a diatomic molecule the energy difference between two adjacent vibrational states in the harmonic oscillator approximation is given by

$$\Delta E = \frac{h}{2\pi} \left(\frac{k}{\mu}\right)^{1/2} .$$

Here μ is the reduced mass of the vibrating nuclei, and k is the proportionality constant between the restoring force and the displacement. (Note that the assumption of harmonic oscillation leads to a constant energy difference between vibrational levels, a prediction that is not borne out by experiment.) For reasonable estimates of k, numerical values of ΔE correspond to those of photons in the mid and near infrared. This portion of a molecule's absorption spectrum thus provides information about restoring forces, that is, about bond strengths.

Since photons in the mid and near infrared have sufficient energy to induce rotational transitions along with vibrational transitions, rotational fine structure is associated with each vibrational absorption feature of a gaseous molecule. Therefore, the rotational-vibrational absorption spectrum also yields much of the information available from the pure rotational spectrum and is of particular interest to molecular spectroscopists. In addition, this spectrum is a powerful tool for qualitative and quantitative analysis.

Photons in the ultraviolet with still higher energies induce transitions between electronic energy states. Thus, the ultraviolet absorption spectrum reveals information about the forces binding valence electrons in molecules. Both vibrational and rotational fine structures are superimposed on the electronic transitions, but this spectrum is more difficult to decode than the rotational-vibrational spectrum.

Shown here are the infrared and adjacent portions of the electromagnetic spectrum. The term infrared radiation refers to radiation with wavelengths between the red limit of the visible spectrum at 0.8 micrometer (μm) and the beginning of the microwave region at 1000 μm. The infrared spectrum thus covers a factor of 1250 in wavelength; in contrast, the extreme limits of sensitivity of the human eye cover only a factor of 2.

Infrared radiation is usually characterized by its wavenumber, or reciprocal wavelength, rather than by its frequency or wavelength. Further, it is customary to use the reciprocal centimeter (cm^{-1}) as the wavenumber unit. Somewhat confusingly, both wavenumber and frequency are designated by the symbol ν. The two quantities are, of course, related by the speed of light, $\nu(cm^{-1}) = \nu(\text{hertz})/c$, so that 1 $cm^{-1} \simeq$ 30,000 megahertz. ■

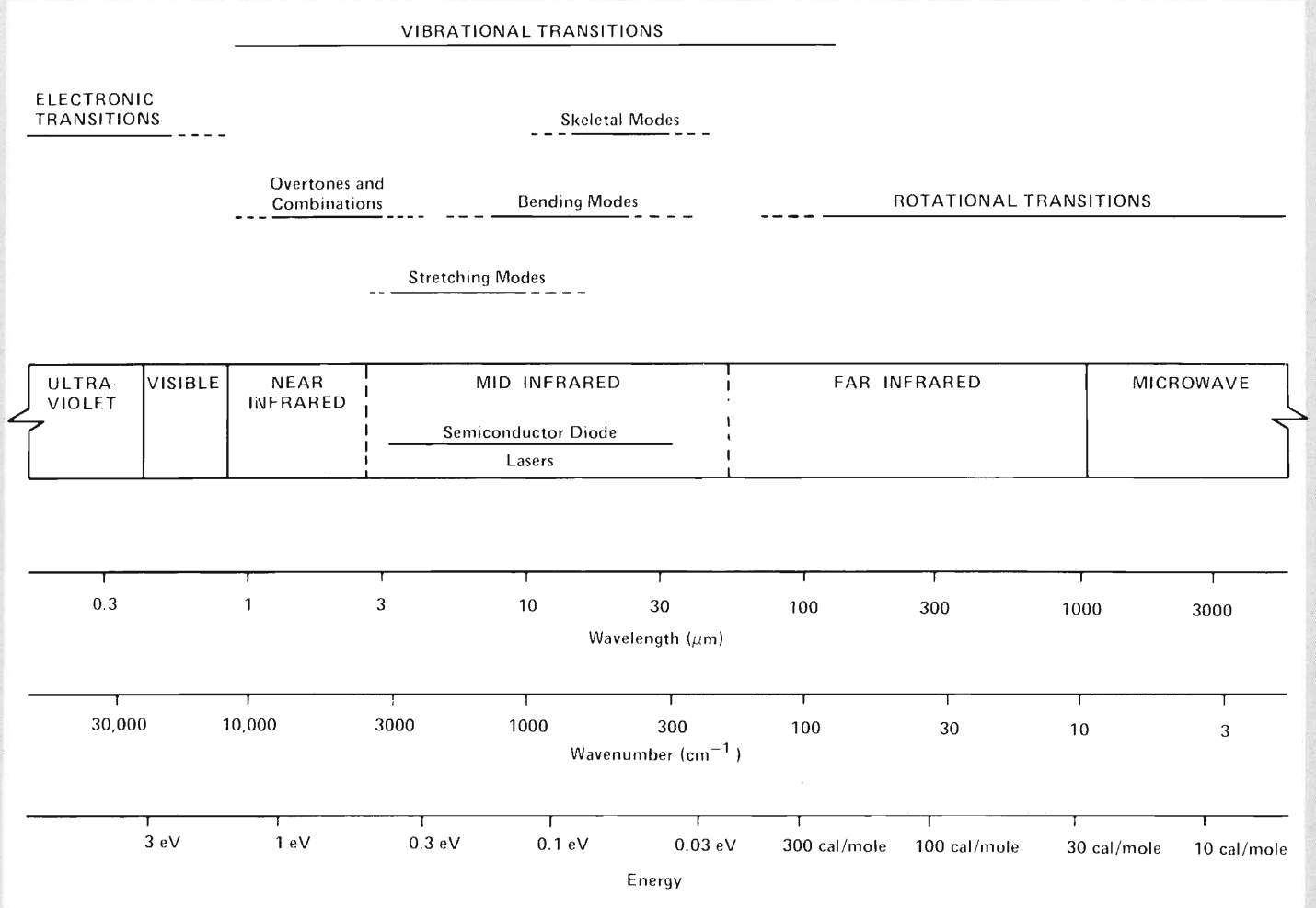

Depending on the energy of a photon, its absorption by a molecule can give rise to rotational, vibrational, or electronic transitions. The energy of a photon equals the product of its frequency and Planck's constant or, equivalently, the product of its wavenumber, Planck's constant, and the speed of light. Various units are used for photon energies. Listed here are electron volts (eV), the customary unit in the ultraviolet, visible, and mid- and near-infrared regions, and calories per mole of photons (cal/mole), the customary unit in the far-infrared and microwave regions.

continued from page 39

energy levels are determined independently of the vibrational motion and then simply superimposed on each vibrational level.

Although this model goes a long way toward describing the energy levels of simple molecules, spectroscopists have always realized there are several approximations inherent in the approach. Especially important is the fact that the various motions of a molecule are not fully independent. For example, when a molecule is both rotating and vibrating, the linear vibrational motion of an atom is subject to the pseudo-forces (centrifugal and Coriolis) of a rotating coordinate system. These forces alter the purely rotational or purely vibrational motion of the molecule.

Also, different molecular motions are coupled through anharmonicities. When the bonding force constraining the motion of an atom is not strictly linear with displacement, the vibration will not be strictly harmonic. The anharmonicities are accounted for with nonlinear terms. When applied as corrections to the simple model, these terms account for the presence in the spectra of overtone and combination frequencies of the normal modes. The anharmonic terms also result in shifts of energy levels and in splitting of states that have approximately the same energy.

The end result of these various effects is that an absorption cannot be represented simply as a vibrational transition with a set of rotational transitions superimposed. Rather, the closer one looks at the spectrum, the more complex it appears, and the more the approximations have to be dealt with in order to understand the detail.

Spectroscopic Resolution

Critical to understanding the detail is the concept of resolution. How close can two spectral features be in frequency and still be distinguished? The more detail we can measure in the spectrum, the more we can hope to understand.

Until recently infrared spectra could only be obtained by methods that, though more sophisticated, are not basically different from those employed in the nineteenth century: the infrared radiation from a glowing source (similar to the heating element on an electric stove) is passed through the sample and then dispersed into its various constituent wavelengths by a prism or diffraction grating. This provides resolutions from about 1 cm^{-1} for commercial grating spectrometers down to 0.1 cm^{-1} or slightly less for some specially built instruments. More recently, interferometry has done somewhat better; in this technique there is no dispersion, but instead the interference between two light beams results in an interferogram from which the desired spectrum can be recovered by performing a Fourier transform. The resolution of Fourier-transform infrared spectrometers varies from about 0.05 cm^{-1} for commercially available interferometers to better than 0.01 cm^{-1} in a very few research instruments.

We see, then, that these conventional spectroscopic techniques can divide the infrared region into at most a few hundred thousand resolved elements. This is a considerable number (the human eye can discriminate only about 200 different visible wavelengths), but much spectral detail of all but the simplest molecules will still be concealed, for the widths of the absorption peaks are much less than these resolutions. Several phenomena contribute to the linewidths, but in a low-pressure gas the dominant broadening mechanism is the Doppler effect caused by the thermal motion of the molecules. The magnitude of the Doppler broadening depends upon the molecular mass, the temperature, and the transition frequency, and is typically between 0.01 and 10^{-4} cm^{-1}. Thus an absorption feature that even the best interferometers show as simply a single "line" may actually consist of many individual transitions that could be revealed with increased resolution.

Over the last decade several different infrared laser sources have been developed (see sidebar "Tunable Lasers—The Tools of the Trade") that combine very narrow linewidths with tunability, so that spectra can be obtained by simply passing the laser emission through the sample and recording the intensity of the transmitted light as the wavelength of the source is changed. Because these devices may have linewidths of the order of 10^{-5} to 10^{-6} cm^{-1}, they can effectively divide the infrared region into several *billion* slices. Furthermore, some of these lasers have enough power to saturate the molecular transition being pumped; as will be discussed in more detail below, this phenomenon can be exploited to obtain spectra whose resolution is not limited even by Doppler broadening.

Figure 2 shows the rich detail revealed in the ν_3 absorption spectra of SF_6 as resolution is increased. Spectrum (a) demonstrates the limited resolution of most grating spectrometers; only a few distinct features are visible. The Fourier-transform infrared trace in spectrum (b) has a resolution of 0.06 cm^{-1} but still does not reveal the underlying structure. The third spectrum is a portion of the ν_3 band at Doppler-limited resolution obtained with a tunable diode laser. Now the true complexity of the band becomes apparent. Some of the rotational-vibrational structure is further resolved in the saturation spectrum (d), in which the Doppler limit is surpassed and a resolving power (the ratio of frequency to resolution, $\nu/\triangle\nu$) of 10^9 is achieved. A plot of the whole ν_3 band at the scale of spectrum (d) would require over a mile of paper; some 10,000 transitions in this band have been observed and assigned. The capability of obtaining spectra such as those in (c) and (d) presents both new opportunities and new challenges to infrared spectroscopists, and such data are providing us with important new insights into molecular structure and dynamics.

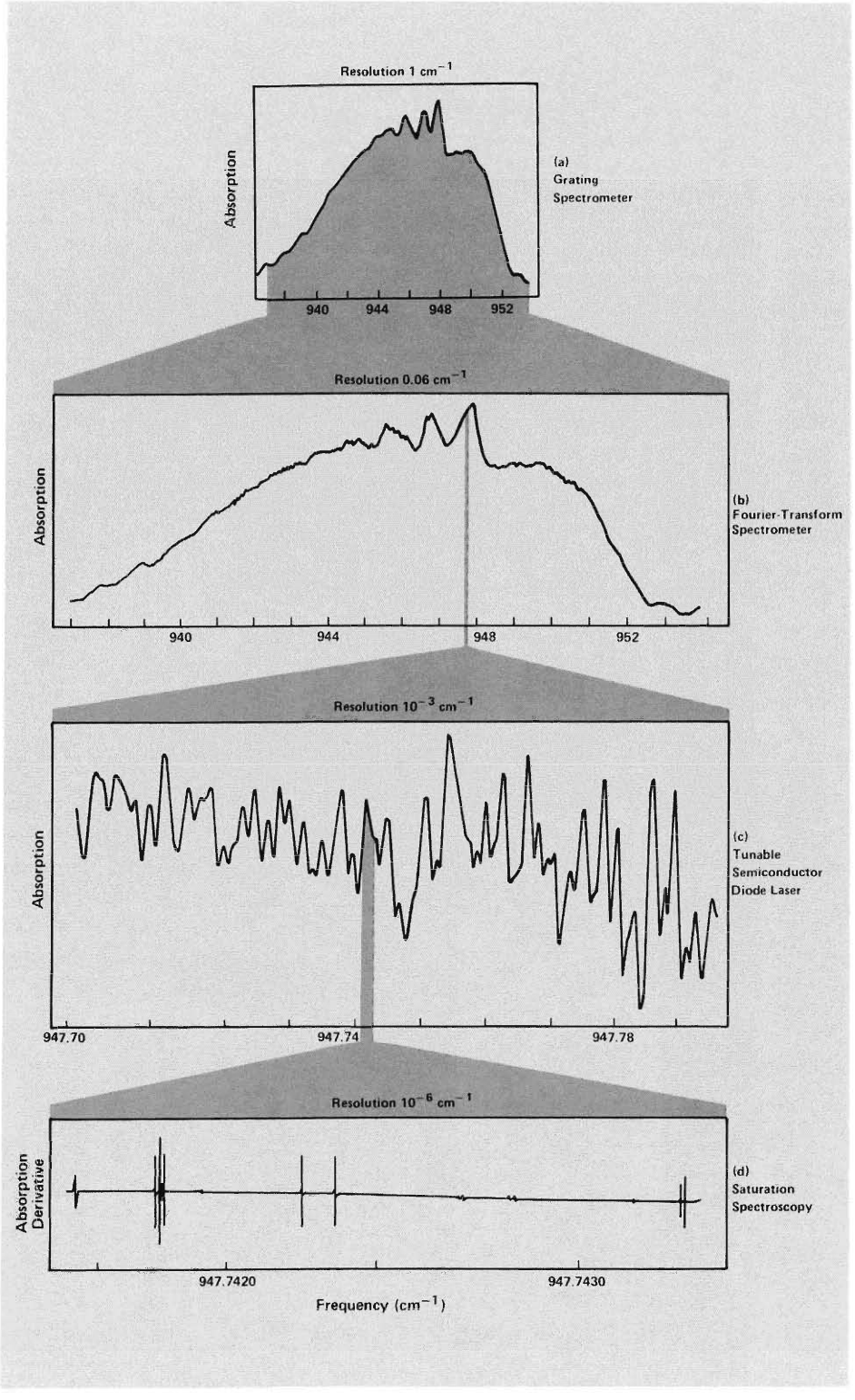

Fig. 2. Infrared spectra of the ν_3 absorption of SF_6 at four resolutions. Spectrum (a) was recorded with a Fourier-transform infrared (FTIR) interferometer, but resolution was degraded to 1 cm^{-1} to match the spectrum produced by a typical commercial grating spectrometer. (b) An FTIR spectrum at a resolution of 0.06 cm^{-1}. (c) A Doppler-limited spectrum obtained by E. D. Hinkley at the MIT Lincoln Laboratory in 1970 using a tunable semiconductor diode laser. The effective resolution is the Doppler linewidth of 0.001 cm^{-1}. (d) Sub-Doppler saturation spectrum recorded by L. Henry at the University of Paris in 1976 with a resolution of better than 10^{-6} cm^{-1}. All of the features in (d) occur inside the small range of frequency possible for the lasing of a single line of a CO_2 gas laser. The trace shows the first derivative of the absorption. Each absorption feature shown in (c) and (d) can be assigned to specific rotational-vibrational transitions of the SF_6 molecule.

tunable lasers-the tools of the trade

SIDEBAR 2:

Molecular spectroscopy has undergone its modern revolution to the tune of lasers whose frequencies can be varied continuously over portions of the infrared spectrum. The most widely useful of such lasers are semiconductor diode lasers, which are similar to the light-emitting diodes familiar from so many display applications. These lasers are characterized by highly monochromatic and widely tunable output frequencies. They are also inexpensive and, although requiring cooling to very low temperatures, simple to operate.

The lasing medium of these devices is a *p-n* junction diode formed in a small crystalline semiconductor. The crystal itself, no bigger than a grain of sand, is mounted on a copper base that serves as an electrical ground and as a thermal connection to a liquefied gas. An injection current applied across the diode causes migration of conduction-band electrons from the *n*-type material and of holes (valence-band electron vacancies) from the *p*-type material into the junction region. There the conduction electrons combine with the holes and emit photons whose frequency depends on the energy difference between the valence and conduction bands of the semiconductor.

The diode lases spontaneously on wavenumbers ranging over several tens of reciprocal centimeters. Within this interval particular wavenumbers (cavity modes) can be amplified by constructive interference within an optical cavity. Such an optical cavity is conveniently at hand in the form of the optically flat and parallel cleaved faces of the crystal. The lasing frequency is thus determined by the index of refraction and length of the crystal. Because these parameters are temperature dependent, the laser can be tuned by varying the temperature of the crystal. In practice this is accomplished by varying the injection current and hence the electrical energy dissipated within the crystal. A semiconductor diode laser can be continuously tuned in this manner over an interval of about 1 cm^{-1}. Adjacent intervals can be accessed by changing the crystal's thermal or magnetic environment, both of which alter not only the index of refraction and length of the crystal but also the diode's spontaneous emission frequency. With these techniques some semiconductor diode lasers can be quasi-continuously tuned over intervals of 100 cm^{-1} with a linewidth of 10^{-5} cm^{-1} or better. However, achieving such a broad tuning range and narrow linewidth requires great care in the fabrication of the diodes, a process involving sophisticated masking and epitaxial growth techniques.

Particularly useful for infrared spectroscopy are semiconductor diode lasers whose spontaneous emission frequency can be varied by altering the chemical composition of the semiconductor from which they are fabricated. For example, lasers made from the semiconductor $Pb_{1-x}Sn_xTe$ (where $0 \leq x \leq 0.28$) can be tailored to emit between 6.6 and 33 μm (between 1520 and 300 cm^{-1}).

This brief account of semiconductor diode lasers has overlooked certain of their faults. Generally, the simultaneous lasing of several different cavity modes, separated by about 1 cm^{-1}, requires the use of a grating spectrometer to select a single mode. Also, competition between the different cavity modes sometimes causes discontinuous frequency jumps, called mode hops, during a scan. Nevertheless, no other laser is so generally useful for high-resolution spectroscopy throughout a very interesting portion of the infrared region. ■

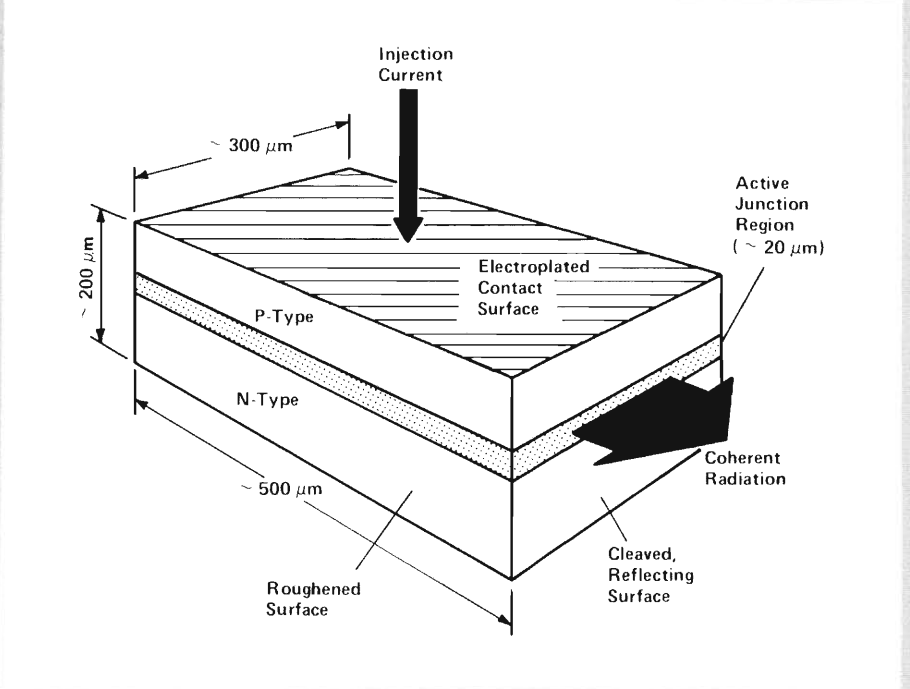

Simplified diagram of a semiconductor diode laser. These tunable lasers have become the workhorses for molecular spectroscopy because of their broad coverage of the infrared region in which rotational-vibrational transitions occur.

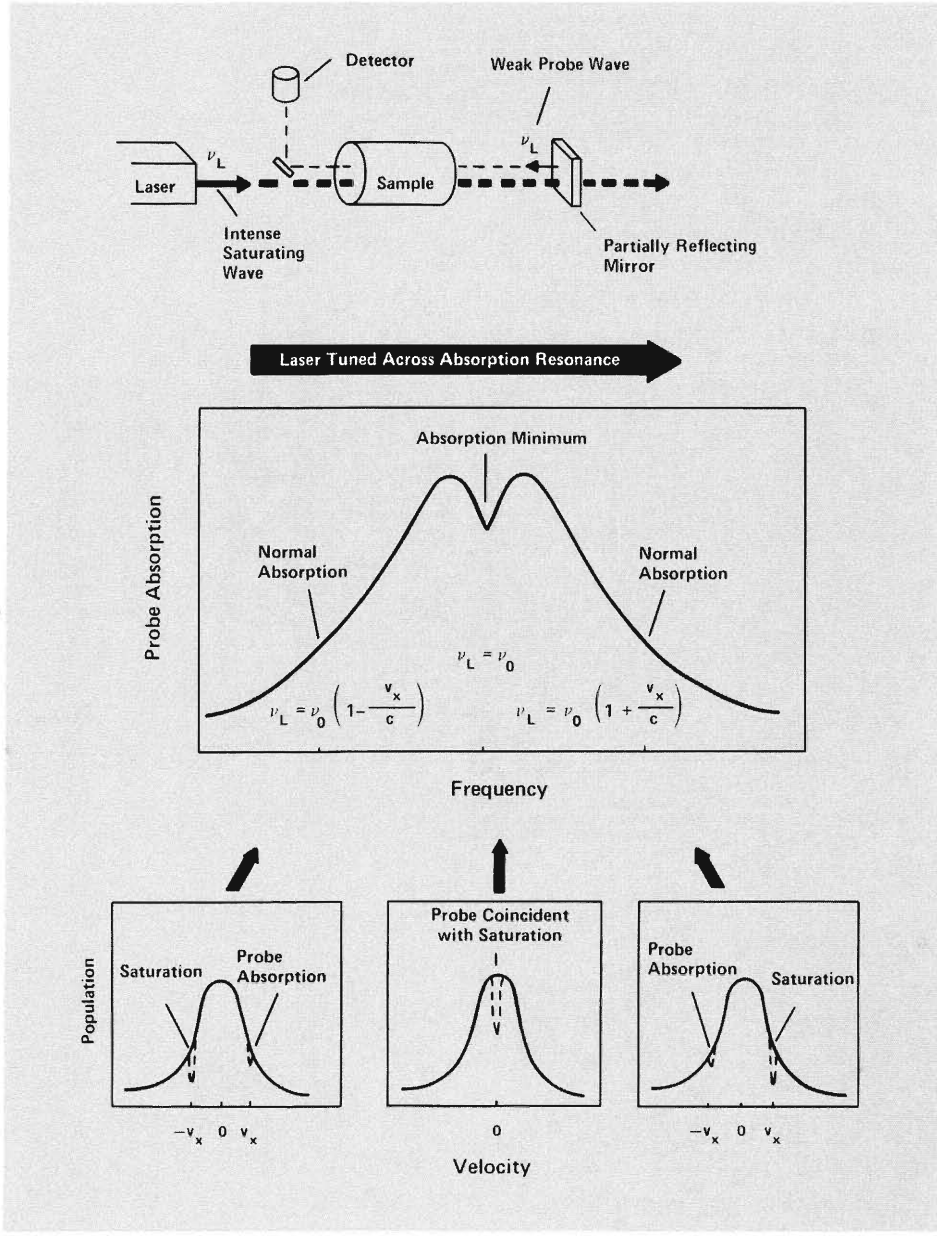

Fig. 3. Saturation spectroscopy. An intense laser at frequency ν_L is tuned across a Doppler-broadened absorption. A small part of this saturating wave is reflected back through the sample as a probe wave. If ν_L does not match the resonance frequency ν_0 of the absorption, the probe and saturating waves see opposite and so different subsets of the velocity distribution and the probe is absorbed normally. If $\nu_L = \nu_0$, then the two waves see the same subset of the velocity distribution, the saturating wave has already depleted the population of that subset, and the probe absorption is reduced. The result is a sharp absorption minimum at the resonance frequency.

Sub-Doppler Spectroscopy

Semiconductor diode lasers and other similar devices have narrower bandwidths than the Doppler linewidth and thus represent a significant advance in infrared instrumentation because they allow spectra to be resolved to the Doppler limit. However, is it possible to circumvent this limit and improve resolution still further? Figure 2d demonstrates that it is. The technique of saturation spectroscopy allows one to examine just those molecules in a particular velocity group rather than the whole thermal distribution. The resulting elimination of Doppler broadening can reveal a wealth of additional spectral detail.

Saturation spectroscopy is conceptually very simple. Say a narrow linewidth laser beam tuned to frequency ν_L is passed in the positive x direction through a sample with an absorbing transition centered at frequency ν_0. As previously mentioned, the broad thermal distribution of molecular velocities gives the absorption a Doppler linewidth that can be much larger than the laser linewidth. A molecule moving in the x direction with velocity v_x will absorb only photons with a frequency $\nu_0(1 + v_x/c)$, where the Doppler shift $\nu_0 v_x/c$ exactly compensates for the difference between the laser frequency and the absorption center, $\nu_L - \nu_0$. Molecules moving in the opposite direction will absorb only photons with a lower frequency $\nu_0(1 - v_x/c)$.

If the laser is sufficiently intense, it can excite molecules out of the lower rotational-vibrational state faster than they can return to that state through relaxation mechanisms such as spontaneous emission and collisional energy transfer. The transition is then said to be saturated: the laser has "burned" a hole in the Doppler distribution of the lower state, depleting those molecules whose velocity allows them to absorb the laser radiation.

Suppose now that a partially reflecting mirror at the far end of the sample cell returns part of the laser beam back through

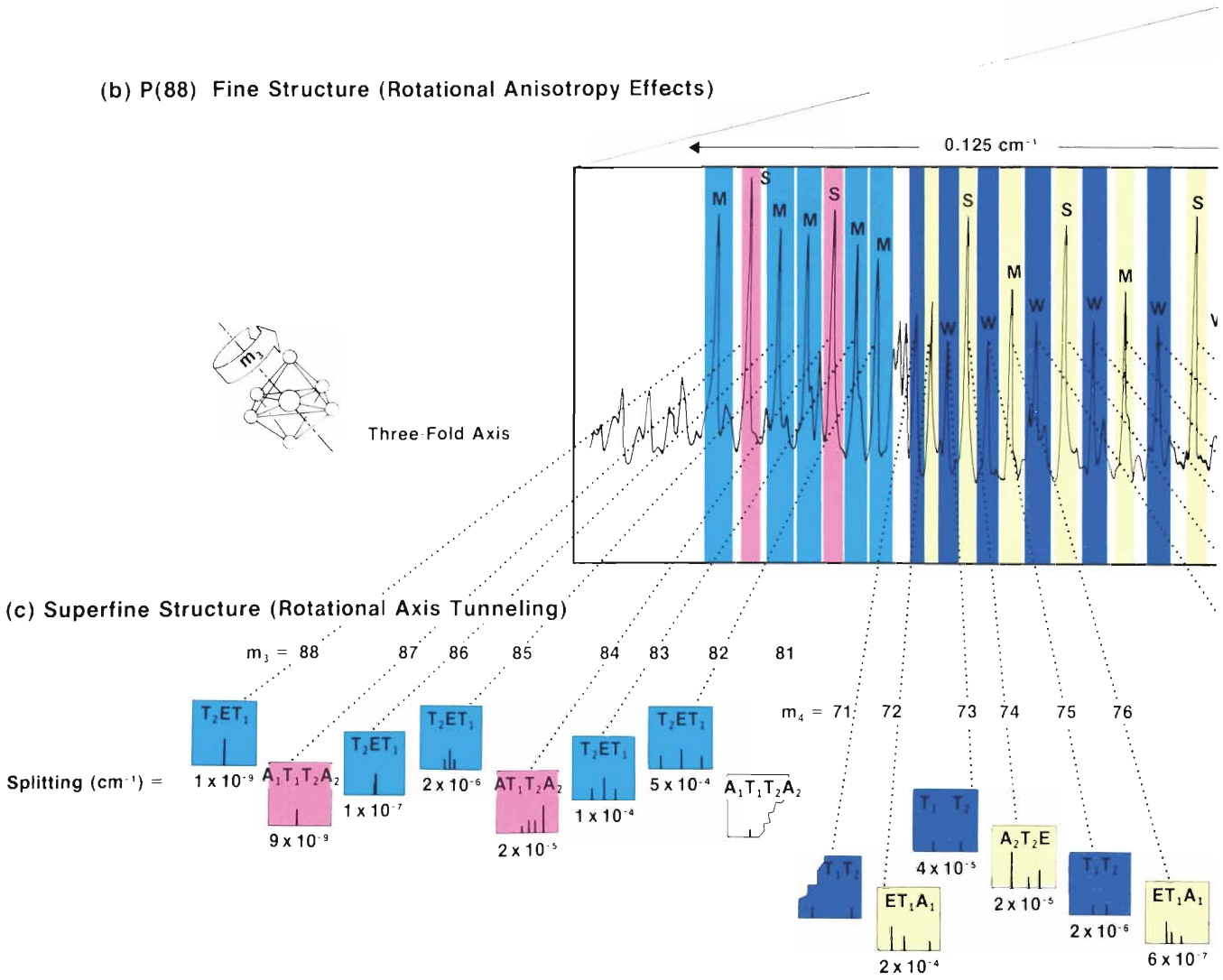

Fig. 4. The bending fundamental ν_4 of SF_6 and its splitting patterns. (a) The gross rotational structure as recorded with a Fourier-transform infrared interferometer at a resolution of 0.04 cm^{-1}. The various rotational-vibrational lines in the P *and* R *branches [designated* P(J) *and* R(J)*] are separated from each other by approximately 0.222 cm^{-1}. The hot-band peaks are ν_4 vibrational transitions that start in an excited vibrational state. (b) Doppler-limited spectrum obtained with a tunable diode laser by K. C. Kim and W. B. Person that shows extensive splitting of the* P(88) *absorption peak. Here the splitting can be attributed to rotational-anisotropy effects; that is, rotation about different axes of the octahedrally symmetric SF_6 molecule results in different amounts of centrifugal distortion. (c) Sketches of superfine structure of the component*

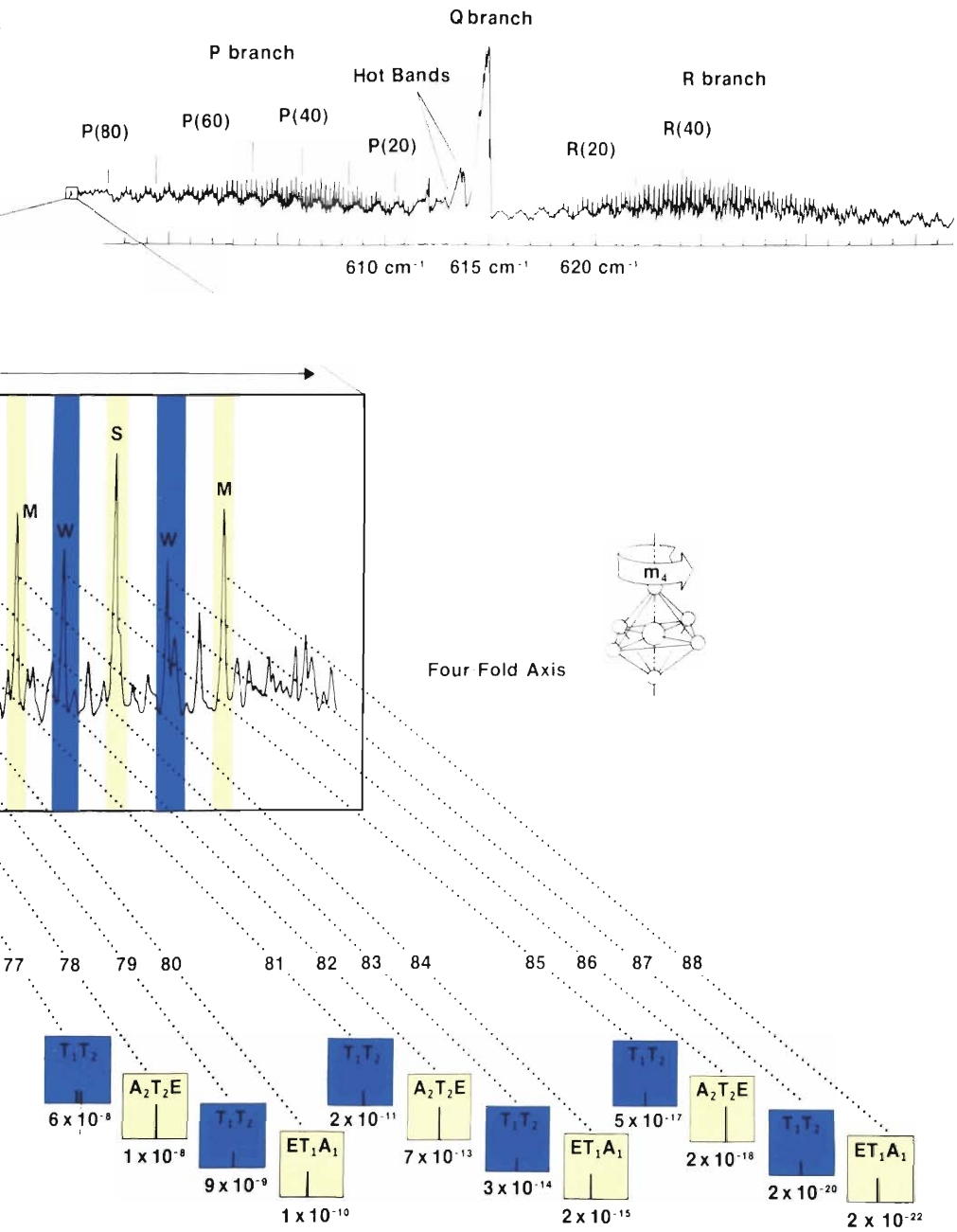

"lines" in P(88), a result of quantum mechanical tunneling from one equivalent rotational axis orientation to another. Resolution of this structure requires sub-Doppler spectroscopy, which has not yet been done on this band. However, a T_2ET_1 triplet similar to what would be observed for $m_3 = 82, 83, 85, 86,$ and 88 is shown at 947.7417 cm^{-1} in Fig. 2d; it belongs to Q(38) of ν_3 with $m = 38$. The absorption peaks in (b) that cannot be assigned to a cluster in (c) are hot-band transitions. The color code used in the figure for the clusters (ATE—light yellow, TT—dark blue, TET—light blue, and ATTA—pink) is the result of mixing the three colors that have been assigned to the three kinds of symmetry species (A—red, E—green, and T—dark blue). This code is also used in Figs. 7 and 14.

the cell as a probe wave (Fig. 3). Since the saturating and probe wave have the same frequency but opposite directions, the returning probe wave will interact with different molecules whose velocity component v_x is opposite to that of the molecules pumped by the saturating beam. This means the probe will be absorbed normally.

If the source is tuned to coincide with the transition frequency ν_0, then the probe will sample a population of molecules whose lower states have just been depleted by the saturating wave. Both beams are then interacting with molecules of the same velocity subset, that for which $v_x = 0$. As a result, the absorption of the probe wave will be reduced. Thus, as the laser is tuned across the Doppler-broadened line, there will be a sharp resonance absorption minimum at exactly the center frequency ν_0. The features shown in Fig. 2d are the derivative traces of such resonances, and the enhanced detail is obvious: over a dozen transitions can be discerned, all of which appear as a single absorption line in the Doppler-limited spectrum of Fig. 2c.

Infrared Spectral Patterns

Infrared spectra range in complexity from a single band of perhaps 20 rotational-vibrational transitions for a light diatomic molecule to the tens of thousands of discrete transitions for heavy polyatomic molecules. The new laser spectroscopy is essential for determining the detailed energy levels of this latter class of molecules. However, even the most complex spectra directly reflect individual physical properties and the allowed motions of the molecule. Our discussion will endeavor to make clear this connection by considering in some detail the spectrum of the octahedrally symmetric molecule SF_6. In addition to having considerable scientific interest in its own right, SF_6 has become the prototype for research on the laser photochemistry and laser isotope separation of such molecules as UF_6.

Since a single atom can move in any of three orthogonal directions, the motion of a molecule composed of N atoms has $3N$ degrees of freedom. Three of these are sufficient to describe the translational motion through space of the center of mass of the molecule, and three more are required to specify its rotational motion (two, if the molecule is linear). There remain $3N - 6$ ($3N - 5$ for linear molecules) vibrational degrees of freedom, which are the fundamental vibrational frequencies or normal modes.

If the molecule is symmetric to the extent of having at least one threefold or higher symmetry axis, then some of these normal modes will occur at the same frequency and are said to be degenerate. Furthermore, for symmetric molecules some of the fundamentals may not induce a change in the molecular dipole moment during the course of a vibration, and thus, according to classical electrodynamics, these fundamentals can not absorb radiation. Such "infrared-inactive" fundamentals may appear as frequency shifts in the spectrum of scattered light (the Raman effect), or, less commonly, they may be totally inactive except in combination with other modes. These considerations will reduce the number of fundamentals seen in the infrared spectrum, though, if inactive modes and degeneracies are properly counted, the total vibrations will always number $3N - 6$ (or $3N - 5$).

For SF_6, the $3N - 6 = 15$ vibrational degrees of freedom are distributed among one nondegenerate Raman-active mode, one doubly-degenerate Raman-active mode, and four triply-degenerate modes of which two are infrared-active, one is Raman-active, and one is inactive. The two infrared-active fundamentals are called ν_3 and ν_4, and the low-resolution contours of their absorption bands were shown in Fig. 1.

ROTATIONAL STRUCTURE. In Fig. 4 we look more closely at the ν_4 absorption (the same considerations apply to ν_3, but the latter is more compact and the details less clear). The ν_4 absorption is the result of a transition from the ground state to the first excited state of the ν_4 vibrational mode (frequently designated $0 \rightarrow \nu_4$). Instead of a single line, however, in Fig. 4a we observe a considerable number of absorptions grouped into three main branches labeled P, Q, and R. As pointed out earlier, this structure is primarily due to small rotational energy changes that accompany the main vibrational energy transition.

As depicted in Fig. 5, rotational energy levels (J) are closely spaced compared to vibrational energy levels (n). Thus, a collection of molecules at room temperature will be found mainly in the lowest vibrational energy level ($n = 0$) but will be distributed among a large number of rotational energy levels. Since the rotational energy for a given angular momentum is inversely proportional to the molecular moment of inertia, the heavier the molecule, the closer the rotational energy spacings. As a result, at room temperature the light hydrogen fluoride molecule significantly populates the lowest 10 or so rotational levels, but the heavier SF_6 molecule populates over 100 levels. This helps explain the abundance of absorption lines in the spectrum.

A transition between rotational-vibrational energy levels is induced by a coupling of the photon's electric field with the molecule's oscillating electric dipole moment. Quantum-mechanical arguments for the harmonic oscillator show that the selection rules for such changes of energy allow only transitions with $\Delta n = \pm 1$ and $\Delta J = -1$, 0, 1. The selection rules for ΔJ correspond, respectively, to the grouping of absorptions into P, Q, and R branches. In Fig. 4a the spectrum is well enough resolved that the individual rotational-vibrational transitions of the P and R branches are apparent. Because there is no change in rotational angular momentum for the Q-branch transitions, the many transitions here tend to be superimposed.

Adjacent to the Q branch in ν_4 are several

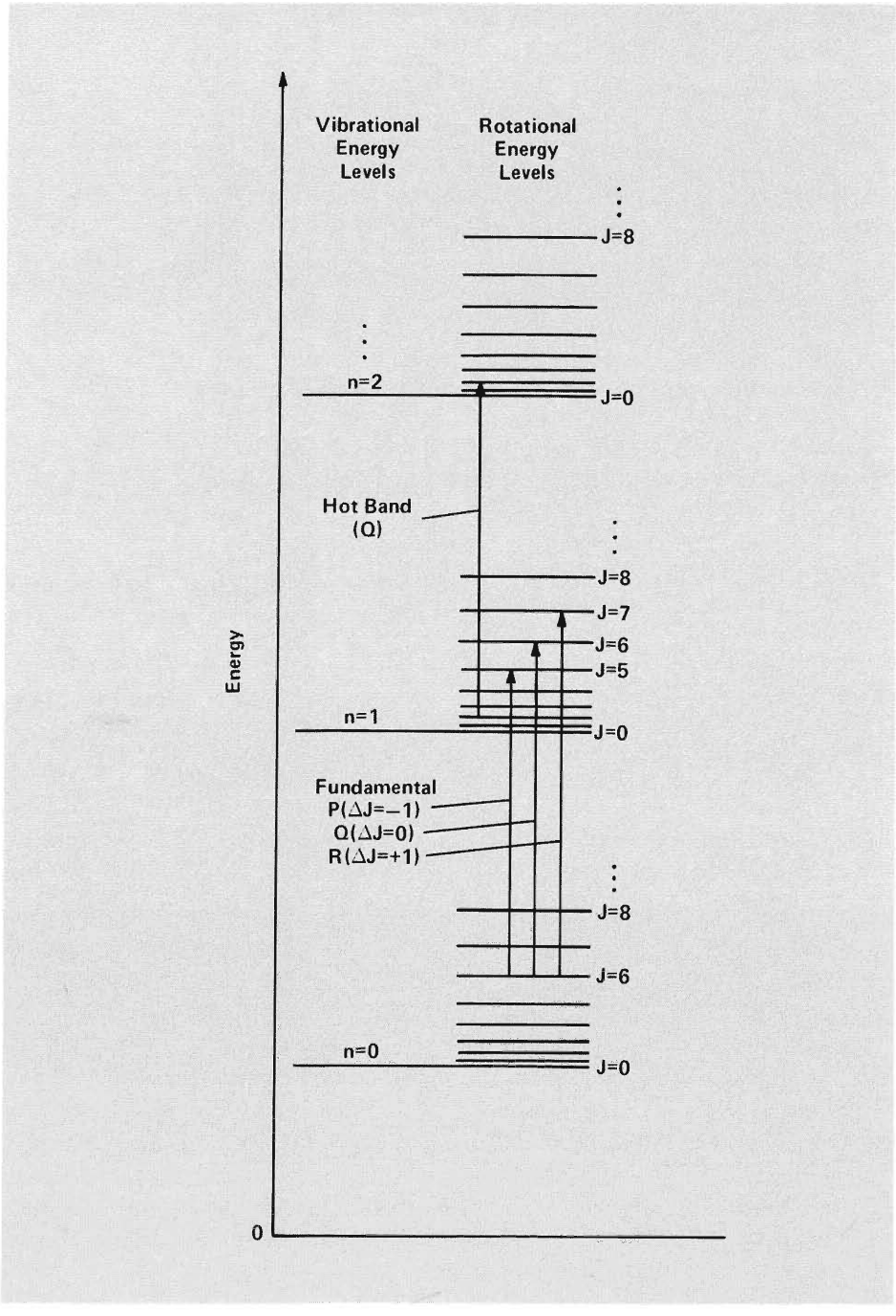

Fig. 5. Rotational-vibrational energy transitions. For a harmonic normal-mode vibration, the energy levels are equally spaced; these are represented here by the quantum number n *with only the three lowest levels shown. The ground vibrational energy level (*n = *0) is not at zero energy because the Heisenberg uncertainty principle requires an oscillator never to be completely at rest. The rotational energy levels are represented by the total angular momentum quantum number* J *and have spacings that increase quadratically with* J. *Thus the frequency of a given energy transition depends on both the* J *of the starting level and the simultaneous change in rotational energy. Examples of allowed transitions out of the vibrational ground state (*n = *0) are shown. The conventional designation is* P(J), Q(J), *or* R(J), *depending on the value of* ΔJ, *plus the value of* J *in the lower state; thus, the three transitions shown are* P(6), Q(6), *and* R(6). *A single hot-band transition from* n = *1 to* n = *2,* Q(2), *is also shown. The relative spacings of the rotational and vibrational energy levels will depend on the bond strengths and the molecular moments of inertia; typically, the rotational energy levels are much more closely spaced than depicted here.*

weaker absorptions called hot bands. These absorptions are due to ν_4 transitions, but originate from an excited vibrational state instead of from the ground state (Fig. 5). The lower excited state either can be ν_4 ($\nu_4 \rightarrow 2\nu_4$ rather than $0 \rightarrow \nu_4$) or can be another vibrational state ($\nu_i \rightarrow \nu_i + \nu_4$). These transitions are seen because they differ slightly in frequency from the central *Q* branch of the fundamental; in fact, they generally occur at lower frequencies. This happens because the vibration is not strictly harmonic. That is, as the bond is stretched further and further, the restoring force does not remain proportional to displacement and higher order anharmonic terms become important. These higher-order terms gradually decrease the equally spaced energy levels of a harmonic oscillator. When the originating states of hot bands can be identified, they provide useful information on the extent of anharmonicity in the vibration. In ν_3 (Fig. 1) the hot-band structure largely obscures the *P* branch.

Single rotational-vibrational transitions can be further resolved with diode spectroscopy. This is shown in Fig. 4b for the *P*(88) transition which corresponds to the absorption of one quantum of ν_4 vibrational excitation accompanied by a change in the rotational quantum number from $J = 88$ to $J = 87$ (that is, $\Delta J = -1$). Obviously *P*(88) is not a single line: at Doppler-limited resolution it displays the detailed structure shown. Even these features, however, consist of discrete clusters of transitions that yield to saturation spectroscopy as shown in Fig. 4c.

These coded messages about the interaction of the molecule with incident photons might seem to be particularly complicated for such a molecule as SF_6. However, the intricate spectra contain rather striking patterns that can be deciphered relatively easily. The simplicity that emerges may help us to understand complex high quantum states in general.

Spectral Clusters— Cracking a High Quantum Code

Why is the $P(88)$ transition a collection of absorptions of different frequencies rather than a single line at one frequency? Basically there is a distinction between rotations caused by the anisotropy of the molecule. If the properties of the molecule were spherically symmetric as depicted in Fig. 6, there would be only one absorption peak for $P(88)$ because the molecule would be distorted in the same way regardless of the orientation of the axis of rotation. However, SF_6 molecules are octahedrally, not spherically, symmetric, and rotations about differently oriented axes produce different distortions in the molecule. These distortions correspond to different rotational energies and consequently to slightly different absorption frequencies.

The orientation of the rotation axis with respect to the symmetry axes of the molecule is the key to understanding the patterns of absorption peaks observed in the spectrum of molecules at high J values. But this classical consideration was not appreciated until after the spectrum was unraveled by a more laborious analysis of the quantum-mechanical Hamiltonian for the molecule. After presenting the quantum approach to this problem, we will show how the classical picture gives intuitive insight into the origin of the many lines in the $P(88)$ spectrum.

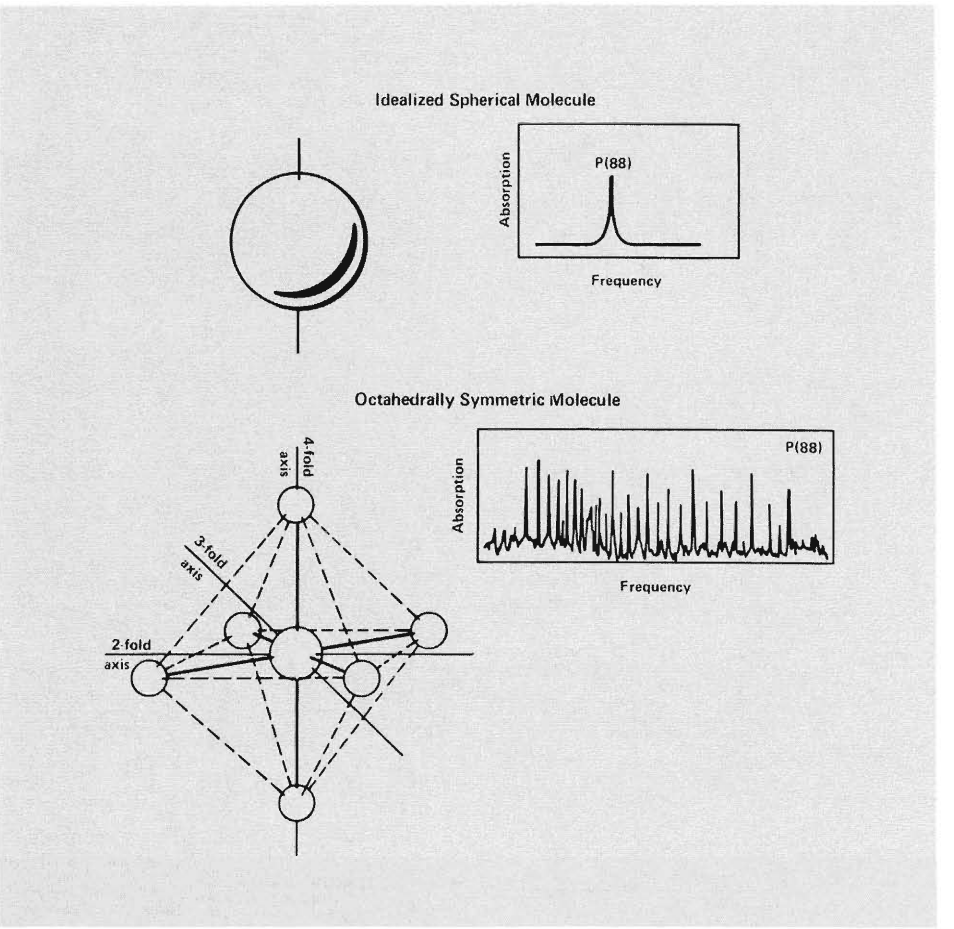

Fig. 6. The effect of molecular symmetry on the absorption spectrum of a rotational-vibrational transition. With a spherically symmetric molecule, all rotational axis orientations are equivalent, so there is only one absorption peak for a given rotational state (here J = 88). However, the SF_6 molecule is octahedrally symmetric, so different orientations of the rotation axis result in distinct energies, producing the complexity of the P(88) absorption band. Examples of axes with 4-fold, 3-fold, and 2-fold symmetry properties are shown; for instance, when the molecule rotates in increments of 360°/4 = 90° about the 4-fold axis, it arrives at positions that are indistinguishable from its starting position.

QUANTUM APPROACH. As we mentioned earlier, the simplest model (or, in mathematical terms, the zeroth-order Hamiltonian H_0) of a molecule is a rigid rotor plus a harmonic oscillator. In order to describe the Coriolis forces experienced by the atoms in a rotating molecule, another term H_1 must be added to the Hamiltonian. H_1 has a very simple form if the molecule is described in a special coordinate system that is fixed in the body of the molecule. In this reference frame the molecule can be described in terms of its angular momentum J and the normal-mode coordinates corresponding to the molecule's independent vibrational motions. So far the Hamiltonian $H = H_0 + H_1$ contains only scalar terms, that is, terms with spherical symmetry. The scalar nature of these terms dictates that a given rotational-vibrational energy level is shifted in energy but not split into different energy components. As a result, this first-order perturbation theory predicts a single absorption frequency for a given J.

In order to account for the observed energy splittings of the rotational states, the Hamiltonian must include second-order octahedrally invariant tensor terms reflecting the symmetry of the molecule ($H = H_0 + H_1 + H_2 = H_{\text{scalar}} + H_{\text{tensor}}$). These tensor terms predict the detailed splitting of each rotational energy level into states at different energies with each state possessing a symmetry compatible with the overall octahedral symmetry of the molecule.

This type of Hamiltonian analysis has been used to identify all the details of complex spectral patterns of high-symmetry molecules. The Hamiltonian predicts relative spacings between energy levels and between absorption peaks. The overall multiplicative constants in the Hamiltonian that determine the size of the spacings are determined by examining the spectra.

Historically, the symmetries of the states into which the rotational levels split were determined by symmetry group analysis in a manner similar to that used by crystal spectroscopists in what is called crystal field theory. According to crystal field theory the various quantum orbitals of an atom located in the anisotropic electrostatic field of a crystal are distorted by that field in a manner determined by the relative orientation of field and orbitals. The consequent shifting of energy levels is called crystal field splitting, and the application of symmetry group analysis allows the number of shifted levels and their relative energy displacements to be identified and labeled.

For example, in crystal systems with cubic, tetrahedral, and octahedral symmetry, the labels for the atomic orbitals are A_1, A_2, E, T_1, and T_2. These labels describe the symmetry character of the orbitals distorted by the crystal field. An atomic s orbital, which has angular momentum $J = 0$, is labeled as a singlet A_1 state. An atomic p orbital, which has angular momentum $J = 1$, is a triplet T_1 state in the crystal field. This triplet state remains degenerate or unsplit in the crystal field, although in the presence of an electric field it splits into three different states corresponding to different orientations of the angular momentum vector relative to the electric field. These orientations are given by the magnetic quantum numbers $m = 1, 0,$ and -1. An atomic d orbital ($J = 2$) has five degenerate states of magnetic quantum numbers $m = 2, 1, 0, -1,$ and -2, which in a cubic crystal field are split into two states, a T_2 (triplet) and an E (doublet). One can represent this energy splitting by the equation

$$d\,(J = 2) = T_2 + E \ .$$

A_2 also labels singlet orbitals, but it appears for the first time in the splitting of an f orbital or $J = 3$ septet:

$$f(J = 3) = A_2 + T_2 + T_1 \ .$$

For the SF_6 molecule, instead of treating external electrostatic fields, the molecular physicist tries to model the effects of the internal electric field on the dynamics of the molecule. But the octahedral symmetry of the SF_6 molecule means that the same formulas used in crystal field theory to derive splitting equations in octahedrally symmetric fields are also applicable to SF_6. For an angular momentum state with $J = 88$, one can derive the splitting equation

$$X(J = 88) = 8A_1 + 7A_2 + 15E + 22T_1 + 22T_2 \ . \qquad (1)$$

Thus the $J = 88$ state is split into 74 octahedrally symmetric states. If one takes into account that A_1 and A_2 are singlets, E is a doublet, and T_1 and T_2 are triplets, then Eq. 1 accounts for all $2J + 1 = 177$ rotational quantum levels associated with this large ($J = 88$) angular momentum.

Since the ground vibrational state has negligible rotational splitting, the splitting observed in the spectrum is essentially that of the excited state. Thus one expects to see one absorption peak for each of the 74 states defined by Eq. 1. In the spectrum of Fig. 4b only about 26 lines are discernible, but in Fig. 4c we see that each of these actually corresponds to a cluster of two to four individual transitions. The clusters consist of the following combinations of symmetry species: A_1T_1E, A_2T_2E, T_1T_2, $A_1T_1T_2A_2$, and T_1ET_2.

The clustering of octahedral states and the identity of these states were predicted by diagonalizing the largest term H_2^* in the second order Hamiltonian, namely the molecular "crystal field potential," or centrifugal distortion potential. This term can be written as

$$H_2^* \propto J_x^4 + J_z^4 + J_y^4 - (3/5)J^4 \ , \qquad (2)$$

where J_x, J_y, and J_z designate the components of total angular momentum along the orthogonal S-F bond axes. A surface representing this potential is shown in Fig. 7a, and the classical physics of the potential will be described below. For now, it is important simply to note that the eigenvalues determined by diagonalizing this approximate H_2 for $J = 88$ predict the exact clustering and level spacing observed in the SF_6 ν_4 spectrum. This procedure leads to the correct assignments not only for the SF_6 ν_4 spectrum but for the rotational substructure for any J in any heavy high-symmetry molecule. Unfortunately, solution or diagonalization of the Hamiltonian to find the energy eigenvalues and rotational substructure requires time-consuming and expensive numerical calculations.

An additional clue to the correct assignment of the rotational substructure of Fig. 4b is provided by the relative intensities of the absorptions. This clue was very useful in both the Q branch of ν_4 and the entire ν_3 band where absorption peaks associated with different J values overlapped. The assignments are made by matching the relative intensities of the absorption peaks with the relative intensities for each cluster predicted from nuclear spin statistics.

The relative intensities of absorptions for the different species depend upon the number of nuclear spin states belonging to each species. This number is found by using the Pauli exclusion principle, which requires the total wave function, which includes nuclear spin, to change sign whenever two identical particles are exchanged. This principle is better known by its application to electronic spin-orbit structure in atoms or to symmetry species of diatomic molecules. For example, the existence of two nuclear-spin isomers of hydrogen (H_2) is well known. Here each nucleus is a proton with a nuclear spin of 1/2 in units of $h/2\pi$; that is, they are fermions with one-half quantum of intrinsic angular momentum. The spins can be aligned parallel ($\uparrow\uparrow$) or antiparallel ($\downarrow\uparrow$); the former results in "ortho" molecules with a unit-spin ($S = 1$) triplet of nuclear-spin states, the latter in "para" molecules with only a

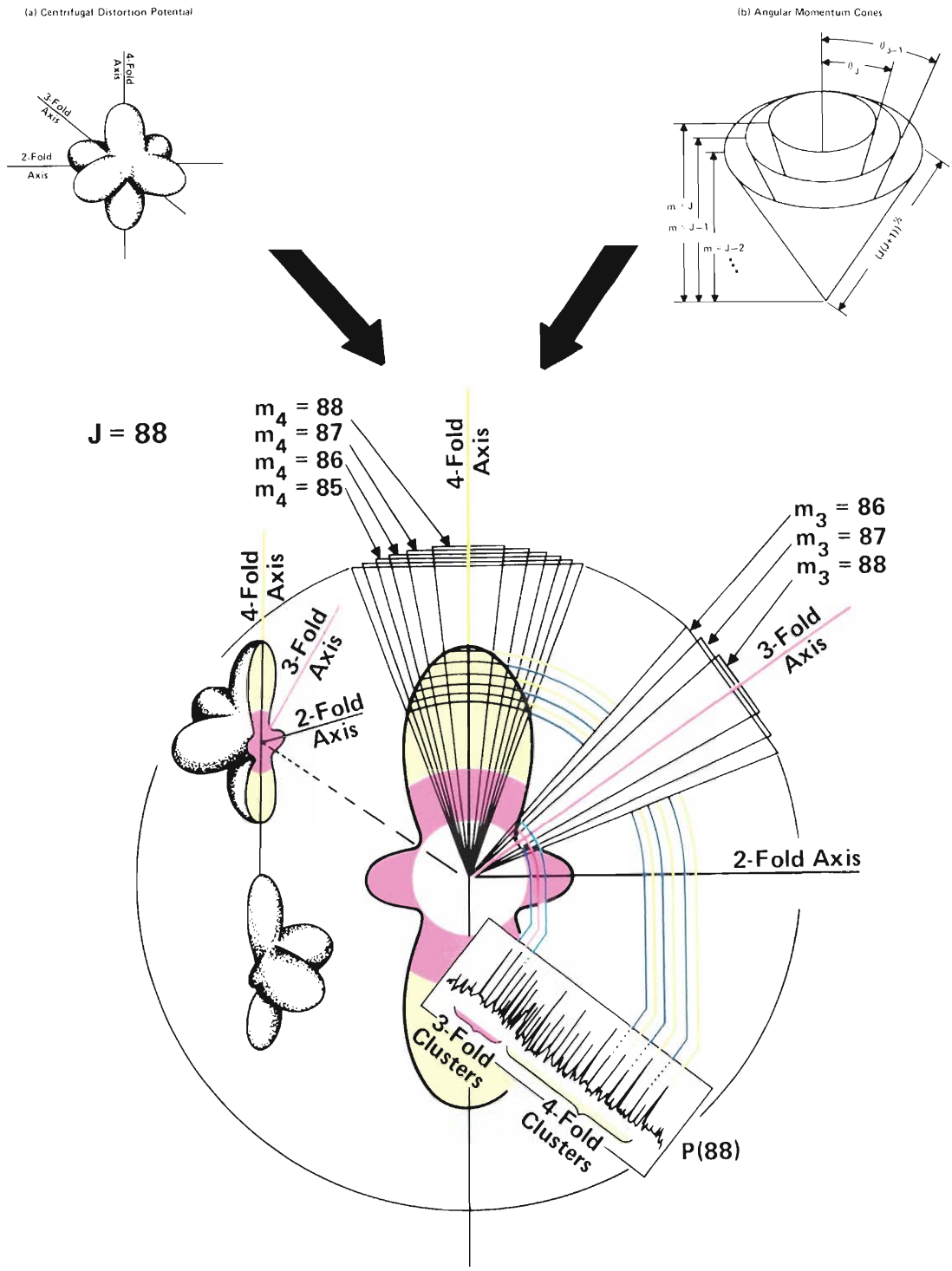

Fig. 7. Rotational axis clustering. (a) A plot of the appropriate centrifugal distortion potential arising from second-order perturbation theory for octahedrally symmetric molecules shows hilltops of maximum rotational energy around the 4-fold symmetry axes and valleys of minimum rotational energy around the 3-fold symmetry axes. There are saddle points at the 2-fold axes that only become obvious in the cross-sectional view of the surface in part (c). (b) Angular momentum cones are the allowed loci of angular momentum vectors for quantum states of magnitude $[J(J+1)]^{1/2}$ *and azimuthal component* m. *(c) In this spectral nomogram for* P*(88), the intersections of the* J = 88 *angular momentum cones with the potential surface approximately determine the spectra near maxima, minima, and saddle points on the symmetry axes. Note that as the cones around the 4-fold axis go to lower* m_4 *azimuthal quantum numbers, the absorption frequency decreases because the point of intersection is moving off the high-energy hilltop. However, for cones around the 3-fold axes, lower* m_3 *quantum numbers correspond to higher frequencies because the point of intersection is moving out of a low-energy valley.*

zero-spin ($S = 0$) singlet. Normal hydrogen thus consists of a 3:1 mixture of the ortho and para species. Consideration of the symmetry of the total wave function, together with the exclusion principle, allows these two to be matched with A_2 and A_1 symmetry species, respectively.

Similar effects will exist in any molecule composed of like nuclei with nonzero spins. The equivalent fluorine nuclei in SF_6 also have a nuclear spin of 1/2. The exclusion principle applied in this case allows the A_1 symmetry species to have only singlet states as in H_2, but in SF_6 there happen to be two A_1 species. The A_2 species in SF_6 have a spin triplet ($S = 1$) and also a septet ($S = 3$), or ten spin states in all. (Recently, the very highest resolution saturation spectra taken by C. J. Bordé at the University of Paris showed evidence of ten sub-peaks in an A_2 absorption, each split about 10 kilohertz apart. This splitting is called hyperfine structure and is due mainly to spin-rotation interactions.) The spin-statistical weights for these and the remaining symmetry species of octahedral molecules were worked out at Los Alamos by H. W. Galbraith and C. D. Cantrell in 1974, and are 2:10:8:6:6 for the A_1: A_2: E:F_1: F_2 levels.

Examining the $P(88)$ fine structure in Fig. 4b (using W for weak, M for medium, and S for strong relative intensities), we see that the main absorption peaks on the right side of the spectrum have a four-peak, repetitive pattern of intensities $MWSW$, which cycles somewhat more than four times. On the left side the three-peak pattern of MSM repeats at least two cycles. By relating the known statistical weights to the relative intensities in the spectra, each absorption can be labeled with the appropriate symmetry species cluster derived from Eq. 2. All 74 symmetry species predicted by Eq. 1 were accounted for in the $P(88)$ manifold of the spectrum.

It is at this point, however, that the remarkable order in the spectrum becomes most apparent. The cyclic pattern of intensities revealed in the fine structure is based on a cyclic ordering of clusters. Thus, on the right in Fig. 4c, reading backwards, there is a cycling of the four clusters A_1T_1E, T_2T_1, ET_2A_2, T_2T_1 (weights 16, 12, 24, 12, respectively, or $MWSW$), and on the left, a cycling of the three clusters T_2ET_1, $A_1T_1T_2A_2$, and T_2ET_1 (weights 20, 24, 20, or MSM). One notices in other rotational-vibrational transitions the regularity of these same sequences repeated over and over. Moreover, a specific order is continued into the superfine structure; each type of cluster has an order and relative spacing of symmetry species within it. Unexplained clusterings of energy levels are sometimes called accidental degeneracies, but it is clear that the SF_6 cluster degeneracies have a meaning.

Hints of clustering have emerged in other theoretical works. Analyses of ion-crystal-field thermodynamics contained some similar clusters in numerical solutions. Computer studies of rare-earth electronic spectra by Lea, Leask, and Wolf in 1962 provided the first evidence of clustering in angular momentum levels. Computer solutions of methane by Dorney and Watson in 1972 provided the first examples of clusters in molecular theory. But it was the spectral scans over a wide range of frequencies made available by tunable lasers at Los Alamos starting in 1974 and the exhaustive computer analyses of the second-order Hamiltonian by Galbraith, Krohn, Louck, and others that finally revealed the full extent and regularity of cluster patterns. However, the reason behind the remarkable regularity of the cluster patterns remained a mystery.

A CLASSICAL APPROACH. The physical origin of the cluster patterns was not understood until a classical, though approximate, approach to the problem was taken. This approach developed from a closer look at the possible orientations of the rotational axis for a given J relative to the symmetry axes of the molecule and the relationship of that orientation to centrifugal distortion of the rotating molecule.

Centrifugal distortion always increases the moment of inertia and therefore decreases the rotational energy for a given J. An octahedral SF_6 molecule has the least centrifugal distortion and thus the highest rotational energy for a given J when rotating around its fourfold symmetry axes, for these axes are along or perpendicular to its strong radial sulfur-fluorine bonds (Fig. 6). The rotational energy decreases if the rotation axis is along a twofold symmetry axis because then centrifugal force tends to bend four of the radial bonds, which is easier than stretching them. The molecule suffers the most distortion and therefore has the lowest rotational energy for a given J when rotating on its threefold symmetry axes, which lie exactly betwen radial bonds, thus allowing all six bonds to bend.

This can be seen if one uses the centrifugal distortion potential of the second-order Hamiltonian (Eq. 2) and plots this part of the SF_6 rotational energy radially on a globe. One finds hilltops, or local maxima, around the fourfold symmetry axes and valley bottoms, or local minima, around the threefold axes (Fig. 7a). The importance of this plot is that for a selected orientation of the axis of rotation one can judge the relative shift in the rotational energy due to centrifugal distortion and, thus, the corresponding relative shift in the absorption frequency.

But what orientations are allowed? The elementary quantum theory of angular momentum describes the allowed orientations of the rotational axis for an orbital state of angular momentum J. It states that the angular momentum vector has a length of $[J(J+1)]^{1/2}$ and that the z-component of the vector equals the azimuthal quantum number m, where m can assume values in integral jumps from J to $-J$. In other words, the J vector is constrained to lie on a cone of altitude m and slant length $[J(J+1)]^{1/2}$ (Fig. 7b). These cones can then be used to locate possible orientations of the axis of rotation with respect to the SF_6 rotational energy surface.

Which cones most closely approximate the cluster patterns? Figure 7c is a nomogram showing the select group of $J = 88$ angular momentum cones that generates the $P(88)$ absorptions of Fig. 4a. One sees that the high-frequency portion of the spectrum is associated with angular momentum cones intersecting the energy surface close to the fourfold-axis hilltops. Evidently the highest-m states ($m_4 = 88, 87, 86 \ldots$) are preferred; these are "low-uncertainty" states with the narrowest cones and the smallest uncertainty in transverse (x and y) components of momentum. The low-frequency portion of the $P(88)$ spectrum corresponds to similar low-uncertainty cones localized around threefold axes. The boundary between these regions contains a few disordered spectral lines. From Fig. 7c it is evident that these are associated with saddle points at the twofold symmetry axes. An angular momentum vector cannot be localized stably around these points; it is free to thread its way all around the globe, going from one saddle point to the next without changing its energy. When this happens, the molecule tumbles wildly like a diver doing uncontrolled gainers. Thus, the appropriate orientations of the rotational axes that account for almost the entire spectrum are those that have a high z-component of angular momentum along a fourfold or

threefold symmetry axis.

For many molecular states, including the SF_6 fundamental vibrational modes, the angular momentum nomograms are a useful alternative to expensive numerical solutions of the detailed Hamiltonian. Computer diagonalization of the Hamiltonian may bog down for angular momenta quanta that range into the hundreds, but the analytic approximations needed to generate the nomogram generally improve with higher quantum numbers. We might say that the analytic results inject a bit of classical common sense into an otherwise difficult quantum problem.

Patterns Within the Clusters

We now have some physical insight concerning the pattern of clusters. As already noted, there is further splitting and order within clusters, again predicted by the second-order Hamiltonian. However, a more classical approach is needed to achieve physical insight concerning this superfine splitting.

All clusters associated with the fourfold axes (*TT* or *ATE*) have six states; for example, the first A_1T_1E cluster on the right of Fig. 4c is made up of a singlet, a triplet, and a doublet—six states in all. This agrees with the fact that a given angular momentum cone can be oriented either up or down about any of three fourfold axes resulting in six equivalent states for each m_4 quantum number. The same reasoning applies to the clusters associated with threefold axes (*TET* or *ATTA*): each cluster has eight states and there are eight equivalent orientations about the four threefold axes for each m_3 quantum number.

But we know from saturation spectroscopy and the Hamiltonian analysis that the states within the clusters are not equivalent. Apparently, the rotational-energy-surface approach in which the orientation of the J axis remains fixed does not take fully into account the octahedral symmetry of the molecule. The additional effect that remedies this incomplete treatment, and that finally breaks the symmetry of the clusters into separate absorptions for each octahedrally invariant symmetry species, involves an interesting interplay between classical and quantum behavior.

ROTATIONAL TUNNELING. Briefly, tunneling of the rotational axis between apparently equivalent states causes the splitting. For example, the A_1T_1E cluster of $P(88)$ in Fig. 4c with $m_4 = 76$ is a cluster with its momentum localized around a fourfold symmetry axis at a hilltop. However, there are six such hilltops, one for each of the directions north, south, east, west, up, and down (Fig. 7a). Quantum theory allows a momentum vector or rotation axis to tunnel from one hilltop to another, which is not permitted in classical mechanics. Quantum tunneling can be understood to occur through resonance between equivalent states and can be expected between any states with the same or nearly the same energy.

It turns out that the tunneling effect is usually quite small and involves hilltops that are nearest neighbors only. For example, the up hilltop has a tunneling rate S with the east, north, west, and south hilltops because those hills surround it. The up-to-down tunneling amplitude, however, is nearly zero since these hills are too distant for appreciable tunneling.

One can find resonant combinations of the six hill states (called stationary states or eigenstates) whose energies are unchanged by the resonant action of nearest-neighbor tunneling. The first such state is an equal sum of all six hill states, so it is labeled by the singlet A_1 symmetry species (Fig. 8). If the classically expected value of a hilltop angular momentum state is H, then the A_1 singlet has an energy $(H - 4S)$ which is the classical value minus the effect of tunneling to the four nearest neighbors. The next three degenerate eigenstates are differences between antipodal hill states, for example, up minus down, and they are labeled by the triplet T_1 symmetry species. All three have the same energy (H) since there is no tunneling in this combination. Finally, there is a pair of E states, with the energy $(H + 2S)$ needed to conserve total energy for the cluster.

In this way one can decipher the intracluster structures. If one resolves an A_1T_1E grouping, three lines will appear with a T_1 line between the A_1 and E lines. The spacing should be $4S$ between A_1 and T_1 and exactly half this much between T_1 and E. This two-to-one ratio of spacing has been seen in virtually all A_1T_1E and A_2T_2E clusters that have been resolved in laser spectra. Similarly, the threefold clusters $A_1T_1T_2A_2$ and T_1ET_2 can be analyzed; one finds that their component lines are all equidistant. This is observed easily and with great precision in computer experiments, which can be as illuminating as those done in the spectroscopy laboratory.

In fact, some of the intracluster splittings due to rotational-axis tunneling will not be resolvable by any spectroscopic techniques. Figure 4c shows that the estimated values of many cluster splittings are so tiny that they will probably never be seen directly. The splitting of the fourfold clusters range from 2×10^{-4} to 2×10^{-22} cm^{-1}, the latter corresponding to a frequency of about one cycle in 50 centuries! The splittings are proportional to the axis tunneling rates S, or the rate at which the molecule may tumble in the absence of other perturbations. It is interesting to note that the smallest splittings are at the two ends of the $P(88)$ spectrum (Fig. 4c), that is for states with high m_4 or high m_3 in which the rotation axis is most localized. As the orientation of the axis moves away from either the fourfold or the threefold axis and toward the unstable saddle point region between, the splitting, and therefore the tumbling, of the molecule increases as expected.

However, whenever the energies of different states come arbitrarily close together, one should expect even small perturbations to have large effects. Most of the clusters in Fig. 4c have intracluster splittings due to axis tunneling that are less than 20 kilohertz, and this is comparable to or less than what is expected for the next level of splittings; the *intra*-species, or hyperfine, splitting. Normally, one would not expect nuclear spin-rotation perturbations to be large enough to have much influence, and the

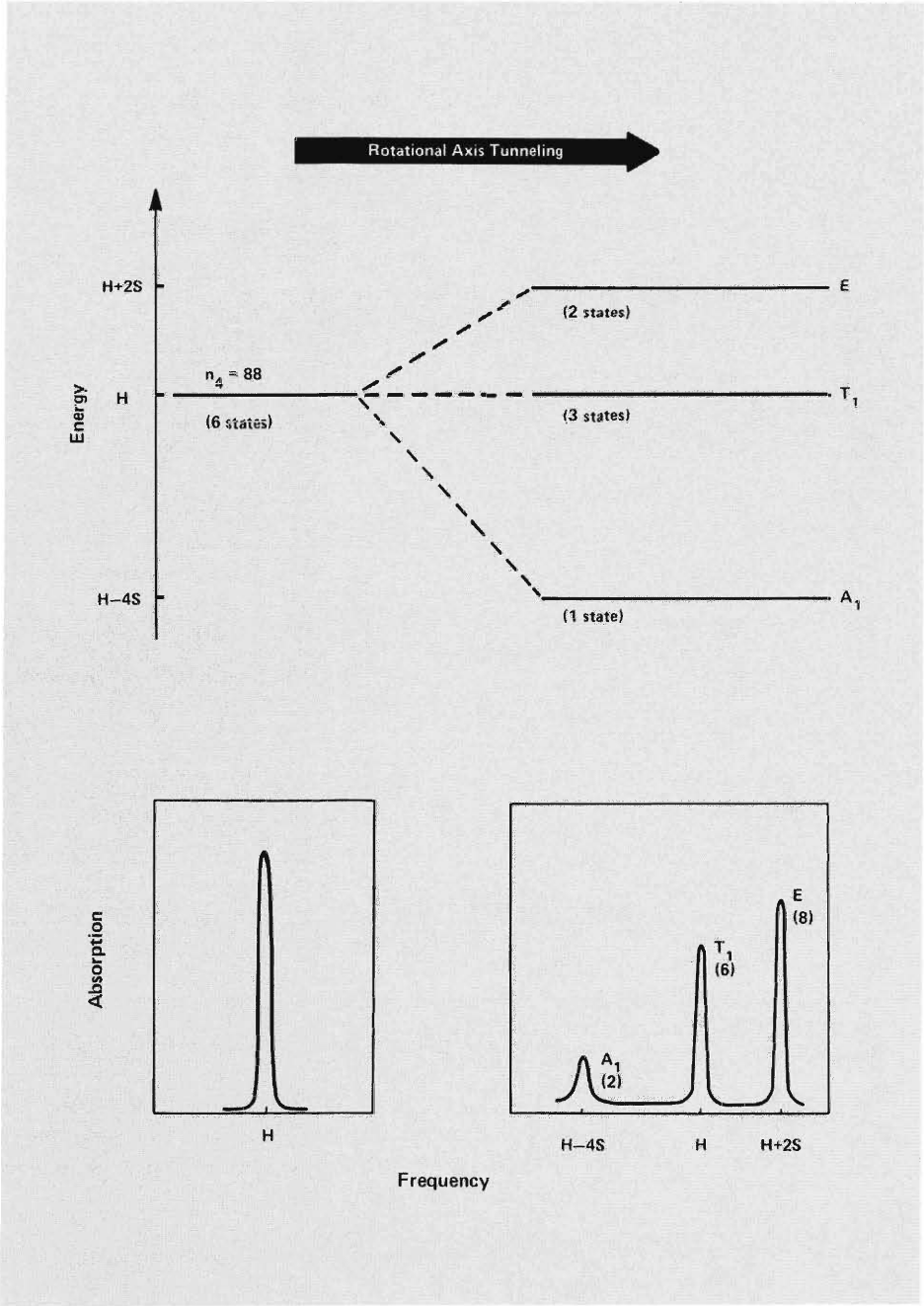

Fig. 8. Superfine structure. The effect of quantum mechanical tunneling between equivalent nearest-neighbor rotational-axis orientations is illustrated for an A_1T_1E *4-fold axis cluster in* P*(88). The mixing of the 6 possible* $m_4 = 88$ *states results in one state reduced in energy by 4 times the tunneling rate* (H − 4S) *and 2 states increased in energy by 2 times the rate* (H + 2S)*. In the absorption spectrum this corresponds to a distinctive 2-to-1 spacing of the peaks. When the relative heights of the* A_1, T_1, E *peaks (the corresponding nuclear-spin statistical weights are shown in parentheses) are also taken into account, the* A_1T_1E *cluster is easily identifiable.*

usual picture is of nuclear spin vectors riding like Ferris-wheel cars around a tumbling molecule. However, the clustering allows the nuclear spin precessional motion to be in resonance with the rotational motion, or for the spins to act in some ways like tiny gyrostabilizers that further retard tumbling. In essence, there must be a strong mixing between individual spin species and their spin multiplets so that A_1, A_2, E, F_1, and F_2 are, by themselves, no longer good labels of molecular states. This is very different from the usual situation in, say, hydrogen, where ortho and para species are like separate compounds. Research on the unexpected hyperfine effects associated with the small superfine splittings is still under way.

Molecular Constants

We now have some understanding of the origins of the complex rotational structure observed in the vibrational spectra of high-symmetry molecules. These considerations allow the spectroscopist to assign each absorption feature to a transition between specific quantized rotational-vibrational levels. If these assignments are used to fit a frequency expression derived from the appropriate Hamiltonian, then various molecular constants can be determined that measure the importance of each of the various effects.

To see how this is done, first consider the rotational absorptions in the P and R branches. To simplify the discussion, we deal only with the scalar approximation, in which $P(88)$, for example, would appear as a single peak.

The "line" positions are given by a polynomial in the total angular momentum quantum number J, which includes both normal rotational and vibrational angular momentum. For the R branch, the frequency expression, somewhat simplified, is

$$\nu_R(J) = \nu_0 + 2B(1 - \zeta)(J + 1) + \Delta B(J + 1)^2 - 4D(J + 1)^3 + \ldots . \quad (3)$$

The same equation holds for the P branch if $(J + 1)$ is replaced by $(-J)$.

The constants in Eq. 3 have the following significance. The first, ν_0, represents the band origin (that is, the frequency of the transition in a hypothetical nonrotating molecule). The constant B is the mean rotational constant of the two vibrational states involved in the transition and is inversely proportional to the mean molecular moment of inertia. The Coriolis constant ζ measures the amount of vibrational angular momentum in the normal mode (this effect will be treated more fully in the next section). The approximate difference $\triangle B$ between the rotational constants in the lower and upper states accounts for the change in the moment of inertia when the molecule is excited vibrationally. Finally, D is a centrifugal distortion constant. To give an idea of the magnitudes involved for ν_4 of SF_6 these parameters in cm^{-1} are

$\nu_0 = 615.020,$
$B(1 - \zeta) = 0.1108,$
$\triangle B = -1.96 \times 10^{-5},$
and
$D = 1.3 \times 10^{-8}.$

The P and R absorption peaks of Fig. 4a are thus spaced by approximately $2B(1 - \zeta) = 0.222\ cm^{-1}$ and their assignment is simply a matter of counting. For ν_3 of SF_6, on the other hand, the manifolds are much closer since $B(1 - \zeta) = 0.0279\ cm^{-1}$. This smaller separation is accompanied by larger tensor splittings in the ν_3 vibration so that the various component peaks overlap much more. As a result, isolated absorptions such as $P(88)$ cannot be observed in ν_3, and this explains the more compact nature of this band. The assignments can still be made, though the process is considerably more tedious.

After the assignments are complete, the energy level expression, including both the scalar part discussed above and tensor terms to describe splitting, is fitted to the data by a least-mean-squares procedure. The spectroscopic constants that result from this analysis specify the frequency of any given rotational-vibrational transition and provide an insight into the dynamics of the molecular motion.

In the Q branch the absorption frequencies, to the same scalar approximation, are given by

$$\nu_Q(J) = \nu_0 + \triangle B'J(J + 1) + \ldots . \qquad (4)$$

Here $\triangle B'$ is a constant similar but not identical to $\triangle B$ (in ν_4 of SF_6, $\triangle B' = 0.97\ \triangle B = -1.91 \times 10^{-5}\ cm^{-1}$). Note that there is no $B(1 - \zeta)$ term since the Q branch represents transitions with no change in rotational angular momentum energy. As a result, spacing between J-transition peaks in the Q branch is obviously much less than in the other branches, and in fact is less than the rotational-anisotropy splitting of each transition, even for small J. The resulting overlap accounts for the sharpness of the Q branch, and it makes assignments extremely difficult. In Fig. 2c, for example, the absorptions seen correspond to transitions arising from $J = 34$ to J values in the nineties, even for this short portion of the Q branch. However, various techniques, including computer synthesis of the branch contours, have enabled spectroscopists to make detailed assignments even in such difficult regions.

The precision with which the molecular parameters can be determined by these methods is remarkable. If the measurements are made with tunable diode lasers over a wide frequency range, the data set may consist of many hundreds of lines, which helps to insure a fit that is mathematically "robust" and resistant to possible errors in a few of the points. Saturation data typically consist of fewer lines, but the frequencies of these can be determined with precisions of the order of $10^{-7}\ cm^{-1}$. In fitting an "isolated" band—one not significantly perturbed by interactions with nearby energy levels—a lower-order spectroscopic parameter such as the band origin, ν_0, might be obtained with an uncertainty approaching that attached to the fundamental physical constants themselves. Results of this precision were beyond the reach of infrared techniques until the development of laser spectroscopy.

The Multiphoton Ladder

Up to this point we have been concerned with vibrational fundamentals, in which the transition is from the vibrational ground state to a singly excited upper vibrational level. Because of the electrical and mechanical anharmonicity of the vibrations, however, combination, difference, and overtone frequencies will also appear in the vibrational spectrum, though with greatly reduced intensities compared with the fundamentals. The hot bands and the overtones ($0 \rightarrow 2\nu_3$, $0 \rightarrow 3\nu_3$, etc.) are of special importance because they give information on the higher vibrational levels, which are very important in laser photochemistry.

When heavy symmetric molecules, such as UF_6, SiF_4, and SF_6, are irradiated using a high-power infrared laser coincident with a certain strong absorption feature, they can be vibrationally excited to the point of dissociation. In the case of SF_6 the dissociation occurs after the molecule absorbs some 30 infrared photons, whereas for UF_6 some 40 photons are required. The multiple-photon absorption of these and other molecules has fascinated chemists who are interested in bond-selective laser chemistry or in laser isotope separation.

Using a simple picture of the overtone levels of a spherical-top molecule, one might conclude that multiple-photon absorption is impossible. The first few energy levels, symbolized by $(n\nu_i)$, of a one-dimensional oscillator, such as the stretching mode ν_i of a linear molecule, are given by

$$(n\nu_i) = n(\nu_0) + X_{ii}n(n - 1) . \qquad (5)$$

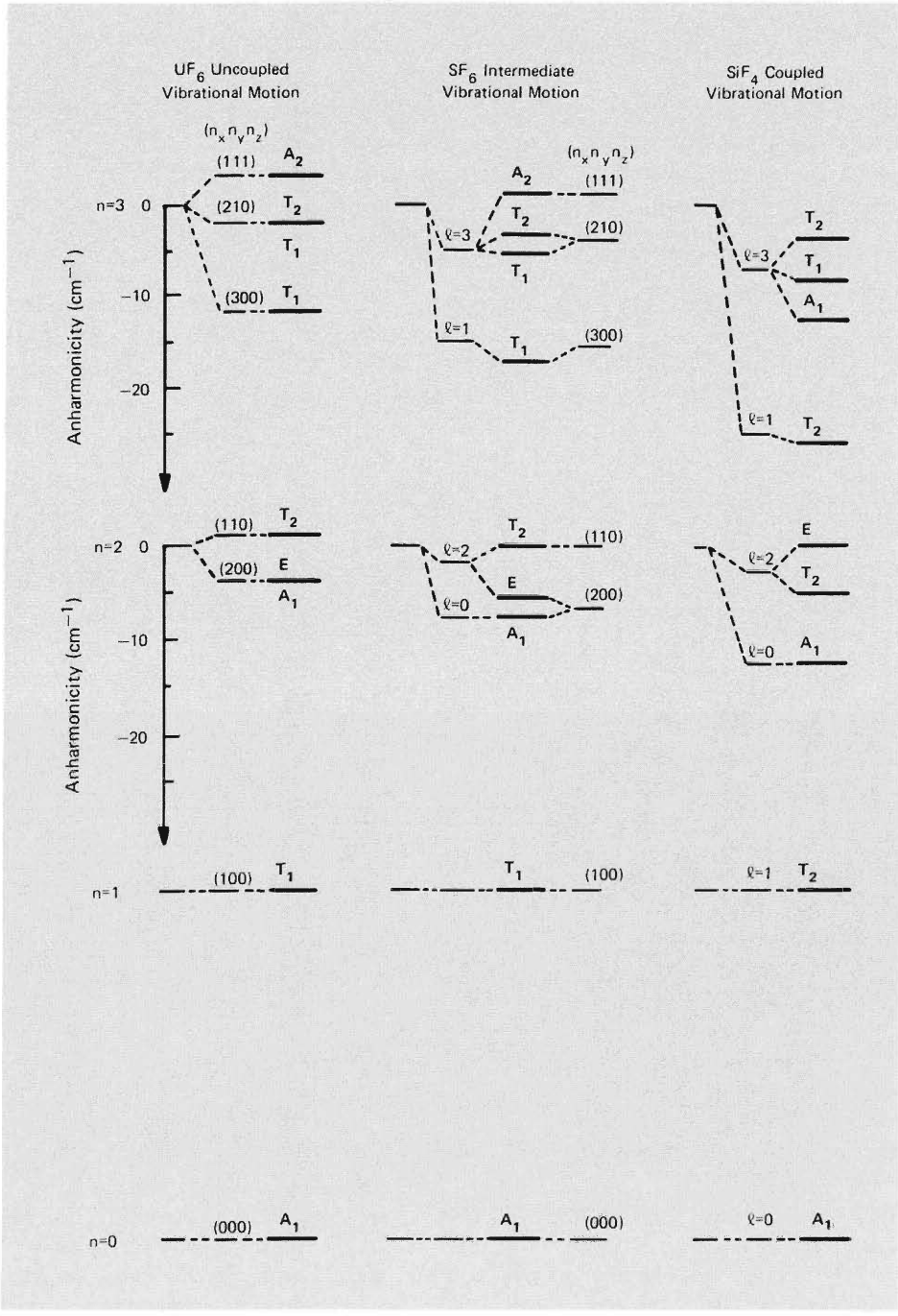

Fig. 9. The lower levels of the $n\nu_3$ *vibrational ladders of* UF_6, SF_6, *and* SiF_4, *showing the effects of anharmonicity and splitting. Because the three degenerate* ν_3 *components are strongly coupled in* SiF_4, *vibrational angular momentum is important and the quantum number* ℓ *is used to label the major energy-level splittings. At the opposite extreme, the large* UF_6 *molecule has uncoupled vibrational motion and the major energy level splittings are best described with separate quantum number* n_x, n_y, *and* n_z *for each of the three orthogonal motions.* SF_6 *is intermediate and must be dealt with as a mixture of both types of motion. The final energy states, after all splitting effects are accounted for, are labeled with their appropriate symmetry species.*

Note that here, as compared to Eqs. 3 and 4, the terms representing rotational structure have been dropped for simplicity, the principal quantum number n is multipled by the band origin of the fundamental to represent the amount of vibrational excitation, and a scalar term has been added to account for the main shift in energy due to anharmonicities. The anharmonic coefficient X_{ii} is usually negative ($X_{33} = -0.95$, -1.7, and -2.9 cm^{-1} for the ν_3 vibration of UF_6, SF_6, and SiF_4, respectively), which means that the energy levels are successively closer with increasing vibrational quanta. Thus for the nth photon absorbed, a laser emitting at frequency ν_0 will be detuned by $X_{ii}\, n(n-1)$ above the resonant energy level of the molecule. When this detuning exceeds the effective laser linewidth, further absorption becomes difficult. The detuning will be reduced somewhat by the rotational structure of the molecule, but this is generally not enough. In fact, linear molecules are known not to absorb many photons even at high laser intensities, for just this reason.

This simple picture does not correctly describe polyatomic molecules because they are multidimensional oscillators and their higher vibrational energy levels ($n \geq 2$) exhibit splitting. This splitting is shown in Fig. 9 for the ν_3 vibrations of UF_6, SF_6, and SiF_4.

The origin of the vibrational splitting lies, once again, in the fact that the various molecular motions are not independent. For example, with degenerate vibrations such as ν_3 or ν_4 the actual motion of the SF_6 molecule will be a combination with arbitrary phase of the degenerate modes. Each nucleus will thus move not in a linear fashion, but on the surface of an ellipsoid. These ellipsoidal motions introduce an angular momentum ℓ to the vibration such that the molecule's total angular momentum J is a vector combination of the vibrational and pure rotational angular momentum. The concept of vibrational angular momentum is most readily illustrated by the degenerate

bending mode of a linear triatomic molecule such as CO_2 (Fig. 10a). This mode consists of two component vibrations that are strictly planar when viewed separately, but when they are combined with a 90° phase difference, the resulting motion has a rotational character that generates a vibrational angular momentum. The more complex combination of just two components of the ν_3 stretching mode of SF_6 is depicted in Fig. 10b.

Because of such coupling phenomena as vibrational angular momentum, the splitting of the ν_3 vibrational energy level needs to be represented by two tensor terms that account for anharmonicities of motion both along the bond and perpendicular to the bond. In SF_6 these anharmonicities correspond, respectively, to bonding interactions between the sulfur and fluorine atoms, and nonbonding interactions between two adjacent fluorine atoms. If these terms are added to Eq. 5, the energies for the nth overtone of ν_3 may be adequately represented for $n < 5$ by

$$(n\nu_3) = n(\nu_0) + X_{33}n(n-1) + (G_{33} + 2T_{33})\ell^2 + T_{33}(10s - 8n - 6n^2) \ . \qquad (6)$$

The first tensor-splitting term, with the coefficient $(G_{33} + 2T_{33})$, is for nonbonding interactions and includes the vibrational angular momentum operator ℓ^2. The last term, with the coefficient T_{33}, includes both the anharmonic splitting operator s and the principal quantum number n; a dependence on n for this bonding-interaction term is not surprising since higher vibrational excitation leads to larger displacements along the bond and so to greater anharmonicities.

Again, because of the octahedral or tetrahedral symmetry of the UF_6, SF_6, and SiF_4 molecules, each vibrational level represented in the splitting belongs to one of the symmetry species A_1, A_2, E, T_1, or T_2. However, the directions and orders of shifting for these levels are seen to be quite

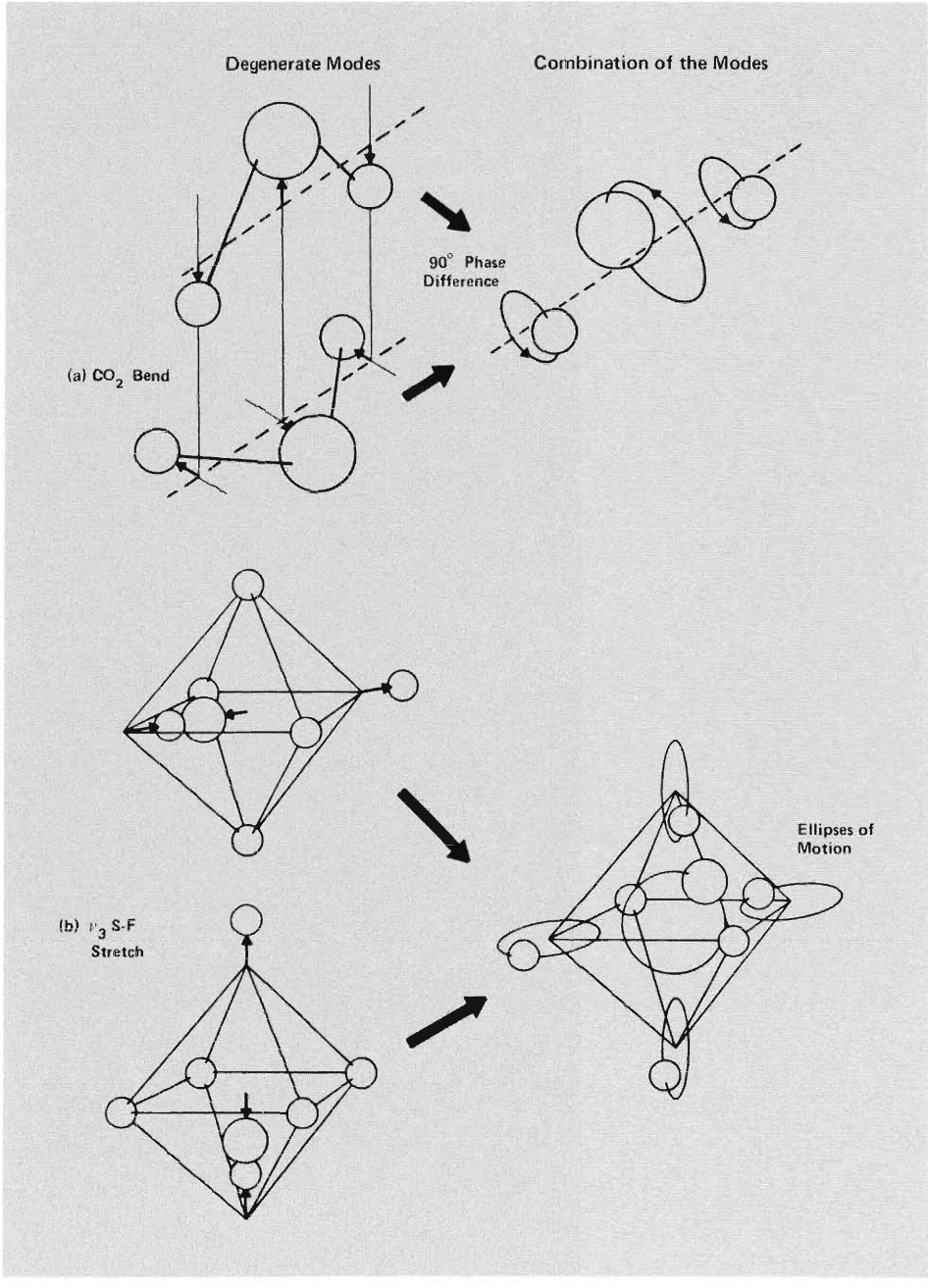

Fig. 10. Vibrational angular momentum. (a) If the two orthogonal components of the degenerate bending vibration of CO_2 are combined with a 90° phase difference, the bent molecule will generate vibrational angular momentum about the bond axis. (b) A similar but more complex situation exists for the degenerate vibrational modes of SF_6. Combination of the components of these modes with arbitrary phase will cause each nucleus to move on the surface of an ellipsoid. The 2-dimensional ellipses of motion that result from the combination of just two of the ν_3 components are depicted (the widths of the four ellipses have been exaggerated for clarity). Vibrational angular momentum ℓ interacts with the angular momentum J of the molecule as a whole and is accounted for in the Hamiltonian with a $J \cdot \ell$ Coriolis force term and higher-order tensor terms.

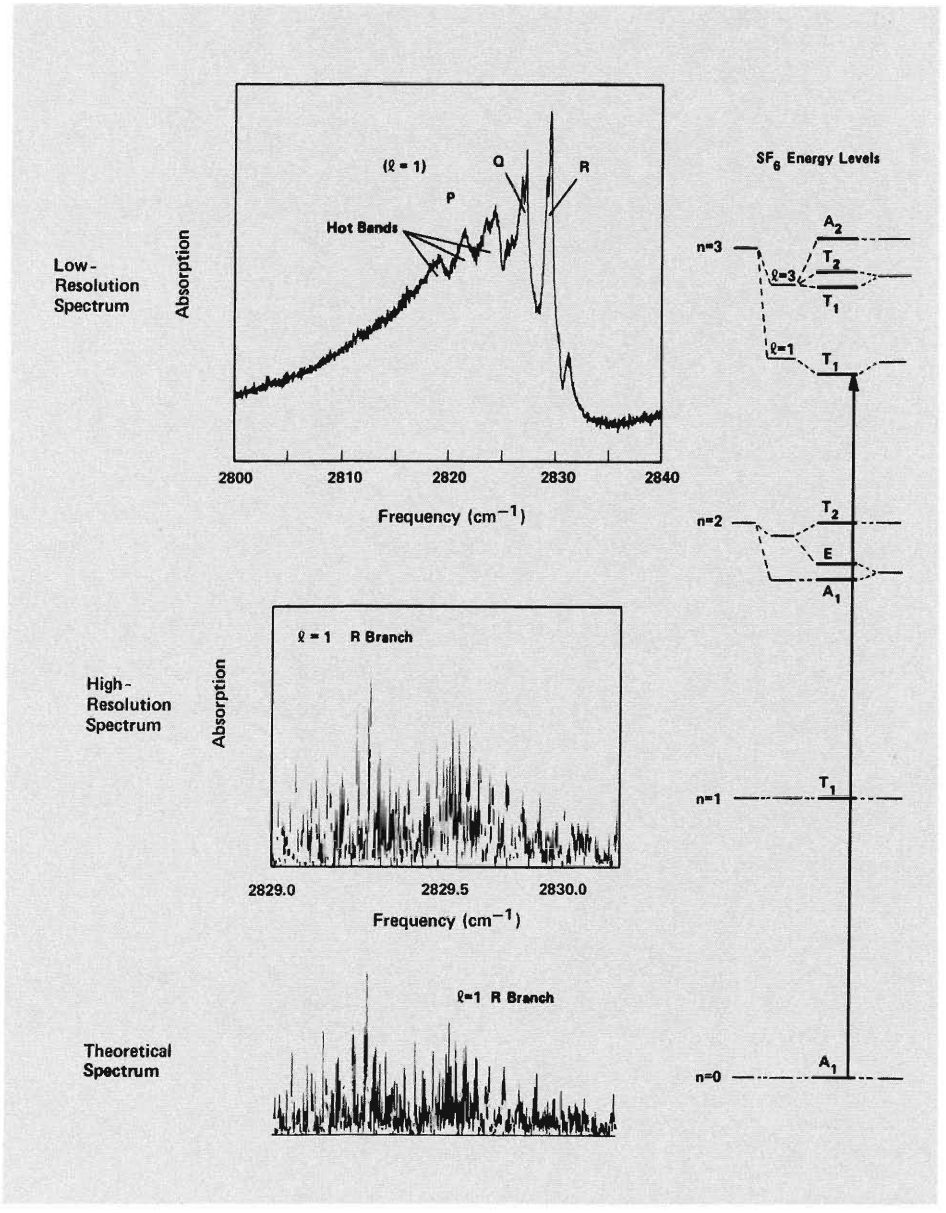

Fig. 11. The overtone $3\nu_3$ of SF_6. The upper spectrum was obtained with a Fourier-transform infrared interferometer at a resolution of 0.04 cm^{-1}. The middle spectrum is a Doppler-limited scan recorded by A. S. Pine at the MIT Lincoln Laboratory using a difference frequency spectrometer. It shows the rotational fine structure of the R *branch of the $\ell = 1$ transition; the vibrational energy transition corresponding to this spectrum is shown on the energy level diagram at the right. The bottom panel illustrates the match that is possible with a theoretical simulation of the spectrum.*

different for the three molecules depicted in Fig. 9. In fact, there is an opposite limiting behavior for SiF_4 and UF_6; SF_6 is intermediate between the two extremes. The reason for the differences lies in the relative importance of the two tensor splitting terms in Eq. 6.

For the case of SiF_4 we find, from analysis of the $3\nu_3$ spectrum, that $T_{33} \ll (G_{33} + 2T_{33})$. In this limit the ℓ^2 operator results in vibrational angular momentum values of the form $\ell(\ell + 1)$, where ℓ is the vibrational angular momentum quantum number. The allowed values of ℓ are n, $n-2$, $n-4$, ..., 1 or 0, and for SiF_4 ℓ is nearly a good quantum number. In other words, the major energy shifts for SiF_4 (labeled in Fig. 9 with ℓ) are due to the ℓ^2 operator. These levels lie at the center of gravity of the smaller shifts (labeled with the appropriate symmetry species) due to the s operator.

The physical significance of the dominance of the nonbonding interaction term for SiF_4 is that the three orthogonal motions of the degenerate ν_3 vibration are strongly coupled by the angular anharmonicity. This should be expected for SiF_4, which has a small, light central atom and crowded fluorine atoms that are able to "see" each other as they vibrate.

For UF_6 we find, again from analysis of the $3\nu_3$ spectrum, that $T_{33} \gg (G_{33} + 2T_{33})$. In other words, bonding interactions dominate here. In this limit the s operator has values of the form $n_x^2 + n_y^2 + n_z^2$, where n_x, n_y, and n_z refer to uncoupled motions in the three perpendicular directions. These three quantum numbers describe excitations of independent simple harmonic oscillators, and each assumes the values 0, 1, 2, ... Thus, in Fig. 9, the major energy shifts for UF_6 are labeled $(n_x\, n_y\, n_z)$ while the finer splittings due to the ℓ^2 operator are labeled with symmetry species labels.

Because of the independence of the oscillations in the three directions, the motions can be described as localized vibrational modes rather than as normal modes of the molecule as a whole. This "local mode" concept has been used extensively in treating certain molecules like benzene (C_6H_6) in which stretching motions of the C-H bonds behave as though each bond were isolated from the rest of the molecule. Although this does not strictly happen in UF_6, each of the three degenerate vibrations of the ν_3 mode does behave here as if it didn't see the other two. In fact, model calculations by B. J. Krohn have shown that when the nonbonding interactions are weak and the mass of the central atom is much larger than that of a fluorine atom (which is the case for UF_6), then the ratio G_{33}/T_{33} approaches -2 and the ℓ^2 term tends to zero.

The drastic difference in the structure of energy levels between SiF_4 and UF_6 also leads to different selection rules, or pathways, for multiple-photon absorption. Since SF_6 is in an intermediate region, it shares some of the characteristics of both SiF_4 and UF_6, and its pathways are the most complicated. In Fig. 9 the effect of its nonbonding interaction term is shown to the right, the effect of the bonding interaction term to the left, and the final energy levels in between.

It is clear from Fig. 9 that the anharmonic splitting of the ν_3 overtones partially compensates for the overall shift of levels to lower energy as discussed above, so that multiple-photon pathways become accessible. The rotational structure of the molecules further splits the levels and helps to minimize laser detunings.

As already mentioned, the anharmonic constants X_{33}, G_{33}, and T_{33} determining the $n\nu_3$ energy levels of Fig. 9 were derived from analyses of the rotational-vibrational levels of the $3\nu_3$ high-resolution spectra for each of the three molecules studied. Typical low- and high-resolution spectra are shown in Fig. 11 for the $3\nu_3$ band for SF_6.

Only the $\ell = 1$ transitions of $3\nu_3$ are shown and, in fact, transitions to the three $\ell = 3$ levels are weak for the three molecules studied. We were able to determine their positions primarily by their influence on the $\ell = 1$ rotational-vibrational levels.

In order to duplicate the complicated structure revealed in Fig. 11, we needed seven rotational-vibrational constants in addition to the three anharmonic constants. With these 10 constants we fitted over 700 lines of the $3\nu_3$ SF_6 spectrum with a standard deviation of 4×10^{-4} cm^{-1}. In constrast, a much simpler ν_3 spectrum of CH_4 recently required over 60 constants to give a fit of 0.02 cm^{-1}. Although the resolution necessary for heavy symmetric molecules causes experimentalists difficulties, such molecules are certainly much nicer for theoreticians!

Once the first few rungs of the ν_3 ladder

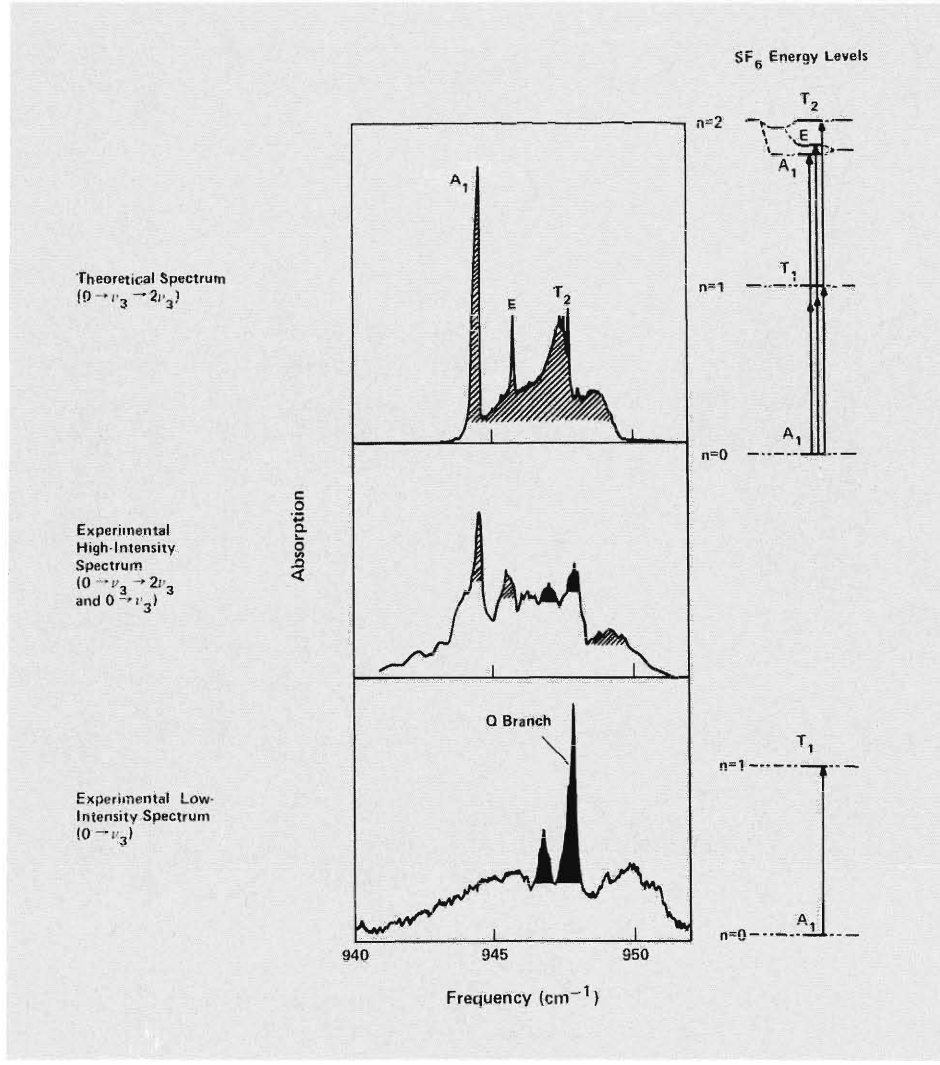

Fig. 12. Two-photon absorption. The lowest panel is a normal low-intensity absorption spectrum for the ν_3 vibrational mode of SF_6 (similar to Fig. 2a, but recorded with fewer absorbing molecules), and thus represents single-photon transitions from the ground state (n = 0) to the first excited state (n = 1) as shown on the right. The high-intensity (3 megawatts per square centimeter) spectrum in the middle (observed by S. S. Alimpiev et al. *at the Lebedev Physics Institute, Moscow) still has the single-photon peaks (black) and, in addition, has peaks that can be attributed to two-photon jumps between the n = 0 and n = 2 levels (shaded). The theoretical shape of just the two-photon contribution to the spectrum, based on an analysis of $3\nu_3$, is shown at the top with the appropriate $0 \rightarrow \nu_3 \rightarrow 2\nu_3$ energy transitions to the right (shifts in the n = 2 levels are exaggerated). The lower-frequency A_1 and E transitions are obvious in the high-intensity spectrum, whereas the T_2 transition apparently overlaps the normal $0 \rightarrow \nu_3$ absorption.*

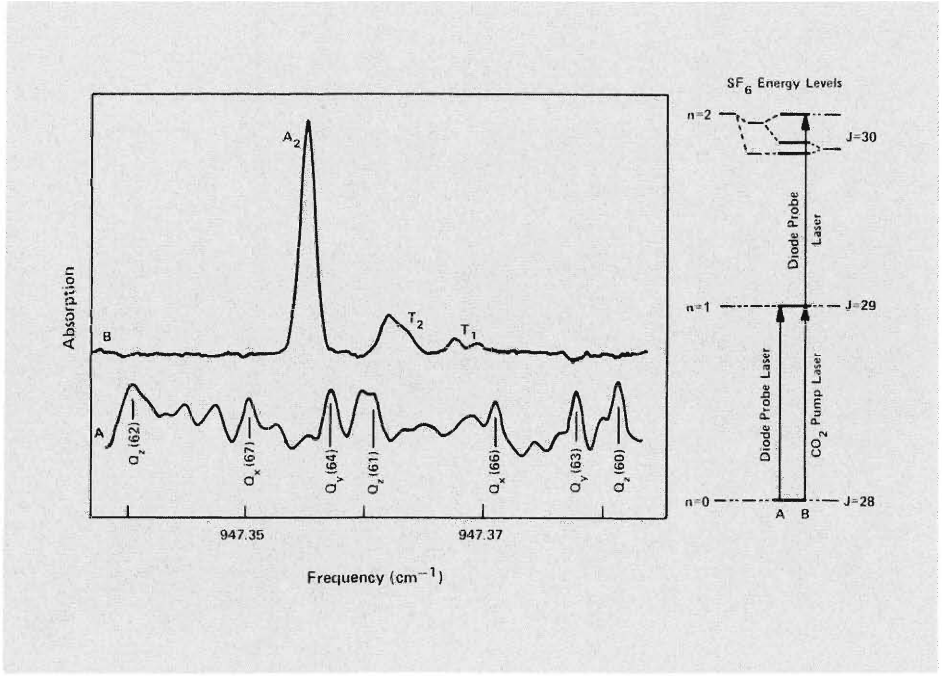

Fig 13. Trace B is a portion of the $\nu_3 \rightarrow 2\nu_3$ double-resonance spectrum of SF_6, recorded by P. F. Moulton and A. Mooradian at the MIT Lincoln Laboratory. A CO_2 laser pumps R(28) of ν_3, populating the J = 29 upper state, while the diode probe laser scans over the $\nu_3 \rightarrow 2\nu_3$ R(29) transition. The diode laser is able to resolve rotational fine structure, and this particular spectrum shows three of the four peaks of an $A_1T_1T_2A_2$ cluster. Trace A is a scan with the pump laser turned off; the resulting ν_3 Q-branch spectrum, similar to that of Fig. 2c, is used to calibrate the frequency.

have been determined, one can characterize the frequency dependence of the multiple-photon absorption. Figure 12 shows a comparison of the theoretical two-photon ($0 \rightarrow$ "ν_3" $\rightarrow 2\nu_3$) absorption spectrum of SF_6 with the high-intensity absorption actually observed using a tunable high-pressure CO_2 laser. In a two-photon resonance, in contrast to a single-photon ($0 \rightarrow 2\nu_3$) transition (which is forbidden), both steps ($0 \rightarrow$ "ν_3" and "ν_3" $\rightarrow 2\nu_3$) are allowed, but the intermediate "ν_3" level is a virtual state that is detuned from the true position of ν_3; this two-photon resonance is shown in the upper set of energy levels of Fig. 12. The one-photon to ν_3 (black) and two-photon to $2\nu_3$ (shaded) spectra account for most of the features seen. The remaining features can be accounted for by higher-order multiphoton resonances. The three peaks in the calculated two-photon spectrum correspond to transitions to the A_1, E, and T_2 levels of $2\nu_3$. The fact that these absorptions range from 944 cm^{-1} for A_1 up to 948 cm^{-1} for T_2 supports the idea discussed earlier that there are good pathways up the ladder at frequencies close to the fundamental at 948 cm^{-1}. Similar analyses for UF_6 have led to predictions of the best pathways for dissociating this molecule in an isotopically selective manner.

With two lasers one can more easily probe the $2\nu_3$ levels of SF_6 by tuning the first laser to a real $0 \rightarrow \nu_3$ transition and the second to allowed $\nu_3 \rightarrow 2\nu_3$ transitions. In such a double-resonance technique, the lasers are both tuned to a particular rotational J level for the intermediate ν_3 step: that is, one laser excites molecules into this J level at ν_3 while the second laser continues the excitation by pumping them out of that level and up to $2\nu_3$. The results of such an experiment are shown in Fig. 13. Here SF_6 is pumped by a CO_2 laser with peak intensity less than 1 kilowatt per square centimeter, so that only the ν_3 rotational-vibrational levels are significantly populated and multiple-photon processes are minimized. The transient change in the absorption of a second (tunable diode) laser beam, caused by the presence of the pump signal, is recorded as the double-resonance signal. The three peaks in the figure represent a small portion of the rotational fine structure of the $\nu_3 \rightarrow 2\nu_3$ $R(29)$ transition. The same constants used in the $3\nu_3$ analysis can be used to analyze the $2\nu_3$ spectrum as well. As a result, some 24 double-resonance signals have been assigned and the predicted $2\nu_3$ vibrational levels in Fig. 9 are now confirmed.

Although even higher anharmonicity contants become important further up the ladder ($n > 5$), we have used the constants X_{33}, G_{33}, and T_{33} to calculate the energy levels of $20\nu_3$ in order to elucidate the generic properties of the vibrational level splitting. In Fig. 14 are plotted the energy levels as a function of T_{33} ($G_{33} = 1.0$) such that the local-mode quantum numbers (n_x n_y n_z) describe the motion on the far left and the vibrational angular momentum quantum numbers ℓ describe the motion on the far right. One may think of this plot as representing UF_6 on the left, SiF_4 on the right, and SF_6 in the middle.

The levels are plotted in Fig. 14 with each class of symmetry species, A, E, and T, represented by a different color (red, green, and dark blue, respectively). Thus, whenever two or more symmetry species coincide or cluster, a new color is formed. For example, an ATE cluster mixes red, green, and dark blue to form a light yellow line while an $A_1T_1T_2A_2$ cluster results in a pink line.

Despite the fact that this analysis represents vibrational rather than rotational excitation, the various levels here appear to cluster as well. This is especially true on the near right for the ℓ-dominated SiF_4 molecule, where the preponderance of pink ($A_1T_1T_2A_2$) and light blue (T_1ET_2) indicates vibrations quantized about the threefold symmetry axis while the dark blue (T_1T_2) indicate vibrations quantized about the fourfold axis. Also, surprisingly, the fourfold axis clusters seem to be conserved even in the intermediate region for SF_6.

The consequences of this for vibrational intramolecular relaxation and multiple-photon pathways are being investigated. In particular, transitions are strongly allowed only between energy levels of the same symmetry species. At the extreme right, with no splitting of energy levels, there is strong coupling between the many states of a given ℓ level, and the density of states available for each vibrational energy transition is large. But as one moves to the left, the splitting breaks up the states into clusters of different symmetry. This clustering, in effect, reduces the density of states connected by vibrational transitions or other intramolecular processes because interactions should occur only between clusters of the same color.

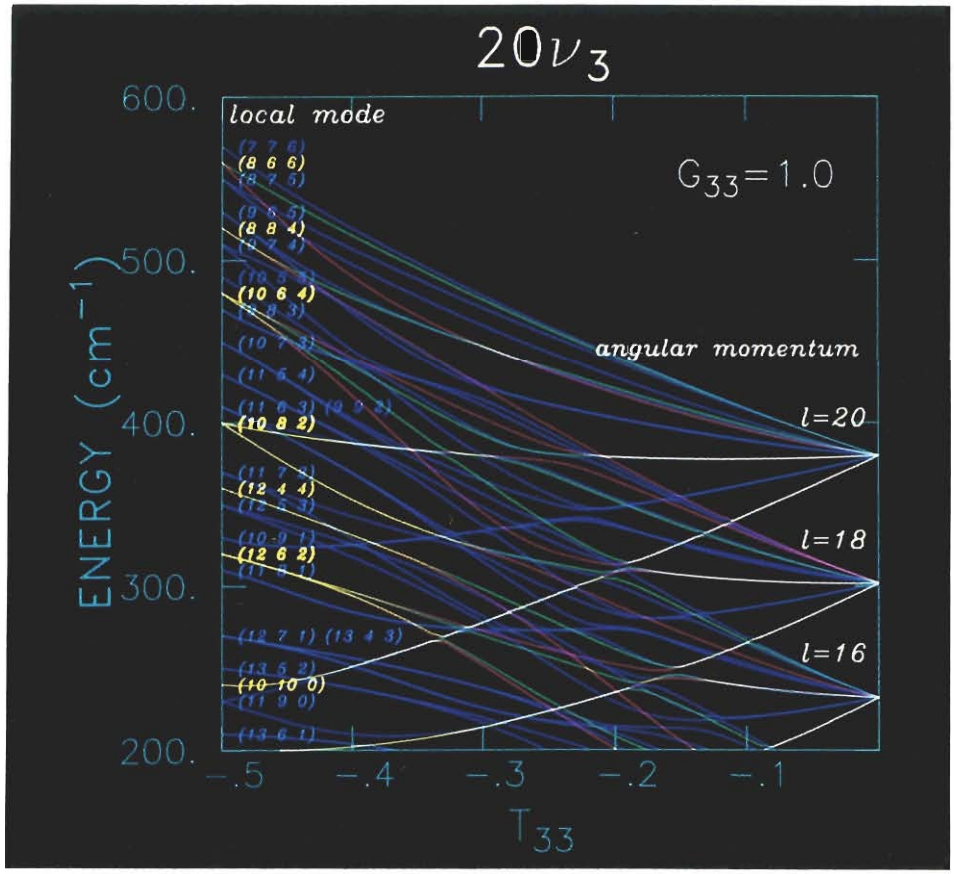

Fig. 14. Model anharmonic splitting in the overtone band $20\nu_3$. The vibrational energy levels shown here as a function of the anharmonicity constant T_{33} are represented with a different color for each class of symmetry species (A—red, E—green, and T—dark blue). Thus, the vibrational clustering of two or more symmetry species forms new colors with 4-fold clusters appearing as light yellow (ATE) and dark blue (TT), and with 3-fold clusters appearing as light blue (TET) and pink (ATTA). An angular-momentum dominated molecule such as SIF_4 would fall to the right of the graph while a local-mode molecule such as UF_6 would be to the left.

Reaping the Benefits

Once the energy-level code had been unraveled for the prototypical molecules, the spectra of other similar molecules became much easier to decode. One dramatic example was CF_4, a material that can be made to lase effectively in the photochemically important 630-cm^{-1} (16-micrometer) region.

J. J. Tiee and C. Wittig first demonstrated in 1976 that when the $\nu_2 + \nu_4$ combination band of CF_4 near 1066 cm^{-1} is pumped with a CO_2 laser, stimulated emission occurs on the $(\nu_2 + \nu_4) \rightarrow \nu_2$ transition (Fig. 15). However, since CF_4 is a heavy, tetrahedrally symmetric molecule, its vibrational bands consist of the typical array of finely spaced absorptions. The actual CF_4 lasing frequency may range from 605 to 655 cm^{-1}, depending on the particular absorption pumped. While this large range of lasing frequencies is potentially an advantage, control and prediction of the actual lasing frequency is a problem. With a given pump frequency overlapping several absorptions, lasing may occur at several widely separated frequencies, and the laser has a marked tendency to switch frequencies from moment to moment.

Analysis of the pump band absorption, $\nu_2 + \nu_4$, showed this degenerate vibrational state to be split by Coriolis forces. Recognition of the origin of the $\nu_2 + \nu_4$ structure led to detailed assignments for the absorptions; selection rules for the lasing transitions

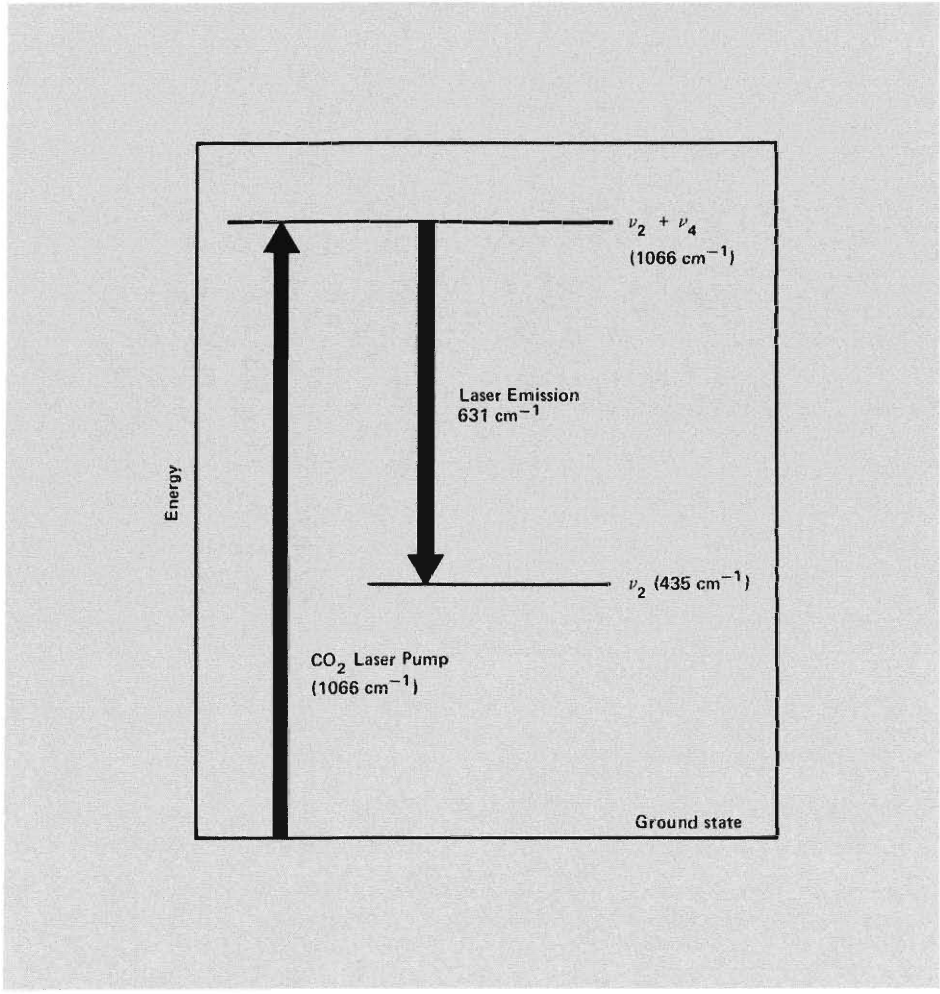

Fig. 15. Vibrational energy level diagram for the CO_2-pumped CF_4 laser.

TABLE I

BOND LENGTH IN CF_4

Vibrational State	C-F Bond Length (angstroms)
ground state	1.31943
ν_4	1.31907
ν_2	1.32062
$\nu_2 + \nu_4$	1.32028

that result from each absorption followed immediately. Using the molecular constants obtained from the $\nu_2 + \nu_4$ analysis and the frequencies of a few dozen known laser transitions, the assignments were made for the difference band $\nu_2 \rightarrow \nu_2 + \nu_4$. The final result was a frequency expression for the lasing transitions that predicts the strongest of these to within a few thousandths of a cm^{-1}, which is more accurate than can be measured at present.

The analysis discussed above has enabled the CF_4 laser to be designed to emit at specific frequencies that might be desirable in particular photochemical experiments. It has also enabled the frequencies of isotopic forms of CF_4 to be predicted. As a by-product of this analysis, the ground- and excited-state rotational constants have been separately determined, which is not possible from the infrared spectrum of a vibrational fundamental alone. From these the effective bond lengths in the various vibrational states can be obtained (Table I), all with an estimated uncertainty of ±0.00009 angstrom. These results should be compared with those obtained by diffraction methods, which are accurate to only a few thousandths of an angstrom at best, and give a bond length that is the effective average over all of the populated vibrational states.

The benefits of high-resolution laser spectroscopy are many. With CF_4, both precise molecular constants and the fine details of a lasing system are provided. With UF_6, the spectroscopy helps map the alternative pathways to photochemical dissociation necessary for the molecular isotope separation of uranium. The analyses of SF_6 and SiF_4 have led to a detailed understanding of the molecular energy levels that are pumped by CO_2 laser radiation in various nonlinear optical experiments. But perhaps the greatest benefits will come from our understanding of molecular dynamics, such as the insight that for heavy, symmetric molecules both rotational and vibrational motion are quantized about symmetry axes. ■

Acknowledgments

The Applied Photochemistry Division high-resolution spectroscopy program has drawn on the expertise of numerous people. It is a pleasure to thank our Los Alamos colleagues who have contributed to this work at one time or another: J. P. Aldridge, R. F. Begley, E. G. Brock, M. I. Buchwald, C. D. Cantrell, H. Filip, H. Flicker, H. W. Galbraith, R. F. Holland, C. R. Jones, R. C. Kennedy, K. C. Kim, B. J. Krohn, G. A. Laguna, J. D. Louck, N. G. Nereson, L. J. Radziemski, M. J. Reisfeld, D. M. Seitz, M. S. Sorem, J. M. Telle, and M. C. Vasquez. We also wish to acknowledge fruitful collaborations with P. Esherick and A. Owyoung (Sandia National Laboratories), K. Fox (University of Tennessee), L. Henry (University of Paris), E. D. Hinkley, A. Mooradian, and P. F. Moulton (the Massachusetts Institute of Technology Lincoln Laboratory), D. W. Magnuson and D. F. Smith (Oak Ridge Gaseous Diffusion Plant), J. Moret-Bailly (University of Dijon), J. Overend (University of Minnesota), W. B. Person (University of Florida), F. R. Petersen and J. S. Wells (National Bureau of Standards, Boulder), A. S. Pine (National Bureau of Standards, Gaithersburg), and A. G. Robiette (University of Reading).

Further Reading

J. I. Steinfeld, *Molecules and Radiation: An Introduction to Modern Molecular Spectroscopy* (Harper & Row, New York, 1974).

V. S. Letokhov, "Problems in Laser Spectroscopy," Soviet Physics Uspekhi (English Translation) **19**, 109-136 (1976).

M. J. Colles and C. R. Pidgeon, "Tunable Lasers," Reports on Progress in Physics **38**, 329-460 (1975).

C. R. Pidgeon and M. J. Colles, "Recent Developments in Tunable Lasers for Spectroscopy," Nature **279**, 377-381 (1979).

R. S. McDowell, "High Resolution Infrared Spectroscopy with Tunable Lasers," Advances in Infrared and Raman Spectroscopy **5**, 1-66 (1978).

R. S. McDowell, "Vibrational Spectroscopy Using Tunable Lasers," Vibrational Spectra and Structure **10**, 1-152 (1981).

J. D. Louck and H. W. Galbraith, "Eckart Vectors, Eckart Frames, and Polyatomic Molecules," Reviews of Modern Physics **48**, 69-106 (1976).

W. G. Harter, C. W. Patterson, and F. J. da Paixao, "Frame Transformation Relations and Multipole Transitions in Symmetric Polyatomic Molecules," Reviews of Modern Physics **50**, 37-83 (1978).

W. G. Harter and C. W. Patterson, "Theory of Hyperfine and Superfine Levels in Symmetric Polyatomic Molecules. I. Trigonal and Tetrahedral Molecules: Elementary Spin-1/2 Cases in Vibronic Ground States," Physical Review A **19**, 2277-2303 (1979).

W. G. Harter, "Theory of Hyperfine and Superfine Levels in Symmetric Polyatomic Molecules. II. Elementary Cases in Octahedral Hexafluoride Molecules," Physical Review A **24**, 192-264 (1981).

H. W. Galbraith, C. W. Patterson, B. J. Krohn, and W. G. Harter, "Line Frequency Expressions for Triply Degenerate Fundamentals of Spherical Top Molecules Appropriate for Large Angular Momentum," Journal of Molecular Spectroscopy **73**, 475-493 (1978).

H. W. Galbraith and J. R. Ackerhalt, "Vibrational Excitation in Polyatomic Molecules," in *Laser-Induced Chemical Processes*, J. I. Steinfeld, Ed. (Plenum Press, New York, 1981), pp. 1-44.

C. W. Patterson, B. J. Krohn, and A. S. Pine, "Interacting Band Analysis of the High-Resolution Spectrum of the $3\nu_3$ Manifold of SF_6," Journal of Molecular Spectroscopy **88**, 133-166 (1981).

C. W. Patterson, R. S. McDowell, P. F. Moulton, and A. Mooradian, "High-Resolution Double-Resonance Spectroscopy of $2\nu_3 \leftarrow \nu_3$ Transitions in SF_6," Optics Letters **6**, 93-95 (1981).

R. S. McDowell, C. W. Patterson, C. R. Jones, M. I. Buchwald, and J. M. Telle, "Spectroscopy of the CF_4 Laser," Proceedings of the Society of Photo-Optical Instrumentation Engineers **190**, 262-269 (1979).

C. W. Patterson, R. S. McDowell, and N. G. Nereson, "Emission Frequencies of the CF_4 Laser," IEEE Journal of Quantum Electronics **QE-16**, 1164-1169 (1980).

AUTHORS

Robin S. ("Rod") McDowell is a molecular spectroscopist who has seen infrared resolving power increase a millionfold over the past 20 years and who was among the first to apply this capability to the detailed analysis of vibrational spectra. He received his Bacheolor of Arts from Haverford College in 1956 and spent two summers at Los Alamos while in graduate school at Massachusetts Institute of Technology. His work with Llewellyn H. Jones in the Inorganic Chemistry Group drew him back to Los Alamos after he obtained his Ph.D. in 1960. After 15 years in the Chemistry-Nuclear Chemistry Division, the spectroscopic opportunities offered by the development of tunable infrared lasers attracted him to Project Jumper, and he is now Assistant Group Leader of the Applied Photochemistry Division's Laser Chemistry Group. In 1975 he and Hal Galbraith first untangled and assigned the complex rotational-vibrational spectrum of SF_6, and he has continued to work on high-resolution infrared and Raman spectroscopy, the analysis of molecular energy levels, and spectroscopic applications to laser development. He has published 80 scientific papers, including two review articles on laser spectroscopy, and shared the Los Alamos Optical Society Award for the Outstanding LASL Paper in Optics in 1979. (Photo by Henry F. Ortega)

Chris W. Patterson was born in Los Angeles, California, on August 1, 1946. He received his Bachelor of Science and Ph.D. degrees in physics from the University of Southern California at Los Angeles in 1968 and 1974, respectively. From 1974 to 1977 he was an Assistant Professor at the Institute of Physics of the University of Campinas, Sao Paulo, Brazil, where he worked on the application of the unitary group to the electronic orbital theory of atoms and molecules. Since 1977 he has been a Staff Member in the Theoretical Division of the Laboratory. His recent work is on the theory of the rotational-vibrational and hyperfine structure of molecules and the modeling of optically pumped molecular lasers in support of the laser isotope separation program. He is a member of Phi Beta Kappa and the Los Alamos Chapter of the Optical Society of America, and shared the Los Alamos Optical Society Award for the Outstanding LASL Paper in Optics in 1979. He was recently named the 1982 recipient of the Coblentz Society Award, which is given in recognition of exceptional work by a molecular spectroscopist before the age of 35. (Photo by Henry F. Ortega)

William G. Harter is a Professor of physics at the Georgia Institute of Technology and a consultant for the Laboratory's Theoretical Division. He received the first doctorate in physics granted by the University of California at Irvine in 1967. After serving a postdoctoral term at Irvine, he joined the physics faculty at the University of Southern California, and in 1974 he took a position at the University of Campinas in Brazil. He was a Visiting Fellow of the Joint Institute for Laboratory Astrophysics at the University of Colorado in Boulder before assuming his present position in 1978. His research interests include symmetry analysis for spectroscopy, applications of permutation and unitary groups, and at present the theory of spectral clusters. Dr. Harter first saw the cluster problem presented by Los Alamos researchers at a symposium in 1975. After constructing some simple rotational cluster model solutions he began a collaboration with Los Alamos from which these models have been further developed and extended. Dr. Harter is even trying to make rotational group theory commercially successful. He is currently marketing a rotational group slide rule and will soon produce an unusual pocket sundial that predicts, among other things, how long human skin can stand the Los Alamos sun on any given day. (Photo by Sarah Harrell, Georgia Institute of Technology)

MULTIPLE-PHOTON EXCITATION

The multiple-photon effect, in which a single polyatomic molecule absorbs many infrared photons, is proving to be a complex and still mysterious phenomenon in laser photochemistry.

by John L. Lyman, Harold W. Galbraith, and Jay R. Ackerhalt

There is no doubt that lasers have revolutionized photochemistry. Initially, the main attraction of lasers was the highly monochromatic nature of the light; many researchers hoped that this feature might serve as the basis for bond-selective photochemistry and for laser-induced isotope separation. However, in the early 1970s another rather surprising feature was discovered involving the interaction of infrared laser light and polyatomic molecules.

This phenomenon, multiple-photon excitation, is the absorption of many infrared photons of the same frequency by a single molecule. Observation of this phenomenon was only possible with the high light intensities typical of lasers. It was a surprising effect because multiple-photon excitation did not fit the established theoretical pictures of how molecules absorb radiation. While considerable experimental and theoretical work has now been directed toward understanding this phenomenon, much remains to be explained.

One can think of multiple-photon excitation or absorption as high-intensity spectroscopy. As such, it is qualitatively different from normal low-intensity spectroscopy. At low intensities relatively small numbers of photons delicately probe individual energy transitions. Typically, the molecules occupy a known equilibrium distribution of energy states, and, for a given absorption frequency, only a small fraction of these are moved to a single excited state. On the other hand, multiple-photon excitation necessarily affects large fractions of the molecules and drives them through many energy states. In fact, since the absorbed energy becomes vibrational energy, the resulting high degree of vibrational excitation drastically alters the chemical nature of the molecule, even to the point of dissociation. The dissociative reaction led to fulfillment of the early hope for laser isotope separation.

As a result of these differences, the interpretation of data for multiple-photon excitation is much more difficult than for normal absorption spectra; a given absorption feature represents the sum effect of many energy transitions in a collection of molecules driven rapidly into a nonequilibrium distribution. Dissociation data, as well as absorption data, are necessary to characterize that distribution. Also, the theoretical picture dealing with the effect is necessarily both statistical and dynamical in nature; it is concerned with the rates at which molecules are driven through the mesh of energy states.

This article will describe the current understanding of multiple-photon excitation and outline both the experimental and theoretical development of this fascinating research area. While the article emphasizes Los Alamos work, we note that scientists in many laboratories have contributed substantially to the understanding of the effect. Multiple-photon excitation is an important phenomenon in laser isotope separation (see "Separating Isotopes With Lasers" in this issue) and is attractive for applications like purification of chemicals, synthesis of new species, and study of chemical reactions. But we have limited our discussion to the phenomenon and its historical development.

The Old Picture

The understanding of the interaction between polyatomic molecules and intense infrared radiation is evolving to give a very different picture from what conventional wis-

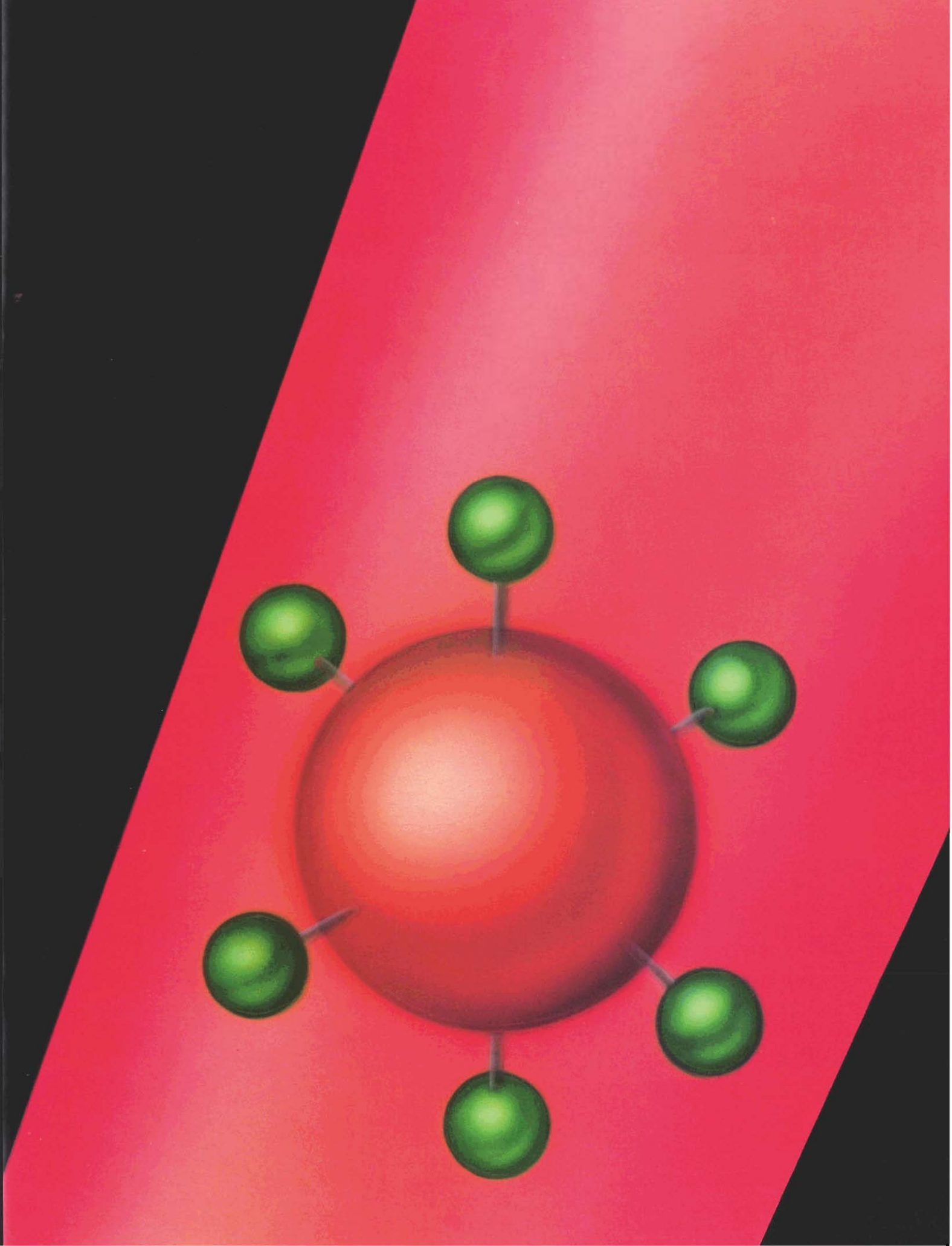

dom portrayed ten years ago. In the late sixties only the most naive thought that one could use infrared lasers to induce dissociation (photolysis) of molecules. Those who knew something of infrared spectroscopy and molecular physics used the following logic to discount the possibility of infrared photolysis.

The photon energy of infrared light is substantially less than the energy required to induce most chemical reactions. In fact, photolysis of molecules that are stable at room temperature requires the energy equivalent of 20 to 50 carbon-dioxide (CO_2) laser photons.

A molecule absorbs infrared radiation by interaction of its vibrating electric dipole with the oscillating electric field of the radiation. The radiant energy becomes vibrational energy in the molecule. Because molecular vibrational energy is quantized, this absorption is best treated as a match between the energy of the photon being absorbed and the gap between the energy levels involved in the transition.

An ideal harmonic oscillator, that is, an oscillator with two masses and a restoring force that remains proportional to the separation between those masses, has equally spaced energy levels. However, all real diatomic molecules deviate from this ideal because the restoring force typically drops toward zero as the bond stretches further and further toward breakage. These molecules are vibrationally anharmonic and the spacing between adjacent vibrational energy levels decreases with excitation.

One can think of the vibrational energy levels as rungs in an interatomic-potential-energy ladder (Fig. 1). The rungs get closer as one moves up the ladder. At the top, where the levels are so close as to be, in effect, continuous, the bond breaks and the diatomic molecule dissociates.

Now if the frequency of the photon being absorbed matches the lowest energy gap (between $n = 0$ and $n = 1$ in Fig. 1), it will not match the next gap, which is smaller.

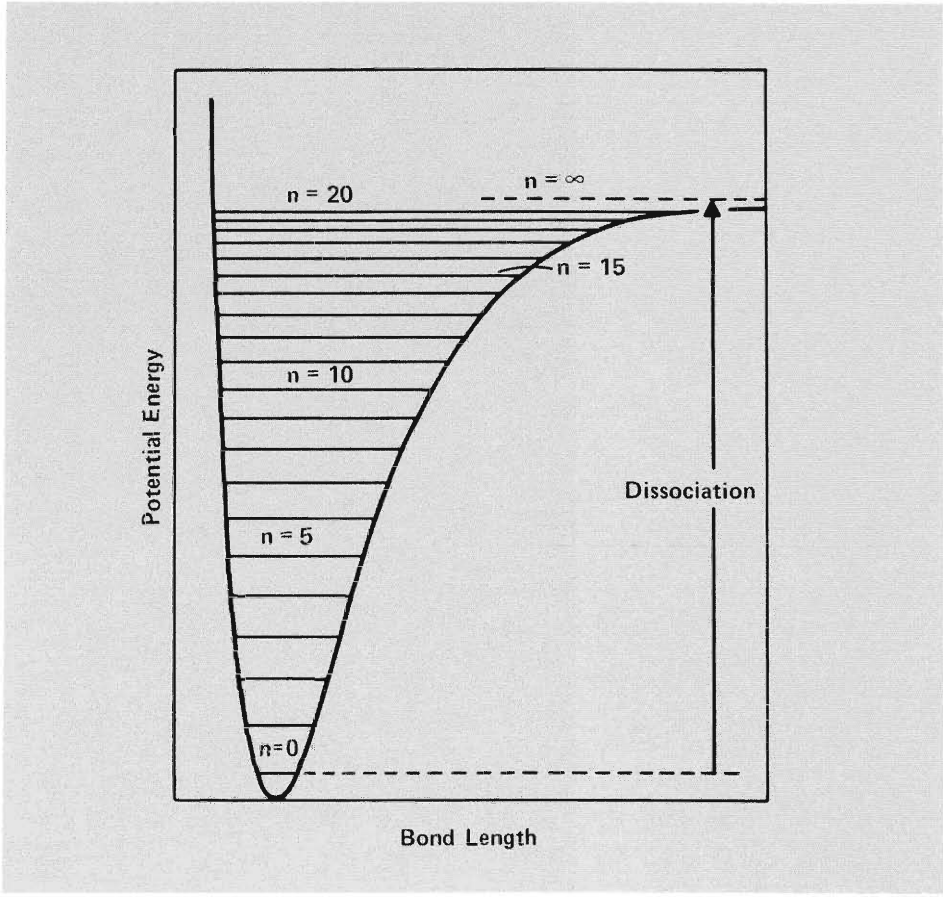

Fig. 1. The potential-energy well of a diatomic molecule. The horizontal lines represent the quantized vibrational energy levels of the molecule with the ground state labeled by $n = 0$. ***Near the ground state the potential-energy well is approximately harmonic and the energy levels approximately equally spaced. As the molecular bond stretches, the potential-energy curve becomes less steep and the levels merge to a continuum. At*** $n = \infty$ ***the molecule will dissociate.***

The mismatch becomes progressively larger with increasing vibrational excitation and precludes the possibility that one diatomic molecule will absorb many photons.

Molecular vibrations of polyatomic molecules are somewhat more complex. However, one can resolve a particular vibrational motion into a superposition of several vibrations called normal modes. To a first approximation, each normal mode vibrates independently and maintains the characteristics of a vibrating, anharmonic diatomic molecule. Therefore, vibrational anharmonicity restricts absorption of photons by polyatomic molecules in basically the same way it does for diatomic molecules.

If this were not enough to prevent absorption of large amounts of infrared energy, another severe restriction exists. All molecules in a gas sample do not respond identically to infrared radiation because of differences in rotational and translational energy of the molecules.

In the case of rotational energy, the molecules of a gas sample are distributed among many quantized rotational states. Each rotational state may contribute differently to the total change in internal energy during an absorption, which means that molecules in different rotational states require different infrared frequencies for efficient absorption. The result is the rotational structure discussed in this issue in "The Modern Revolution in Infrared Spectroscopy."

Likewise, the translational energies (or velocities) of the molecules cover a wide thermal distribution. Each velocity component along the path of the light propagation will produce a different Doppler shift in the frequency of the infrared light as viewed by the molecule. Because the optimum frequency for absorption varies with the rotational and translational energy state, the fraction of molecules that can absorb even the first photon for vibrational excitation is greatly reduced.

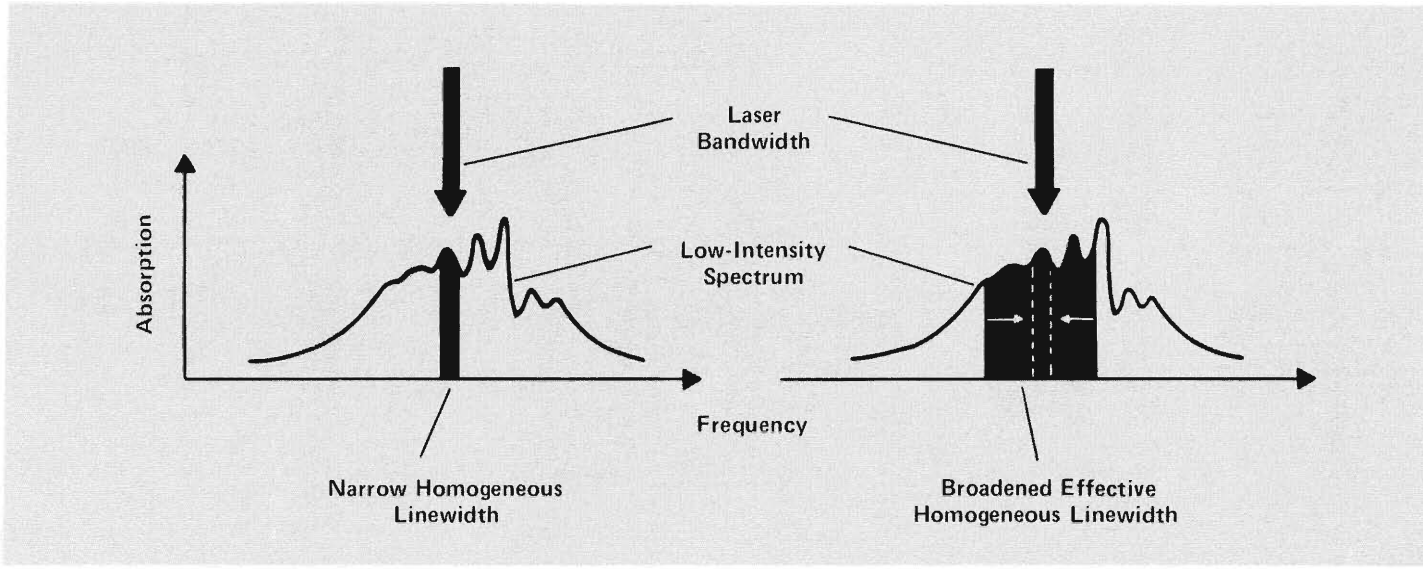

Fig. 2. Homogeneous and effective homogeneous linewidth. The low-intensity spectrum of an absorption band represents the distribution of molecules among various molecular energy states, each state with absorbing transitions at different frequencies. For the absorption on the left, the laser photons interact only with that fraction of the molecules whose states have transition frequencies falling approximately within the laser bandwidth. This fraction of molecules are said to be absorbing homogeneously because they all interact in the same way with the photons. For this absorption the homogeneous linewidth matches the laser bandwidth. However, certain mechanisms, such as collisions that change energy states or multiphoton absorption, can cause molecules outside the laser bandwidth to absorb photons in a manner identical to those within the homogeneous linewidth. The effective homogeneous linewidth (right) has a larger frequency range that includes this larger fraction of absorbing molecules.

Molecules that all interact in a like manner with the photons are said to absorb homogeneously. Molecules in different states that interact differently with the photons are said to absorb inhomogeneously. Certain mechanisms, such as collisions, can alter the rotational and translational energy states. Thus, during a laser pulse molecules from one homogeneous collection that is not absorbing strongly can be transferred by these mechanisms into another homogeneous collection that *is* absorbing. This increases the fraction of molecules affected in a like manner by the photons. The effective homogeneous linewidth is a measure, in terms of frequency, of the extent of such mechanisms (Fig. 2). However, calculations suggest that many collisions during a pulse from an infrared laser are necessary for even a small fraction of the molecules to absorb the photons needed for dissociation. Those same collisions would tend to distribute the absorbed energy randomly among many molecules in the sample. The net effect of this particular broadening mechanism, then, would be similar to heating the sample by more conventional methods.

Photolysis might be accomplished by *multi*photon absorption, which is a single, resonant interaction between several photons and two widely separated states. This effect is another mechanism broadening the homogeneous absorption linewidth; it requires only that the sum of the photon energies match the gap between the initial and final states, thus bypassing unmatched intermediate states. However, the thirty-photon process that would be necessary for dissociation would have a vanishingly small probability of occurrence.

(Catastropic dielectric breakdown could lead to dissociation, but this sudden ionization can only be produced in a molecular gas with extremely high-intensity infrared radiation and is quite different from multiple-photon dissociation.)

The line of reasoning outlined above led to the conclusion that a single polyatomic molecule could not, in the absence of collisions, absorb sufficient energy from an infrared laser pulse to dissociate. The arguments appeared to have no serious deficiencies; they were based, for the most part, on sound principles of infrared spectroscopy. The conclusion, however, was wrong.

The Historical Development of the Multiple-Photon Effect

In the late sixties people in several laboratories began to induce chemical reactions with the newly developed CO_2 laser. The experiments tended to fall into two categories. In the first category, absorbed laser energy induced reactions that involved the collision between two molecules. The researchers concluded that a single absorbed photon enhanced the reaction rate. In the second category, the pressure of the sample was high enough to produce rapid collisional scrambling of the absorbed energy. Both types of experiments gave results that fit well into the old picture we portrayed above.

With the advent of high-intensity, pulsed infrared sources, such as a pulsed version of the CO_2 laser, that picture began to show defects.

In 1971 researchers for the National Research Council of Canada showed that when they irradiated low-pressure SiF_4 gas with intense CO_2 laser pulses, the molecules dissociated to give electronically excited SiF fragments. The laser intensity that produced these reactions was close to, but below, the threshold for dielectric breakdown. At these low pressures, the absorption took place under nearly collisionless conditions. This experiment showed that a single, isolated molecule (and its fragments) could absorb well over one hundred photons during a laser pulse.

During the next year experiments at Los Alamos demonstrated that increased pres-

sure, and so increased collisions, impeded, rather than enhanced, the rate of laser-induced dissociation of N_2F_4 to NF_2. A dissociation reaction that depended on simple conversion of laser energy to thermal energy in the gas would have shown the opposite pressure effect. However, these experiments were still not an unequivocal demonstration of laser-induced dissociation in the complete absence of collisions.

In the period from 1972 to 1974 several experiments gave strong evidence that CO_2-laser pulses of modest fluence (time-integrated intensity per unit area) could induce chemical reactions producing atomic fragments. At Los Alamos CO_2-laser pulses were used to initiate explosive reactions in mixtures of H_2 with either the absorber N_2F_4 or SF_6. These experiments suggested that during the laser pulse the radiant energy fragmented the absorber molecule (N_2F_4 or SF_6) to produce fluorine atoms. These atoms then reacted rapidly with the H_2 to generate energy and more reactive species. This accelerating chain reaction resulted in explosion of the gas mixture. An important finding was the fact that the laser energy absorbed was significantly less than would be required in an equivalent thermally induced reaction.

Experiments at the Institute of Spectroscopy in the Soviet Union demonstrated that the laser-induced reaction of BCl_3 in the presence of oxygen produced electronically excited BO molecules. These reactions were isotopically selective. When the CO_2-laser frequency was near the vibrational frequency of a particular isotopic form of BCl_3, the BO fragment favored that boron isotope. About the same time researchers at the National Bureau of Standards demonstrated the laser-induced, isotopically selective reaction of BCl_3-H_2S mixtures. The isotopic selectivity in the latter two experiments was particularly strong evidence of a nonthermal, infrared photolytic reaction.

But the experiments that demonstrated unequivocally the phenomenon of multiple-photon excitation were performed by the Institute of Spectroscopy in late 1974 and Los Alamos in early 1975. These experiments demonstrated direct photolysis of SF_6 with extremely high isotopic selectivity under conditions where molecular collisions could not have played a major role. Similar demonstrations with other species followed rapidly, as well as a broad range of explanations for the phenomenon.

The Experimental Characterization of Multiple-Photon Excitation

Multiple-photon excitation experiments exhibit many features that are independent of the particular molecular species. These features, which must be included in any successful theory of the process, will be presented below. We will start by giving a qualitative picture of the absorption and dissociation processes and then show how generic properties of the molecules, the laser pulse, and the gas sample influence the phenomenon.

QUALITATIVE FEATURES. Typical laser-induced photolysis experiments examine only the end products of the dissociative reaction. How then can multiple-photon excitation be distinguished from other possible dissociation mechanisms? For example, the dominant process might be laser ionization, rather than vibrational excitation, of the absorbing molecules. In laser ionization the observed products would be generated by ion-molecule reactions rather than single-molecule, or unimolecular, dissociation. But, since experiments have shown that laser pulses produce no ions under conditions of extensive chemical reaction, researchers now feel that the general mechanism most consistent with available data is one in which the polyatomic molecule absorbs the infrared laser energy in the form of vibrational energy. Then, if the molecule absorbs sufficient energy, the molecule may dissociate into fragments.

What type of molecules undergo multiple-photon excitation? Many of the early successful experiments were with highly symmetric molecules like SF_6 and SiF_4. Is high symmetry an essential feature? Does molecular size play a role? From Table I, which gives a partial list of molecules that dissociate by multiple-photon excitation, we see that it is a general phenomenon. Molecular symmetry is not a restriction. Molecular size is only a partial restriction: diatomic molecules do not dissociate; some triatomic molecules like OCS and O_3 dissociate when irradiated with very intense infrared radiation; and very large molecules like uranyl-bis-hexafluoracetylacetonate·tetrahydrofuran dissociate very easily.

One of the impressive features of multiple-photon excitation is high isotopic selectivity. We define isotopic selectivity as the ratio of dissociation probabilities of two isotopic forms of a molecule. With appropriate laser frequencies and gas pressures one can induce isotopically selective reactions in most polyatomic molecules.

Isotopic selectively depends strongly on the isotopic shift of absorption features in the infrared spectrum. Basically, the shift is due to a change in the vibrational frequency of the molecule when one of the vibrating atoms has a different isotopic mass. As a result, isotopic selectivities tend to be large for light isotopes, where the relative change in the mass is large, and small for heavy isotopes, where the relative change is small. For example, isotopic selectivities for heavy metals like molybdenum (in MoF_6), osmium (in OsO_4), and uranium [in $U(CH_3O)_6$] fall in the range between 1.0 and 1.1. Selectivities for light isotopes like hydrogen (in CF_3H) may be as high as 20,000. For the well-studied molecule SF_6, the selectivity for ^{33}S relative to ^{32}S is about eight, and for ^{34}S relative to ^{32}S, it is about fifty. These values are typical for intermediate atomic weight isotopes.

Isotopic selectivity observed in a wide range of molecules gave clear evidence that a

TABLE I
SPECIES DISSOCIATED BY MULTIPLE-PHOTON EXCITATION

OCS	CH_3OH	MoF_6	Benzene
O_3	CH_3CN	UF_6	Cyclopropane
NH_3	CH_3NC	CF_3CHCl_2	Propylene
H_2CO	C_2H_3Cl	CF_3CH_3	Hexafluorocyclobutene
BCl_3	C_2H_3F	C_2H_5F	Perfluorocyclobutane
CCl_4	CF_2CH_2	C_2H_5NC	Ethylvinylether
CF_2HCl	C_2H_4	C_2H_5OH	Ethyl acetate
CF_2Cl_2	N_2F_4	SF_5NF_2	*sec*-Butyl acetate
CF_3I	SF_6	CF_3COCF_3	Tetramethyldioxetane
CrO_2Cl_2	SF_5Cl	S_2F_{10}	Uranyl-bis-hexafluoroacetyl-acetonate·tetrahydrofuran
HCOOH	CH_3NH_2	C_6F_5H	
OsO_4	CH_3NO_2	$U(OCH_3)_6$	
CHF_3	SeF_6	CH_2FCH_2Cl	

single molecule can absorb many infrared photons with no help from collisional processes and that the resulting vibrational energy is sufficient to induce a unimolecular chemical reaction.

These results suggested that the reactions might be bond selective. That is, if molecules absorbed laser energy under collisionless conditions, perhaps the vibrational energy remained in a single normal mode and cleaved the chemical bond that experienced the highest vibrational amplitude. If this were so, then one could select the point of reaction within the molecule by matching the laser frequency to the frequency of the appropriate normal mode.

Arguments for bond-selective dissociation by multiple-photon excitation rely heavily on many features of the old picture for the absorption of infrared radiation. Because the old picture can't explain multiple-photon excitation in the first place, one should be highly suspicious of the possibility of such a reaction. Many people claimed to have demonstrated bond-selective reactions, or at least some degree of vibrational-energy localization within a polyatomic molecule. However, in all cases that we are aware of, alternate explanations are more plausible.

Researchers at the Berkeley campus of the University of California performed experiments that not only suggested that bond-selective reactions were unlikely, but also demonstrated the collisionless nature of the multiple-photon excitation process. These experiments involved dissociating the molecules in a molecular beam with CO_2-laser pulses. A molecular beam is a low-density stream of molecules passing through a vacuum. These conditions virtually eliminate collisions between molecules during the time the beam is in the irradiation region. When the molecules dissociate, recoil of the separating fragments frequently causes the reaction products to leave the path of the beam. This altered trajectory permits detection and identification of the fragments.

Reactions of over fifteen species containing from four to eight atoms per molecule were studied. Multiple reaction pathways were available for many of these species. However, all species reacted by the energetically most favorable pathway. This result is consistent with statistical redistribution of the available vibrational energy prior to dissociation. The velocities of the separating molecular fragments were also consistent with a statistical energy distribution.

DENSITY OF VIBRATIONAL STATES. We noted that heavier molecules dissociate more easily than lighter ones. People generally attribute this fact to the increasing density of vibrational states with increasing mass of the molecule. The density of states is simply the number of available vibrational states per unit energy interval of the molecule and is one of the profound differences between a diatomic molecule and a larger polyatomic molecule. ("The Modern Revolution in Infrared Spectroscopy" discusses the origin of this high density of vibrational states for polyatomic molecules.)

From spectroscopic constants one can obtain an adequate estimate of the density of vibrational states. Figure 3 shows how this density depends on vibrational energy for several representative molecules. We see a huge difference in the state density between a small molecule like OCS and a larger one like S_2F_{10}, even at modest energies.

A high state density gives an immense statistical advantage to absorption by large molecules. For example, at an energy near the dissociation threshold of S_2F_{10} (20,000 cm^{-1}), the densities of vibrational states for S_2F_{10} and OCS differ by a factor of 10^{22}. This means that if molecules of both species were in equilibrium with some environment (such as a radiation field or a thermal gas), the probability that the S_2F_{10} molecule is in a vibrational state near 20,000 cm^{-1} could be as much as 10^{22} times the same probability for the OCS molecule. Of course, absorption of laser radiation is certainly not an equilibrium process. Moreover, as the energy or temperature of the environment increases and both molecules become distributed throughout a large range of energy levels, the probability ratio will decrease below the 10^{22} factor. Nevertheless, the huge statistical advantage remains for larger molecules.

Recent dissociation experiments with polyatomic molecules have demonstrated the effect of the density of vibrational states on multiple-photon excitation. To facilitate comparison of these experiments we define two parameters, $\Phi_{1\%}$, the fluence needed to dissociate 1% of the molecules in the laser beam, and $N(10{,}500)$, the density of vibra-

tional states for each molecule at 10,500 cm^{-1}, which is about half the energy needed to dissociate a typical molecule.

Figure 4 shows the relationship between these two quantities in many different experiments with a wide range of experimental conditions. We see the trend of decreasing $\Phi_{1\%}$ (easier dissociation) with increasing N(10,500) (higher density of vibrational states).

There are, of course, many other variables in these experiments. These include: absorption cross section, chemical bond strength, frequency relative to the infrared absorption band, gas pressure, laser pulse shape, and laser spectral width. To eliminate some of this diversity we report the results of a set of experiments performed under more controlled conditions (Table II). These results all came from the same laboratory (Los Alamos), and the laser pulse shape and gas pressure were nearly the same for all experiments. The species all have the structure SF_5X allowing the laser frequency to be set near the center of a strong infrared absorption band of a sulfur-fluorine stretching vibration for each species. The main parameter that still varies is the strength of the weakest chemical bond: from 50 kilocalories per mole for SF_5NF_2 to 93 kilocalories per mole for SF_6. However, the most dramatic effect obvious from Table II is the decrease in $\Phi_{1\%}$ with increasing density of states.

The strength of the chemical bond that breaks when the molecule dissociates plays a weaker role in determining $\Phi_{1\%}$. For example, SiF_4 and OsO_4 have similar vibrational-state densities. But SiF_4 has a bond strength of 142 kilocalories per mole and a $\Phi_{1\%}$ of 8.9 joules per square centimeter; OsO_4 has a strength of only 73 kilocalories per mole and a $\Phi_{1\%}$ of 1.1 joules per square centimeter.

The correlation with bond strength is not as strong as the correlation with certain of the other factors. In fact, it is not difficult to find a pair of molecules where the more strongly bound molecule dissociates more

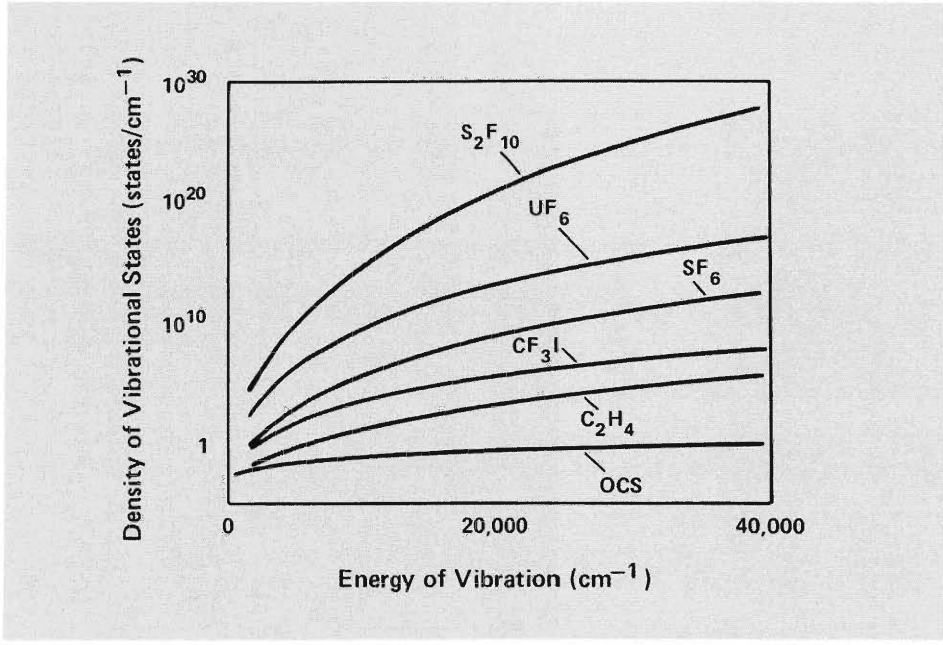

Fig. 3. Density of vibrational states for various molecules as a function of vibrational energy. The density of vibrational states, that is, the number of available states per unit energy interval, increases for all molecules as vibrational excitation increases. However, the large molecules have considerably larger densities than the small molecules at all but the lowest energies. [Here, frequency in wavenumbers is used as an energy unit: 1 reciprocal centimer (cm^{-1}) = 1.24 × 10^{-4} electron volt (eV). Also note the logarithmic scale for density of vibrational states.]

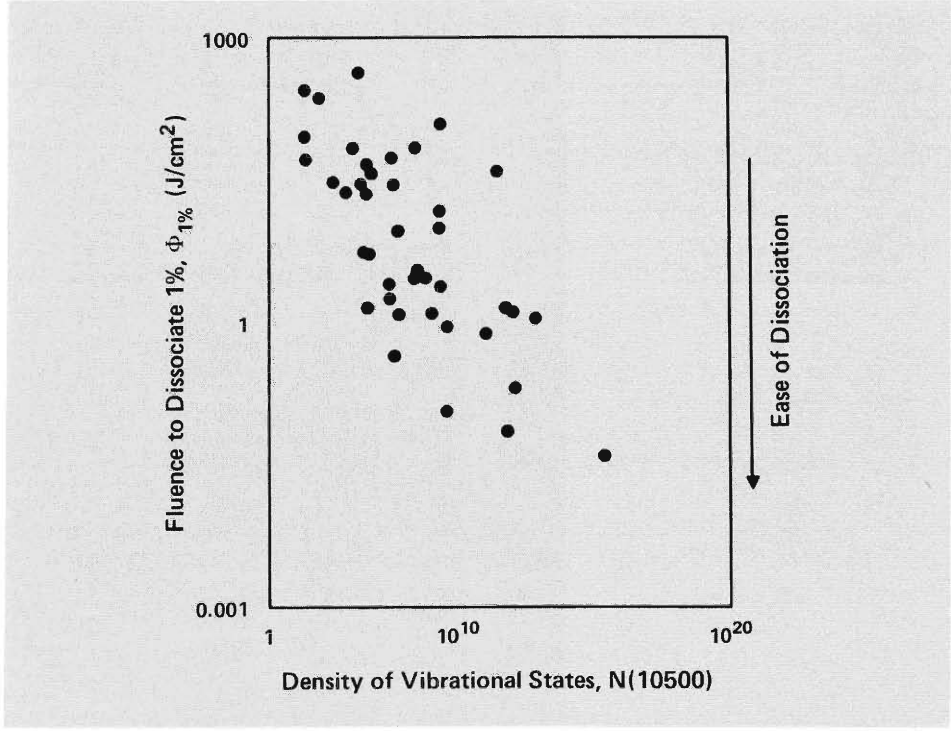

Fig. 4. The dissociation efficiency for various molecules as a function of vibrational state density. The parameter $\Phi_{1\%}$ is the laser fluence (in joules per square centimeter) needed to dissociate 1% of the molecules. Thus, a lower $\Phi_{1\%}$ implies easier dissociation. The overall trend is easier dissociation for larger molecules with higher vibrational state densities (here measured for each molecule at an energy of 10500 cm^{-1}).

TABLE II

COMPARISON OF FLUENCE NECESSARY TO DISSOCIATE 1% OF MOLECULES IN BEAM

Species	N(10500) (1/cm^{-1})	Bond Strength (kcal/mole)	$\Phi_{1\%}$ (J/cm^2)
SF_6	8.5×10^8	93	2.8
SF_5Cl	2.1×10^9	61	0.6
SF_5NF_2	2.6×10^{12}	50	0.05
S_2F_{10}	3.1×10^{17}	58	0.018

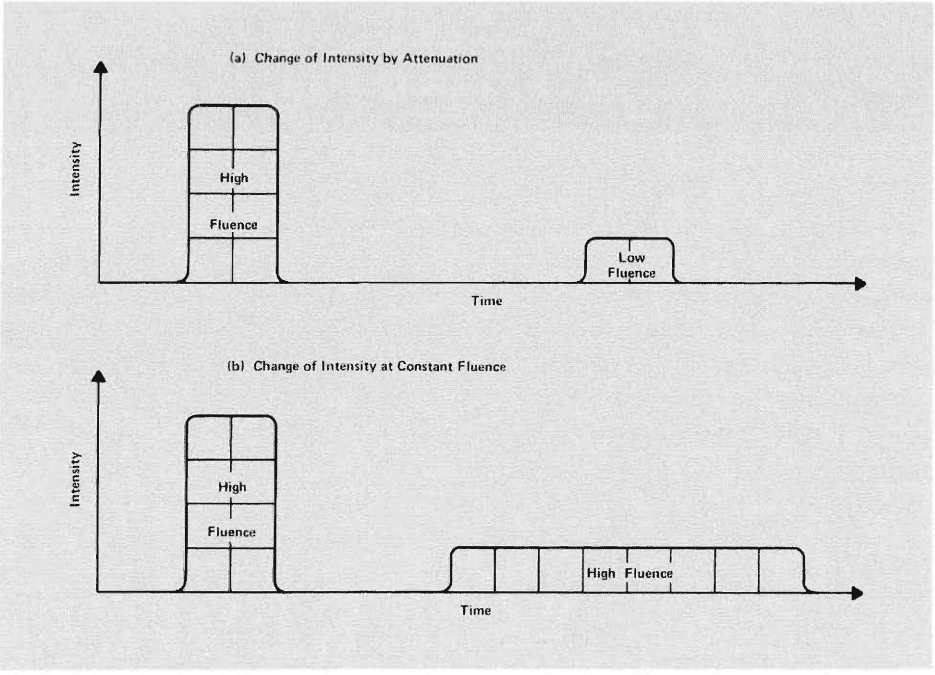

Fig. 5. The intensity-fluence relationship. Laser intensity (power per unit area) is given as a function of time by the height of these idealized laser-pulse curves. The fluence (energy per unit area) is the time-integrated laser intensity, or the area under each curve. (a) If the laser pulse is attenuated (by placing a partial absorber in the beam or by refocusing to a larger area) both the intensity and the fluence are reduced. (b) If the laser pulse is attenuated but, at the same time, the pulse length is increased proportionately, the fluence can be held constant while the intensity is reduced.

easily. Again, from Table II, the density of vibrational states for S_2F_{10} is larger than for SF_5NF_2, and this fact appears to be more important for ease of dissociation than the weaker bond strength of SF_5NF_2.

FLUENCE EFFECTS. One of the more easily varied parameters in a multiple-photon excitation experiment is the laser fluence. The fluence can be varied by placing attenuators in the beam or by focusing the beam differently in the sample (Fig. 5a). As observed by many researchers, variations in fluence produce profound changes in the dissociation probability and the absorption cross section.

Figure 6 shows how the laser fluence, Φ, affects the absorption cross section, σ, and dissociation probability of a large molecule (SF_5NF_2). Figure 7 shows the corresponding curves for a somewhat smaller molecule (C_2H_4). Both the differences and similarities between these figures are instructive.

At the threshold for dissociation, the fluence, Φ_{TH}, differs for the two molecules by a factor of about 10^3. However, the absorption cross section at threshold, σ_{TH}, also differs by about this factor, only inversely, so that the product $(\sigma\Phi)_{TH}$ is about the same for both molecules ($\approx 10^{-19}$). The fluence times the cross section is proportional to the energy absorbed per molecule, E_{ab}.

$$E_{ab} \propto \sigma\Phi \ .$$

Thus both molecules need to absorb approximately the same energy to reach the threshold for dissociation. Furthermore, the observed value of $(E_{ab})_{TH}$ corresponds to about half the energy needed to dissociate either of the molecules. If only a small fraction of the molecules were absorbing the energy, the dissociation reaction would have started at a much lower fluence. These facts suggest that the molecules behave similarly at high levels of excitation and that the absorbed energy must be distributed among many molecules.

For the large molecule (Fig. 6), the cross section remains almost constant from low fluence up to the threshold for dissociation (for both long and short pulses). The drop in cross section at this point is probably due, for the most part, to dissociation of the molecules during the laser pulse. In other words, the probability for absorption of a photon by the molecule remains constant from the low-fluence limit where the molecule's initial state of excitation is low to near the threshold for dissociation where the molecule is highly excited. This behavior contrasts dramatically with the old-picture prediction that the absorption cross section would drop rapidly with excitation due to a growing anharmonic mismatch between photon energy and the gaps in the vibrational energy ladder.

A high absorption cross section over a broad range of fluence suggests that all of the molecules are absorbing laser radiation regardless of their translational or rotational energy states. In terms of linewidth, this means the effective homogeneous linewidth

is on the order of the frequency width of the entire low-intensity absorption band; a broadening mechanism is apparently at work. The high cross section at high fluence suggests than any anharmonic frequency shift with increasing vibrational excitation is less than this effective homogeneous linewidth.

We reach opposite conclusions with the smaller molecule (Fig. 7). The low absorption cross section suggests that at low fluence only a small fraction of the molecules are able to absorb laser radiation. The immediate drop in cross section with increasing fluence suggests that this small fraction is easily depleted. Thus, the homogeneous linewidth for the absorption is much less than the frequency width of the low-intensity absorption band and there is no significant broadening mechanism at low fluence. The low, but finite, cross section at high fluence suggests that the anharmonic frequency shift substantially reduces, but does not eliminate, the probability that an excited molecule absorbs more photons.

Other types of experiments confirm these conclusions. Increasing the pressure (collision rate) increases the absorption cross section for small molecules at high fluence whereas pressure has little effect on the cross section for large molecules. As pointed out earlier, collisions change the energy state of the molecules, bringing more of them into states where absorption is favorable. Similar changes in large molecules are insignificant because the already larger homogeneous linewidth makes absorption somewhat independent of energy state.

In summarizing the above findings for small molecules, we see an intriguing difference between the extremes of low and high fluence. At low fluence only a small fraction of the small molecules absorb photons. This conclusion follows from the large effect pressure has on the effective homogeneous linewidth and the early drop in cross section with increasing fluence. At high fluence a much larger fraction of the small molecules absorb photons. This follows from the facts that, on the average, the molecules absorb

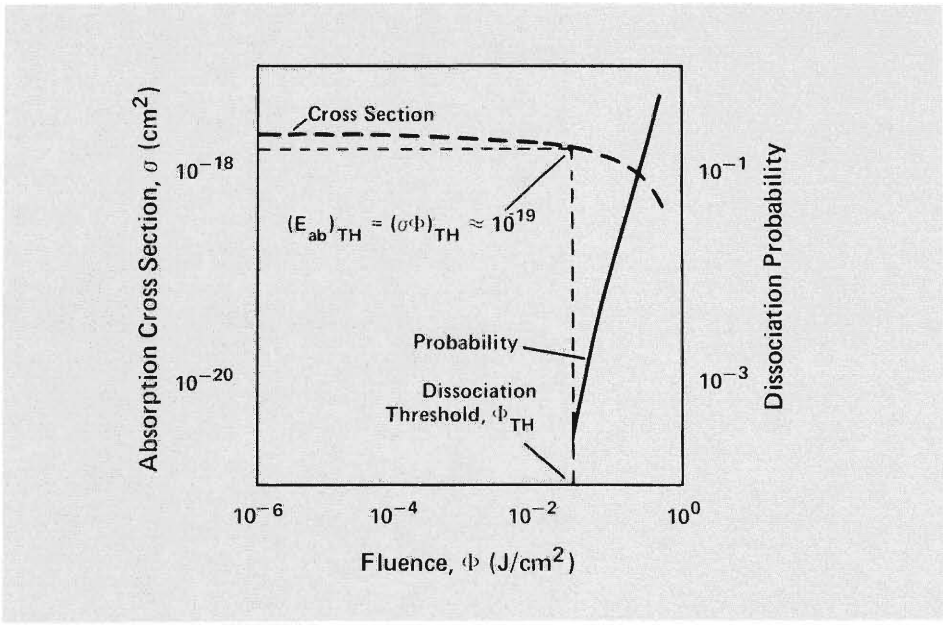

Fig. 6. Absorption cross section (dashed curve) and dissociation probability (solid curve) for SF_5NF_2. For this large molecule the absorption cross section remains fairly constant with laser fluence out to the threshold fluence, Φ_{TH}, at which dissociation starts. The product of Φ_{TH} and the corresponding threshold absorption cross section is proportional to the average energy absorbed per molecule at threshold conditions; this average is about 10^{-19} joule and represents about half the energy needed for a molecule to dissociate. Data are from John L. Lyman, Wayne C. Danen, Alan C. Nilsson, and Andrew V. Nowak, Journal of Chemical Physics, 71, 1206-1210 (1979).

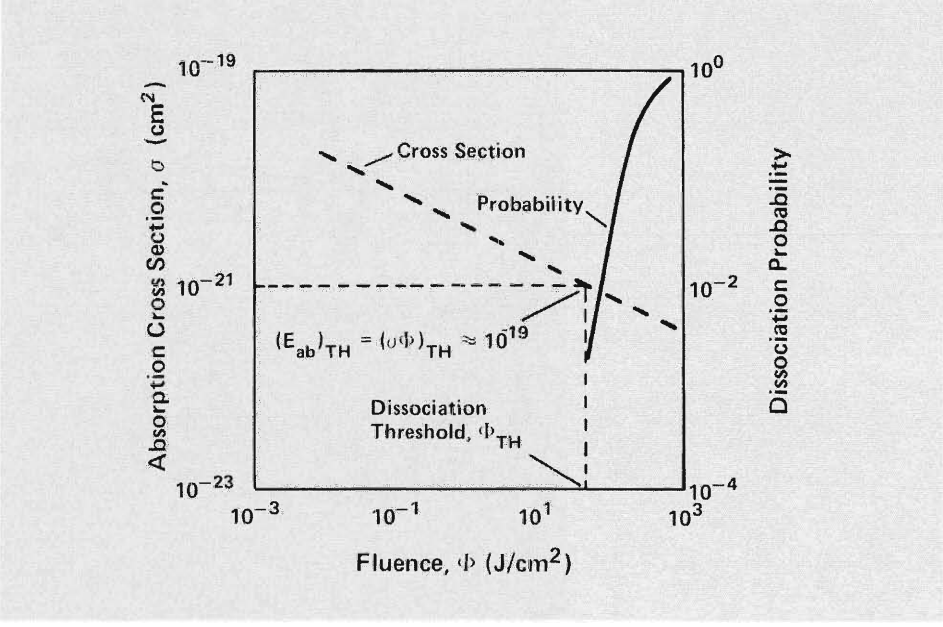

Fig. 7. Absorption cross section (dashed curve) and dissociation probability (solid curve) for C_2H_4. The absorption cross section for this smaller molecule decreases with increasing fluence long before the threshold fluence for dissociation is reached. Despite large differences in threshold fluence and cross section between this molecule and SF_5NF_2 (Fig. 5), the energy absorbed per molecule at the dissociation threshold is approximately the same. This suggests that both molecules behave similarly at high levels of excitation. The resemblance in the rise of dissociation probability with fluence for both molecules further strengthens this suggestion. Data are from O. N. Avatkov, V. N. Bagratashvili, I. N. Knyazev, Yu. R. Kolomiiskii, V. S. Letokhov, V. V. Lobko, and E. A. Ryabov, Soviet Journal of Quantum Electronics 7, 412-417 (1977).

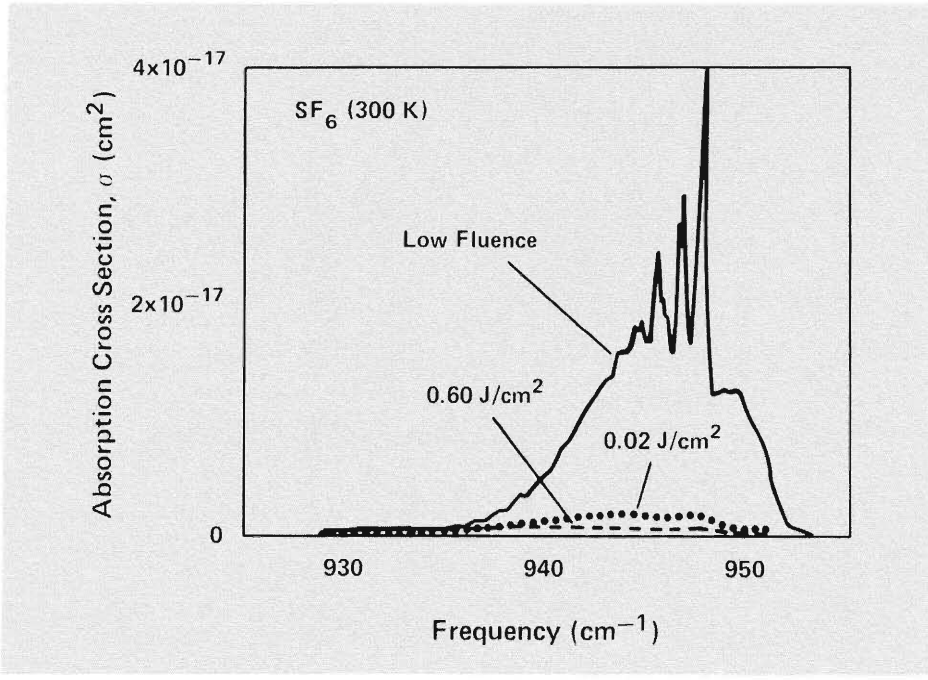

Fig. 8. Fluence dependence of the ν_3 absorption band of SF_6 at 300 kelvin. The low-fluence spectrum was obtained at a fluence typical of conventional spectroscopy, whereas the two high-fluence spectra were obtained with a pulsed CO_2 laser. The most obvious effect of high fluence is a significant drop in the absorption cross section. There is also an indication of a shift to lower frequencies. The high-fluence data are from Wei-shin Tsay, Clyde Riley, and David O. Ham, Journal of Chemical Physics 70, 3558-3560 (1979); the low-fluence data are from A. V. Nowak and J. L. Lyman, Journal of Quantitative Spectroscopy and Radiative Transfer 15, 945 (1975).

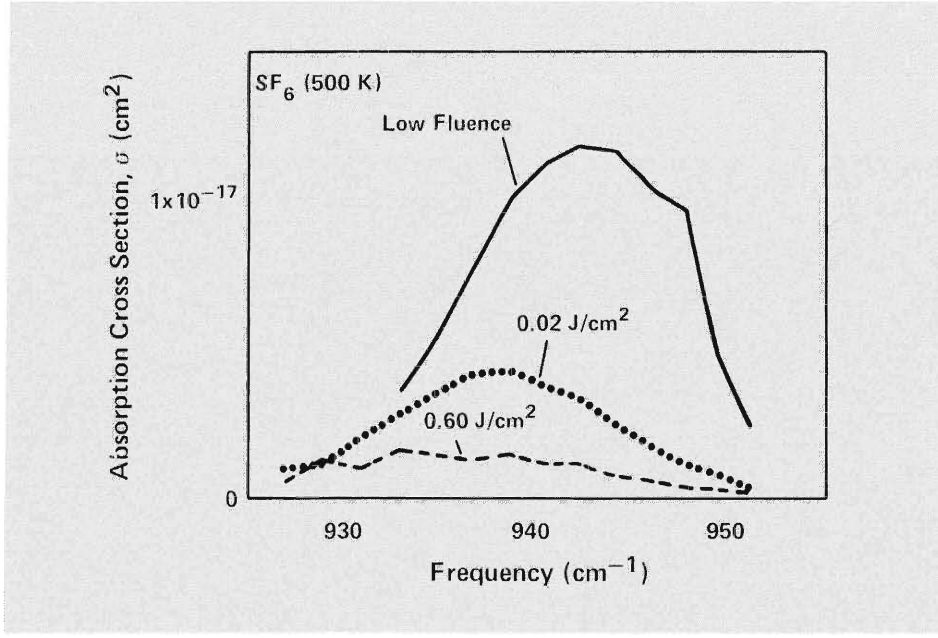

Fig. 9. Fluence dependence of the ν_3 absorption band of SF_6 at 500 kelvin. The increase in temperature (from 300 kelvin in Fig. 7) eliminates the structure in the low-fluence spectrum. Also, the drop with increasing fluence in the absorption cross section is less precipitous, making obvious the shift to lower frequencies. The data are from the same references cited in Fig. 8.

half the energy needed for dissociation before reaching the threshold, and that thereafter, the reaction probability increases as rapidly as for large molecules.

INTENSITY EFFECTS. When the fluence is varied with attenuators or by focusing the beam differently, the intensity (laser power per unit area) also changes (Fig. 5a). To separate the effects of intensity and fluence, researchers usually vary the intensity while holding the fluence constant. This is a difficult task because it requires changing the temporal shape of the laser pulse while keeping the total pulse energy constant (Fig. 5b). For instance, rapid electro-optical shutters can change the pulse length at the sample, but, at the same time, one must either refocus the beam or change the attenuation to keep the total energy per unit area constant.

The general observation from experiments of this type is that, unlike the effects of fluence, only in special situations does intensity play a major role. One of these situations is for high gas pressures when frequent collisions redistribute the absorbed energy. Thus, the critical effect is the number of these collisions that take place during the laser pulse, rather than the interaction between the laser field and an isolated molecule. As intensity is varied by changing pulse length, the total number of collisions during the pulse will change, altering the ultimate energy distribution.

FREQUENCY DEPENDENCE. Polyatomic molecules absorb low-fluence infrared radiation in frequency bands that correspond to the frequencies of normal-mode vibrations (or some combination of those frequencies). We would expect multiple-photon excitation to have a similar frequency response, but with some modification because of the fact that high-fluence laser pulses severely perturb the absorbing sample. Early experiments verified this approximate relationship between low- and high-fluence spectra.

Figures 8, 9, and 10 compare low- and high-fluence spectra in the region of an

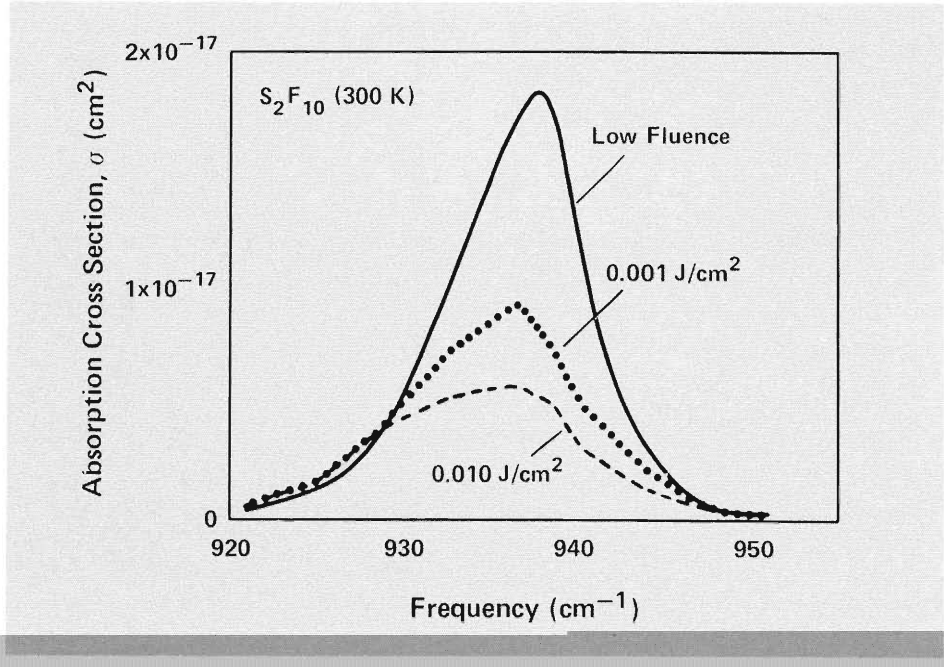

Fig. 10. Fluence dependence of an absorption band of S_2F_{10} at 300 kelvin. Higher fluence here results in a moderate drop in absorption cross section and a shift to lower frequencies. This behavior resembles that of the small SF_6 molecule at high temperature (Fig. 9). Data are from John L. Lyman and Kevin M. Leary, Journal of Chemical Physics 69, 1858-1864 (1978).

absorption band for SF_6 at two temperatures and for S_2F_{10} at one temperature. In all three examples we see a similarity between the spectra at high and low fluences, but with a shift to lower frequencies at high fluence. This is most certainly related to the anharmonic frequency shift. High-fluence absorption involves excitation up several rungs of the anharmonic ladder with the resonant frequency quickly becoming mismatched. A somewhat lower frequency that matches an intermediate rather than the lowest energy gap is optimum because it averages the mismatch over more levels. Moreover, as suggested earlier, multiphoton absorption necessarily occurs at lower frequencies. As one would expect from our previous discussion, we also see a decrease in absorption cross section at high fluence, and that decrease is most pronounced for the lighter molecules (SF_6) at the lower temperature (300 kelvin).

The effect of temperature on high-fluence spectra is most interesting. For SF_6 the absorption cross section drops quickly with increasing fluence at 300 kelvin but drops much less quickly at 500 kelvin. This could be related to the degree of initial vibrational excitation in the molecule because most SF_6 molecules are not excited at 300 kelvin whereas most *are* excited at 500 kelvin. For larger molecules, such as S_2F_{10}, even at 300 kelvin there is little loss of cross section with increasing fluence. Again, this could be related to vibrational excitation because these molecules have pliant bending modes with lower energy levels and even at 300 kelvin virtually all molecules have some degree of vibrational excitation. In terms of linewidth, it appears that increased vibrational excitation increases the effective homogeneous linewidth so that a larger fraction of the molecules are able to absorb photons. This trend with vibrational excitation parallels the previously observed trends with density of vibrational states and molecular size. Thus, vibrational excitation may be one, but perhaps not the only, reason for the state-density trend.

EXPERIMENTAL CONCLUSIONS. Clearly, conclusions drawn from the data for multiple-photon excitation experiments do not fit the old picture of the absorption of photons. Most significantly, at high fluence the laser frequencies need not match the absorption features exactly. We suggest four phenomena that contribute to this observation.

1. Absorption in the wings of a spectral line is possible because the cross section does not go to zero, but decreases with the square of the distance from line center.

2. The laser field itself can broaden the absorption lines by a process called Rabi broadening (this will be discussed in more detail later).

3. Muliphoton absorption, which bypasses one or more intermediate states, occurs at frequencies displaced slightly from the single-photon spectrum.

4. Most of the larger molecules have some degree of vibrational excitation *prior* to laser irradiation (because of the higher density of vibrational states), while the smaller molecules do not, and this excitation may play a role similar to collisions in allowing for homogeneous absorption.

The first effect means that there will always be a small amount of off-resonant energy absorbed and that this amount will increase with fluence. The next two effects increase the effective homogeneous linewith with increasing fluence, and the last effect accounts for differences between large and small molecules at low fluence.

Collisionless Multiple-Photon Excitation Theory

A theory of multiple-photon excitation should be consistent with the experimental observations that we have outlined above. The theory should explain the effect of vibrational-state density. It should give the proper fluence and frequency dependence. It should give an increasing homogeneous linewidth with the degree of vibrational excitation. And it should also suggest additional experiments whereby one could further check the theory.

Early attempts at theories ranged from strict compliance with the old picture to complete rejection of that picture. Enough experimental evidence has accumulated now

to force recognition of two points: multiple-photon excitation is a general, not a peculiar, limited, phenomenon; and theoretical explanation will require an expansion and modification of the old picture in terms of a variety of effects such as absorption line broadening, multiphoton absorption, higher-order interactions among normal-mode states, and intramolecular energy flow between states.

THEORETICAL APPROXIMATIONS. Generally, one bases a theory of light absorption on a quantum-mechanical description of the absorbing medium and either a classical or quantum-electrodynamic description of the light. In the case of multiple-photon excitation, the question is not whether fundamental concepts such as the Schrödinger equation or Maxwell's equations are correct, but rather, what degree of approximation is necessary in the application of the basic theories to this complex problem. In our opinion, the major problem with the old picture was that it used approximations appropriate for spectroscopy problems but not for the multiple-photon problem.

Before we begin to consider the more detailed physical process of multiple-photon absorption in polyatomic molecules, let us review those properties of a molecule that allow it to absorb electromagnetic radiation and point out in this review the various approximations that are needed. First, a molecule consists of some number of atoms bound together by interatomic electromagnetic forces at fixed separation distances and at fixed relative orientations. These positions are obviously not absolutely rigid, but are only relative equilibrium locations for each nucleus.

As a result of the very large mass difference between the electrons and the nuclei, it is valid to treat the electronic and nuclear motions as independent. This approximation, due to Born and Oppenheimer, assumes that the electrons produce a potential in which the nuclei vibrate. For the SF_6 molecule, the approximation reduces the complexity of the description of vibrational motion from 77 particles (70 electrons and 7 nuclei) to 7 particles.

Because the negative charge of the electrons and the positive charge of the nuclei are spatially separated, it is possible to establish or change an electric dipole moment in the molecule by displacement of any charged particle from its equilibrium position. Typically, it is photons in the infrared whose frequencies match those of the changing dipole moments generated by nuclear displacements (vibrations). The ensuing interaction leads to the absorption of infrared photons.

Displacements of the nuclei from their equilibrium positions can be described by harmonic motions that are referred to as the normal modes of the molecule. The normal-mode approximation allows one to describe the motion as many uncoupled motions. This further reduces the 7-particle problem to a set of 1-particle problems. Furthermore, in conventional infrared spectroscopy one treats interactions between normal modes as minor perturbations on the initial uncoupled motions. This set of approximations gives excellent solutions to infrared-spectroscopy problems when the molecules are in or near the ground vibrational state. This approach is discussed at several levels of perturbation in "The Modern Revolution in Infrared Spectroscopy."

In any octahedral XY_6 molecule there are fifteen normal modes, but, because symmetry leads to mode degeneracies, only six are at different frequencies. Of these only the triply degenerate modes ν_3 and ν_4 generate a changing electric dipole moment and therefore absorb infrared radiation. These normal modes behave initially like harmonic oscillators, but as energy is put into these motions their anharmonic nature becomes more pronounced until dissociation is reached.

In addition to the vibrational motion just discussed, a molecule also undergoes rotational and translational motion. Because translational motion does not affect the internal molecular structure, but leads only to small Doppler broadening of the absorption features, we will neglect it in further discussions. The combined motion of vibration and rotation leads to a greater wealth of possible transitions so that a single vibrational absorption feature actually consists of a broad absorption band containing thousands of individual rotational-vibrational transitions. This rotational broadening is not unlike Doppler broadening in nature, but the effects in frequency dispersion are far greater and must be included here.

So far our discussion has dealt mainly with theory used for conventional spectroscopy, in which only the lowest vibrational excitations are induced by low-intensity light. Do the same assumptions apply when vibrational excitation is high enough to cause dissociation of the molecule? The most well-established theory for the unimolecular dissociation of polyatomic molecules is the so-called RRKM unimolecular reaction-rate theory. Without describing the RRKM theory in detail, we can say that it retains the first approximation of separability of electronic and nuclear motion. However, instead of assuming a very weak coupling among normal modes of vibration, the theory assumes that the interaction among the vibrational states at high vibrational energies is strong enough to continuously maintain a statistical distribution of population among those states. The normal-mode approximation is used in the RRKM theory only to count vibrational states at energies near that needed to dissociate the molecule. This theory explains a large body of data on unimolecular reaction rates for dissociation of molecules with high levels of vibrational energy.

A successful theory of multiple-photon excitation would probably contain elements of both of the previous theories. The initial

absorption of intense infrared radiation produces low vibrational excitation where the normal-mode approximation of the old theory applies. But at excitation energies near the dissociation limit, the molecule is in a state where the approximations of the RRKM theory apply. Also, a theory for multiple-photon excitation can no longer treat the laser radiation simply as a probe because it severely perturbs the absorbing sample.

We will further restrict our theoretical description to the absorption of infrared laser photons by isolated molecules. The introduction of collisions into the theory precludes any first principle description of the problem and, in fact, masks the more interesting phenomena we wish to study here.

A NEW PICTURE. We begin a theoretical explanation of collisionless multiple-photon excitation by sketching a new picture with the three major parts shown in Fig. 11: the region of discrete, low-energy levels described by conventional spectroscopic theory; the region of high-energy levels and high density of states described by RRKM theory; and a region called the molecular quasicontinuum that connects these two extremes. The discrete, low-energy region of Fig. 11 shows resonant absorption at the frequency of the laser, ν_L, in the fundamental of an infrared-active mode, such as ν_3 for SF_6. As excitation advances, the anharmonicity necessarily causes a gradual mismatch between the laser frequency and the resonance frequency for excitation to the next higher state.

However, at about the energy level where the mismatch becomes significant, the multiple-photon excitation process merges into the second part of our theoretical picture. In this middle region the excited states of the resonant mode mix with other "background" states (vibrational states at the same energy with different normal mode character.) Briefly, this mixing occurs because the normal mode vibrations are not truly independent, but rather are loosely coupled to each other.

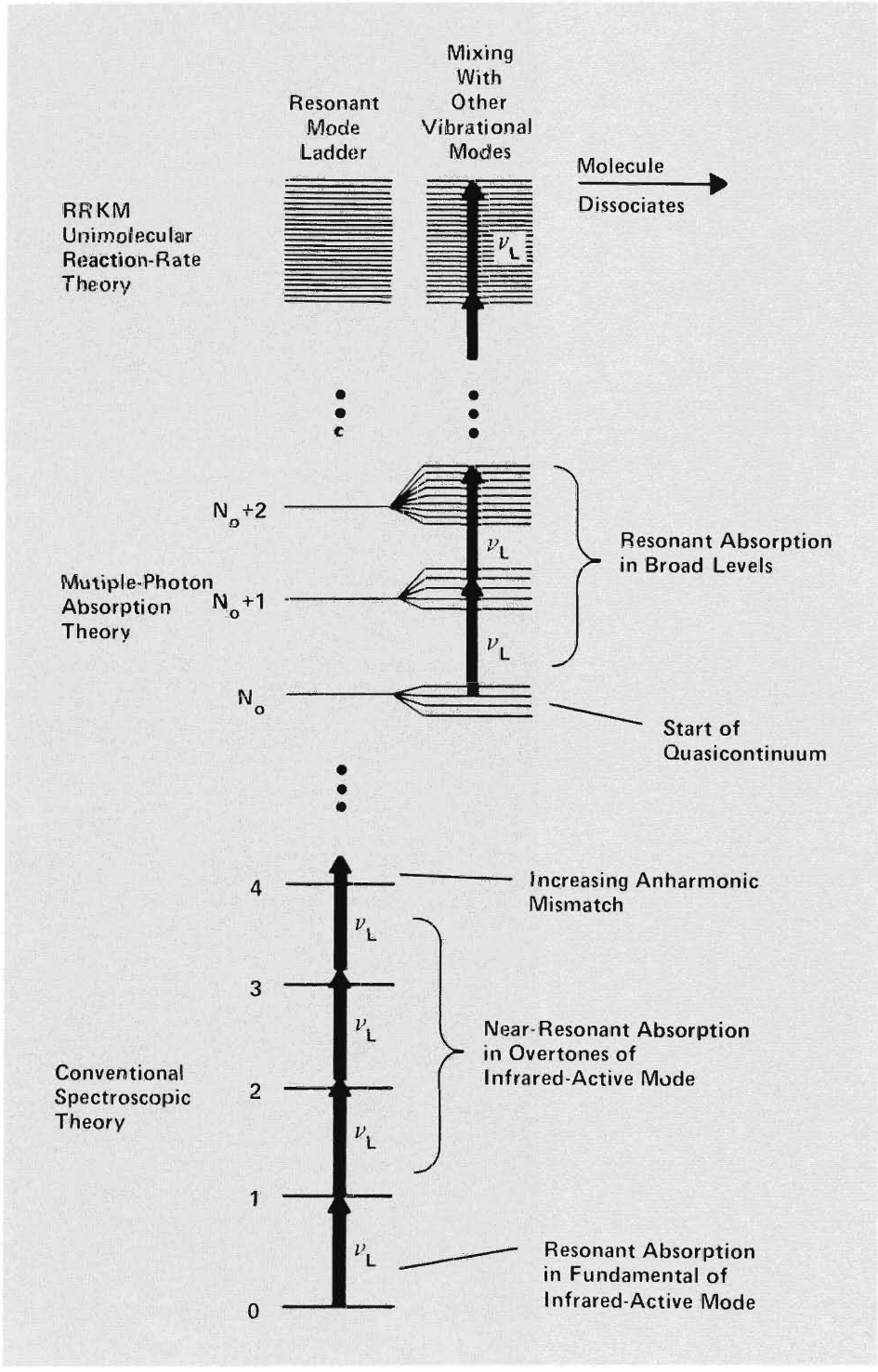

Fig. 11. Theoretical framework of multiple-photon excitation.

Most importantly, this mixing process causes shifts and broadenings of the excited states of the molecule. With enough mixing a fine mesh of states, the molecular quasicontinuum, is formed that compensates for the anharmonicities and allows further absorption of laser photons. The mixing allows access to the full density of vibrational states with its huge statistical advantage for absorption. Laser excitation through the quasicontimuum is resonant, but of a nature different from the simple normal mode excitation that occurs at the low molecular levels; the quasicontinuum states obey quite different dynamics owing to their "strong admixture" character.

Finally, the third part of our theoretical picture in Fig. 11 is reached when enough energy for dissociation has been absorbed. In this region, a statistically random dissocia-

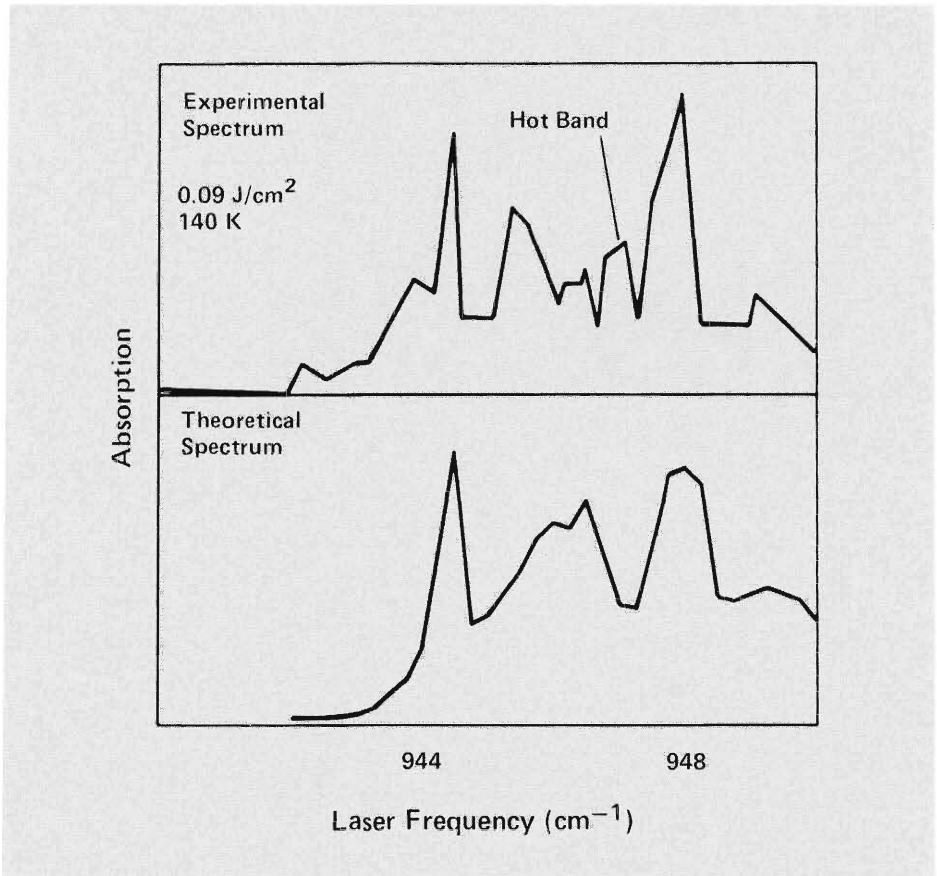

Fig. 12. Experimental and theoretical high-fluence spectra in the region of the ν_3 absorption of SF_6. The theoretical spectrum was computed for coherent transitions within the three-level system of $0\nu_3$, $1\nu_3$, and $2\nu_3$. Since all molecules were assumed to be initially in the ground state, the theoretical spectrum does not include the hot-band absorption ($\nu_6 \rightarrow \nu_6 + \nu_3$) present in the experimental spectrum. The experimental spectrum is based on data from S. S. Alimpiev, N. V. Karlov, S. M. Kikiforov, A. M. Prokhorov, B. G. Sartakov, E. M. Kohkhlov, and A. L. Shtarkov, Optics Communications 31, *309-312 (1979).*

tion occurs that can be described by the RRKM unimolecular reaction-rate theory.

Let us now proceed more slowly through the stages of excitation within the framework of a more detailed model constructed by workers at Los Alamos and applied to SF_6, S_2F_{10}, and UF_6. All of these molecules have been dissociated with infrared laser photons and, therefore, must proceed through these stages of excitation. A molecule that cannot be dissociated may simply be reaching a bottleneck at the first stage of excitation because the quasicontinuum may not occur low enough in the molecule's vibrational ladder to overcome the anharmonicity.

THE DISCRETE, LOW-ENERGY REGION. We have obtained very-high-resolution spectra, for both SF_6 and UF_6, of the ν_3 fundamental band (transitions from the ground state to the first excited state: $0 \rightarrow \nu_3$) and of the second overtone of ν_3 (transitions from the ground state to the third excited state: $0 \rightarrow 3\nu_3$). By using the spectroscopic data as a basis, a great wealth of information has been obtained about the multiple-photon ladder in the discrete, low-energy region for these molecules.

Two important conclusions follow from this work. First, vibrational splittings that relate to the octahedral symmetry of the SF_6 molecule are a dominant feature of the degenerate energy levels of the ν_3 overtones and may provide levels that compensate for anharmonicity in the discrete, low-energy region. These octahedral splittings are due to interactions between the degenerate components *within* the ν_3 vibrational ladder. As such, octahedral splittings are not the same as the mixings that generate the molecular quasicontinuum, namely, the mixings between levels with different normal-mode character. Octahedral splittings were anticipated in early work at Los Alamos, but there was no empirical confirmation until infrared spectra of overtones had been obtained. These splittings are discussed in "The Modern Revolution in Infrared Spectroscopy."

The second conclusion drawn from the spectra is the fact that the quasicontinuum and coupling to other vibrational modes play no role below or even at the $3\nu_3$ level. This is a surprising result because the background vibrational density of states is already $\approx 10^4$ states per cm^{-1} at $3\nu_3$. The data clearly indicate a very weak coupling strength between the $3\nu_3$ overtone levels and this multitude of background states, although the data do not preclude mixing within the background states. The data also show us that simple state counting is not enough for a determination of the energy level that marks the beginning of the quasicontinuum. In fact, a determination of the level and the mechanism for the start of the quasicontinuum with respect to the background state mixing is one of the major outstanding theoretical problems.

These conclusions about the start of the quasicontinuum apply only to molecules that are initially in the ground vibrational state. Excitation in lower vibrational states of other modes prior to laser excitation may substantially alter the quasicontinuum character of the absorber by providing an interaction pathway between the ν_3 mode and states that are not directly coupled to ν_3-mode states. Because temperature alters the population of the lower vibrational states, absorption features whose transitions originate in these states are usually referred to as hot bands. At 0 kelvin all of the molecules are in the ground state.

The analysis of multiple-photon absorption up the ν_3 ladder begins with the solution of the time-dependent Schrödinger equation for multiple-level systems. The Hamiltonian used is

$$H = H_m - \vec{\mu} \cdot \vec{E}(t) \ .$$

Here H_m describes the energy levels of the

molecule and $-\vec{\mu} \cdot \vec{E}(t)$ describes the interaction between the laser photons and the molecule. The molecular Hamiltonian, H_m, has been developed to second order of perturbation for octahedral molecules, and many of the molecular parameters have been evaluated using the spectra of ν_3 and $3\nu_3$ ("The Modern Revolution in Infrared Spectroscopy"). Typically, H_m contains terms of both scalar and tensor nature that account, respectively, for energy-level shifts and energy-level splittings, including the vibrational octahedral splittings.

The wave function for the total Hamiltonian, H, is expanded in the basis of the first-order molecular energy states so that all operators, except those associated with the octahedral splitting and the photon-molecule interaction, are already diagonal. Ignoring collisions, each rotational state in the ground vibrational state can be chosen to be independent; that is, the absorption for different rotational states is inhomogeneous. Excitation modeling is then done individually for each rotational ground state and the resulting populations are averaged with the appropriate Boltzmann distribution factors at the end of the calculation.

If the number of quanta in the pumped mode is small, simple solutions to the Schrödinger equation can be found by eigenvector techniques using the rotational-state angular momentum as the Hamiltonian matrix index. The multiple-photon spectrum computed for the lowest levels of the ν_3 mode of SF_6 is compared in Fig. 12 with experimental data obtained at the Lebedev Institute in the Soviet Union. Considering that the hot-band peak ($\nu_6 \rightarrow \nu_6 + \nu_3$) at 947 cm^{-1} is not included in our calculation, we find a very good agreement with the measured multiple-photon spectrum. By including the coherent dynamics of the time-dependent Schrödinger equation for the three-level system, the calculated resonances are in better proportion to the experimental spectrum than if one had simply used the population-counting technique typical of conventional spectroscopic analysis. This result shows that the anharmonicities of the pumped mode lead naturally to the observed shift to lower frequencies that is characteristic of high-fluence, multiple-photon absorption.

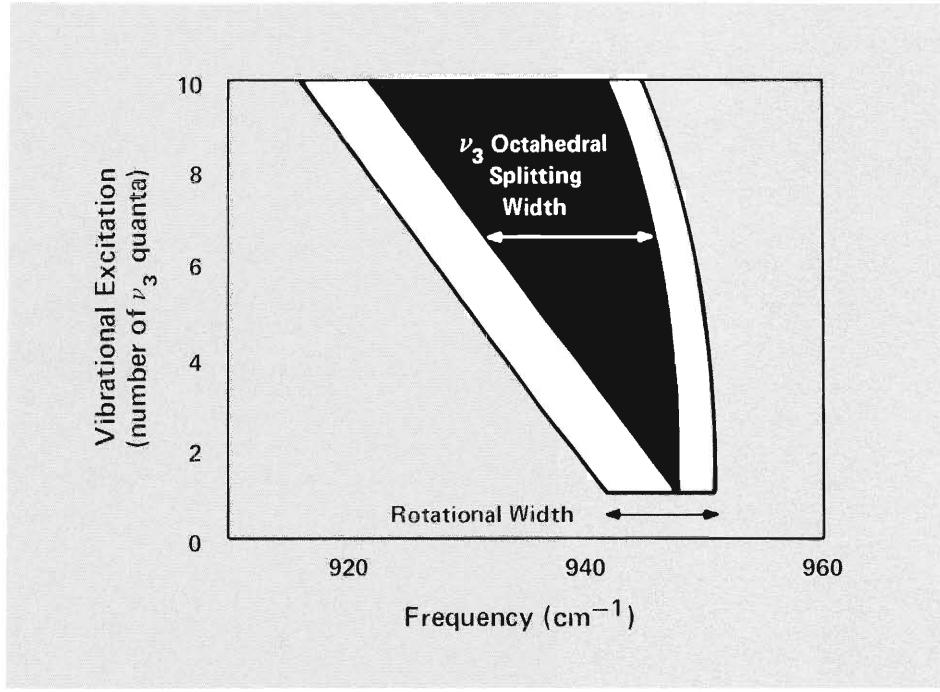

Fig. 13. Range of possible absorption frequencies for the ν_3 mode of SF_6. The white areas represent the frequency width of the ν_3 absorption band ($0 \rightarrow \nu_3$) due to rotational structure. The black area represents the increase in the range of absorption frequencies that results from the octahedral splitting of ν_3 overtone levels. This latter range increases with vibrational excitation in such a way that it compensates for much of the anharmonic shift up to $10\nu_3$.

At this fluence (0.09 joule per square centimeter) the average number of photons absorbed per SF_6 molecule is ≈ 0.7. Since some molecules are not excited, this average implies levels of excitation possibly as high as $4\nu_3$ or $5\nu_3$ for the absorbing molecules. However, above $2\nu_3$ the octahedral splitting operator effectively couples all rotational states, making both the detailed structure unobservable and this method of solution intractable. New methods to cope with this complication are currently being developed. The computed spectrum in Fig. 12, however, reflects the structure of only one and two quanta absorption.

Before leaving the discrete low-energy region of multiple-photon excitation, we need to discuss two important issues: 1) the level N_0 at which resonant normal-mode coupling occurs, that is, the energy level for the start of the quasicontinuum, and 2) the role of "coherence" in the absorption process.

First, consider Fig. 13, which illustrates how the range of possible absorption frequencies in the ν_3 mode of SF_6 changes as vibrational excitation increases. For example, $n = 1$ on the vertical axis represents the $0 \rightarrow \nu_3$ transition and the horizontal line at $n = 1$ from about 942 cm^{-1} to 951 cm^{-1} represents the width of the ν_3 absorption band resulting from the various rotational-energy transitions. At higher excitation energies this rotational width is shown as the white area split into its traditional low- and high-frequency branches. The black area expanding upward between the rotational-energy branches represents the additional frequency range for absorptions that result from the octahedral splitting of ν_3 overtone levels. We note that Fig. 13 is an idealization: many holes are certainly present within the given range where no transitions exist. However, the figure can be used to determine for a given frequency how high in the vibrational energy ladder it may be possible to resonantly excite the ν_3 mode.

As a result of the growing anharmonic mismatch, the center of the frequency range shifts to lower frequencies. However, the increase in frequency range due to the octahedral splitting compensates for the anharmonic shift for many levels of excitation. About eight photons resonant with the center of the ν_3 fundamental band at 948 cm^{-1} can be absorbed before the next excita-

tion is outside the range of possible absorption frequencies. If the laser is tuned to lower frequencies, say around 944 cm^{-1}, about ten photons can be resonantly absorbed up the ν_3 ladder of SF_6. This calculated increase explains, in part, the observed shift of high-fluence absorption spectra to lower frequencies.

Conversely, for the excitation to proceed much above $10\nu_3$ we *must* have coupling with other normal modes, that is, the start of the quasicontinuum must be below $10\nu_3$ or SF_6 would never dissociate. By considering an explicit expansion of the molecular vibrational potential in normal coordinates and strong tensor splitting of background states, we have predicted the start of the quasicontinuum in SF_6 to be at $N_0 \approx 8$. Indeed, this most recent work leads to a new counting of all coupled states and shows that the average density of interacting states becomes roughly constant as the molecule is excited to high levels.

The above arguments allow roughly one-quarter of the excitation dynamics to be described by the time-dependent Schrödinger equation in the discrete levels. This description requires the excitation to be coherent, reflecting the fact that the molecule develops a transition dipole moment in phase with the laser. In particular, populations in near-resonant or resonant laser-coupled energy levels are seen to cycle between these levels, that is, to "Rabi oscillate." The absorption and ensuing stimulated emission of energy depends on the product of the magnitudes of the electric field and the transition dipole moment.

When the difference between the laser frequency and the transition resonance frequency is large, that is, for off-resonant states, the populations oscillate rapidly at this detuning frequency, but with very little net transfer of population between states. However, because the Rabi frequency depends on the magnitude of the electric field, increasing the intensity decreases the effect of the detuning; that is, at higher laser powers an off-resonant state behaves in a resonant manner with population flow between states. This phenomenon is the Rabi broadening mentioned earlier.

An inhomogeneously broadened absorption feature consists of many independent transitions that are separately coherent. For example, the time-dependent Schrödinger equation correctly gives the dynamics of each transition in a typical, rotationally broadened absorption band. However, the excitation that is observed experimentally (as in Fig. 12) is made up of a sum over all these transitions. Because each transition has a slightly different detuning frequency determined by its location in the band, the coherent Rabi oscillation period for each transition is also slightly different. These differences give rise to a dephasing, or loss of coherence, in the dynamics observed for the entire band. In addition, each rotational transition has only a small fraction of the population available to it (determined by the Boltzmann thermal distribution of rotational energy states). Therefore, the overall excitation may not execute simple coherent Rabi oscillation.

The inhomogeneous character of the total absorption process helps explain the observed weak dependence of multiple-photon excitation on laser intensity. Solutions of the Schrödinger equation show strong intensity dependence, especially when multiple-photon resonances are important. However, solutions that are summed over rotational-energy states are a much weaker function of the intensity than the individual terms. Thus, the observed weak intensity dependence in the absorption shows that the excitation does not have the character expressed by a single Schrödinger equation.

Of course, if the laser power is sufficiently great, the middle, or quasicontinuum, region of the molecule also contributes to the excitation. Most models of multiple-photon excitation that incorporate the molecular quasicontinuum ignore coherent effects and use instead a set of population-rate equations for the dynamics. These rate equations are single-step in nature and do not exhibit Rabi oscillation. They automatically provide for fluence-dependent absorption. The rate equations are derived on the basis of a collisionless, unimolecular damping mechanism whereby energy flows out of the resonant mode into other coupled vibrational background states. However, the fact that the phenomenon can be described as a sum of many different coherent processes shows that the data do not *require* a rate-equation description.

To test these hypotheses experiments are needed that measure the lifetimes of excited states, thereby providing information about damping mechanisms by which energy flows out of one state into others. The Heisenberg uncertainty principle relates the lifetime of a state to frequency linewidths. Thus, measurements are needed of the linewidths of various processes, such as absorption from excited states, double resonance absorption, and fluorescence.

EXCITATION THROUGH THE QUASICONTINUUM. The model for multiple-photon excitation developed at Los Alamos in 1978 is illustrated in Fig. 14. To be definite, we will use as an example the absorption of CO_2-laser photons by SF_6. The discrete levels of the ν_3 resonant-mode ladder are treated as described above. However, at some level of excitation, N_0, a coupling occurs from the ν_3 overtones (the leftmost column in Fig. 14) to the background subdensity of states (the second column) having $(N_0 - 1)$ ν_3 quanta, but still at the total energy $N_0\nu_3$. (Figure 14 is drawn, for simplicity and definiteness, with $N_0 = 3$.) This background subdensity is, in turn, coupled to the subdensity having $(N_0 - 2)$ ν_3 quanta (third column), and so forth. The model is therefore distinguished by the selection rule $\Delta n = \pm 1$, where n is the quantum number for the vibrational excitation of ν_3.

The loss of a single ν_3 quantum to another vibrational mode causes the molecule to

drop back one level in its ν_3 content. In other words, this construction is convenient since the transition dipole moment is carried by the resonant ν_3 mode. Further, the $\Delta n = \pm 1$ selection rule for ν_3 is reasonable because ν_3 is the highest energy mode in SF_6 and a constant energy change of two or more ν_3 quanta would require coupling to many other modes, making such couplings higher order and much less probable.

At a sufficiently large subdensity of states, Fermi's Golden Rule can be used to describe the rate at which the population flows from a given state in the ν_3 ladder to the coupled background states with one less ν_3 quantum. The Golden Rule rate is proportional to the density of the coupled background states and to the anharmonic coupling strength averaged over the states with one less ν_3 quantum. The problem of low-level excitation in the ν_3 ladder coupled with leakage into the quasicontinuum is independent of the dynamics of further excitation or energy transfer within the quasicontinuum. This first problem can thus be solved exactly, giving the population at different locations in the quasicontinuum as a function of time.

Heller and Rice have shown that, for molecules in the quasicontinuum, if the signs of the level coupling are random, then sequential population flow is observed to the subdensities having $(N_0 - 2)$, $(N_0 - 3)$, ..., ν_3 quanta. This leakage leads to phase interruption and hence loss of coherence. The dynamics can then be determined by population-rate equations provided that the Golden Rule rates exceed the laser upward pumping rates. Our calculations are made self-consistently as follows. We assume the population-rate equations are valid and then obtain the coupling constant and, thus, the Golden Rule rates by fitting the data for absorption versus fluence. We then check to see if these rates do, in fact, exceed the laser pumping rates for the range of intensities considered. Our fit to such absorption data (circles) is shown in Fig. 15. We have also computed the fraction of molecules dissociated using standard RRKM theory

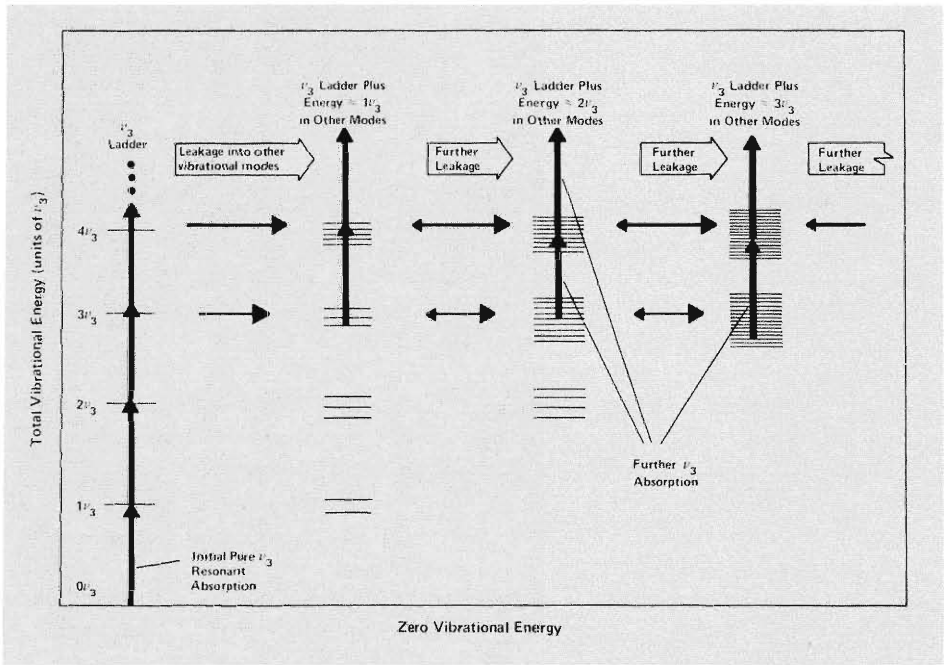

Fig. 14. Transfer of vibrational energy from the resonant, absorbing mode to other vibrational modes. Each column represents a vibrational ladder with the large steps approximately equal to one ν_3 quantum of energy. The left column is the ladder for the pure ν_3 mode. The next column represents the situation in which one quantum of ν_3 energy has leaked into other vibrational modes. This loss of ν_3 energy causes the molecule to drop back one level in its ν_3 content. Thus a new "ground state" (combination modes with no ν_3 content) is fixed at $1\nu_3$ of total energy. Each further column depicts the same situation with an additional quantum of ν_3 energy transferred to other modes and new "ground states" for the ν_3 mode at ever increasing levels of total vibrational excitation. Multiple states are drawn at each level to depict the density of modes coupled between ladders. The size of the arrows and arrowheads between ladders indicates the relative strength of coupling in both directions. The lowest level for which coupling is significant (here depicted for convenience at the $3\nu_3$ level) is defined as the start of the quasicontinuum.

(black region). The lower edge of the region was defined by using RRKM theory just during the laser pulse, and the upper edge was defined by continuing the calculation after the pulse for all population above the $33\nu_3$ level. Molecular-beam data (triangles) for SF_6 at 140 kelvin, a temperature at which almost all of the molecules are initially in the ground vibrational state, fit the theoretical curve well. The other data (squares) are included to show a typical range for dissociation data, but are not expected to correspond as well to the calculated curves because of less favorable experimental conditions (a closed cell rather than a molecular beam experiment; a temperature of 300 kelvin and, therefore, higher initial vibrational excitation).

Figure 16 shows the calculated population distributions versus the level of excitation (in terms of CO_2 photons) for various laser energies. Below a laser fluence of 0.5 joule per square centimeter we see a population bottleneck due to the transition from the discrete, low-energy region to the quasicontinuum. Below the bottleneck we see that a fraction of the molecules are unaffected by the laser photons and remain in ground states because of inhomogeneous absorption. We also note that the population distributions are quite broad. The tail of each curve above the $33\nu_3$ level represents the molecules with enough energy to dissociate.

There is no way to measure these population distributions separately; however, we can compare our results with those predicted

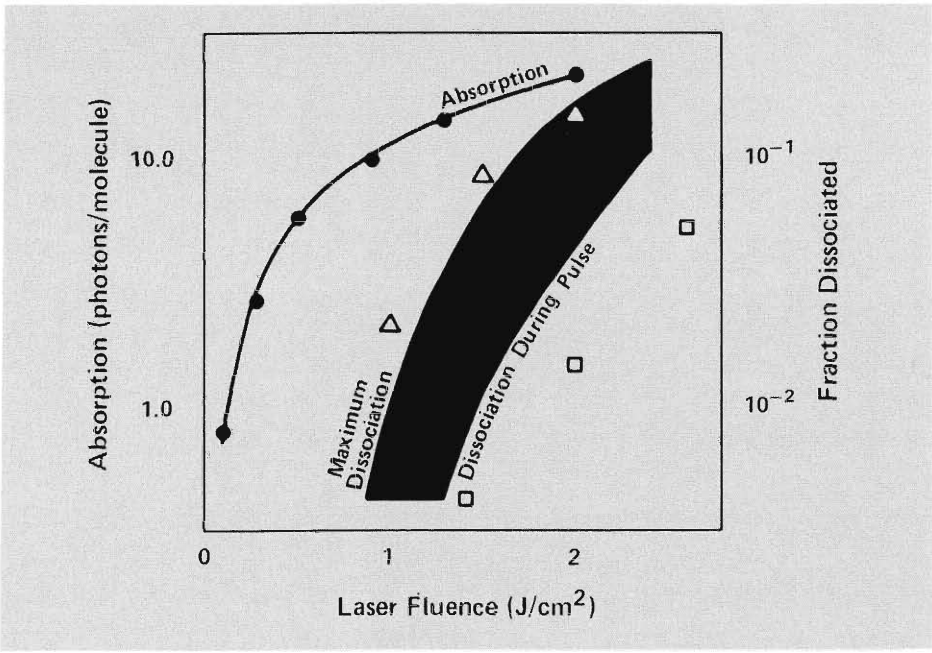

Fig. 15. Theoretical fit for SF_6 of absorption data and the fraction of molecules dissociated as a function of fluence. Absorption data (circles) for SF_6 [T. F. Deutsch, Optics Letters 1, 25 (1977)] has been used to evaluate the single coupling constant in the Los Alamos quasicontinuum model for multiple-photon excitation. The fraction of dissociated SF_6 molecules can be calculated when the RRKM unimolecular dissociation theory is combined with the Los Alamos quasicontinuum theory. The curve defining the lower edge of the black region is for the dissociation that occurs during the laser pulse only; the curve defining the upper edge is the result of continuing the rate calculations after the laser pulse for molecules excited above the $33\nu_3$ level. The triangles are molecular-beam data for dissociation of SF_6 at 140 kelvin [F. Brunner and D. Proch, Journal of Chemical Physics 68, 4978 (1978)], which agress well with the maximum dissociation curve. The squares are other data [J. G. Black, P. Kolodner, M. J. Shultz, E. Yablonovitch, and N. Bloembergen, Physical Review A 19, 704-716 (1979)] taken under conditions less favorable for comparison with theory.

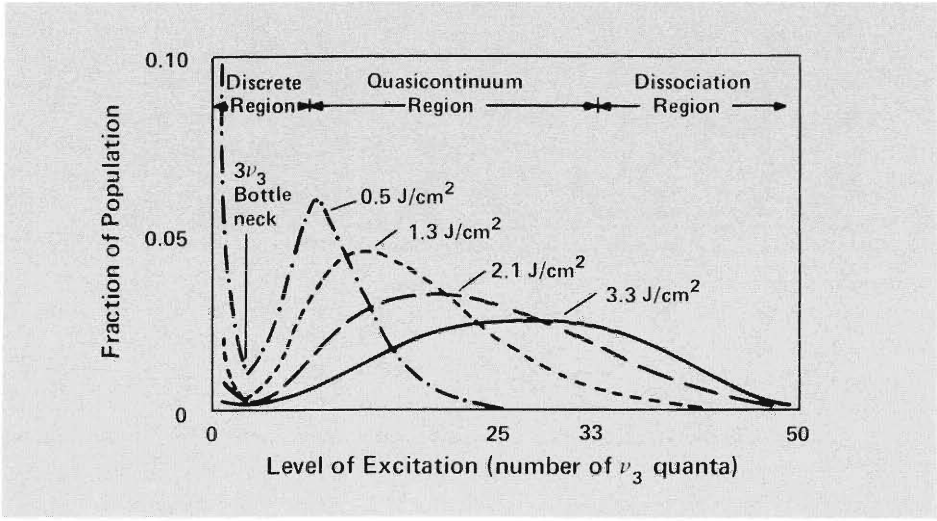

Fig. 16. The distribution of molecules with respect to level of excitation. The distribution curves calculated from the Los Alamos quasicontinuum model become broader with increasing fluence so that more molecules are in the high-energy tail of the dissociation region above $33\nu_3$. The fraction of molecules below the $3\nu_3$ bottleneck represent those molecules that are unaffected by the laser photons because, for instance, they are in rotational-energy states that do not absorb at that frequency.

by a thermal quasicontinuum model. This model is based on the idea that laser excitation leads to a thermal population distribution, that is, a Boltzmann distribution among *all* vibrational modes. A key assumption for the model is constant absorption cross section in the quasicontinuum. This assumption is equivalent to strong coupling between all modes as opposed to our assumption of the $\Delta n = \pm 1$ selection rule for ν_3 that represents weak coupling in the quasicontinuum.

An assumption of constant cross section for all levels from the ground state up leads to a Boltzmann thermal distribution with no $3\nu_3$ bottleneck and a narrow distribution with negligible dissociation (see curve with long dashes in Fig. 17). Surprisingly, however, if the thermal model is solved with a ν_3 energy ladder, that is, discrete energy levels are used for the energy levels below N_0, the population distribution (short dashes) is almost identical with that calculated from the Los Alamos model (solid line). While the thermal model with the ν_3 ladder does not result in a large inhomogeneous fraction of molecules below $3\nu_3$, the fraction of molecules in the high-energy tail is almost the same.

In summary, the modeling efforts to date on the SF_6-CO_2 laser multiple-photon problem have demonstrated a possible mechanism for this phenomenon. The observed effects of fluence and intensity and the shift to lower frequencies for high-intensity absorption are mostly accounted for by the hot bands and the discrete, low-energy region of the model. The trends in absorption cross section due to temperature and molecular size are accounted for by the vibrational state density of the quasicontinuum. Also, the resonant-mode vibrational ladder has been identified as a critical element of the model in that, without it, the calculated distribution curves are too narrow for significant dissociation to occur.

But there are difficulties. Calculations in the resonant-mode ladder above the first overtone are formidable, and the data appear to be unable to distinguish quasicontinuum

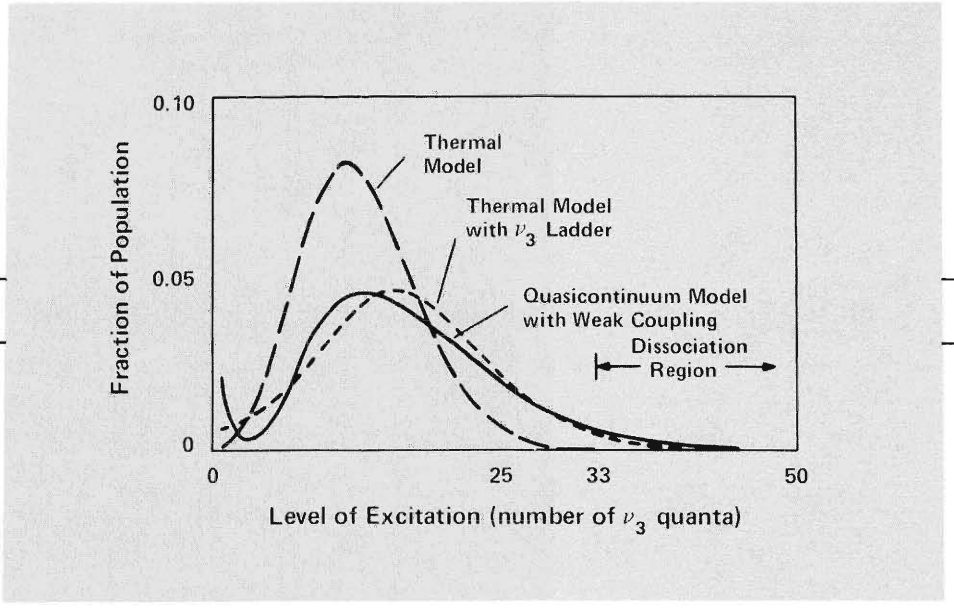

Fig. 17. Distribution curves for thermal and quasicontinuum models. The thermal model (long dashes) results in a Boltzmann thermal distribution with no $3\nu_3$ bottleneck and a narrow overall distribution. The addition of a ν_3 energy ladder to the thermal model broadens the distribution (short dashes). Surprisingly, the high-energy tail nearly matches the tail predicted by the Los Alamos quasicontinuum model (solid curve).

models that originate from opposing hypotheses. It is our belief that new quasicontinuum models must be based upon (if not explicitly derived from) accurate potential-energy surfaces for the molecule. A new model based upon a potential-energy expansion already indicates that the so-called weak coupling model with the $\Delta n = \pm 1$ selection rule for ν_3 overcounts the number of coupled states. The overcounting results from the fact that the selection rule applies only to changes in ν_3, thus limiting the vibrational coupling of ν_3 with other modes to low order, but not limiting in a similar manner the couplings between all other modes in the quasicontinuum.

There are at least two other important aspects that need eventually to be incorporated into the model for multiple-photon excitation. The first is the effect of initial vibrational excitation. This effect may explain important differences in absorption behavior for different molecules and temperatures by providing alternate pathways for multiple-photon excitation. The second is the effect of collisions, an extremely difficult modeling problem. Nevertheless, many photochemical or laser isotope separation schemes require high molecular concentrations to insure the generation of significant amounts of reaction product. An adequate model for such conditions must necessarily account for collisions.

Concurrently with theoretical advances, experimental techniques need to be developed that reveal more detail about the distribution of vibrational energy, both among the collection of molecules and within given molecules. Presently, dissociation experiments measure the total number of molecules above the dissociation energy, that is, the area under the tip of the high-energy tail of the population distribution curve. Likewise, absorption experiments determine only the average number of photons absorbed per molecule, that is, the mean of the distribution curve. Experiments need to be designed that map the detailed shape of the curve and so distinguish between alternate models. Also, once photons are absorbed, how is the energy distributed among the vibrational modes of the molecule? Are there pathways of rapid energy flow between certain states, but restricted flow between others?

Much has been learned about the surprising phenomenon of multiple-photon excitation. But there are experimental and theoretical challenges yet to be overcome—many of which undoubtedly harbor further surprise. ■

Further Reading

N. Bloembergen and E. Yablonovitch, "Infrared-laser-induced unimolecular reactions," Physics Today **31**, No. 5, 23-30 (1978).

Ahmed H. Zewail, "Laser selective chemistry—is it possible?," Physics Today **33**, No. 11, 27-33 (1980).

V. S. Letokhov, "Laser-induced chemical processes," Physics Today **33**, No. 11, 34-41 (1980).

J. L. Lyman, G. P. Quigley, and O. P. Judd, "Single-infrared-frequency studies of multiple-photon excitation and dissociation of polyatomic molecules," in *Multiple-Photon Excitation and Dissociation of Polyatomic Molecules*, C. D. Cantrell, Ed. (Springer-Verlag, Berlin, to be published).

N. R. Isenor and M. C. Richardson, "Dissociation and breakdown of molecular gases by pulsed CO_2 laser radiation," Applied Physics Letters **18**, 224-226 (1971).

L. Allen and J. H. Eberly, *Optical Resonance and Two-Level Atoms* (John Wiley & Sons, New York, 1975).

Harold W. Galbraith earned his Bachelor of Science degree in 1967 at Pennsylvania State University and a Ph.D. in physics from the University of Pennsylvania in 1971. He came to Los Alamos on a postdoctoral appointment in 1973 to work with James D. Louck on group theoretical approaches to the few-nucleon problem. He became interested in molecular spectroscopy in 1974 and began working on problems of interest to the Applied Photochemistry Division. His research interests moved to quantum dynamics in 1976 with the discovery of isotopic selectivity in multiple-infrared-photon dissociation of polyatomic molecules. (Photo by Henry F. Ortega)

AUTHORS

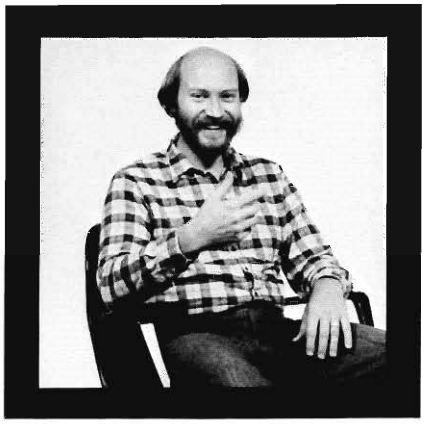

Jay R. Ackerhalt earned his Bachelor of Science (1969) from Hobart College and his Master of Arts (1972) and his Ph.D. (1974) in physics, specializing in quantum optics, from the University of Rochester. Before joining the Laboratory in 1977, he held postdoctoral positions at the Institute for Theoretical Physics of the University of Warsaw, Poland, at the Department of Physics and Astronomy of the University of Rochester, and at the Physics Department of Johns Hopkins University. At Los Alamos he has worked on a theory of multiple-photon excitation in polyatomic molecules, primarily SF_6 and UF_6, and has shared with Harold Galbraith the Laboratory's Distinguished Service Award for this research and its application to the uranium enrichment program. His present interests include self-focusing effects in polyatomic molecules. (Photo by Henry F. Ortega)

John L. Lyman received his Bachelor of Science and his Ph.D. in chemistry from Brigham Young University in 1968 and 1973, respectively. He performed the research for the Ph.D. degree at Los Alamos under Reed J. Jensen. That research included some of the first experimental studies of infrared-laser-induced reactions of polyatomic molecules. He also worked on HF chemical lasers. After joining the Laboratory in 1973, Lyman, along with Stephen Rockwood, Reed Jensen, C. Paul Robinson, and Jack Aldridge, was active in the early research on multiple-photon excitation. These scientists hold the patent for isotope separation by that process. Lyman has authored over thirty-five papers, including several review articles, on this and related phenomena. He is currently the Assistant Group Leader of the Laser Chemistry Group in the Applied Photochemistry Division. Most of his time is spent working on problems related to the uranium enrichment project. These problems include infrared self-focusing effects in UF_6 gas and the chemical reactions of UF_6 dissociation fragments. (Photo by Henry F. Ortega)

R. V. Ambartsumyan, Yu. A. Gorokhov, V. S. Letokhov, and G. N. Makarov, "Separation of sulfur isotopes with enrichment coefficient $>10^3$ through action of CO_2 laser radiation on SF_3 molecules," JETP Letters **21**, 171 (1975).

John L. Lyman, Reed J. Jensen, John Rink, C. Paul Robinson, and Stephen D. Rockwood, "Isotopic enrichment of SF_6 in S^{34} by multiple absorption of CO_2 laser radiation," Applied Physics Letters **27**, 87-89 (1975).

J. R. Ackerhalt and J. H. Eberly, "Coherence versus incoherence in stepwise laser excitation of atoms and molecules," Physical Review A **14**, 1705-1710 (1976).

N. Bloembergen and E. Yablonovitch, "Collisionless Multiphoton Dissociation of SF_6: A Statistical Thermodynamic Process," in *Laser Spectroscopy III*, J. L. Hall and J. L. Carlsten, Eds. (Springer-Verlag, New York, 1977).

T. F. Deutsch, "Optoacoustic measurements of energy absorption in CO_2 TEA-laser-excited SF_6 at 293 and 145 K," Optics Letters **1**, 25-27 (1977).

F. Brunner and D. Proch, "The selective dissociation of SF_6 in an intense ir field: A molecular beam study on the influence of laser wavelength and energy," Journal of Chemical Physics **68**, 4936-4940 (1978).

S. S. Alimpiev, N. V. Karlov, S. M. Nikiforov, A. M. Prokhorov, B. G. Sartakov, E. M. Khokhlov, and A. L. Shtarkov, "Spectral Characteristics of the SF_6 Molecules Excitation by a Strong IR Laser Field at Continuously Tuned Radiation Frequency," Optics Communications **31**, 309-312 (1979).

Jerry G. Black, Paul Kolodner, M. J. Shultz, Eli Yablonovitch, and N. Bloembergen, "Collisionless multiphoton energy deposition and dissociation of SF_6," Physical Review A **19**, 704-716 (1979).

O. P. Judd, "A quantitative comparison of multiple-photon absorption in polyatomic molecules," Journal of Chemical Physics **71**, 4515-4530 (1979).

Harold W. Galbraith and Jay R. Ackerhalt, "Vibrational Excitation in Polyatomic Molecules," in *Laser-Induced Chemical Processes*, J. I. Steinfeld, Ed. (Plenum Press, New York, 1981), pp. 1-44.

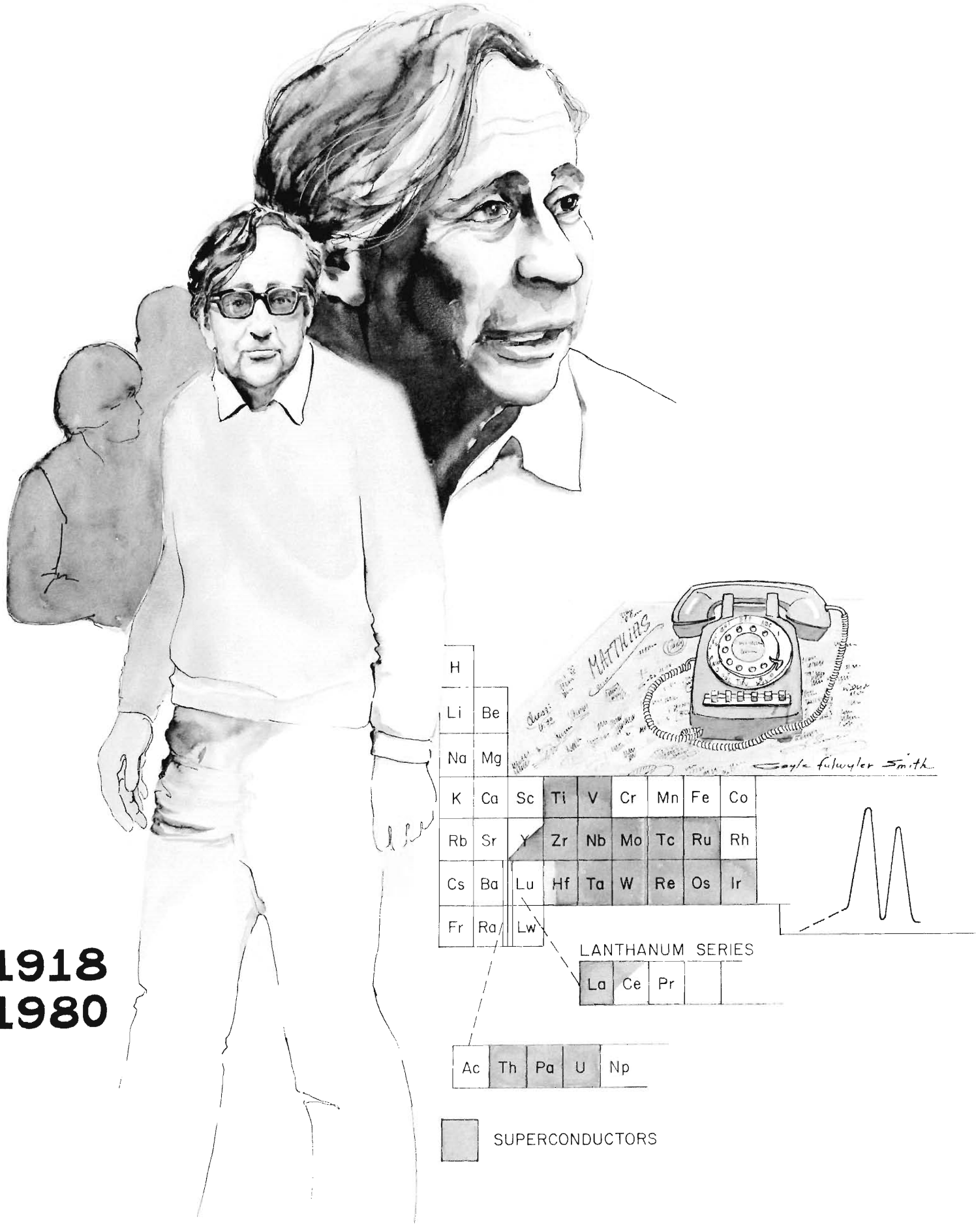
MATHIS
Gayle Fulwyler Smith
H
Li Be
Na Mg
K Ca Sc Ti V Cr Mn Fe Co
Rb Sr Y Zr Nb Mo Tc Ru Rh
Cs Ba Lu Hf Ta W Re Os Ir
Fr Ra Lw
LANTHANUM SERIES
La Ce Pr
Ac Th Pa U Np
SUPERCONDUCTORS
1918
1980

Bernd Matthias

A Personal Memoir by Paul R. Stein

Some time on the morning of October 27, 1980, Bernd Matthias suffered a fatal heart attack. The news reached relatives and some close friends before mid afternoon; by the next day, hundreds knew. The common reaction among all these people, at least initially, was disbelief. How could a man so vital, so filled with creative energy, be cut down without reason or warning? There were so many plans, so many irons in the fire, so many people depending on him. It was unthinkable, in fact, ridiculous. Of course, acceptance and grief soon followed. But even now, months afterward, there are a few old friends who would say that if they saw Bernd in the street or heard his voice in a crowd, they would not be astonished.

What I have just described is a familiar, much-studied syndrome. The surprising thing is how many people exhibited the symptoms, usually restricted to intimates of the deceased. One is moved to conclude that all these people really felt themselves to be close to Bernd. In my opinion, that conclusion is certainly right.

Early Years

Now for some facts, and, as they say, a little bit more. Actually, in what follows I shall not attempt a strict separation of fact and hearsay except where scientific achievement is involved. Much of Bernd's history is embodied in anecdotes; very often a story, even though merely *ben trovato*, contains more truth than a register of dates and deeds. But first let me apologize to more formally-minded readers for the practice of referring to my subject, Professor Dr. B. T. Matthias, simply as Bernd. I am not invoking the privilege of long and close friendship; it is rather a matter of what sounds best. Bernd himself had absolutely no use for academic stuffiness, and was unimpressed by titles of any sort. Applied to him, the formal mode of address has a false ring; here I have adopted what I hope is a suitably informal style.

Bernd was born on the 8th of June, in either 1918 or 1919; he himself stuck by the second date, but most others opt for the first. At least there is general agreement that the place was Frankfurt, Germany. There is

Matthias
A Personal Memoir

something mildly ambiguous about the record of Bernd's early years, and I shall not be concerned with trying to clear things up. This may be the proper occasion for proposing a new uncertainty principle à la Heisenberg. Although the principle has not yet been clearly formulated, one symbol suggests itself: Δt_B, a time measured in years representing the absolute uncertainty for a subset of significant dates in Bernd's life. Evidently $\Delta t_B \approx 1$.

The milieu Bernd entered was upper middle-class, and there were apparently no financial problems. His father, a successful leather merchant, died when the boy was two. In 1925, Frau Matthias moved her family (Bernd and his younger sister Judith) to nearby Königstein, where she owned a country house with extensive grounds. It must have been a wonderful place indeed, if the tales of idyllic childhood that have come down to us are accurate. All the usual children's games are recorded, the difference being that the playmates were offspring of the aristocracy and the very rich. The boy was bright, unconventional, and undoubtedly spoiled by his mother, who doted on him. Marta Matthias had grand ambitions for her son; she wanted him to be an international figure, preferably in the physical sciences. According to Bernd, as reported by his wife Joan, his mother thought a fitting role would be that of a great astronomer. This suggests that maternal influence was the principal factor in Bernd's choice of career.

Frau Matthias believed in the British system of educating the well-to-do. Accordingly, Bernd attended a series of boarding schools, most of them in Switzerland, which were predominantly international in character. It was probably during this period of secondary education that Bernd laid the foundation for his command of Swiss German, to be perfected during his university years. His remarkable ability to handle—and occasionally manipulate—people, so evident to all who knew him, must also have had its development in this period. The following fairly well-attested story suggests that this is so. In one of the boarding schools, Bernd had as a classmate the scion of a very rich and aristocratic Italian family. This young man was easily the most disliked student in the entire school. Recognizing the problem and its cure, Bernd offered to make the noble youth one of the most popular boys in the class; for this he would receive, if successful, a certain sum. As the story goes, Bernd succeeded brilliantly, and collected the money. Shortly thereafter the boy's mother came to visit. Bernd feared she would angrily demand return of the fee, which was not precisely in the chicken-feed range. Instead, the lady was overjoyed, and Bernd became a lifelong friend of the family.

The University

In 1936, after a mysterious last fling in Rome, during which he reportedly cashed in on the standing invitation occasioned by the boarding school feat mentioned above, Bernd entered the Eidgenössische Technische Hochschule (E.T.H.) in Zurich. His major was physics. The death of his mother in 1938 seemed to strengthen his resolve to succeed in his chosen field, and he became, by contemporary accounts, a very hard worker. It is said that he was not particularly strong in mathematics. I can believe this, even though in later years he displayed a lively interest in the facts of number theory. Perhaps it was this attitude toward mathematics that kept him away from theoretical physics, despite the presence among his teachers of two very strong theorists, Wolfgang Pauli and Gregor Wentzel. (Later, at the University of Chicago, Wentzel tried, without success, to interest Bernd in field theory.) Bernd became an experimentalist, and his subsequent brilliant career attests the correctness of this choice.

Bernd's thesis advisor was Paul Scherrer, a man in his late forties, whose considerable zest was the equal of Bernd's own. After receiving his Ph.D. in 1943, Bernd became a research associate, evidently Scherrer's favorite. Despite the age difference, the two were close friends, "even to the extent of exchanging girl friends," as one former schoolmate has remarked. Bernd was admired and envied for his ability to attract pretty girls. "He was an expert in arranging to have girl friends in strategic positions," girls with access to fancy foods (then hard to come by) and girls with political connections. The former provided him and his friends with gourmet fare at his laboratory every morning; the latter enabled him to maintain his work permit despite his lack of Swiss citizenship.

Bernd's thesis involved some properties of ferroelectric crystals; this was to be his main professional interest for the next six years. It soon became apparent that he would not be content merely to refine and extend the work of his predecessors. Bernd was not especially interested in proving or disproving other people's theories. (Perhaps his work in the 1960s on the superconducting isotope effect should be considered an exception.) Instead, he adopted an empirical approach, testing many hundreds (later thousands) of alloys and compounds, regardless of prevailing theories, to find new examples of whatever phenomenon currently interested him. As we know, this approach paid off in the most handsome fashion for superconductors. But even in the early days, before he became interested in superconductivity, he carried out this sort of research on ferroelectrics, most of it in collaboration with John Hulm at Chicago. At E.T.H., from 1944 to 1949, he used much of his time developing his experimental skills and, by no means incidentally, learning to grow pure crystals of barium titanate. As it happened, Bernd's technique became known to crystallographers at the Cavendish Laboratory in Cambridge, and their product was used by Hulm for some important research. Bernd was, in effect, scooped; this

occasioned some acrimonious argument when he and Hulm first met at Chicago in 1949. They soon became close friends, however, and enjoyed many years of fruitful collaboration.

Bernd's empiricism was, I think, a symptom of his intellectual independence. To some, however, he seemed merely brash and impertinent, especially when he challenged in public the views of senior professors. No doubt there was in his character an innate irreverence coupled with a youthful desire to shock. One old friend from the Zurich days recounts a typical incident. Bernd had been invited by some colleagues to join them in a Sunday climb near Schwyz, in the central part of Switzerland. Because he had seemed less than enthusiastic, the others were not surprised when he failed to meet them at the train station. The party of four, clad in all their mountaineering gear, had boarded and the train had started to pull out, when Bernd appeared, casually dressed in shirt, slacks, and sneakers, and carrying a small parcel of pastry for his lunch. So they all climbed together, four in full regalia and one dressed for tennis. Of course Bernd had a cover story, but to me the whole thing sounds like pure panache.

America

By 1947, Bernd was an expert on ferroelectric crystals. This got him an invitation from Arthur von Hippel to come to MIT for a year. The invitation was accepted and, in effect, Bernd emigrated to the New World. At MIT he continued his work on barium titanate; most of this work appeared in *Physical Review* during 1948. When his year at MIT was up, he joined the staff of Bell Laboratories in Murray Hill, New Jersey. Perhaps the most important event in Bernd's professional life during this period was making the acquaintance of Willie Zachariasen. They were introduced by Ray Pepinsky (who had been one of Willie's early graduate students) during a crystallography meeting at Yale in March 1948. By this time Willie had been recognized as a "world-class" crystallographer, in the forefront of his profession. The two hit it off to an extent that could scarcely have been predicted. It may be that Willie assumed the semipaternal role played previously by Scherrer. At any rate, Bernd and Willie became very close friends, and Willie taught Bernd a great deal about crystal structure, indispensable knowledge for future endeavors. The relationship could not be described as serene. Both men were very outspoken. From 1962 on, I myself witnessed numerous arguments, mostly about technical matters, but occasionally having to do with the relative merits of fellow scientists. Willie was perhaps the sounder of the two, but he was also the more stubborn. So far as I could judge, the really substantial arguments were draws.

The relationship developed during Bernd's two years (1949-1951) as assistant professor at the University of Chicago, where Willie was chairman of the Physics Department. As I remarked earlier, John Hulm was there at the time, and he and Bernd did much work together. It was Hulm who, with the not inconsiderable help of Enrico Fermi, aroused Bernd's interest in superconductivity. Fermi pointed out that superconductivity was much less well understood than ferroelectricity, for which some reasonable theoretical models existed. I don't know what Bernd thought of these models of ferroelectricity. Much later he would claim that ferroelectrics and superconductors are similar in structure: "Superconductivity is a phase which is just on the verge of disappearing; small variations can convert a superconductor into a ferroelectric metal or a semiconductor, or possibly cause the crystal to fall apart entirely."

From a list of Bernd's publications, I would conclude that his serious interest in ferromagnetism also dated from the Chicago period. Twenty-eight years later, in 1978, Bernd had this to say about the relation between ferromagnetism and superconductivity:

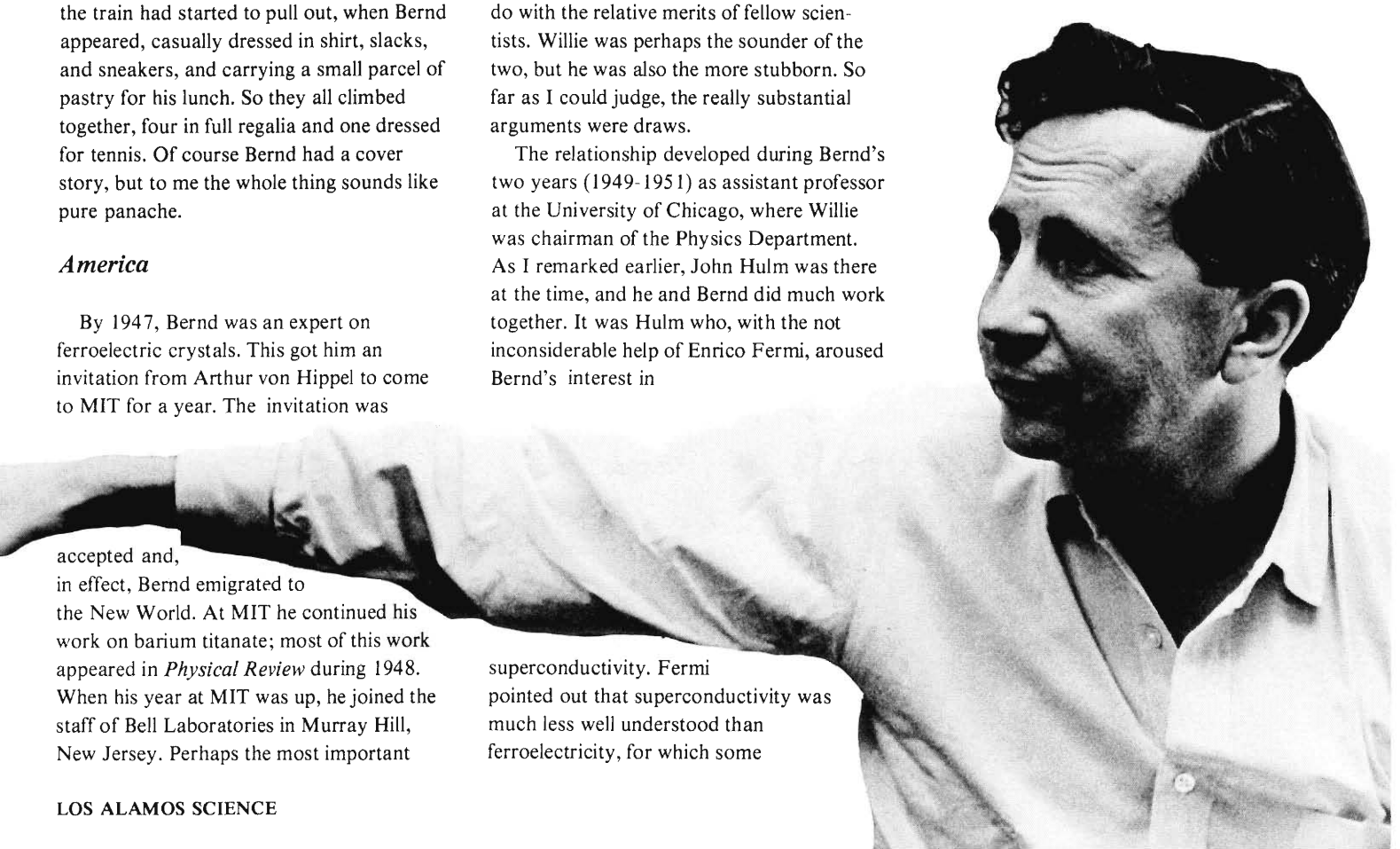

Matthias
A Personal Memoir

It is well known that a sufficiently large magnetic field will destroy superconductivity (by interfering with the alignment of the Cooper pairs). One might think this means that magnetic compounds are never superconducting, but that is not so (the example of cerium under pressure has already been mentioned). Superconductivity and magnetism are, after all, kindred phenomena (both ordered states, or condensations) differing, one might say, in sign (superconductivity can be considered an extreme case of diamagnetism). It is therefore not surprising that the presence of magnetism often indicates where one should look for superconductivity. What is surprising is the relative scarcity of magnetism; it is much more interesting to look for magnetic compounds than for superconducting compounds, since the latter can be found nearly everywhere.

According to one source, Bernd thought for many years that magnetism and superconductivity were incompatible. As for the electron-phonon interaction, the principal mechanism in the theory of superconductivity proposed by Bardeen, Cooper, and Schrieffer in 1957, Bernd seems not to have fully accepted it until the West Coast Gordon Conference of 1970.

Bernd did not stay long at Chicago, returning to Bell Laboratories after only two years. He was on leave, and it could be that Jim Fisk, then president of Bell, told him to come back or pack up. I myself have always assumed that his leaving Chicago so soon had something to do with the unlikelihood of achieving tenure. Apart from Zachariasen, and to a lesser extent Fermi and Wentzel, Bernd had no influential supporters at either the University or the Metals Institute. Perhaps it was a case of the Bright Young Man ruffling some establishment feathers. Precisely this is said to have happened when Bernd was being interviewed for a job at Princeton. The anecdote, considerably condensed from Bernd's Standard Version, goes as follows. Eugene Wigner arranged the interview and, just before it took place, pleaded with Bernd to be on his best behavior. (That in itself may have been a mistake.) One senior professor, apparently irritated by Bernd's self-possessed manner, proceeded to unsheathe the needle. This did not sit well with Bernd. Things came to a head when the professor, with some sarcasm, asked Bernd about his interest in extrasensory perception. Bernd quickly admitted his concern with this dubious phenomenon, adding that he had always wanted to disprove the second law of thermodynamics, which he had never liked anyway. The professor, falling into the trap, said he failed to see the connection. "Oh, it's quite elementary," said Bernd; "you have to remember that when something eerie happens, there's usually a chill in the air."

Bernd's supposed interest in extrasensory perception is the occasion for another anecdote which, if not true, is at least characteristic. Here, though, Bernd comes out the loser. I follow the version of George Feher, a colleague of Bernd's on the physics faculty at La Jolla. As Feher tells it:

One of Bernd's passions was betting. A particular bet that comes to mind took place at Bell Labs in the fifties. Several of us were complaining at lunch one day how hard it was to get Bell Labs to pay for trips abroad. Bernd shook his head and said, "That's just because you are all ribbon clerks" (one of his favorite expressions). "I'll bet you I can get Bell to pay me for a trip to Tibet and an extended stay there." I didn't believe he could pull it off, and took him up on it immediately. The next week Bernd arranged a luncheon with Jim Fisk (then president of Bell Labs) and, between the soup and the main course, he said, "Jim, I want to go to Tibet for a few months, and I expect Bell Labs to pay for my trip." When Jim quietly asked why, Bernd replied, "Well, I know of a guru there who

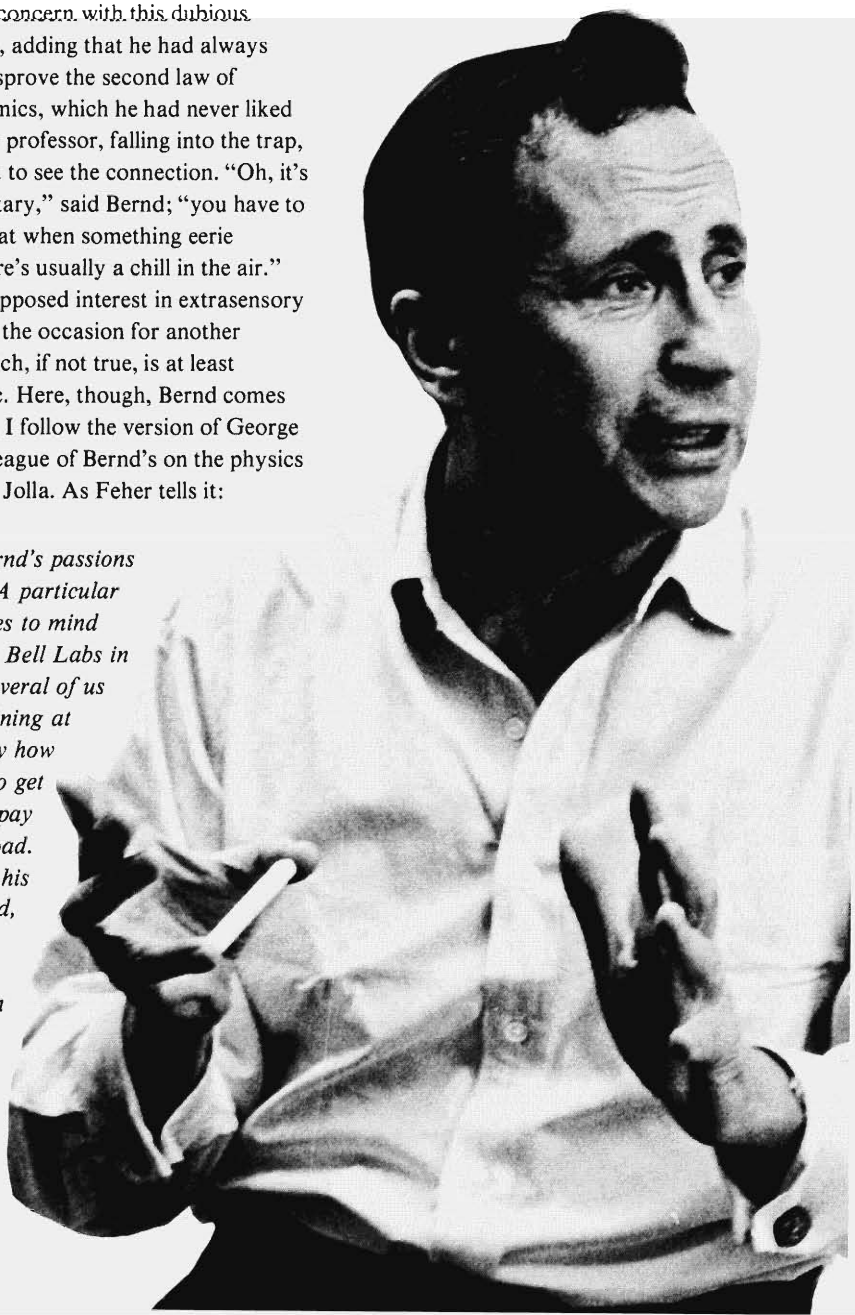

can teach me ESP. Knowing about this should be of enormous importance to the phone company. If ESP became commonplace and everybody could practice it, nobody would need phones, and Bell Labs would go broke." Jim thought for perhaps a second and said, "Bernd, I'm afraid you're behind the times; we already have a department that does nothing but work on the jamming of ESP."

Success

Back at Bell Laboratories, Bernd settled down to some hard work in his new field of superconductivity. "Settled down" may be too strong; at least he had taken the first step toward solid citizenship in 1950 by marrying Joan Trapp—a move that certainly did not hurt his reputation for finding and influencing pretty girls.

The attempt to understand superconductivity led to a search for new superconducting materials. Among Bernd's collaborators in this effort were Ted Geballe, Joe Remeika, the theorist Harry Suhl, and "Bernd's secret weapon" Ernie Corenzwit, who was a coauthor with him on at least 60 papers.

A word about Bernd's publications is in order here. The corpus of 309 papers through 1978 seems at first glance to consist mainly of experimental reports with titles like "Superconductivity in the Y-Rh and Y-Ir Systems" (Matthias, Geballe, Compton, Corenzwit, and Hull). A closer look reveals that about a quarter of the entries are review or state-of-the-art papers; of many of these Bernd is the sole author. In a rapidly changing field there is much demand for such continual updating. The existence of these articles indicates not only that Bernd was fast becoming (and by the early 1960s had become) the authority on practical superconductivity, but also that at fairly regular intervals during the course of his investigations Bernd would attempt to generalize from experience.

As I have remarked, for many years Bernd found it difficult to accept the electron-phonon interaction as the basic mechanism of superconductivity. When I first asked him about it, the BCS theory was roughly five years old. Even in the early days he did not disparage the theory, but merely declared it irrelevant to the discovery of new superconducting materials. His brilliant success in that very endeavor tended to prove his point. Bernd's quarrel with the solid-state theorists grew in intensity through the 1960s, the acrimony reaching a peak in the early 70s. He did not, of course, fight with all of them. Notable exceptions were his friend Harry Suhl, Phil Anderson, Charlie Kittel, Conyers Herring, and probably John Bardeen. Then there was J. H. Van Vleck, whom he admired and with whom he did some important work on europium oxide. But I would have to say that he did not have many friends in the theoretical camp. In the last few years, I thought I detected some signs of mellowing, but now I am not so sure. As late as 1978 he was capable of publishing some very bitter remarks.

The argument between Bernd and the theoretical establishment in solid-state physics had more than a single cause. One was the claim of some theorists to be able to predict superconducting phenomena. In my opinion, Bernd showed convincingly that these claims were empty. Although a considerable showman himself, Bernd would not tolerate charlatanism in science, and that is just how he viewed these attempts at prediction. To be sure, he sometimes carried his criticism to ludicrous extremes—for example, to the point of stating that the mere writing down of a Green's function was a sign of fraudulent intent. If failure to predict was bad, "prediction after the fact" (as he called it) was worse. What Bernd meant by this phrase was the promulgation of theories so full of arbitrary constants that they could be made to fit almost any situation. Experimentalists would discover new phenomena, and the villains of the piece would adjust their formulae so that in due course they could "explain" the results. Unfortunately, it often happened that the supply of constants was exhausted before everything could be explained—a sure sign of a bankrupt theory.

There was also a philosophical disagreement at the root of the trouble; readers will recognize it as nothing more than the ancient battle between induction and deduction. Bernd's commitment to the empirical method was very strong. He was convinced that constructing a theory and then designing experiments to verify it was the wrong way to study a phenomenon as complicated as superconductivity. The right way was to try everything, in flexible sequence—for example, substituting elements from the same part of the periodic table while maintaining the same crystal structure—to see how the transition temperature T_c actually varied as these changes were made. This "pay-as-you-go" inductive method is not congenial to most theoretical physicists, and it is easy to see a source of conflict here. But Bernd had tangible progress on his side. Not only was he extremely successful in his program, he is also given credit by some for a modest revival of scientific empiricism in this country.

During the eight or nine years at Bell Laboratories, Bernd and his coworkers had many triumphs, but two stand out. One was the discovery in 1954 of the superconductivity of Nb_3Sn at 18 kelvin; the transition temperature was a record high at the time. Although several people were involved—Matthias, Geballe, Geller, and Corenzwit—Bernd seems to have been the driving force behind the work, and he received much acclaim for his efforts.

Niobium-tin has the so-called beta-tungsten crystal structure (a misnomer arising from an early, mistaken identification of a "new" form of tungsten), which is still the most favorable structure known for high transition temperatures in binary

Matthias
A Personal Memoir

compounds. Nb_3Sn is a "type II" superconductor with a high critical field. Commercially useful superconducting magnets came into being in 1960 when long wires of Nb_3Sn became available for winding solenoids.

The other outstanding triumph was the formulation of an empirical rule to guide the search for superconductors with high transition temperatures. Over the years, Bernd and his coworkers had observed that, in those parts of the periodic table where superconductors generally occur, there is a correlation between transition temperature and the number of valence electrons per atom. For non-transition-metal superconductors, the peak transition temperature is found at about 5 valence electrons per atom; for transition-metal superconductors, there are peaks at both 5 and 7 e/a. In the case of binary compounds one uses the weighted average for the two components. Of course, this prescription is not infallible; it cannot, for example, distinguish between La_3In and $LaIn_3$, (lanthanum and indium have the same number of valence electrons), yet these two compounds have quite different transition temperatures (10.5 and 0.7 kelvin, respectively). Further, it fails completely for ternary compounds. Nevertheless, the "electron counting" prescription, first published in 1955, proved to be one of Bernd's principal tools in his discovery of over 1000 superconducting materials.

Los Alamos and La Jolla

In the early 1950s Nick Metropolis suggested to Carson Mark, then leader of the Laboratory's Theoretical Division, that Bernd would be a good man to have on the Division's consultant list. Nick had come to know Bernd at Chicago and had formed a very favorable opinion of his abilities. Carson was persuaded, and the wheels were set turning. Apparently they turned rather slowly (the clearance check proved hard to complete), but finally Bernd appeared at Los Alamos. The vexed question of just when this happened is further proof that $\Delta t_B \approx 1$; circumstantial evidence points to 1956, but strong, unshakable memories say 1957.

Bernd's consultant duties were at best loosely prescribed; based as he was in the eclectic corridors of the Theoretical Division, he was free to look into anything that interested him. Chemistry, Metallurgy, and Cryogenics were where one might have expected to find him, but early on one was more likely to run into him in one of the weapons-design divisions, where he dispensed expertise on piezoelectric switches. It was not until 1962 that a paper on superconductivity appeared bearing his name along with those of Laboratory members. Very early he began to be used in an advisory capacity; he also acted as self-appointed liaison between initially incompatible groups. Ultimately, of course, there was a great deal of superconductivity research done at Los Alamos either under his direction or with the benefit of his advice. After 1970 Bernd had closer contact with the Director's Office, and in 1971 Harold Agnew appointed him a Fellow of the Laboratory, the first to be so honored.

A branch of the University of California was established in La Jolla in 1960; in 1961 Bernd was appointed Professor of Physics at the new institution (named, for some reason, UCSD rather than UCLJ). Despite the move to California he maintained his connection with both Bell Laboratories and Los Alamos. This meant there were now three laboratories at which Bernd's superconductivity research could be pursued. Among those who from time to time worked with Bernd at Los Alamos were Al Giorgi, Gene Szklarz, Clayton Olsen, Bernd's student the late Hunter Hill, and, in later years, Jim Smith and Greg Stewart. Smith and Stewart, along with Giorgi, collaborated with Bernd in a remarkable study of the eutectic structure of yttrium-iridium; this was the last project Bernd was involved with at Los Alamos.

In La Jolla Bernd had his old friend Harry Suhl, the only theorist with whom he published regularly. Between 1965 and 1980 he supervised 22 doctoral theses, and several of his former students remained at La Jolla for extended periods. Among these were Brian Maple, George Webb, Zach Fisk, Angus Lawson (now at Pomona), and the late John Engelhardt.

In these years Bernd developed a coherent view of the nature of superconductivity and the limits on the transition temperature. To mention only one aspect, Bernd came to believe that in binary compounds with the beta-tungsten structure, perfect stoichiometry was essential for attaining high transition temperatures. This is well illustrated by the case of Nb_3Ge. The original niobium-germanium compound had the composition $Nb_{3.3}Ge$, and was superconducting at 6 kelvin. It took many years to develop techniques for making a compound with a composition closer to the 3-to-1 ratio, for example, $Nb_{3.1}Ge$, with a transition temperature of 18 kelvin. Finally, in 1973, using the "sputter" technique, John Gavaler at Westinghouse Research Laboratories was able to make the compound Nb_3Ge; it has a transition temperature of 23 kelvin, the highest of all superconducting materials. Of course, Nb_3Ge is quite unstable; just dropping the sample on the ground will lower the transition temperature. It would be technically advantageous to find a superconductor with a transition temperature of 25 kelvin or higher, because then liquid hydrogen rather than liquid helium could be used as the coolant. Such a material has so far eluded discovery. Bernd conjectured that niobium-silicon would be such a compound if it could be made in the exact stoichiometric ratio of 3 to 1, that is, as Nb_3Si, but went on to say, ". . .this does not seem possible at present. The basic reason for this is that the silicon atom is just too small; in the beta-tungsten structure, stoichiometry seems to require atoms with

comparable radii." I am told that the question is very much alive.

Because of the extremely unstable nature of superconductors with high transition temperatures, Bernd believed that T_c values greater than about 30 kelvin were unattainable with any material, and that 25 kelvin was probably an upper limit for binary compounds with the beta-tungsten structure. Therefore, he was greatly incensed to discover that much government money was being used to support a search for organic superconductors (in the form of thin polymers) that would, it was hoped, be superconducting at room temperature or thereabouts. Bernd was adamant (his favorite word) in his opinion that such things did not and could not exist. Around his laboratory one could hear occasional jokes about "superconducting carrots" and "high T_c celery." Privately, Bernd did not deny the possibility that some organic crystals might be superconducting, but if such things were found, they would (he said) have very low transition temperatures. When a meeting on organic superconductors was announced, Bernd stated (probably incorrectly) that it was "the first conference ever on a nonexistent subject." Bernd said on more than one occasion that if the government wanted to waste its money on ridiculous projects, it would do better to fund the development of antigravity paint—because if anyone ever managed to make that, the payoff would be beyond imagining. The existence of some superconducting organic crystals has recently been reported; as Bernd suspected, these materials have low transition temperatures and are of no immediate practical interest.

The Professor

Bernd had been a professor before, but his new position bore no resemblance to the previous one at Chicago. All of a sudden he was on top of the academic heap, with perquisites that effectively freed him from the more onerous duties. For one thing, his relation to the University curriculum was extremely tenuous; he was never required to teach a regular course, graduate or undergraduate. To be sure, he did conduct some advanced seminars in solid-state physics. I heard him lecture at the first meeting of one such seminar. To me it seemed an unabashed exercise in one-upmanship. I trust the subsequent sessions were more productive. The real thrust of his teaching was directed at his many graduate students. According to the testimony of some of these former students, Bernd was a splendid teacher. His method was to probe and challenge, aiming to develop self-reliance in the pupil. Despite his advocacy of the Socratic method, he did not withhold advice. I have often heard him giving his views to a student in informal discussion. It is reported that much of this teaching occurred in his laboratory after midnight (I was not a witness to that); he would touch base with his students after having spent an hour or so carefully looking through the current literature.

Bernd was quick, and exceptionally good at thinking on his feet, very much in the style of the best theoretical physicists I have known. And like them, he was not invariably sound. This was never more evident than when he and Zachariasen argued. Willie, too, was quick, but his response tended to be more of a lecture than the series of rather aphoristic remarks one usually heard from Bernd. Willie, by the way, came out to La Jolla almost every spring to work his indispensable and irreplaceable magic. He also talked with Bernd's students (on request), sometimes, it seems, to great effect.

In a short piece published last year, three of Bernd's former students (Zachary Fisk, Brian Maple, and George Webb) gave a moving description of what it was like to study under him. Among other things, they remarked on the great social rapport he maintained with his students: "Friendship and science became intertwined. Interaction spilled over into parties, weekend trips, and countless sessions at the famous El Sombrero cantina in the village of La Jolla." (One gratuitous comment: for anyone with a musical ear, the now defunct Sombrero was a dismal swamp.)

One gift that heightened the impact of Bernd's personality on his students and nonstudents alike was his eloquence. Bernd spoke a fluent, imaginative, and slightly inaccurate English. I think his unconventional phraseology was actually an advantage for him; it tended to fix metaphors in the listener's memory. In retrospect, I regret having persuaded him to suppress some of the more unusual locutions. One I unfortunately helped get rid of was "forth and back" (from the German *hin und her*). Bernd put up a weak logical argument in its favor, but finally bowed to the overwhelming evidence that "back and forth" was the accepted form. His accent was not bad and rarely caused problems. I do, however, remember one occasion when it almost got him into trouble. The Matthiases, Zachariasens, and Steins were driving through the border checkpoint at Tijuana, on our way to Ensenada. Two burly Mexican cops spotted Bernd as a foreigner, and started to give him a hard time. Bernd very wisely adopted a docile, conciliatory attitude, and eventually we got through. As we drove away, I thought to ask "Willie, how about you? Why didn't they pick on you too?" "Ah," he said, in his unmistakable Norwegian accent, "when they heard me talk, no doubt they thought I was from New England."

In writing, Bernd's exotic style proved to be a handicap. Many a student and ex-student took his turn at Englishing Bernd's prose. He finally pressed me into service, probably because I affected an (unwarranted) air of absolute confidence in this field. Curiously, Willie, whose written English was hypercorrect, never offered to help with any of these rewriting chores.

It didn't take many years for the Professor

Matthias
A Personal Memoir

to become known, not only on campus, but as far away as downtown San Diego. Even the police would recognize the tall, bespectacled figure with wavy hair, dressed in a black sweater or dark blazer, and driving a slightly disreputable but vintage Oldsmobile convertible. Bernd was certainly familiar to a large body of undergraduates who knew little or nothing of his scientific achievements. This may account for the immediate success of his experimental general education course "Frontiers of Science," which was meant for, and in fact attracted, a large untutored audience. (To some of us, the course was known by a less flattering name which pointed up its lack of significant content.) In conducting this course, Bernd depended heavily on his friends to provide 45-minute lectures on almost anything. He even managed to persuade four or five of us from Los Alamos to run the gantlet of inattention or restless incomprehension that characterized the audiences of the earlier years. I came to talk about some simple aspects of so-called elementary number theory; "elementary" here has a technical meaning that does not include the notion of simplicity. Bernd liked number theory. On introducing me, he said (inaccurately) that it remained the one subject that was of no use to the military. For my talk a great concession was made: dogs, especially dogs in heat, were barred from the lecture hall. In the course of my short lecture I had occasion to refer to quantities like 10^3, 3^{27}, and so forth. My wife, Carol, was in the audience and heard one young lady ask her companions "What does he mean by 'ten-to-the-three'?" Her friends laboriously explained. At the end, Bernd announced the topic for the next meeting. He pointed to an extremely attractive girl in the front row and told us that she would reveal what she had learned about the mystery of the Bermuda Triangle. I'm sorry I missed it.

The Social Animal

Just as there were for Bernd three main centers of low-temperature research, so there were three crowded and demanding social schedules. I saw the Bell Laboratories version only twice, but I got to know something of the La Jolla scene from 1962 to 1980, when Carol and I went out almost every February to spend two or three weeks. During this time I would work for Bernd; the tasks were always different, but they had in common the property of being well within the range of any number of indigenous mathematicians. As it was, Bernd didn't know any of them, and he would only let his friends do his work. In the 1960s—when we were still young enough to stand the pace—Carol and I would seem to be caught up in a whirlwind. Joan always maintained that things had been much less hectic before we arrived and would settle down again after we left. I must say that neither my wife nor I was ever convinced of this, and I think that Willie and Mossa Zachariasen shared our skepticism. But La Jolla was just two weeks for us; in Los Alamos it was all summer. Here the Matthiases maintained a brutal pace from the early 1960s until Bernd's death. After Joan's parents moved to Santa Fe, we would see the Matthiases over Christmas too.

Bernd and Joan needed no help from us or anybody else in making friends either in Los Alamos or Santa Fe. By 1968 they probably had a larger circle of New Mexico friends than we did, and they had spotted us 15 years. If I remember correctly, however, I did introduce Bernd and Joan to Eliot and Aline Porter, a social act that I view as a positive contribution. (I had known Eliot for several years; at the time Bernd met him, I had just taken up large-format photography at his suggestion.) After an uncertain start, Bernd and Eliot became close friends, spending their time in verbal give-and-take whenever they were together. Both of them were unflappable in argument, vehement but without rancor; it was a very good match.

In their memoir, Fisk, Maple, and Webb say of Bernd: "Like most people who are never bored, he demanded excitement. This meant that much of the time he would produce it himself." He could do this because in social situations he was totally aware of everything that went on about him. If conversation was in danger of stagnating, or if some awkwardness threatened to intrude, he always knew exactly what to do. Somewhat paradoxically, he was at his best in private conversation—what current jargon calls one-on-one situations. It was not a matter of charm; his interest in others was sincere, and was therefore reciprocated. As I wrote in another place, he was a collector—not of material things (as I am) but of friends. All these friends thought they had a special place in Bernd's life. I think that all of them were correct.

Iceland

In the summer of 1972 Carol and I went to Iceland as part of a group of eight, the others being Eliot Porter, his son Jonathan and daughter-in-law Zoe, Joan Matthias, and Tad Nichols and his wife, Mary Jane. The males in the party were all photographers with various degrees of professional commitment, with Eliot the acknowledged leader. It was a busy summer for Bernd, but he had promised to join us for a few days at the beginning of our stay. This was the year of the Fischer-Spassky world championship chess match in Reykjavik, so the date is not in doubt, and for once $\Delta t_B = 0$.

We all arrived on the same day—all but Bernd, that is—and, after collecting the duty-free alcohol of our choice, we repaired to the hotel Borg, a small, neat establishment with an excellent dining room. The mood was euphoric, the promise of adventure heightened by exotic details like the signs with impossibly long and unpronounceable names, reminiscent to me of the road signs in Turkey.

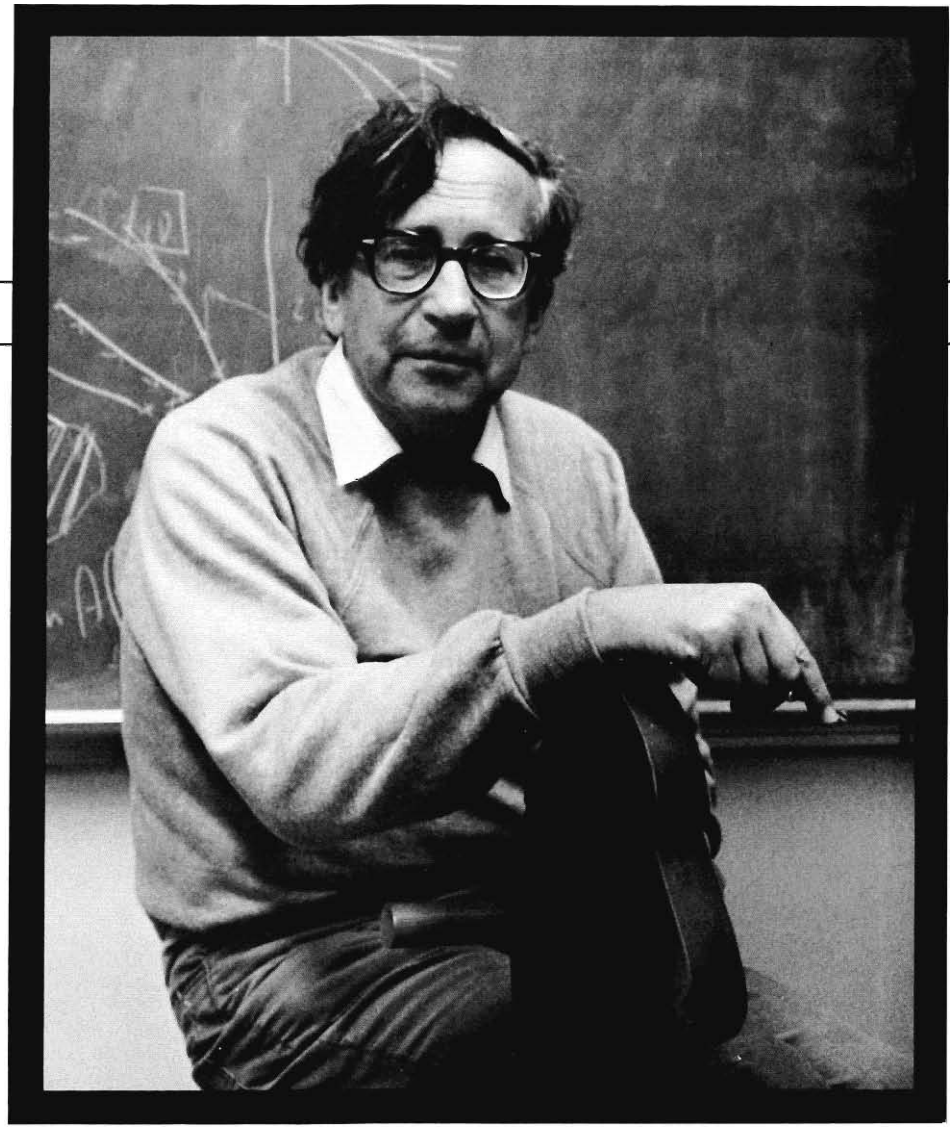

In the next few days we were busy with preparations, but there was time to explore the nearby countryside, in particular the desolate, wind-eroded landscape of Krysuvik to the east of the city, where the rocks resemble the wings of fabulous animals. In Reykjavik itself the leaden skies exhilarated me as the bland blue of New Mexico has never done (a photographer's reaction). I wanted to get going. But where was Bernd? Joan was in touch with him; it seemed uncertain whether he would make it. And then he was there, for him reasonably well equipped. At least he'd brought suitable footwear and a selection of sweaters (it was mid June, but the temperature rarely exceeded 45 degrees). Exactly half the group were strangers to him, but that obstacle was swept away in an hour or two. That night in the hotel dining room Bernd absorbed the ambient euphoria and began to talk. After a bit, voices started to rise. Eliot accused Bernd of talking too much, the accusation was returned, and of course there had to be a bet: the first of the two to say a word would forfeit five dollars. Eliot won by deceit. He left the table, ostensibly to go to his room. Instead, he lingered outside the elevator for a minute or so, then re-entered the dining room and caught Bernd talking. Bernd was outraged by this trickery, but he paid.

Bernd stayed with us for three or four days. We took him to the starkness of Krysuvik and to the fantastic geothermal displays near the city, great roaring jets of steam rushing out of the earth. We took our rented Land Rovers cross-country through the heather. Bernd good-naturedly criticized other people's driving over the non-roads, and when it was his turn at the wheel, got as good as he gave. Each night we tried another restaurant, happily discussing its merits and faults vis à vis those of the previous night's choice. All through this Bernd kept up a running commentary on the state of the union, the coming presidential election, the condition of physics in the United States, the administration of the Laboratory, in short, anything that had interested him lately. It was as though a much-traveled relative had come home, bursting with tales of distant lands and exotic customs. In reality, we were the ones in the distant land, but it didn't matter.

I think Bernd would have liked to stay longer, but a Senate committee had requested his testimony. So suddenly he was gone. We were not concerned; we knew we would see him soon again, and of course we did. This time it is different, and that hurts. ■

Acknowledgment

I wish to thank the following people for supplying information used in preparing this memoir: Zach Fisk, Kees Gugelot, Carson Mark, Joan Matthias, Nick Metropolis, Clayton Olsen, Ray Pepinsky, Eliot Porter, Jim Smith, Rolf Steffen, Jacob Trapp, and Renate Zinn.

Further details about Bernd and his work may be found in the following publications.

Journal of the Less-Common Metals 62 (November/December 1978). This volume, titled "On the Physics and Chemistry of Solids," is dedicated to Bernd T. Matthias on the occasion of his 60th birthday and contains much information about Bernd and his professional career.

B. T. Matthias and P. R. Stein, "Superconducting Materials," in *Physics of Modern Materials II* (International Atomic Energy Agency, Vienna, 1980), pp. 121-148.

John K. Hulm, J. Eugene Kunzler, and Bernd T. Matthias, "The Road to Superconducting Materials," Physics Today 34, 34-43 (January 1981).

Zachary Fisk, M. Brian Maple, George W. Webb, "Some Recollections of Our Years with Professor Bernd T. Matthias," in "Proceedings of the Ternary Superconductor Conference," Lake Geneva, Wisconsin, September 23-26, 1980 (Elsevier/North Holland, New York, 1981).

* U.S. GOVERNMENT PRINTING OFFICE: 1982- 576-088/16